

SNAKES Manipulator and ARD Sluicer Testing

Prepared for the U.S. Department of Energy
Assistant Secretary for Environmental Management

Project Hanford Management Contractor for the
U.S. Department of Energy under Contract DE-AC06-96RL13200

Approved for public release; distribution is unlimited

SNAKES Manipulator and ARD Sluicer Testing

Magnox Electric PLC

Date Published
April 1997

Prepared for the U.S. Department of Energy
Assistant Secretary for Environmental Management

Project Hanford Management Contractor for the
U.S. Department of Energy under Contract DE-AC06-96RL13200

RECORD COPY

Approved for public release; distribution is unlimited

LEGAL DISCLAIMER

This report was prepared as an account of work sponsored by an agency of the United States Government. Neither the United States Government nor any agency thereof, nor any of their employees, nor any of their contractors, subcontractors or their employees, makes any warranty, express or implied, or assumes any legal liability or responsibility for the accuracy, completeness, or any third party's use or the results of such use of any information, apparatus, product, or process disclosed, or represents that its use would not infringe privately owned rights. Reference herein to any specific commercial product, process, or service by trade name, trademark, manufacturer, or otherwise, does not necessarily constitute or imply its endorsement, recommendation, or favoring by the United States Government or any agency thereof or its contractors or subcontractors. The views and opinions of authors expressed herein do not necessarily state or reflect those of the United States Government or any agency thereof.

This report has been reproduced from the best available copy. Available in paper copy and microfiche.

Available to the U.S. Department of Energy
and its contractors from
U.S. Department of Energy
Office of Scientific and Technical Information (OSTI)
P.O. Box 62
Oak Ridge, TN 37831
(615) 576-8401

Available to the public from the U.S. Department of Commerce
National Technical Information Service (NTIS)
5285 Port Royal Road
Springfield, VA 22161
(703) 487-4650

Printed in the United States of America

DISCLM-1,CHP (8-95)

Westinghouse Hanford Company
P.O. Box 1070
Richland, WA 99352

**APPLICATION FOR PERMISSION TO USE
YOUR COPYRIGHTED MATERIAL**

To: MAGNOX Electric plc
Berkeley Centre
Berkeley, Glos GL13 9PB

Date: May 16, 1997

Permission is requested to reproduce the following copyrighted material from:

HANFORD SINGLE SHLL TANKS WASTE RETRIEVAL, PHASE 1-ACTR INTEGRATED TESTING, MAGNOX Electric Team Final Report-Track 3: Task 5 - Prepared for Fluor Daniel Hanford

Selections from text (specify by date of issue, page, paragraph, or illustration; if desired, attach a copy of the material in question):

Complete Report

Title of work or project in which this material will be included:

HNF-MR-0538, Rev. 0

Estimated publication date: May 23, 1997

Author: Eric J. Berglin

Publisher (if applicable): N/A

If the copyrighted material is not to be used in a published work, please provide a brief description of how it is to be used:

Will be placed on the Hanford HTI web page, document is being released to the public.

A self-addressed stamped envelope is enclosed for your reply.

Name: Eric Berglin

MSIN: 115-61

Date: May 16, 1997

Signature: *Eric Berglin*

Westinghouse Hanford Company

Credit line (if required):

Application approved by:

Name: S. A. BARNES

Date: 20 May 1997

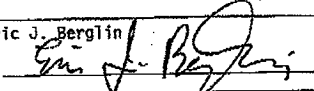
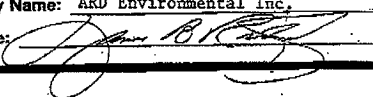
Company Name: MAGNOX ELECTRIC PLC

Signatory's Position: Project Mgr.

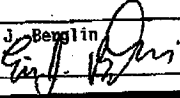
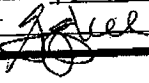
Signature: *[Signature]*

(on behalf of) N. S. BEESEFORD

PostNet Fax Note	7871	Date	5-16-97	12 of 1
To	Stuart Barnes	From	Eric Berglin	
Outbox	MAGNOX	Co.	SEEC	
Phone #	44-1322-290022	Phone #	(509) 372-1824	
Fax #	44-1322-290118	Fax #	(509) 373-6100	

Westinghouse Hanford Company P.O. Box 1970 Richland, WA 99352	APPLICATION FOR PERMISSION TO USE YOUR COPYRIGHTED MATERIAL
To: ARD Environmental, Inc 9116 Whiskey Bottom Road Laurel, MD 20723	Date: May 16, 1997
<p>Permission is requested to reproduce the following copyrighted material from:</p> <p>HANFORD SINGLE SHELL TANKS WASTE RETRIEVAL, PHASE I-ACTR INTEGRATED TESTING, MAGNOX Electric Team Final Report-Track 3: Task 5 - Prepared for Fluor Daniel hanford</p> <p>Selections from text (specify by date of issue, page, paragraph, or illustration; if desired, attach a copy of the material in question):</p> <p>ARD sluicer data and photos in support MAGNOX testing; primary Appendix B</p> <p>Title of work or project in which this material will be included:</p> <p>HNF-MR-0538, Rev 0</p> <p>Estimated publication date: May 23, 1997 Author: Eric J. Berglin</p> <p>Publisher (if applicable): N/A</p> <p>If the copyrighted material is not to be used in a published work, please provide a brief description of how it is to be used:</p> <p>Will be placed on the Hanford HTI web page, document is being released to the public. All proprietary data has been removed from the report.</p>	
A self-addressed stamped envelope is enclosed for your reply.	
Name: Eric J. Berglin Signature: 	MSIN: H5-61 Date: May 16, 1997 Westinghouse Hanford Company
Credit line (if required): <hr/>	
Application approved by: Name: James B. Ridgely Date: 5-21-97 Company Name: ARD Environmental Inc. Signatory's Position: Director, Operations Svs. Signature:  (on behalf of) _____	

Post-It Fax Note	7671	Date	5/21/97	# of pages	1
To	Jim Ridgely	From	Eric Berglin		
Co./Dept	ARD	Do.	SESC		
Phone #	(301) 497-0477	Phone #	(509) 372-1024		
Fax #	(301) 497-1645	Fax #	(509) 373-6101		

Westinghouse Hanford Company P.O. Box 1970 Richland, WA 99352	APPLICATION FOR PERMISSION TO USE YOUR COPYRIGHTED MATERIAL
To: McCrometer 3255 West Statson Avenue Honnet CA 92545 c/o Gregg McCall Fax (909) 652-3078	Date: May 16, 1997
<p>Permission is requested to reproduce the following copyrighted material from:</p> <p>McCrometer Brochures - MF100 Flowmeter Information Engineering cutsheets to be included in reports.</p> <p>Selections from text (specify by date of issue, page, paragraph, or illustration; if desired, attach a copy of the material in question):</p> <p>See Attached</p> <p>Title of work or project in which this material will be included:</p> <p>HNF-MR-0538, Rev 0, HNF-MR-0534</p> <p>Estimated publication date: May 23, 1997 Author: Eric J. Berglin</p> <p>Publisher (if applicable): N/A</p> <p>If the copyrighted material is not to be used in a published work, please provide a brief description of how it is to be used:</p> <p>Will be placed on the Hanford HTI web page, document is being released to the public.</p>	
A self-addressed stamped envelope is enclosed for your reply.	
Name: Eric J. Berglin Signature: 	MSIN: H5-61 Date: May 16, 1997 Westinghouse Hanford Company
Credit line (if required): 	
Application approved by: Name: <u>Gregg A. McCall</u> Date: <u>5/20/97</u> Company Name: <u>McCrometer, Inc.</u> Signatory's Position: <u>V.P. Marketing</u> Signature:  (on behalf of) _____	

Post-It [®] Fax Note	7571	Date <u>5/20/97</u>	# of pages <u>7</u>
To	<u>Gregg McCall</u>	From	<u>Eric Berglin</u>
Co./Dept.	<u>McCrometer</u>	On	<u>SESC</u>
Phone #	<u>(909) 652-3078</u>	Phone #	<u>(509) 372-1824</u>
Fax #	<u>(909) 652-3078</u>	Fax #	<u>(509) 372-6101</u>

Westinghouse
P.O. Box 1970
Richland, NA 99352

YOUR COPYRIGHTED MATERIAL

To: Thienschmidt
77 East Main Street
Newark, Delaware 19711

Fax (302) 454-7366

Date: May 16, 1997

Permission is requested to reproduce the following copyrighted material from:
Godwin Pump Brochures - CD809CD150N Pump Information, Engineering cutsheet to be included in reports.
Selections from text (specify by date of issue, page, paragraph, or illustration; if desired, attach a copy of the material in question):
See Attached
Title of work or project in which this material will be included:
HNF-MR-Q538, Rev 0, HNF-MR-0534
Estimated publication date: May 23, 1997 Author: Eric J. Berglin
Publisher (if applicable): N/A
If the copyrighted material is not to be used in a published work, please provide a brief description of how it is to be used:
Will be placed on the Hanford HTI web page, document is being released to the public.

A self-addressed stamped envelope is enclosed for your reply.

Name: Eric J. Berglin
Signature: *[Handwritten Signature]*

MSIN: H5-61 Date: May 16, 1997
Westinghouse Hanford Company

Credit line (if required):

Application approved by:

Name: JOSEPH L. ABBOTT JR.
Company Name: GODWIN PUMPS OF AMERICA
Signature: *[Handwritten Signature]*

Date: 5/28/97
Signatory's Position: NOMINAL SALES
(on behalf of) FRB

Post-It Fax Note	7671	Date	5/28/97	# of Pages	6
To	Paul Thienschmidt	From	Eric Berglin		
Co./Dept	Thienschmidt	Co.	SESC		
Phone #	(302) 454-7233	Phone #	(509) 372-1824		
Fax #	(302) 454-7366	Fax #	(509) 373-6101		

Defined and Revisited

ARA Environmental
Test High Pressure
Nongel device to clean
waste Retrieval
System
non Radioactive
Radioactive

Unclassified

**HANFORD SINGLE SHELL TANKS
WASTE RETRIEVAL**

PHASE 1 - ACTR INTEGRATED TESTING

MAGNOX ELECTRIC TEAM

FINAL REPORT - TRACK 3: TASK 5

to

FLUOR DANIEL HANFORD

Contract Reference: MSJ - SLD - A15104

April 1997

SNAKES Manipulator and ARD Sluicer Testing

Issue 1 April 1997

Confidentiality classification:
Unclassified

SNAKES Manipulator and ARD Sluicer Testing
Fluor Daniel Hanford, Contract Ref: MSJ - SLD - A15104

April 1997

Approved for Issue:

A. T. Stewart

Date: 9/4/97

Dr A T Stewart, Branch Manager,
Systems and Remote Engineering

EXECUTIVE SUMMARY

Long reach arms represent one of the options available for deployment of end effectors which can be used in the retrieval of radioactive waste, from the Hanford single shell tanks. The versatility of an arm based deployment system is such that it has the potential to improve the performance of a wide range of end effectors compared with stand-alone or other deployment methods.

The long term reliability and availability of the deployment system is central to the timely completion of a waste retrieval programme. However, concerns have been expressed over the dynamic performance of long reach arms and it is essential that an arm based system can cope with operational dynamic loads generated by end effectors.

The test programme conducted, set out to measure static and dynamic loads and responses from a representative arm and sluicer, with the objective of extrapolating the data to a long reach arm system, that can be used for in-tank waste retrieval.

As an arm with an appropriate reach was not available, the test programme was undertaken to measure dynamic characteristics of a Magnox Electric 18 ft multi-link, hydraulically actuated SNAKES manipulator. This is the longest reach unit in service, albeit only one third of the 50 ft length required for in-tank waste retrieval. In addition operational performance and loading measurements were obtained from a low pressure confined system sluicer under development by ARD Environmental, to add to the end effector data base.

When subject to impulse loading, the arm was found to behave in a repeatable manner having fundamental natural frequencies in the vertical and transverse directions of ~ 1 Hz. There were also a large number of higher natural frequencies measured up to 100 Hz.

The mode shapes for these natural frequencies appear to follow classical shapes as would be expected for a continuous beam. Hence, it should be possible to calculate natural frequencies for an arm for retrieval of waste from a Hanford tank based on mass and stiffness distributions. Indeed, in developing a long reach arm for Hanford tanks, fundamental natural frequencies have been calculated at between 1.1 Hz to 1.3 Hz. Hence the dynamic response could be expected to be similar to the shorter arm. The responses at the lower natural frequencies were shown to be relatively highly damped. Whilst this could be expected to be applicable to a scaled-up system, damping could be dependent on the detail joint design of the long reach arm.

A study was undertaken to determine the sensitivity of response to variations in payload, stiffness, geometry, reach and force level, the parametric changes that would be encountered in operational duty. Variations were detected and these were broadly in line with expectations.

The low pressure confined sluicer has been developed to improve upon the performance of other sluicing systems. The sluicer spray nozzle system has been shown to be effective in breaking up saltcake and hardpan materials. However, the prototype had only limited success in containing water.

The sluicer was primarily designed for deployment with a remote vehicle and there is clearly a mis-match in the 200 lbf payload for an arm deployment system and the 400 lb weight of the sluicer. The sluicer produces relatively large, broadband dynamic forces which will inevitably excite some of the natural frequencies in the long reach arm. However in view of the high damping, it is not expected that the resulting vibration would be detrimental to the integrity of the arm system. To realise the potential benefits of the low pressure confined sluicer, a design optimisation and development programme would need to be undertaken.

The test programme has provided data that goes some way to allaying concerns on the issue of dynamic response of a long reach arm affecting long term endurance capabilities for waste retrieval. Since the SNAKES system is considerably shorter than a system for in-tank waste retrieval it is recommended that an integrated development programme for the sluicer and deployment arm should be undertaken that includes rigorous combined testing, prior to "hot waste retrieval".

LIST OF CONTENTS

SECTION	TITLE	PAGE
1.0	INTRODUCTION	1
2.0	DESCRIPTION OF TESTS	1
2.1	SNAKES Manipulator	2
2.1.1	Base Line Test	2
2.1.2	Sensitivity to Payload	2
2.1.3	Sensitivity to Configuration	3
2.1.4	Sensitivity to Force Level	3
2.2	Sluicer	3
2.2.1	Reaction Forces	3
2.2.2	Performance against Waste Simulants	4
2.2.3	Blockage Effects	4
3.0	TEST METHOD AND TEST EQUIPMENT	4
3.1	SNAKES Manipulator	4
3.1.1	Mechanical Arrangement	4
3.1.2	Instrumentation	5
3.1.3	Static Loading	6
3.1.4	Dynamic Loading	7
3.1.5	Sensitivity to Force Level	8
3.2	Sluicer	8
3.2.1	Mechanical Arrangement	8
3.2.2	Instrumentation	9
3.2.3	Static Loading	10
3.2.4	Dynamic Loading	10
4.0	TEST RESULTS	11
4.1	SNAKES Manipulator	11
4.1.1	Static Loading	11
4.1.2	Dynamic Loading	11

4.2	Sluicer	14
4.2.1	Static Loading	14
4.2.2	Dynamic Loading	15
5.0	CONCLUSIONS AND RECOMMENDATIONS	16
5.1	Manipulator and Sluicer Compatibility	16
5.2	Applicability of Results to Hanford Scale-up	16
5.3	Operational and Design Lessons Learned	17
5.4	Recommendations	17
6.0	REFERENCES	18
	TABLES	19 - 21
	FIGURES	22 - 32
	PHOTOGRAPH	33

1.0 INTRODUCTION

Long reach arms represent one of the options available for deployment of end effectors which can be used in the retrieval of radioactive waste, from the Hanford single shell tanks. The versatility of an arm based deployment system is such that it has the potential to improve the performance of a wide range of end effectors compared with stand-alone or other deployment methods.

The long term reliability and availability of the deployment system is central to the timely completion of a waste retrieval programme. However, concerns have been expressed over the dynamic performance of long reach arms and it is essential that an arm based system can cope with operational dynamic loads generated by end effectors.

Magnox Electric has a range of long reach arms in-service with a reach of up to 18 feet and a payload capability of 200 lbf. Whilst in-service experience of deploying a range of end effectors with these arms has not highlighted dynamic instability as a problem, there is limited data to support this position. Similarly, there is limited data available on the forces generated by waste retrieval end effectors.

Theoretical analysis of a long reach arm system of 50 ft reach, designed for in-tank waste retrieval at Hanford predicted natural frequencies for the first order modes of between 1.11 Hz and 1.29 Hz. Against this background, measurements of the excitation forces generated by the government designed confined system sluicer, albeit of a low level of the order of a few pounds, has a fundamental frequency of vibration, when operating at optimum conditions, of 1 Hz. Thus reinforcing the need to resolve this issue prior to employing a long reach arm system for waste retrieval. Similarly, a better understanding needs to be gained of the forces generated by typical waste retrieval end effectors.

As an arm with an appropriate reach was not available, the test programme was undertaken to measure dynamic characteristics of a Magnox Electric 18 ft multi-link, hydraulically actuated SNAKES manipulator arm. This is the longest reach unit in service, albeit only one third of the 50 ft length required for in-tank waste retrieval. In addition operational performance and loading measurements were obtained from a low pressure confined system sluicer under development by ARD Environmental, to add to the end effector data base. The test programme also covered static load measurement on the sluicer and a limited amount of static deflection measurement of the manipulator arm.

2.0 DESCRIPTION OF TESTS

The test programme conducted, set out to measure static and dynamic loads and responses from a representative arm and sluicer, with the objective of extrapolating the data to a long reach arm system, that can be used for in-tank waste retrieval. In evaluating the dynamic characteristics of long reach arm systems, it is important to consider the potential sources of excitation. The 1 Hz

excitation generated by the high pressure sluicer is attributable to the rotational head. The Past Practice Sluicer (PPS) loading will primarily be that of reaction force from the water jet and could be expected to induce transient and broad band frequency excitation. The low pressure confined sluicer under development could be expected to induce hydro-dynamic loading and broad band excitation from turbulence in the sluicer chamber. In view of the long flexible hoses for the services to the sluicer, the driving machinery and pump induced excitation could be expected to be de-coupled from the arm. The fundamental mode of a long reach arm is anticipated as being at a frequency of the order of 1 Hz. The frequency range of testing was thus limited to 0-100 Hz, which is considered adequate to cover the frequency range of all possible excitation mechanisms.

Testing on the deployment arm was conducted at Magnox Electric premises in the UK. The manipulator arm made available by Magnox Electric for the tests whilst having an equivalent payload capability, at 18 ft reach is only approximately one third of the 50 ft required for in-tank waste retrieval.

To better understand the forces generated by end effectors, measurements were taken on the novel low pressure confined sluicer under development in the programme for the deployment of end effectors from remote vehicles. This work was conducted by ARD Environmental at their works in Maryland USA (Ref 1).

2.1 SNAKES Manipulator

2.1.1 Base Line Test.

The manipulator arm, fully extended in a horizontal attitude, with all rotational joints aligned for planar motion in the vertical plane, was subject to multi-directional transient excitation employing impulse methods. The measured responses in the three orthogonal planes were used to characterise the manipulator arm modal behaviour and establish the frequencies of vibration and damping factors. Additionally, measurements were made of static deflections and attempts were also made to measure torsional vibrations.

This base line test was used to establish a basic understanding of the manipulator arm dynamic response characteristics and identify the potential for adverse resonant behaviour. This test was also used to formulate the testing programme for a sensitivity study of boundary condition changes during operation.

2.1.2 Sensitivity to Payload.

The payload capacity was expected to be of limited significance in relation to the self weight of the manipulator arm although it could take up backlash and lost motion in the joints. Nevertheless the sensitivity of response to a range of loads applied to the manipulator arm was investigated

2.1.3 Sensitivity to Configuration.

Changes in dynamic characteristics could be anticipated as a result of changes in configuration when the manipulator arm is subject to transient excitation. The sensitivity of response to configuration changes was evaluated in three ways; by rotating links to investigate changes in stiffness of the extended manipulator arm, by progressively altering the geometry of the arm and finally by reducing the extended reach.

The supports to the pivots of the gear driven articulated joints of the manipulator arm are believed to exhibit maximum stiffness in the plane of articulation. By operating the two rotate joints of shoulder and wrist in 45° steps, changes in local stiffnesses were evaluated through investigations of dynamic responses.

For in-tank waste retrieval, the deployment system will be required to operate avoiding interaction with in-tank hardware. This would lead to geometric changes to the configuration of the manipulator. The sensitivity of dynamic response to such changes was examined with a range of articulations of the arm and wrist joints in steps of 45°.

All retrieval work will not demand the reach of the deployment system to be fully extended. Thus the effects of reduced reach on dynamic response were examined by retracting the arm's upper link assembly into the outer vertical deployment tube, thereby reducing the reach by some 2 feet.

2.1.4 Sensitivity to Force Level

In assessing the dynamic behaviour of the manipulator, it is important to establish its consistency of response over a range of force input levels. Therefore, a 'linearity' test was conducted in which the proportionality of the response was evaluated against changes in input force excitation levels.

2.2 Sluicer

In attempting to resolve the issue of dynamic performance of long reach arms as a deployment system for waste retrieval, a pre-requisite is to better understand the operational loading regime generated by typical waste retrieval end effectors. The low pressure confined sluicer, under development, potentially offers benefits in waste retrieval performance but represents an "unknown" in terms of reaction forces generated in operation.

2.2.1 Reaction Forces

To provide a rigid mounting, whilst retaining manoeuvrability of the sluicer head, the instrumented sluicer was mounted on a hydraulically actuated back-hoe. The sluicer assembly was suspended in free space and the reaction forces of the water jets were monitored for comparison with theoretical assessment. The effects of variations in efflux angle from the nozzles was also monitored.

2.2.2 Performance against Waste Simulants

One of the predicted attributes of the low pressure confined sluicer would be the ability to break-up and retrieve saltcake and hardpan type wastes at a rate practical for a major retrieval programme. During performance evaluation of the sluicer against simulants of this type of waste with a simple mining strategy of 'plunging', the loads generated during the process were monitored in terms of forces transmitted through the mounting structure and hydro-dynamic forces as a result of pressure fluctuations from 'loss of confinement' and turbulent flow in the sluicer chamber.

2.2.3 Blockage Effects

In operation, the suction pump would limit the release of free water when the sluicer was buried in the waste by extracting the water and waste from the shroud. Loss of suction through pump failure or extract pipe blockage would lead to pressure build-up in the sluicer shroud, generating an up-thrust on the deployment arm, that would cause the arm to lift and thereby release the pressure. A long reach arm would be expected to have greater compliance than the back-hoe used for deployment of the sluicer and oscillatory behaviour might be induced by the pressure forces. The pressure build-up and the upthrusts generated by conditions of loss of suction were measured over a range of conditions from a buried sluicer, through loss of suction pumps to a fully blocked suction pipe to provide a data base to support future designs.

3.0 TEST METHOD AND TEST EQUIPMENT

3.1 SNAKES Manipulator

3.1.1 Mechanical Arrangement

Magnox Electric has a range of heavy duty hydraulically actuated multi-limb manipulators (HDM) in service. The unit used for this series of tests was the SNAKES variant, which has sixteen degrees of freedom, a horizontal reach of 5.334 m (17 ft 6 in) and a payload capacity of 90 kg (200 lbf) at full extension.

The manipulator support is formed of two concentric tubes, which would be mounted vertically in operation. The inner tube, which carries the articulated manipulator arm assembly at its lower end, runs in axial keys on the inside of the outer tube and is raised and lowered via a lead screw drive. The gearbox for this vertical drive and that for the azimuthal drive of the manipulator arm are mounted at the top of the outer structural tube.

The articulated manipulator arm assembly is made up of nine links and extends out of the lower end of the outer tube under the control of the vertical drive. Each link is hydraulically powered by an independent supply to avoid any possible interaction between circuits during operation. The hydraulic actuator for each of the links is an integral part of the link assembly. In the case of the

upper five links, a conventional piston/cylinder actuator with an offset pivot is used. The lower four links, the tool arm, wrist/lower arm, middle arm and the upper arm, which together provide the dextrous motion, use bevel gears to translate axial motion into 'bend'. The joint rotation is direct drive.

The manipulator assembly was supported in the high bay test facility for this series of tests in a different way to the normal reactor use. Instead of being rigidly supported at the lower end of the outer tube by the riser, the upper end of the outer tube was rigidly fixed and only a 'weak' restraint was provided mid-span of the outer tube. This arrangement is comparable to that envisaged for operations in a Hanford tank where no contact would be made with the riser.

To ensure long term positional stability of the manipulator, the individual link joint controllers incorporate a 'position hold' feature that automatically restores the joint position to a pre-set value. This feature is intended to cater for effects of slow load changes, small hydraulic leakage and thermal expansion effects. The frequency response of the system is less than 0.5 Hz. Thus to avoid possible interaction during induced motion, the facility was disabled during the testing programme.

In view of the limited time available for testing and the short ACTR phase 1 schedule, the tests had to be conducted with the manipulator assembly in the pre-existing configuration. Time constraints precluded adapting to an optimum arrangement. For the purposes of these tests, a steel block was clamped in the parallel jaws of the tool post. This block was used as a target for impulse loading and as a point of attachment for the static loads. The tool arm itself, had 'extend' and 'rotation' motion and the jaws were attached to the tool arm by a pinned linkage.

3.1.2 Instrumentation

Excitation was induced into the manipulator arm by a hand held impulse hammer fitted with a piezo-electric force transducer through which the applied force is transmitted and provides a measure of force level.

The piezo-electric accelerometer used to measure the response was mounted on a magnet to provide a mobile attachment for measurements at various locations and directions along the length of the manipulator. The mass of the accelerometer and magnet was very small compared with the mass of the structure being tested and consequently errors caused by loading of the structure by the transducer can be ignored.

A reference accelerometer at a fixed location close to the impulse site was used to check the constancy of the structure for the duration of a test.

In view of the inaccessibility at mid span along the vertical outer tube a further accelerometer was permanently positioned close to the outer tube restraint. Its orientation was aligned as required depending on the direction of excitation.

For detecting torsional or rotational response of the manipulator arm about its centre-line, an additional accelerometer was used in conjunction with the response accelerometer to form a pair, positioned equi-distant from the manipulator arm centre-line. The difference of the two output signals was used to derive the torsional response.

The accelerometer and force transducer output signals were conditioned through charge amplifiers to provide calibrated outputs in terms of either mV/N for force or mV/m/s² for acceleration.

Because of poor low frequency signal to noise ratios associated with piezo-electric accelerometers, Linear Variable Differential Transformers (LVDTs) were used to obtain response measurements for frequencies below 1.5 Hz. These transducers have an output proportional to displacement for frequencies in the range 0 to 15 Hz.

The force and response signals were digitally processed to produce frequency response functions using a two channel frequency analyser. This data is then post-processed using appropriate modal analysis software to extract the natural frequencies, damping and mode shapes.

Analysis of the impulse testing was performed with the vibration analyser set to exponential "windowing" to improve the accuracies of amplitude and frequency measurements. This "window" achieves its improved accuracy by superimposing artificial damping on the signal to improve signal to noise ratio during data capture. However, this damping must then be removed numerically from any measurements of damping coefficients. Damping values were derived from analysis of the frequency response spectra, using Nyquist plots, computer fitted to manually selected data points around each natural frequency.

As a back up, all test signals were recorded on an frequency modulated (FM) magnetic tape recorder.

The arrangement of the instrumentation and data capture analysis system is shown in figure 1. Appendix A Section 2 provides details of the instrumentation used and calibration details.

3.1.3 Static Loading

With the manipulator arm fully extended horizontally, static loads were progressively applied at the tool post both along the axis of the manipulator arm and vertically by means of suitable arrangement of hangers, weights and pulleys. Static deflections were measured using LVDTs or dial gauges. Measurements were made whilst loading and unloading the manipulator arm.

It was intended to carry out static tests horizontally transverse to the manipulator arm's axis and rotationally but these were abandoned due to practical difficulties.

3.1.4 Dynamic Loading

This series of tests was designed to characterise the dynamic response of the manipulator arm at frequencies up to 100 Hz. Excitation was induced via an instrumented hammer applied at the tool post, either translational along one of three orthogonal axes or offset from the manipulator arm's centre-line to produce a moment.

The force waveform generated by a hammer impulse is a short duration transient event or impulse, with a continuous frequency spectrum, having a useful frequency range determined by the hammer mass and the stiffness of the hammer tip which acts as a filter and enables the cut-off frequency to be adjusted to suit the application. For measurements taken with accelerometers, a plastic hammer tip was used having a useful range up to 120 Hz (-3 dB), but for the LVDT measurements, the impulse was through a softer high density foam rubber which provided uniform excitation at frequencies up to 20 Hz and thus eliminating the possibility of LVDT tip contact rattle which might have occurred if vibrational frequencies above this level were induced.

The structural response was measured with either a roving accelerometer which gave sufficient data to determine full modal information (natural frequencies, damping and mode shapes), or a fixed LVDT for each axis at the driving point (tool post), which gave only natural frequencies and damping for the low frequency modes (less than 10 Hz).

In some of the tests it was judged that no significant new information was being obtained, and in those cases, the testing was restricted to a single driving point accelerometer measurement and a single driving point LVDT measurement for each axis.

The number of degrees of freedom (accelerometer locations) was chosen to ensure accurate representation of the total dynamics of the structure and the complexity of the expected mode shapes within the frequency band of interest. Acceleration measurements were always made in the direction of the excitation but in some cases additional measurements were made in a second direction where the vibration resulted in significant motion in this direction. The measuring positions are shown in figure 2 and correspond to the ends of each link, either side of the wrist and shoulder rotation joints, the vertical restraint, and intermediate and bottom vertical outer tube locations. Accelerometer derived response spectra were analysed on-line and recorded for measurement positions corresponding to the tool post and at the end of each link assembly.

LVDT derived response spectra were analysed on-line and recorded for the fixed tool post positions.

Each frequency response function stored was the result of four averages, with each individual impulse being accepted or rejected on the basis of the pulse shape, and the absence of under or over-loading of the instrumentation.

Modal analysis was performed using the MODENT • suite of programs (Ref 2). These programs allow a highly interactive modal analysis of either Single- or Multi-Degree of Freedom systems

and is designed to run on a PC. After completing the analysis it can display an animated simulation of the calculated normal or complex mode shapes.

Rotational tests were discontinued since the data produced was inconsistent and therefore considered unreliable. This was caused by the fact that the rotational motion produced by the off centre application of the force was coupled to a much larger, unwanted, translational component which dominated the accelerometer signals resulting in a poor signal to noise ratio for the rotational component.

3.1.5 Sensitivity to Force Level

This test was devised in order to determine whether the response characteristics of the manipulator arm changed with the excitation force level. This may have to be considered in the long reach arm design if the change is significant. It was originally intended to carry out this test using an electromagnetic shaker to provide a control over the level of excitation being applied to the manipulator arm. However, this proved impractical with the Position Hold feature on the manipulator arm being switched off, see Sec 3.1.1, allowing a slow drift downwards of the manipulator. Although the amount of drift is small for normal manipulator operation, it was considered sufficient to damage the relatively delicate force mechanism of the shaker. Therefore, this test was substituted by an equally valid alternative of using the hammer technique and applying impulse loads of several distinctly different levels of magnitude. With the configuration as in the base line test, impulses were applied at the tool post and the driving point inertance noted. This was done for all the three orthogonal directions.

3.2 Sluicer

3.2.1 Mechanical Arrangement

The sluicer was mated to a backhoe to simulate installation on a long reach arm, and tests were performed to determine the forces generated and the effectiveness of the sluicer. The tests were conducted against saltcake and hardpan to determine the effectiveness of the sluicer in mobilizing and removing waste, with the sluicer blocked to determine the maximum forces generated, and with the sluicer suspended to determine reaction forces. The test materials used were saltcake formulations #'s 1 and 3, and hardpan # 2 (see Ref 1). These were poured in layers 1' thick x 8' x 12', in dumpsters per the simulant preparation instructions.

The low pressure sluicing device, shown in figure 3, consists of an external shroud approximately 24" W x 8" D x 12"H. Inserted in the external shroud is a central 3" diameter suction pipe with 14 off 0.182" diameter water nozzles arranged on a manifold around it. For the tests performed, the nozzles were extended to within 2" of the bottom of the external shroud. The nozzles face downwards at 22.5° to the mount axis and direct streams of water against the face of the material to be removed, disrupting the material and providing the transportation medium for removing the material.

Photograph 1 shows the sluicer, nozzles and suction intake. The skirt shown in the photograph was removed after it became damaged early in the testing. The sluicer performance improved after the skirt had been removed, since it had inhibited downward motion of the sluicer.

The sluicer suction pipe is equipped with two 1" lines at +/- 45° to the vertical. These are used to provide priming water to the pump, and clog-clearing water for the shroud. The nozzle manifold is fed from two locations to insure uniform flow to the nozzles. All connections to the sluicer were via standard cam-lock couplings.

The backhoe used to simulate a long reach arm was equipped with an extensible boom that permitted linear adjustment of the sluicer position. This enabled the sluicer to be moved straight down into the simulant as the material was eroded by the water jets.

The equipment for pumping and sluicing tests was set up at ARD's facility (See Ref 1). Water at approximately 200 gpm and 400 psi was supplied via two Paco model 38-15955-7B6F01 centrifugal pumps connected in parallel, each driven by a 75 hp electric motor. The Paco pumps were powered by a portable 3 phase 480 Volt diesel-driven generator. Water feed to the Paco pumps was via a Godwin HL80 centrifugal pump driven by a diesel engine. The suction pump was a Godwin HL150M "dri-prime" pump, also diesel driven. The piping arrangement is shown in figure 4.

3.2.2 Instrumentation

The instrumentation included pressure and flow sensors in the supply pipework to the nozzles to permit pressure setting and flow sensors in the suction pump discharge line to determine the effectiveness of water extraction. The shroud was modified for the blocked sluicer tests by the addition of a pressure sensor to measure the internal pressure directly. This sensor was also used to determine the dynamic forces exerted on the backhoe arm. Pancake load cylinders were fitted between the sluicer and the backhoe to determine static loading and triaxial accelerometers were mounted on the sluicer shroud to determine vibration responses.

Figure 3 is a drawing showing the details of the sluicer assembly and location of the pancake cylinders as well as the interface assembly for mounting on the backhoe.

The flow sensors initially installed were Doppler acoustic units with digital readouts and 4-20 mA current loop outputs for computer logging. The Doppler acoustic flow meters proved to be unreliable and were later replaced with turbine-type meters that had to be read manually. These provided accurate readings but could not be logged by computer.

The Labview * data acquisition package from National Instruments (Ref 3) was used to log and process data. The data were sampled at a rate of 2000 samples/second to capture any significant high frequency energy in the accelerometer signals. The data acquisition flow chart and the instrumentation block diagram is enclosed in Appendix B.

The data were processed in two ways. The raw data files were scanned in Labview to identify areas that might be of interest for further processing. Since the software used to perform Fast Fourier Transforms (FFTs) is limited to a data record of 2048 points or less, 1 second sections of data were selected for high frequency processing, thus there is no information in these records below 1 Hz.

In order to process the low frequency data, it was necessary to filter the files to remove high frequency energy, and then decimate them to limit their length to 2048 samples. This was also accomplished with Labview. The decimated files provide a history of the main features of each run, but do not contain any significant data above 1 Hz, as this was filtered out.

Following tests against saltcake and hardpan, the depth was measured with a ruler as the water was trapped in the depression caused by the sluicing.

3.2.3 Static Loading

The static loading and thrust tests were performed by suspending the sluicer assembly and measuring outputs from the load cells attached to the backhoe. The assembly weight was recorded with the sluicing water off and then on. Sluicing pressure at the measurement point was generally in the range of 400 to 430 psi, and flow was in the range of 190 to 210 gpm.

In addition, static loadings were measured during a series of tests with the sluicer in operation against saltcake and hardpan materials. Finally the sluicer shroud was positioned against a rubber mat on an asphalt surface and pressure was applied with the backhoe. This sealed the mouth of the sluicer shroud and loads were measured to determine the maximum forces generated by the sluicer on the backhoe arm. Three tests were conducted: (1) Blocked sluicer, no suction; (2) Blocked sluicer with the suction turned on; and (3) Blocked sluicer with the suction blocked.

3.2.4 Dynamic Loading

The sluicer mounting load cell was used for measurements of static forces in the backhoe arm but the measurement technique did not have the dynamic capability for determining the dynamic forces. The accelerometers mounted on the shroud did have the capability of producing dynamic responses but because the assembly vibration characteristics were unknown, they could only be used for comparative measurements. The sluicer shroud pressure measurements were therefore the only measurements which could be used to derive absolute levels of dynamic forces. These had sufficient dynamic range and have been used to derive the dynamic forces generated in the backhoe arm, based on a known area.

Dynamic responses from the accelerometers were observed during operation against saltcake, hardpan and for the blocked sluicer tests. In addition, the shroud internal pressure was measured during the blocked sluicer and hardpan tests using the pressure sensor.

4.0 TEST RESULTS

4.1 SNAKES Manipulator

Test directions were defined, based on 3 orthogonal axes with their origin centred at the tool post. Horizontal Impulse forces and displacements along the axis of the extended manipulator arm, directed towards the vertical riser (support) were designated as in the +X direction. Impulse forces and displacements in the vertical plane, directed upwards were designated as in the +Y direction and horizontal impulse forces and displacements transverse to the axis of the extended manipulator arm, directed to the left when looking in the +X direction were designated as in the +Z direction.

4.1.1 Static Loading

The manipulator arm static stiffness, determined from the measured deflection during the addition and subsequent removal of incremental loads at the tool post, is given in the table below. These results show significant tolerances, particularly along the axis of the arm, which correspond to the load increasing and load decreasing. This difference is caused by hysteresis and not measurement error.

Load Direction	Along the arm axis		In the vertical plane	
	+X	-X	+Y	-Y
Stiffness N/mm	460±60	195±7	8.2±0.1	7.8±1.2
Stiffness lbf/in	2600±340	1100±40	47±0.6	45±6.9

It can be seen that the stiffness is higher along the axis of the arm, ie along the arm's length, and shows a significant dependence on the direction of application of the load as it is higher in compression. The stiffness in the vertical plane is relatively low in both directions.

Testing transverse to the axis of the arm and with torsional loading was terminated without conclusive results because of high hysteresis (slip-stick friction originating at the temporary restraint) causing erratic large stepped displacements.

4.1.2 Dynamic Loading

The results of the dynamic loading tests are contained in Tables 1a and 1b and are discussed here in the following sections.

4.1.2.1 Natural Frequencies

Natural frequencies of the manipulator arm have been derived from the results of impulse tests. Responses below 10 Hz were measured using LVDTs, while from 2 Hz to 100 Hz, accelerometers were used. This gives some overlap which was used to verify the accuracy of the results. Repeat impulse tests were also performed and these demonstrated repeatable behaviour and good measurement repeatability.

Natural frequencies derived from the measured responses are summarised in Tables 1a and 1b. These show that measurements using the accelerometers missed the fundamental (lowest) natural frequency but there is good agreement in the natural frequencies between the LVDT and accelerometer derived results at the second natural frequency. These results also show that there are a range of natural frequencies from ~ 1 Hz upwards, some of which were excited by impulses in more than one direction.

Examination of the frequencies in the base line test suggests that impulses along the axis of the arm have excited frequencies at 1.5, 3.3, 29/30 and 35 Hz which are common with the natural frequencies in the vertical plane, while frequencies at 19.1/19.7, 30 and 53 are common with those transverse to the axis of the arm. Where impulses along the axis of the arm have excited responses in common with other orthogonal directions, the response to an impulse in the other direction was in each case greater than the response to an impulse along the axis of the arm. Hence, the 12.3 Hz frequency is considered to be the only natural frequency for vibrations along the axis of the arm.

Following the baseline test, an assessment was made of the sensitivity of the dynamic characteristics to changes in payload, manipulator arm stiffness, arm geometry and reach.

In Tables 1a and 1b, it can be seen that increasing the payload from 10 kg (22 lb) to 32 kg (70 lb) and 62 kg (136 lb) progressively reduces the fundamental natural frequency (by up to 13 %) in the vertical plane. However, this same addition of mass did not effect all natural frequencies in the same manner and even had the effect of increasing some of the frequencies transverse to the axis of the arm.

In the tests to investigate possible stiffness changes, rotation of the wrist and shoulder joints by $\pm 45^\circ$ and $\pm 90^\circ$, simultaneously increased the fundamental natural frequencies in both the vertical plane and transverse to the axis of the arm. However, this effect was inconsistent across other natural frequencies.

In the tests to check the effects of configuration, a dog-leg was produced in the manipulator arm in the vertical axis by operating two bend joints. The results show no change in the fundamental natural frequency in the vertical plane and a slight increase in other natural frequencies. There was however a more marked reduction in natural frequency, transverse to the axis of the arm. Changing the configuration of the manipulator arm also had the effect of introducing a number of higher natural frequencies, increasing the complexity of vibration responses.

Reducing the length of the manipulator arm by retracting one of the links into the support tube, had the effect of shortening the arm by approximately 2 ft. As expected, this increased the natural frequencies in all directions.

4.1.2.2 Damping

The damping values are also shown in Tables 1a and 1b.

Damping values are generally relatively low at the higher frequencies (3% to 18% loss factor) where the displacements are small, indicating small levels of energy loss per vibration cycle. Whereas, at the lower frequencies (such as at the fundamental natural frequencies) where displacements are much larger, damping is significantly higher (16% to 56% loss factor). This difference is probably caused by additional energy loss from friction and fluid damping in the joints.

4.1.2.3 Mode Shapes

Mode shapes for natural frequencies f_1 to f_6 have been produced from accelerometer measurements. Examples of these mode shape plots are shown in figures 5 to 10, for impulses in the vertical plane and along the axis of the arm for the base line test. Comparison of these figures confirms that many of the modes excited by impulses along the axis of the arm correspond closely to those excited by vertical plane impulses. Analysis of the 12.3 Hz mode has shown it to be a complex mode with a travelling vibration "wave" and no fixed nodal points. Hence, it has not been possible to plot it, in the same manner as other modes. In this case the shape plotted represents a single instant in time, at other times in the cycle the vibration nodes will be elsewhere. Other complex modes were discovered in tests to investigate stiffness changes and in tests to investigate the effects of reducing the length of the manipulator arm.

Examination of the modes shows the manipulator arm vibrating as would be expected from simple beam theory, with an additional nodal point in each successive mode. The mode shapes are smooth with no step changes, indicating there is no excessive clearance in the joints. Examination of the vertical support tube shows significant movement, indicating flexibility in the clamping arrangement.

In tests with increased payload, the mode shapes remained essentially the same as in the baseline test and it was only the frequency that changed as mass was added. Similarly, from the tests to investigate possible changes in stiffness, there was no change in the mode shapes.

In tests to investigate the effects of changed configurations, the mode shapes were more elaborate due to the configuration of the beam and some of the modes were essentially modes of the two end segments of the manipulator arm alone.

In the tests to examine the effects of shortening the manipulator arm, the mode shapes were essentially the same as in the base line test and it is only the frequencies which changed with

change of arm length.

Vibration mode shapes are shown in Appendix A, Section 5.

4.1.2.4 Sensitivity to Force Level

Response inertances were measured for varying force levels, a typical example of which is shown in figure 11 (transverse direction response). This shows a fairly constant degree of force sensitivity across the frequency spectrum. However along the axis of the arm, the sensitivity to force level changes with frequency, as does the response in the vertical direction. Response inertances changed by up to approximately a factor ~ 2, over the range of forces tested.

4.2 Sluicer

4.2.1 Static Loading

The tests, test runs and files generated are tabulated in Table 2.

The weight of the sluicer head was measured as 400 lb. This does not include the weight of the flexible hoses (4 off 1" diameter and 1 off 3" diameter, up to 50 ft long) and water, which could add considerably to the overall weight to be lifted depending on the orientation of the deployment arm.

When the supply water is on, this produces water jets from the spray nozzles which in turn produce reaction forces in the sluicer. At the nominal operating pressure for the sluicer (430 psi) and a 22.5° angle on the sprays, this reaction force was measured as 177 lbf. This reaction force acts in a direction away from the surface being worked on, so that for a horizontal surface the reaction force will tend to counteract the weight of the sluicer.

Results were as follows:

Assembly Weight: 466 pounds, water off.

Assembly Weight: 289 pounds, water on.

Flow Rate: 190 gpm

Pressure: 430 psi

All the nozzles were angled inwards by approximately 22.5°, resulting in a reduced vertical component of thrust.

Measured thrust: 177 pounds.

Theoretical thrust $T = 0.0526 \times Q \times \cos(22.5) \times \sqrt{P} = 191$ pounds.

The theoretical and measured values agree to within 8%, and are within experimental error.

During the tests on saltcake and hardpan, it was found that additional reaction forces were

produced by the sluicer and that significant thrust loads were required to prevent excessive leakage at the sides of the sluicer. Thrust loads were also required to overcome resistance from the surrounding material as the sluicer was driven into it. These thrust loads induced by the backhoe peaked at over 3000 lbf but they were still insufficient to prevent all leakage. The resistance of the saltcake to downward loads also caused damage to the soft skirt around the shroud which had to be removed after the first test.

During the "blocked shroud" tests the reaction forces increased further due to pressure build-up within the shroud. Here, the pressure reached 25 psi with a thrust load of 4280 lbf, at which point leakage occurred (having lifted the backhoe to produce a small clearance between sluicer and mat). In operation, if a plunging type mining strategy is used, it is possible that the pressure may not be relieved by only a small degree of lift on the sluicer. Hence, additional up-thrust of this nature may need to be accommodated by the deployment arm and if excessive, this could exceed the capacity of the arm. The impressions made by the sluicer jets and the rim of the shroud were clearly visible as indicative of the loading imposed on the sealing mat.

4.2.2 Dynamic Loading

For operation against saltcake, sluicing pressure was generally in the range of 400 to 430 psi, and flow was in the range of 190 to 210 gpm.

The sluicer penetrated 8" during the first test, requiring about 15 minutes to do so. During this test it was observed that the skirt inhibited the ability of the sluicer to move downwards, because of its width and resistance of the saltcake. During the third test, the sluicer penetrated 9" in 10 minutes. The holes created by the sluicing jets were clearly discernable.

During the second test, the sluicer penetrated fully, and although the test ran for 12 minutes, full penetration occurred sometime before that. This breakthrough to the bottom of the saltcake and dumpster surface was first evidenced by large amounts of free water pouring out of the dumpster from beneath the simulant. In addition, large amounts of free water also escaped at the surface during sluicing.

The sluicer was also deployed against hardpan. Material removal rates were not determined, however the sluicer was very effective in breaking up the material.

Photographs of these tests are included in Appendix B Section 5.

Vibration levels measured by the accelerometers were observed to increase generally with sluicer shroud pressure indicating the turbulent flows inside were affecting the dynamic forces. There were also some indication of 30 and 40 Hz vibration responses from the accelerometers but these were not at frequencies generated by the pumps and are believed to be transmitted from the backhoe. However, these frequencies are also seen in the shroud pressure measurements when testing against hardpan and the possibility that they are generated by the sluicer sprays cannot be ruled out (although the forcing levels are relatively small).

The shroud pressure measurements show dynamic levels to be highest during the blocked shroud tests when the levels were less than 1 psi at 1 Hz. The test results show broadband forcing up to approximately 40 Hz with maximum levels at low frequencies and levels decreasing as the frequency increases. The 1 psi pressure reading at 1 Hz equates to approximately 170 lbf.

5.0 CONCLUSIONS AND RECOMMENDATIONS

5.1 Manipulator and Sluicer Compatibility

Concern has been expressed at the dynamic characteristics of long reach arms when deploying end effectors for waste retrieval. The Magnox Electric SNAKES manipulator arm has been the subject of experimental evaluation to examine its dynamic characteristics. The manipulator arm was found to behave in a repeatable manner having fundamental natural frequencies in the vertical and transverse directions of ~ 1 Hz. There were also a large number of higher natural frequencies up to 100 Hz.

With excitation induced in three orthogonal directions, the seven lowest order modes of vibration in each plane have been evaluated and estimates made of their frequency, mode shape and damping. The responses at the lower natural frequencies are relatively highly damped. A study was undertaken to determine the sensitivity of response to variations in payload, stiffness, geometry, reach and force level. Variations were detected and these were broadly in line with expectations.

The sluicer was primarily designed for deployment with a remote vehicle and there is clearly a mis-match in the 200 lbf payload for an arm deployment system and the 400 lb weight of the sluicer which will need to be accommodated in the optimisation of the sluicer design.

The sluicer produces relatively large, broadband dynamic forces which will inevitably excite some of the natural frequencies in the manipulator arm. In view of the high damping, we do not expect the resulting vibration to be detrimental to the integrity of a long reach arm.

Clearly mining strategy is important. An arm based system would require a download force of 3000 lbf to be applied to penetrate the saltcake.

The fault condition of a blocked suction line could generate unacceptably high upthrust. Whilst this is likely to be relieved by deployment arm deflection, the consequences of oscillatory motion would need to be addressed.

5.2 Applicability of Results to Hanford Scale-up

The mode shapes for these natural frequencies appear to follow classical shapes as would be expected for a continuous beam. Hence, it should be possible to calculate natural frequencies for a long reach arm for retrieval of waste from a Hanford tank based on mass and stiffness

distributions. Indeed, in developing a long reach arm for Hanford tanks, fundamental natural frequencies have been calculated at between 1.1 Hz to 1.3 Hz. Hence the dynamic response could be expected to be similar to the shorter manipulator arm.

Although the damping at low frequencies has been shown to be high, the applicability to a scaled up system could be dependent on the detail joint design. Damping values may also be expected to change if alternative methods of arm actuation are used.

Despite the shortcomings identified in sluicer performance, its potential benefits to waste retrieval still stand.

5.3 Operational and Design Lessons Learned

The low pressure confined sluicer has been developed to improve upon the performance of other sluicing systems. The sluicer spray nozzle system has been shown to be effective in breaking up saltcake and hardpan materials. However, the prototype had only limited success in containing water.

The test programme was in two independent phases; the dynamic testing of a manipulator arm and the measurement of operational loading from a sluicer. The testing highlights a need for system design and integrated testing. The potential operational loading generated by the sluicer is strongly influenced by the mining strategy and the sluicer system will need to provide deployment arm overload protection.

The loading regimes and arm response characteristics have been found on the ARD low pressure sluicer and Magnox Electric manipulator arm. No account has been taken at this stage of hose weights and hose and umbilical handling.

5.4 Recommendations

The test programme has provided data that goes some way to allaying concerns on the issue of dynamic response of a long reach arm affecting long term endurance capabilities for waste retrieval. Since the SNAKES system is considerably shorter, we therefore recommend future stages of this project are based on an integrated development programme for the sluicer and deployment arm and that this programme should include rigorous combined testing.

To realise the potential benefits of the low pressure confined sluicer, a development programme should be undertaken.

6.0 REFERENCES

- 1 Test Report: Tests of ARD Sluicer for use on the Magnox SNAKES Manipulator. ARD Environmental, February 1997.
- 2 MODENT/MODESH/MESHGEN V4.3B Software °
Imperial College, ICATS, London
- 3 Labview is a Trade Mark of National Instruments

Acronyms

- SNAKES** Sizewell Nine Arm Knuckle End Steered. This is an acronym used for a specific hydraulically actuated manipulator arm, designed originally for Sizewell Power Station.
- ACTR** Acquire Commercial Technology for Retrieval. This is an acronym used for part of the Hanford Tank waste retrieval programme.

Natural Frequency f (Hz) and Loss Factor (η %)

LVDT f_0 (η_0)	LVDT f_1 (η_1)	Test No	accel f_1 (η_1)	accel f_2 (η_2)	accel f_3 (η_3)	accel f_4 (η_4)	accel f_5 (η_5)	accel f_6 (η_6)
		1	Fully extended horizontally rotational joints aligned for vertical operation (with a 10 Kg (22 lb) payload)					
1.5	3.3 (12)	1X	3.2 (6)	12.3 (5)	19.1 (5)	29.9(5)	35.5 (7)	53.0 (10)
1.5 (23)	3.4	1Y	3.2 (6)	7.7 (10)	18.3 (12)	28.9 (7)	35.0 (8)	46.9 (11)
0.9	4.4 (11)	1Z	4.3(3)	8.3 (13)	19.7 (10)	30.0 (12)	39.3 (3)	53.0 (12)
		2	As Test 1 but with additional 50 kg (110 lb) added mass at tool-arm (Total payload including hanger = 62 Kg (136 lb))					
1.2	3.2 (13)	2X	3.7		21.9	31.0	46.4	56.8
1.3 (29)	3.3	2Y	3.1 (3)	6.4 (10)	16.9 (10)	28.4 (8)	36.0 (9)	41.3 (18)
1.1	5.0 (3)	2Z	4.3 (3)	8.7 (13)	20.4 (6)	30.8 (9)	38.8 (6)	53.8 (13)
		2a	As Test 1 but with additional 20 kg (44 lb) added mass at tool-arm (Total payload including hanger = 32 Kg (70 lb))					
1.4	3.2 (12)	2aX	3.8		21.4	30.2		
1.4 (56)	3.2	2aY	3.1 (13)	6.9 (10)	17.2 (10)	28.7 (6)	35.0 (7)	41.8 (11)
1.1	5.0 (2)	2aZ	4.3 (3)	8.1 (13)	19.8 (9)	30.2 (9)	39.7 (3)	53.0 (11)
		3	As Test 1 but with the wrist rotated +45° and the shoulder rotated -45°					
		3X	3.8	7.9		13.0	18.8	31.1
		3Y	3.4	8.1	9.1	13.1	18.6	30.6
		3Z	4.5	7.7	9.0	13.2	19.0	30.5

Results in **Bold** are based on multi-point testing, others on a single point test.
 Complex modes are shown shaded. Where no damping is shown, this is due to un-reliable data.

Table 1a Tests 1, 2, 2a & 3 Natural Frequencies and Damping (Loss Factor η %)

Natural Frequency f (Hz) and Loss Factor (η %)

LVDT f_0 (η_0)	LVDT f_1 (η_1)	Test No	accel f_1 (η_1)	accel f_2 (η_2)	accel f_3 (η_3)	accel f_4 (η_4)	accel f_5 (η_5)	accel f_6 (η_6)
		4	As Test 1 but with the wrist rotated +90° and the shoulder rotated -90°					
1.6 (36)	3.8	4X	3.9	9.3		18.8	31.5	39.4
1.6	3.6	4Y	3.3 (21)	9.1 (11)	12.8 (18)	18.5 (17)	30.3 (4)	39.1 (7)
1.0 (22)	4.8	4Z	4.1 (12)	6.0 (30)	15.6 (25)	26.7 (20)	28.2 (16)	33.4 (20)
		5	As Test 1 but with pivot A rotated +45° and pivot B rotated -45°					
		5X	3.8	8.0		26.7	34.5	46.6
		5Y	3.5	7.8		18.4	26.1	34.5
		5Z	4.0	6.5	11.8	13.7	16.0	18.1
		6	As Test 1 but with pivot A rotated +90° and pivot B rotated -90°					
1.6 (16)	3.8	6X	3.9	8.5 (11)	13.2 (14)	18.1 (15)	22.1 (7)	32.3 (5)
1.5	3.9	6Y	3.8 (16)	8.3 (12)	15.3 (15)	18.3 (9)	20.3 (9)	31.5 (5)
		6Z	3.5 (39)	5.5 (11)	9.6 (17)	12.5 (18)	13.7 (16)	16.5 (8)
		7	As Test 1 but pivot J at 0°, pivot H at 45° and pivot G at 45°					
1.7 (37)	3.5	7X	3.6 (2)	9.2 (4)	21.1 (9)	27.5 (5)	46.5 (5)	
1.7	3.5 (11)	7Y	3.4 (1)	8.5 (10)	20.0 (9)	26.8 (7)	40.4 (6)	45.4 (6)
1.1	4.5 (9)	7Z	4.4 (9)	9.0 (20)	19.0 (12)	27.5 (9)	50.2 (6)	60.2 (3)

Results in **Bold** are based on multi-point testing, others on a single point test.
 Complex modes are shown shaded. Where no damping is shown, this is due to un-reliable data.

Table 1b Tests 4, 5, 6 & 7 Natural Frequencies and Damping (Loss Factor η %)

SUMMARY OF TEST RUNS - SLUICER ON BACKHOE				
TEST # AND DESCRIPTION	DATA RUNS	FIGURES	DESCRIPTION	LABVIEW FILES
1: STATIC THRUST	N/A	N/A	SLUICER SUSPENDED FROM LOAD CELL	N/A
2: SALTCAKE	1 2 3 4 5	LF1,2 LF3,4 LF5,6 LF7,8 LF9,10	HF1,2,3,4 HF5,6 HF7	SSLUICE1.BIN SSLUICE2.BIN SSLUICE3.BIN SSLUICE4.BIN SSLUICE5.BIN
3: BLOCKED SHROUD	7, SUCTION OFF 8, SUCTION ON 9, SUCTION BLOCKED	LF11,12 LF13,14 HF10,11,12 LF15,16	HF9	SSLUICE7.BIN SSLUICE8.BIN SSLUICE9.BIN
4: HARDPAN	10	LF17,18 HF14,15,16	SLUICER ON BACKHOE OPERATING AGAINST SIMULANT SLAB	SSLUIC10.BIN

SUMMARY OF TEST RUNS

Table 2

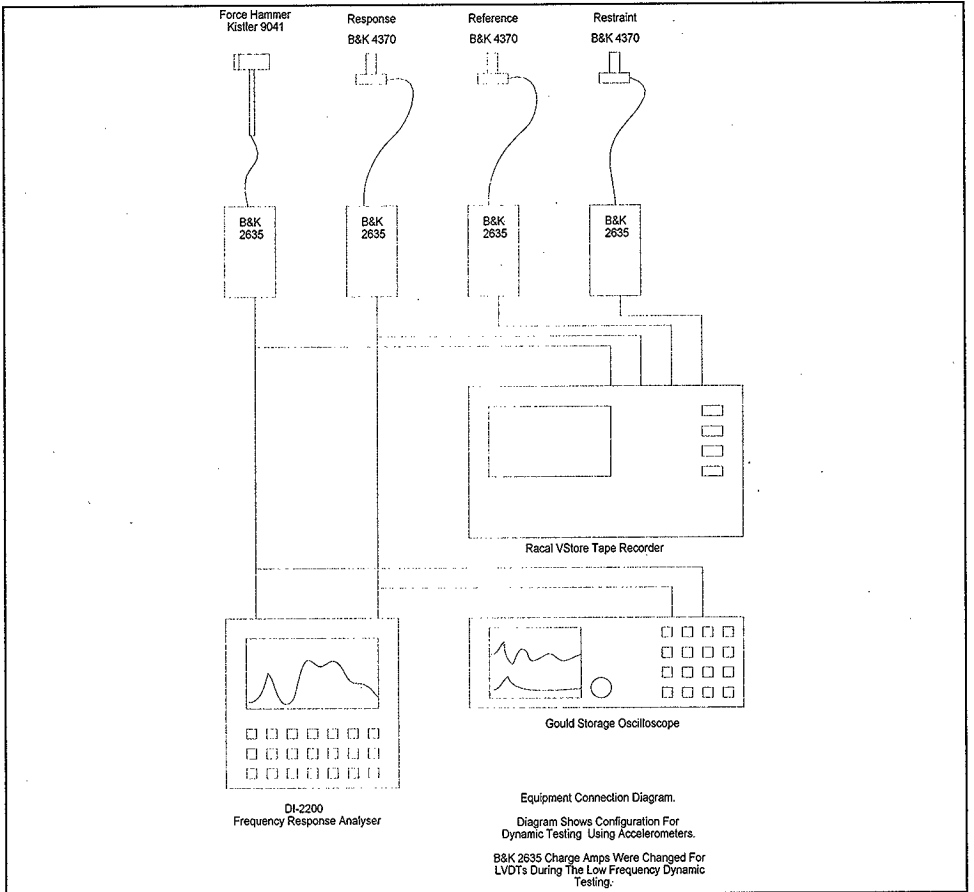


Figure 1 Equipment Connection Diagram

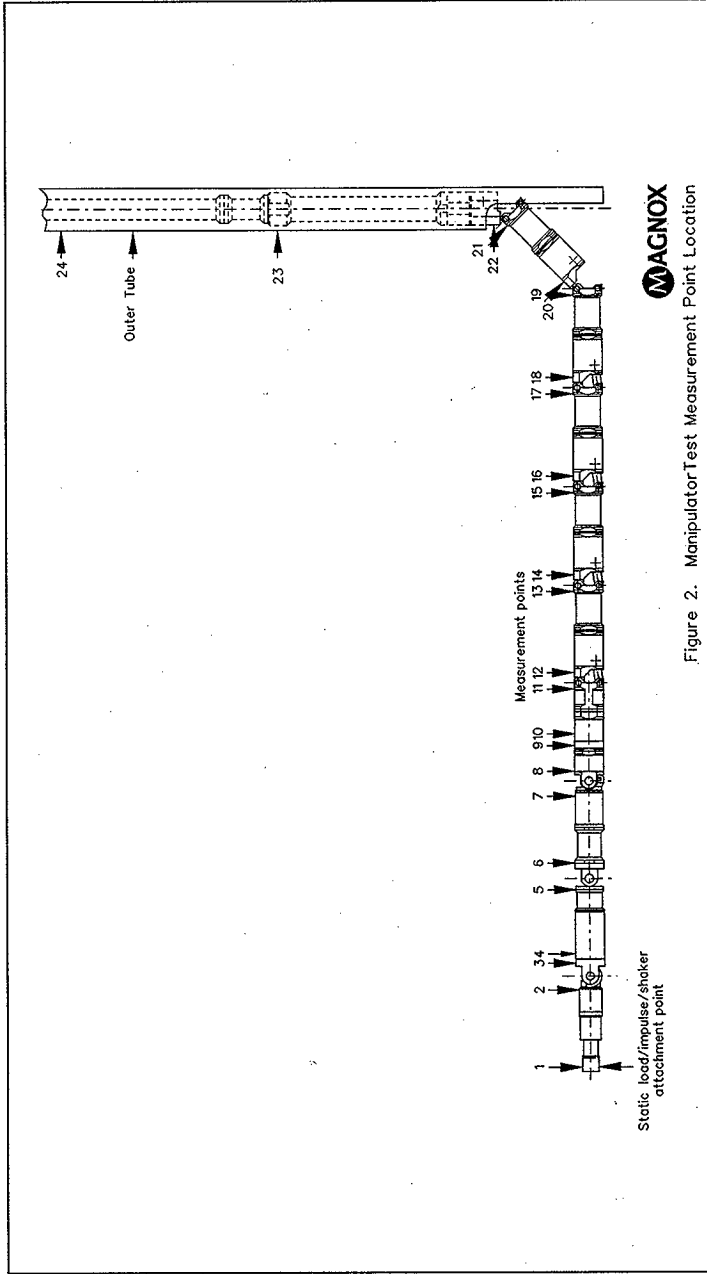


Figure 2. Manipulator Test Measurement Point Location

Figure 2 Test Measurement Locations

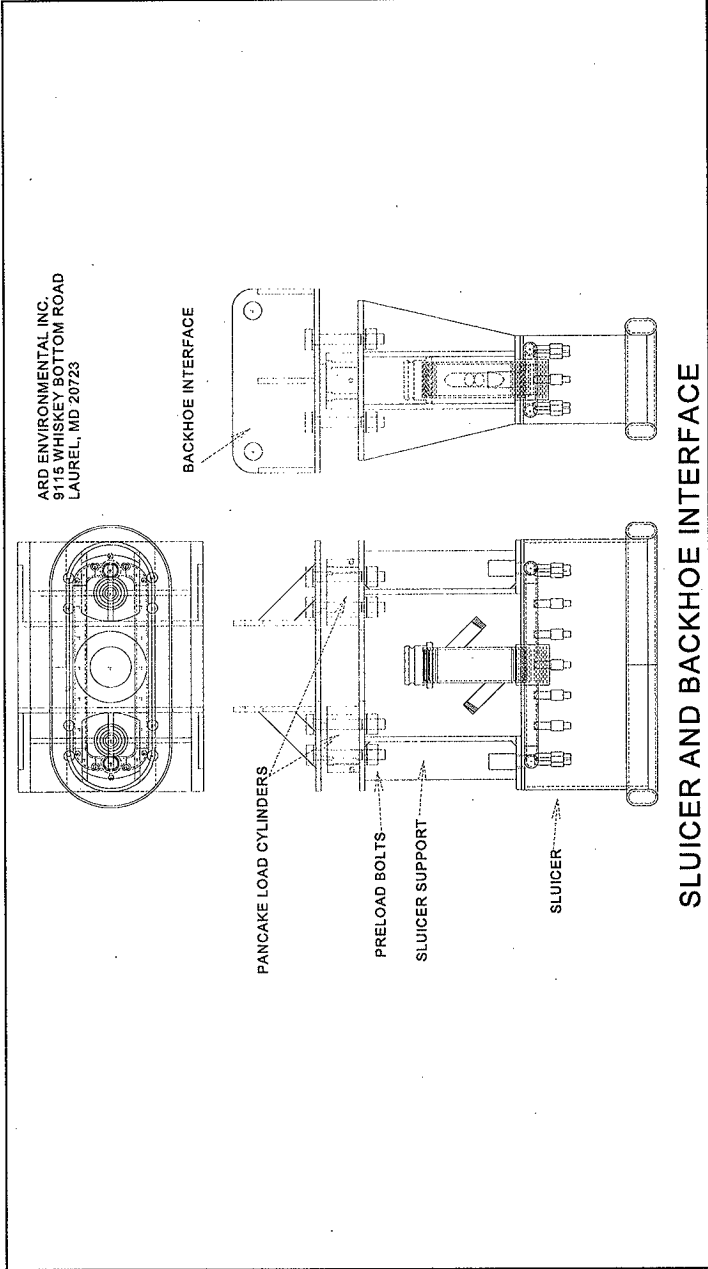


Figure 3

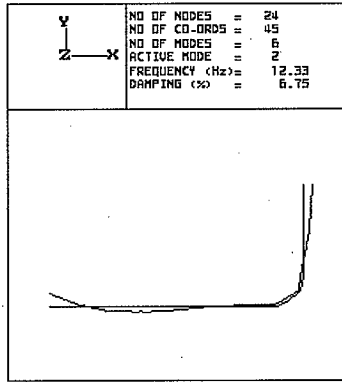
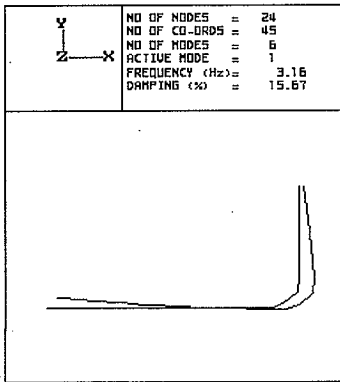


Figure 5 TEST 1X Modes 1 & 2

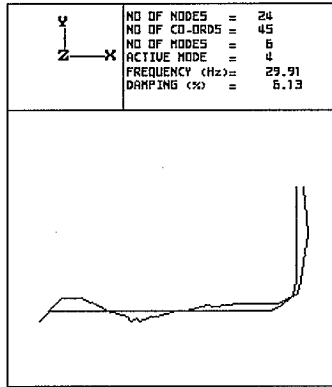
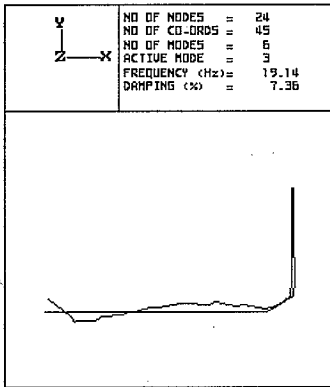


Figure 6 TEST 1X Modes 3 & 4

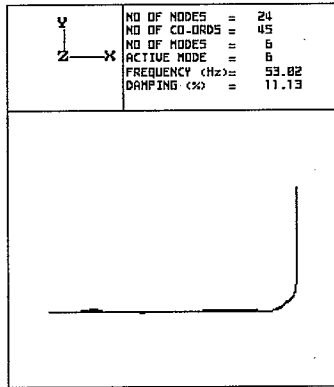
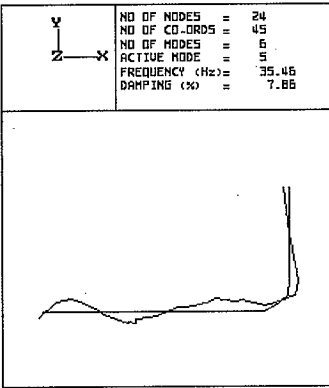


Figure 7 TEST 1X Modes 5 & 6

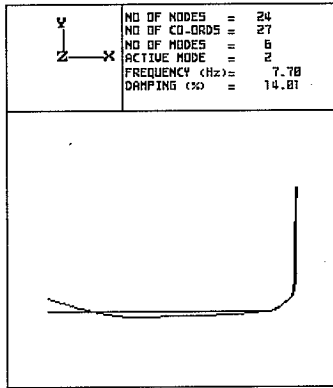
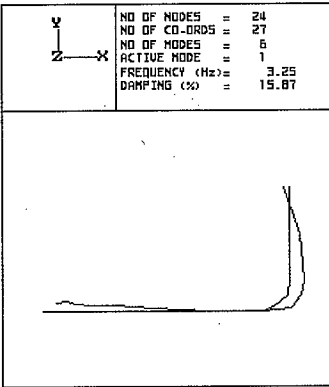


Figure 8 TEST 1Y Modes 1 & 2

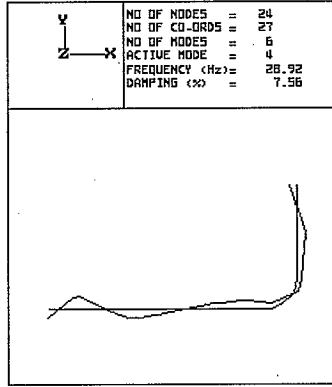
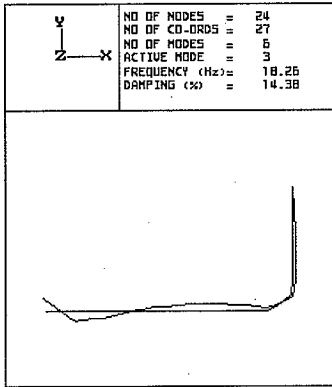


Figure 9 TEST 1Y Modes 3 & 4

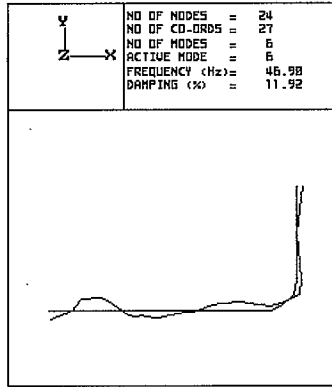
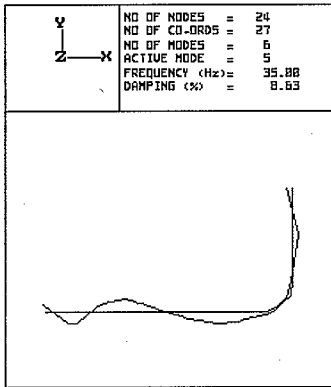


Figure 10 TEST 1Y Modes 5 & 6

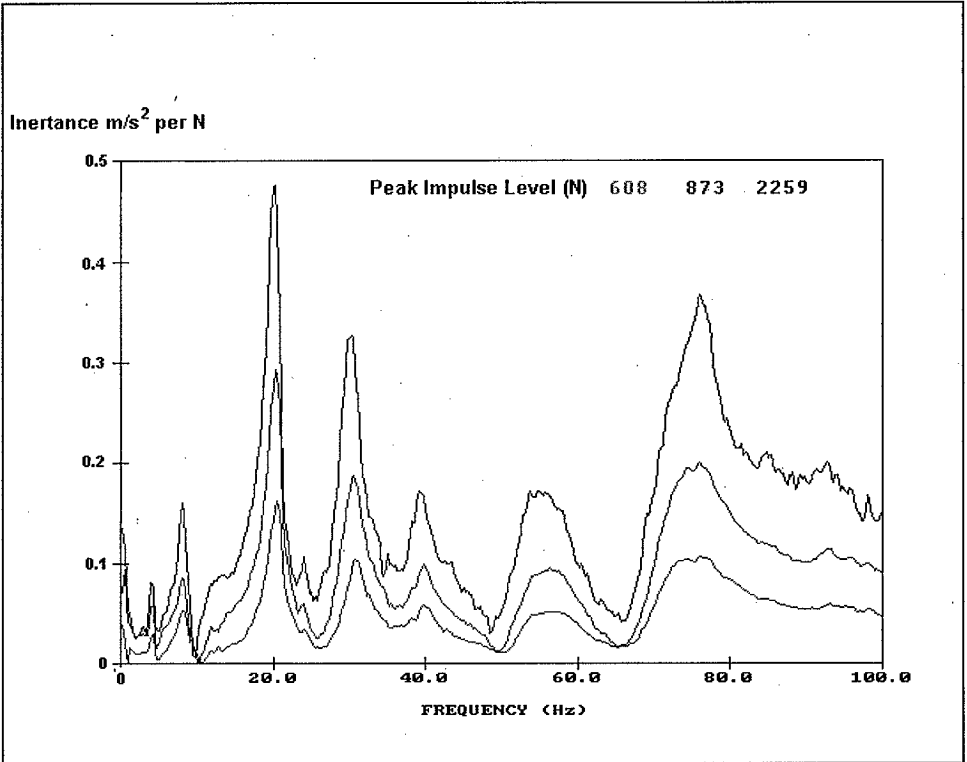
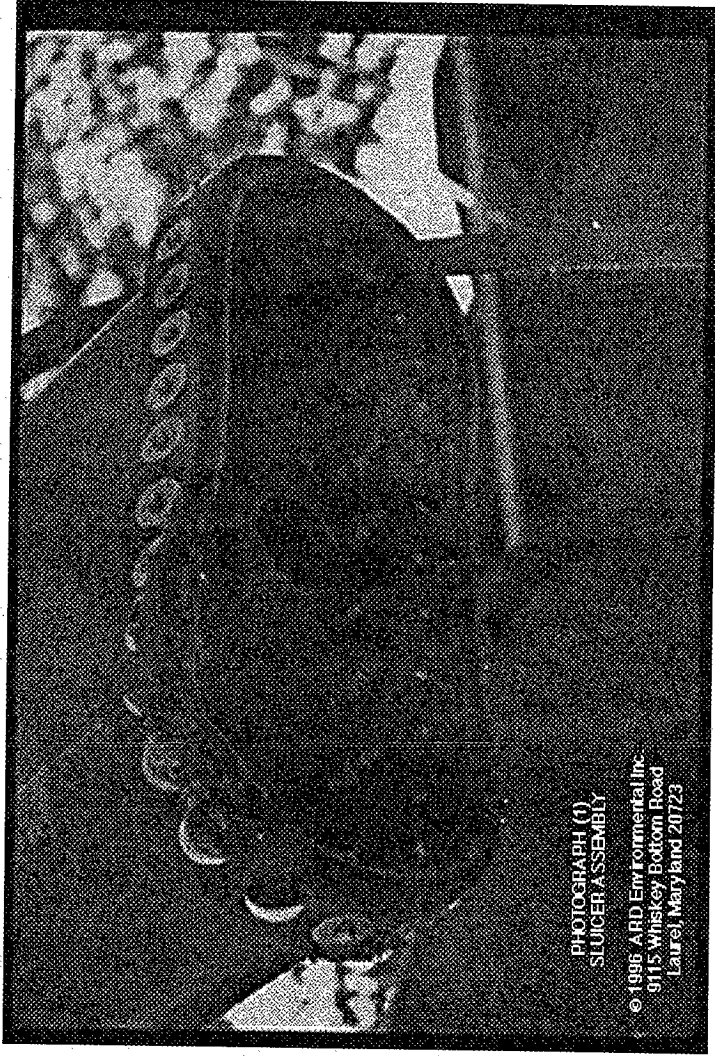


Figure 11 Sensitivity to Dynamic Loading in the Z Direction



Photograph 1

APPENDIX A
MANIPULATOR DATA

SECTION	CONTENTS	Page No.
1	Layout, Test Notations and Definitions.	A2
2	Instrumentation.	A12
3	Correction Factor for Exponential Windows.	A32
4	Summary of Natural Frequencies and Damping.	A34
5	Mode Shape Plots.	A39
6	Driving Point Compliance Plots.	A86
7	Driving Point Inertance Plots.	A103
8	Sensitivity to Loading Plots.	A119

SECTION 1

LAYOUT, TEST NOTATIONS & DEFINITIONS

Figure No.	TITLE	Page No.
A1.1	Schematic Layout of Work SNAKES Manipulator.	A3
A1.2	Test Measurement Locations.	A4
A1.3	Co-ordinate System used in Tests.	A5
A1.4	Summary of Tests.	A6
A1.5	Measurement Locations in Tests 1, 2, 2a, 3 & 4.	A7
A1.6	Measurement Locations in Test 5.	A8
A1.7	Measurement Locations in Test 6.	A9
A1.8	Measurement Locations in Test 7.	A10
	Definitions, Filename Convention & Units.	A11

MANIPULATOR JOINT DATA

VERTICAL	206 inches
AZIMUTH	+/- 270 DEG
TOOL ARM EXTEND	0 - 4 inches
TOOL ARM ROTATE	+/- 90 DEG
WRIST ROTATE	+/- 90 DEG
SHOULDER ROTATE	+/- 90 DEG
PIVOT 'A'	+/- 90 DEG
PIVOT 'B'	+/- 90 DEG
PIVOT 'C'	+ 50, -40 DEG
PIVOT 'D'	+ 50, -40 DEG
PIVOT 'E'	+ 50, -40 DEG
PIVOT 'F'	+ 50, -40 DEG
PIVOT 'G'	+ 50, -40 DEG
PIVOT 'H'	+ 50, -40 DEG
PIVOT 'J'	+ 50 DEG

MANIPULATOR LINK DATA

TOOL ARM	86 lbs	19.7 inches
WRIST ASSY	10 lbs	24 inches
ELBOW ASSY	106 lbs	24 inches
SHOULDER ASSY	150 lbs	24 inches
LINK ARM ASSY 1	100 lbs	24 inches
LINK ARM ASSY 2	100 lbs	24 inches
LINK ARM ASSY 3	100 lbs	24 inches
LINK ARM ASSY 4	100 lbs	24 inches
LINK ARM ASSY 5	100 lbs	24 inches

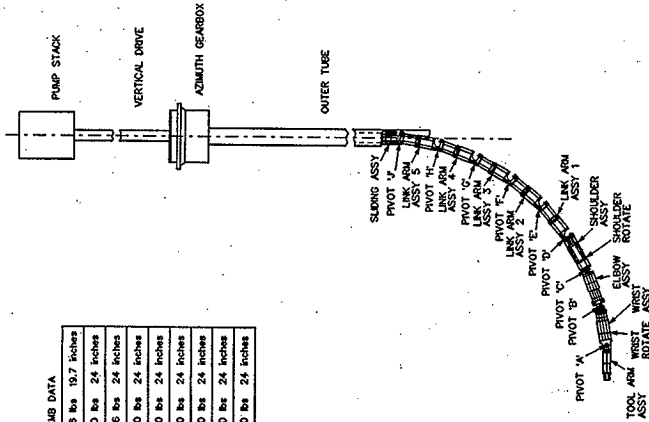


Figure 1. Schematic Layout of Work Snakes Manipulator

Fig A1.1 Schematic Layout of Work SNAKE Manipulator

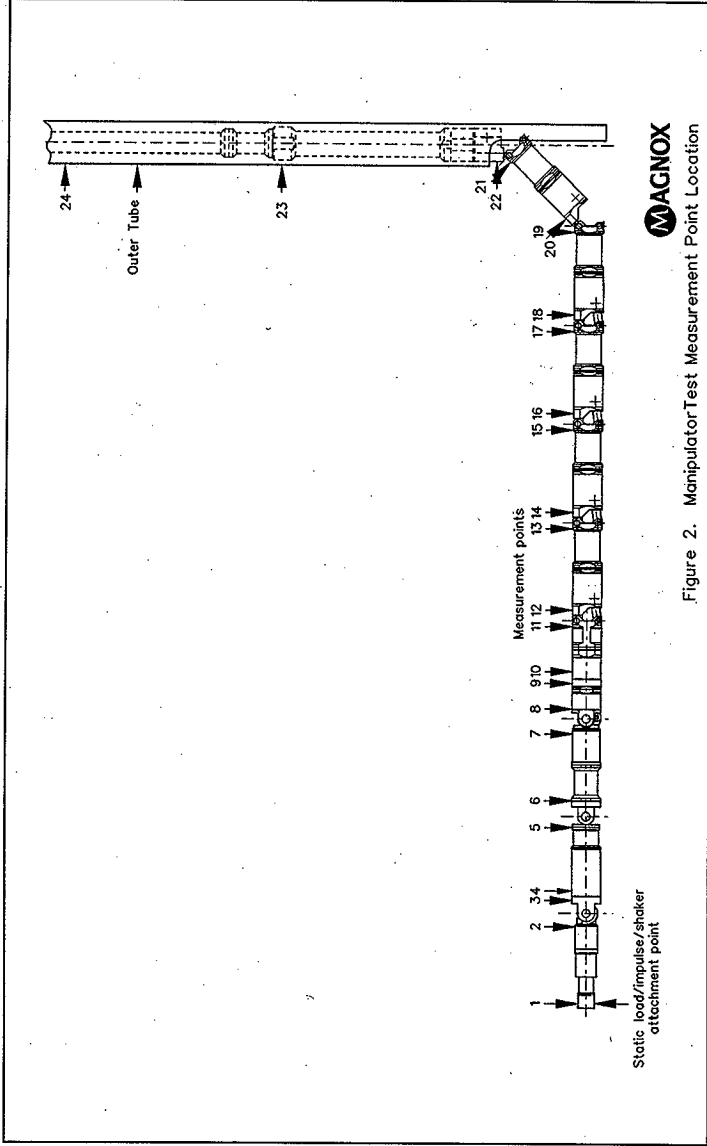
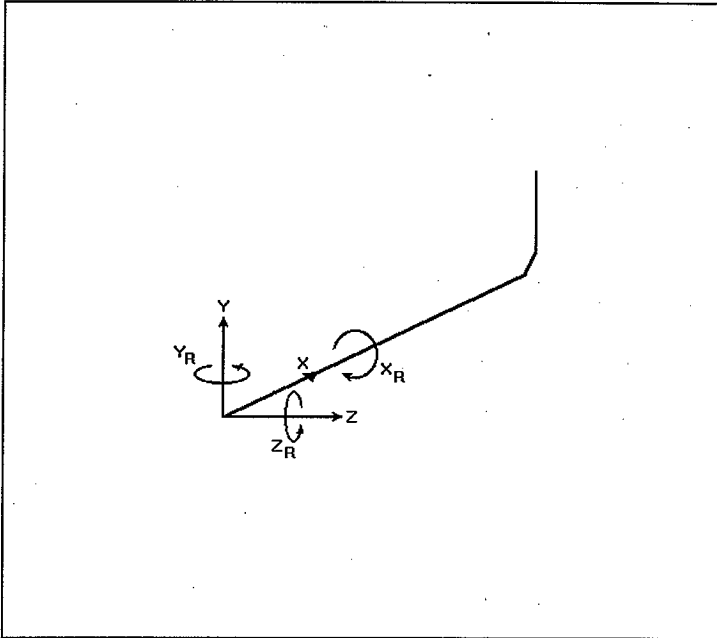


Fig A1.2 Test Measurement Locations



Direction	+X	+Y	+Z	+X _R	+Y _R	+Z _R	-X	-Y	-Z	-X _R	-Y _R	-Z _R
Direction Code	1	2	3	4	5	6	7	8	9	A	B	C

Subscript_R indicates rotation about axis

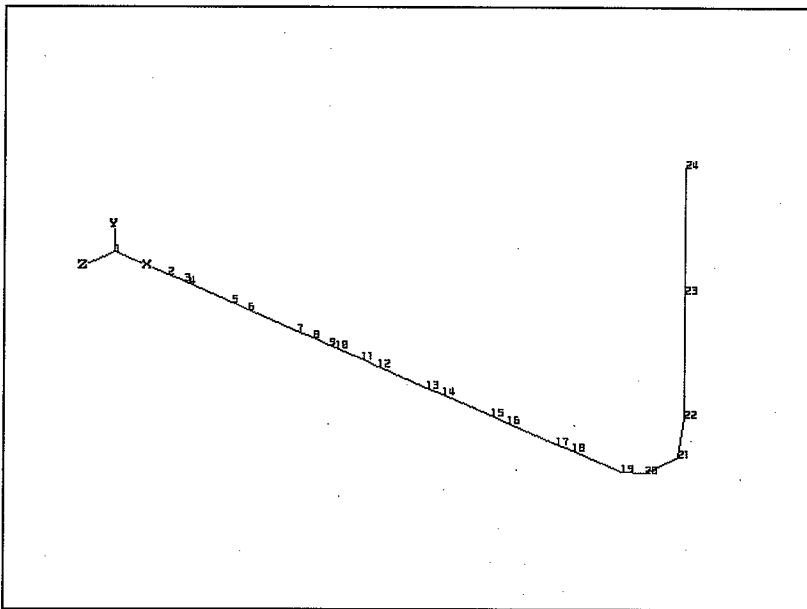
Fig A1.3 Co-ordinate System used in Tests.

	Test Number							
	1	2	2a	3	4	5	6	7
Manipulator Configuration (Section 7)	Fig2(2)	Fig2(2)	Fig2(2)	Fig2(2)	Fig2(2)	Fig2(3)	Fig2(4)	Fig2(5)
Static Load*	10 kg 22 lb	62 kg 136.4 lb	32 kg 70.4 lb	10 kg 22 lb				
Modal Test (accelerometer)	X Y Z	Y Z	Y Z		Y Z		X Y Z	X Y Z
Driving Point Compliance Test (LVDT)	X Y Z	X Y Z	X Y Z		X Y Z		X Y	X Y Z
Sensitivity to Dynamic Loading	X Y Z							
Driving Point Inertance Test (accelerometer)		X	X	X Y Z	X	X Y Z		

* The tool post test block weighed 10 kg and was always present. A hanger weighing 2 kg was used to hold the 50 kg and 20 kg test weights.

- Test 1 The manipulator arm was fully extended horizontally, with the rotational joints aligned for vertical in-plane operation with all link assemblies in-line.
- Test 2 As Test 1 but with 50 kg (110 lb) added mass at tool arm.
- Test 2a As Test 1 but with 20 kg (44 lb) added mass at tool arm.
- Test 3 As test 1 but with wrist rotated +45° and the shoulder rotated -45°.
- Test 4 As test 1 but with wrist rotated +90° and the shoulder rotated -90°.
- Test 5 As test 1 but with pivot A rotated +45° and the pivot B rotated -45°.
- Test 6 As test 1 but with pivot A rotated +90° and the pivot B rotated -90°.
- Test 7 As Test 1 but pivot J at 0°, pivot H at 45° and pivot G at 45°.

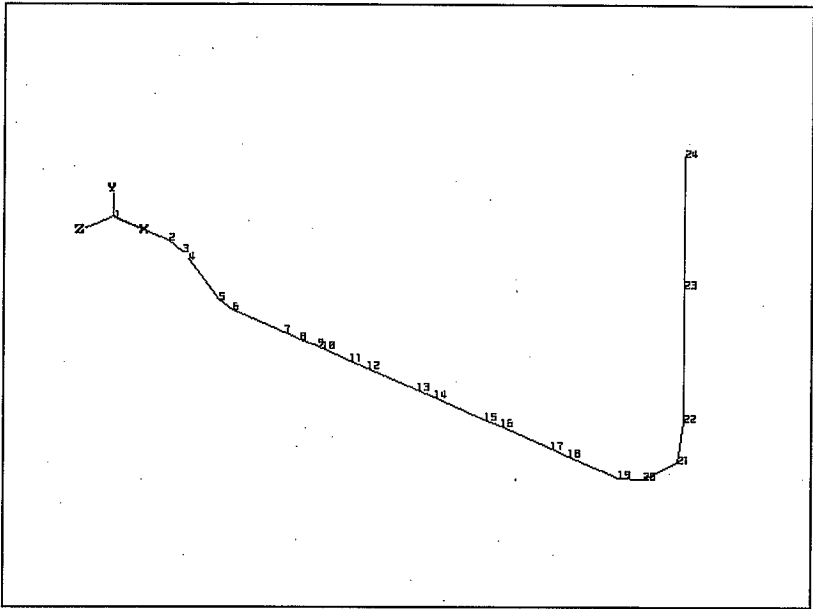
Fig A1.4 Summary of Tests



Point No	1	2	3	4	5	6	7	8	9	10	11	12
X (inches)	0	19	25	27	43	49	67	73	79	81	91	97
Y (inches)	0	0	0	0	0	0	0	0	0	0	0	0
Z (inches)	0	0	0	0	0	0	0	0	0	0	0	0

Point No	13	14	15	16	17	18	19	20	21	22	23	24
X (inches)	115	121	139	145	163	169	187	196	208	210	210	210
Y (inches)	0	0	0	0	0	0	0	4	17	35	88	141
Z (inches)	0	0	0	0	0	0	0	0	0	0	0	0

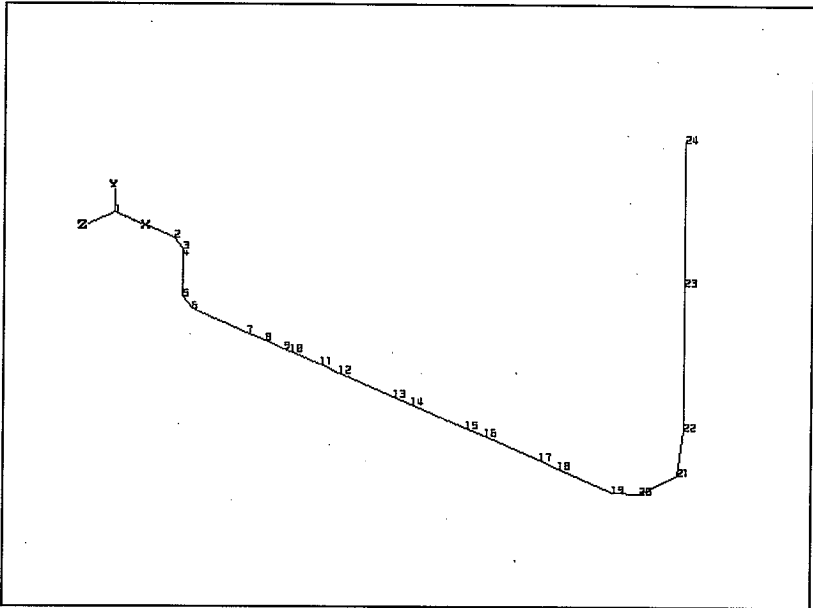
Fig A1.5 Modal Measurement Locations used in Tests 1, 2, 2a, 3 & 4



Point No	1	2	3	4	5	6	7	8	9	10	11	12
X (inches)	0	19	24	26	37	42	60	66	72	74	84	90
Y (inches)	0	0	2	4	15	17	17	17	17	17	17	17
Z (inches)	0	0	0	0	0	0	0	0	0	0	0	0

Point No	13	14	15	16	17	18	19	20	21	22	23	24
X (inches)	108	114	132	138	156	162	180	189	201	203	203	203
Y (inches)	17	17	17	17	17	17	17	21	34	52	107	161
Z (inches)	0	0	0	0	0	0	0	0	0	0	0	0

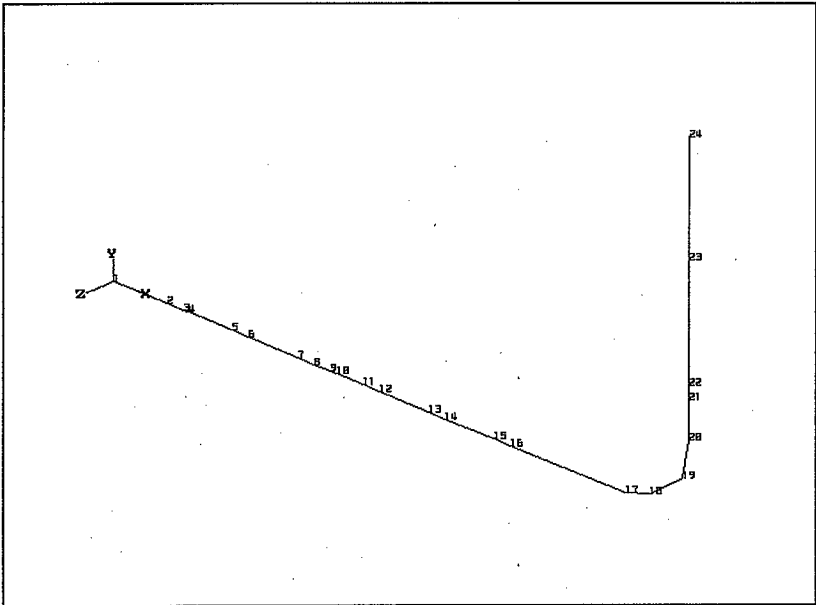
Fig A1.6 Modal Measurement Locations used in Test 5



Point No	1	2	3	4	5	6	7	8	9	10	11	12
X (inches)	0	19	22	22	22	25	43	49	55	57	67	73
Y (inches)	0	0	3	5	21	24	24	24	24	24	24	24
Z (inches)	0	0	0	0	0	0	0	0	0	0	0	0

Point No	13	14	15	16	17	18	19	20	21	22	23	24
X (inches)	91	97	115	121	139	145	163	172	184	186	186	186
Y (inches)	24	24	24	24	24	24	24	28	41	59	114	168
Z (inches)	0	0	0	0	0	0	0	0	0	0	0	0

Fig A1.7 Modal Measurement Locations used in Test 6



Point No	1	2	3	4	5	6	7	8	9	10	11	12
X (inches)	0	19	25	27	43	49	67	73	79	81	91	97
Y (inches)	0	0	0	0	0	0	0	0	0	0	0	0
Z (inches)	0	0	0	0	0	0	0	0	0	0	0	0

Point No	13	14	15	16	17	18	19	20	21	22	23	24
X (inches)	115	121	139	145	187	196	208	210	210	210	210	210
Y (inches)	0	0	0	0	0	4	17	35	54	59	114	168
Z (inches)	0	0	0	0	0	0	0	0	0	0	0	0

Fig A1.8 Modal Measurement Locations used in Test 7

DEFINITIONS

In the general case Acceleration/Force = INERTANCE.

If the acceleration is measured at the point of application of the force then this is known as the DRIVING POINT INERTANCE

In the general case Displacement/Force = COMPLIANCE .

If the displacement is measured at the point of application of the force then this is known as the DRIVING POINT COMPLIANCE

The damping figures referred to in the analysis, are not purely viscous damping but more correctly LOSS FACTORS. These account for losses originating in hysteresis of the flexing structural material, friction at the structural joints, friction with attached non-structural items (e.g. cables, hoses etc.), gears, bearings as well as viscous damping at lubricated sliding surfaces.

FILENAME CONVENTION

The frequency response functions generated during a test are either in the form of an inertance or compliance depending on the transducer used. They are designated according to the transducer type, impact position and direction, and the response position and direction.

INERTANCE

e.g. The accelerometer derived frequency response function 10018012 corresponds to:-

- 1 force direction code (+X)
- 001 measurement location for point of application of force
- 8 response direction code (-Y)
- 012 accelerometer measuring location

COMPLIANCE

e.g. The LVDT derived frequency response function X001X001 corresponds to:-

- X force direction
- 001 measurement location for point of application of force
- X force direction
- 001 LVDT measurement location

UNITS

ACCELERATION	$g = 9.81 \text{ m/s}^2$	$= 32.2 \text{ ft/s}^2$
COMPLIANCE	m/N	$= 14.23 \text{ ft/lb}_f$
DISPLACEMENT	m	$= 3.2808 \text{ ft}$
FORCE	N	$= 0.2248 \text{ lb}_f$
INERTANCE	$\text{m/s}^2/\text{N}$	$= 14.23 \text{ ft/s}^2/\text{lb}_f$

SECTION 2
INSTRUMENTATION

FIGURE No	TITLE	Page No.
	Instrumentation Details.	A14
A2.1	Equipment Connection Diagram.	A17
A2.2	BRUEL & KJAER Type 2635 Charge Amplifier, Inst. No. 06089.	A18
A2.3	BRUEL & KJAER Type 2635 Charge Amplifier, Inst. No. 07233.	A19
A2.4	BRUEL & KJAER Type 2635 Charge Amplifier, Inst. No. 07234.	A20
A2.5	BRUEL & KJAER Type 2635 Charge Amplifier, Inst. No. 07235.	A21
A2.6	BRUEL & KJAER Type 2635 Charge Amplifier, Inst. No. 06088.	A22
A2.7	BRUEL & KJAER Type 4381 Accelerometer, Serial No. 1308998.	A23
A2.8	BRUEL & KJAER Type 4370 Accelerometer, Serial No. 1068009.	A24
A2.9	BRUEL & KJAER Type 4370 Accelerometer, Serial No. 1405021.	A25
A2.10	BRUEL & KJAER Type 4370 Accelerometer, Serial No. 1068008.	A26
A2.11a	SCHLUMBERGER Type DG 5.0, LVDTs Serial Nos, 6950, 6951, 6954, 6955, 6957, 6966. Table of calibration results.	A27
A2.11b	SCHLUMBERGER Type DG 5.0, LVDTs Serial Nos, 6950, 6951, 6954, 6955, 6957, 6966. Calibration Graph.	A28

FIGURE No	TITLE	Page No.
A2.12	DIAGNOSTIC INSTRUMENTS Type DI-2200, Serial No 532. Dynamic Signal Analyser.	A29
A2.13	RACAL 14 Channel 'V-STORE' FM Tape Recorder, Serial No T562-005. Certificate of Conformity to Manufacturers Specification.	A30
A2.14	KIAG Force Gauge type 9041, Serial No 85199 Statement of Calibration.	A31

Acceleration Transducers

B&K type 4370 and 4381 delta shear piezo-electric accelerometers (Magnetically mounted)

Type	Name	Serial No
4370	Response	1068008
4370	Reference	1405021
4370	Restraint	1068009
4381	Rotational	1308998

Force Transducers

Kistler force transducer (integral part of impulse hammer)

Name	Serial No
Force	85199

Signal Conditioning

Bruel & Kjaer type 2635 charge amplifiers (settings shown below)

Name	Serial No	Output	Hi pass	Low pass
Response	07233	10 mV/m/s ²	0.2 Hz	1 kHz
Reference	07235	10 mV/m/s ²	0.2 Hz	1 kHz
Restraint	07234	10 mV/m/s ²	0.2 Hz	1 kHz
Rotational	06088	10 mV/m/s ²	0.2 Hz	1 kHz
Force	06089	0.316 mV/N	0.2 Hz	1 kHz

Displacement Transducers

Sangamo/Solartron Type DG5.0 Linear Voltage Differential Transformers (LVDT)
(used for the low frequency vibration measurements)

Name	Serial No	Output
+X	06954	597 mV/mm
+Y	06950	585 mV/mm
+Z	06957	599 mV/mm
+X _R	06951	603 mV/mm
-X _R	06966	596 mV/mm

Mercer type 259A and 250 dial test indicators with a resolution of 0.01mm.
(Used to measure the displacements caused by the static loading)

These were fixed to a substantial steel bracket mounted on a surveying tripod.

Signal Analysis

Diagnostic Instruments Model Type DI-2200 Serial No. 532

Tape Recording

16 channel Racal VStore tape recorder Serial No. 06152

(The recorder allows voice annotation and automatic recording of time, date, tape identification number and tape recorder configuration. Tape recorder log sheets were maintained for each test and are stored in the task file. Each tape is uniquely identified by a serial number and contains the following information:

Tape Number	Test Number
2200	1
2201	4
2202	2, 2a,
2203	3, 4, 5, 6
2204	7

Quality Assurance

Technology & Central Engineering Division (T & CED) operates a Quality Management System to British Standard BS5882 (ISO9001). The system uses a structured suite of procedures to ensure consistently graded standards are maintained along with traceability. The work involved in this investigation has been designated as Grade 2. The job has been allocated the 'Task number' ETABZ/38797 which used as the common reference for all data, information and other media relating to the job. A task file bearing this number contains an index of all items of relevance to the job, documents, magnetic tapes floppy discs etc. and details of where they are stored.

Calibration

Equipment used during testing has been calibrated either in house or by the original manufacturer to traceable National/International standards. Copies of calibration certificates, certificates of conformity etc. can be found at the end of this Appendix.

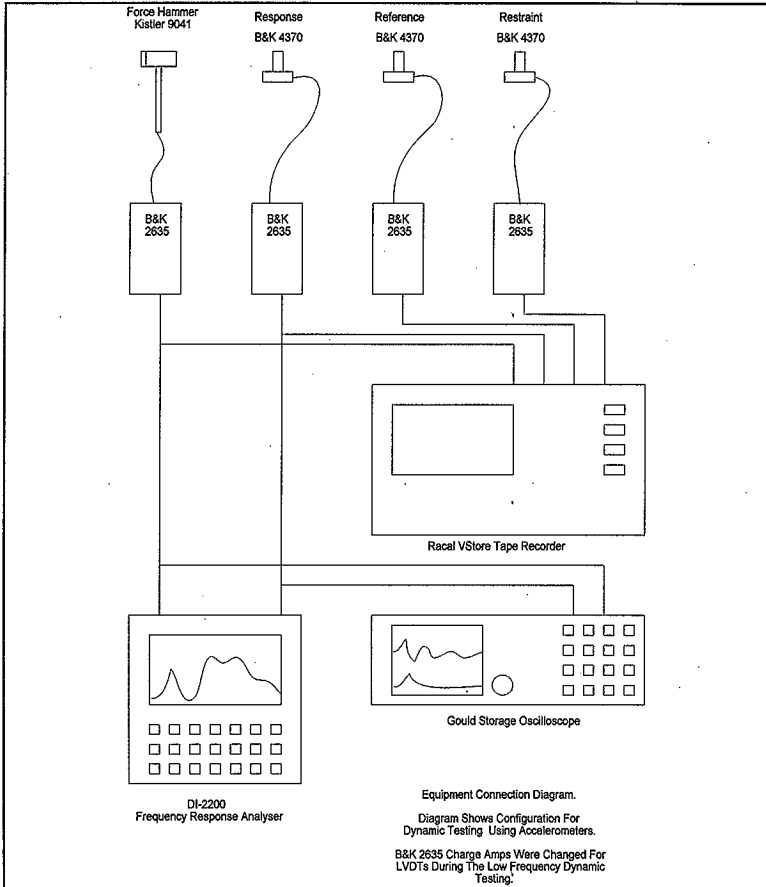


Fig A2.1 Equipment Connection Diagram

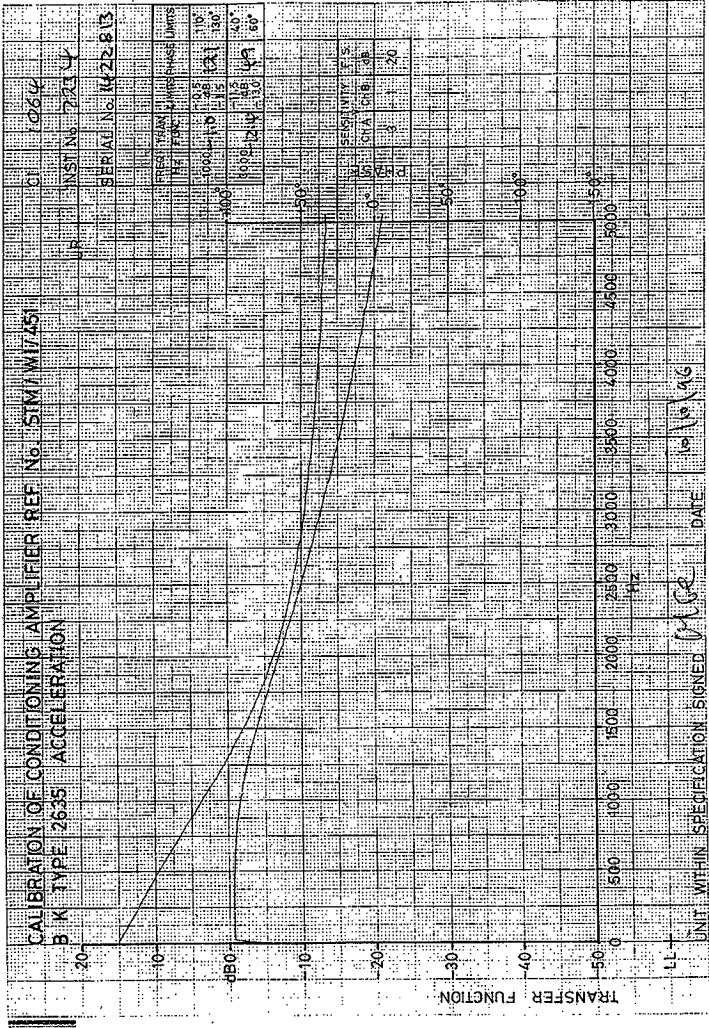


Fig A2.4

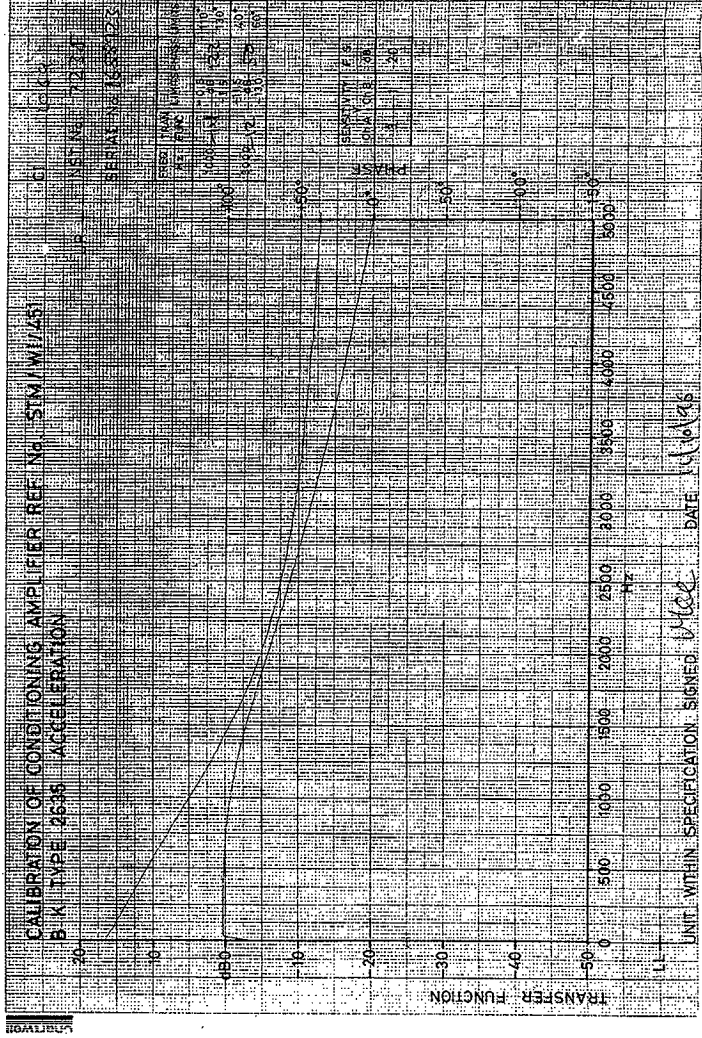


Fig A2.5

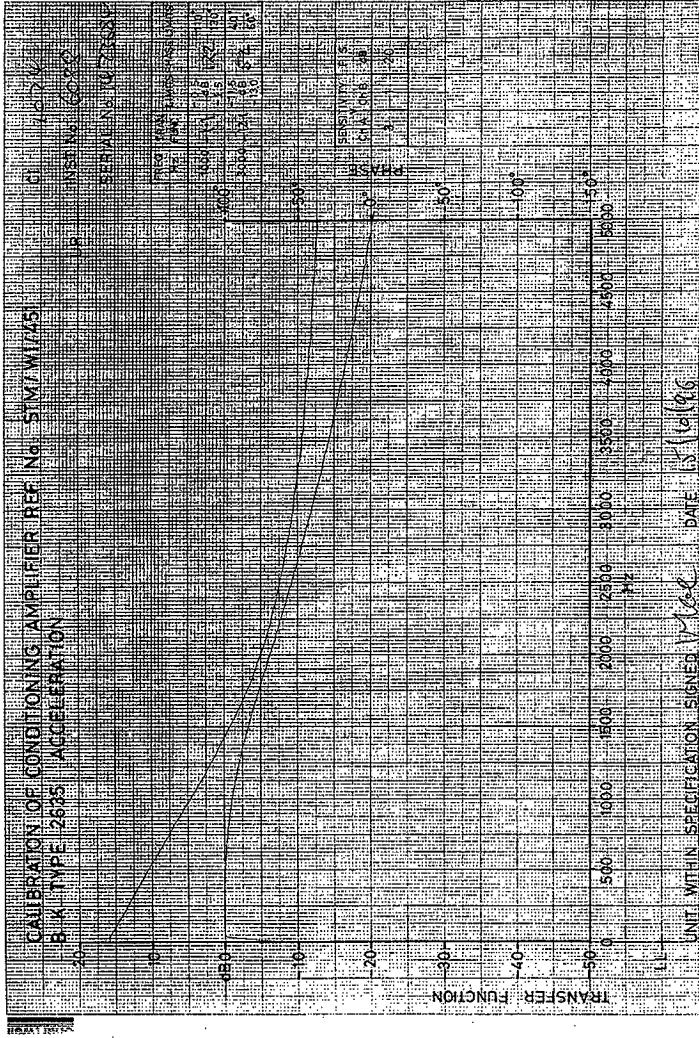


Fig A2.6

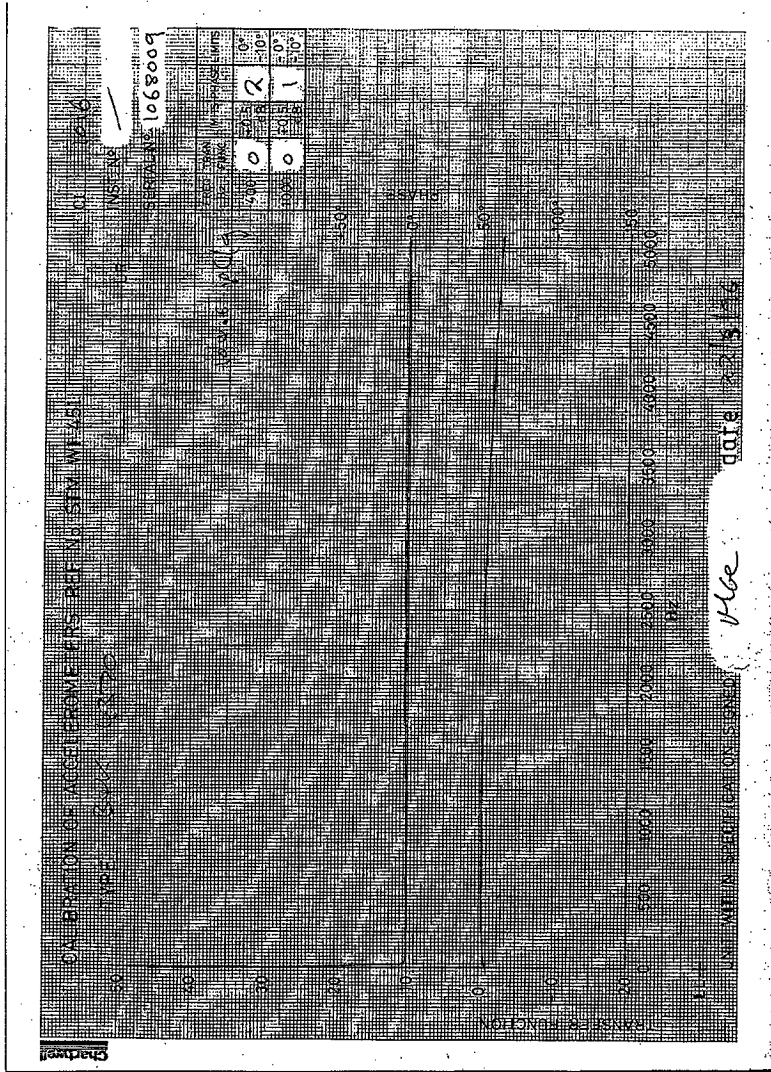


Fig A2.8

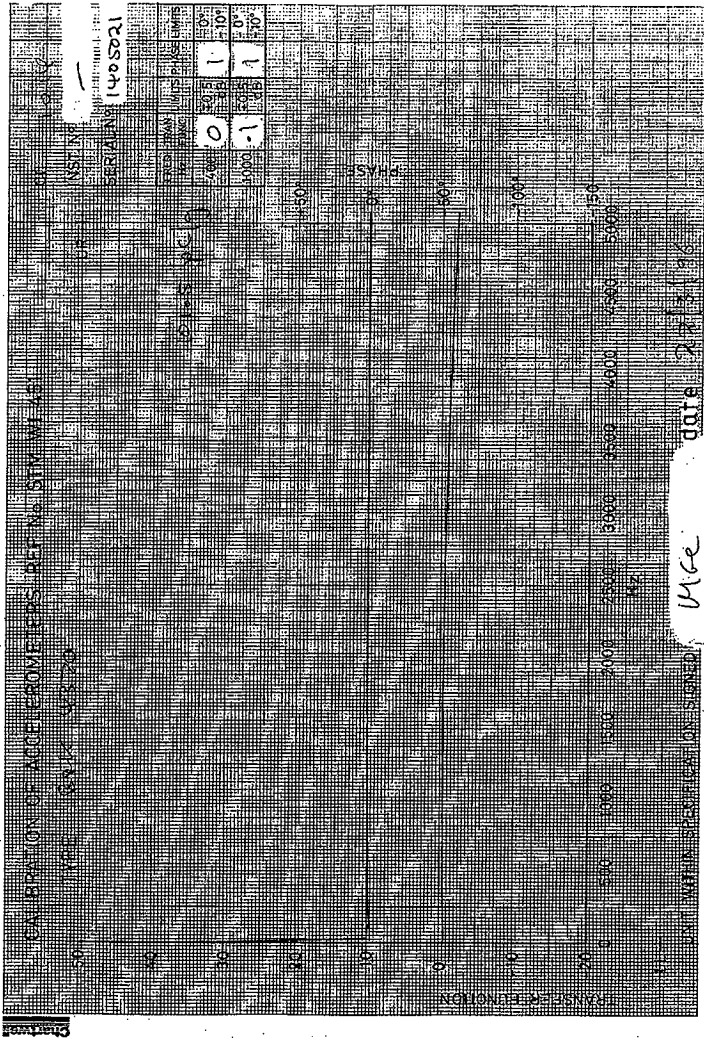


Fig A2.9

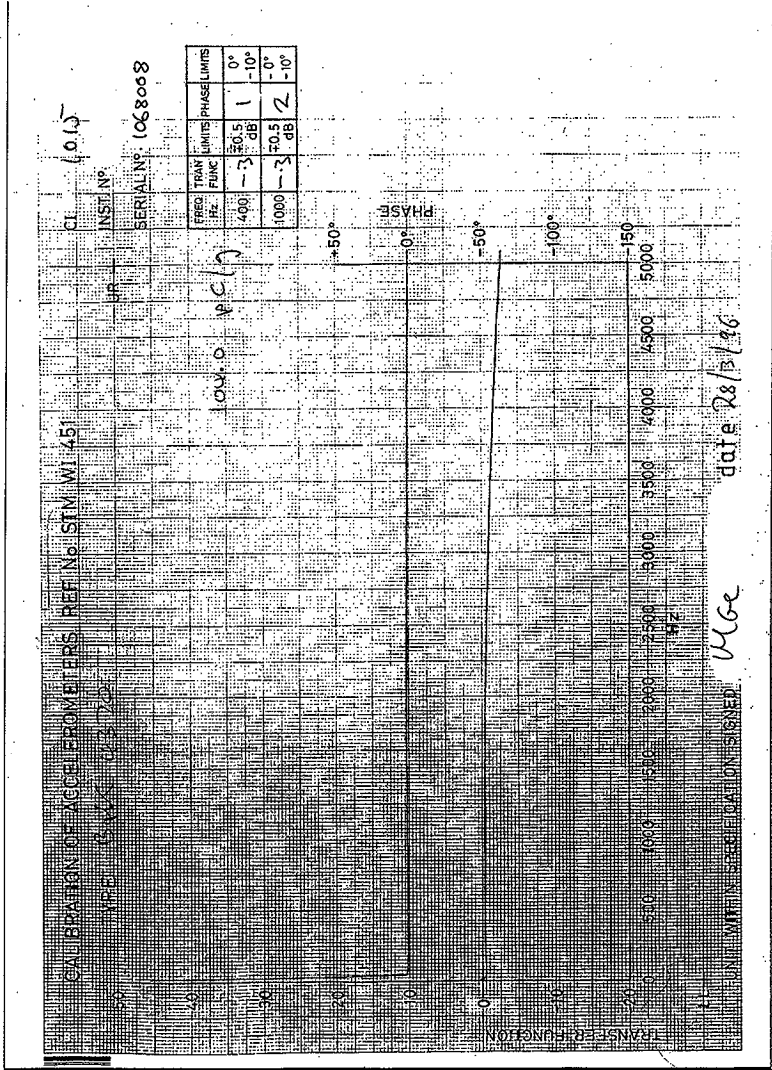


Fig A2.10

LVDT Calibration 21/0/96

Calibration of the LVDTs was performed, measuring the voltage output for a given displacement. The results are tabulated below and are displayed graphically.

Calibration Results

V _{in} = 10.05		S/N 6954 Y = 0.60X - 3.13		S/N 6955 Y = 0.60X - 3.16		S/N 6957 Y = 0.60X - 3.15		S/N 6956 Y = 0.60X - 2.63		S/N 6951 Y = 0.61X - 3.08	
Displacement	Vout	Displacement	Vout	Displacement	Vout	Displacement	Vout	Displacement	Vout	Displacement	Vout
0	-3.052	0	3.142	0	-3.144	0	3.144	0	-2.618	0	-3.062
0.25	-2.905	0.33	-2.943	0.48	-2.887	0.46	-2.873	0.39	-2.862	0.44	-2.802
0.75	-2.816	0.83	-2.641	0.98	-2.566	0.96	-2.57	0.89	-2.396	0.94	-2.508
1.25	-2.303	1.33	-2.34	1.48	-2.268	1.46	-2.269	1.39	-1.803	1.44	-2.208
1.75	-2.023	1.83	-2.041	1.98	-1.967	1.96	-1.971	1.89	-1.45	1.94	-1.909
2.25	-1.736	2.33	-1.739	2.48	-1.669	2.46	-1.673	2.39	-0.912	2.44	-1.611
2.75	-1.44	2.83	-1.447	2.98	-1.372	2.96	-1.376	2.89	-0.566	2.94	-1.31
3.25	-1.145	3.33	-1.147	3.48	-1.073	3.46	-1.076	3.39	-0.22	3.44	-1.007
3.75	-0.848	3.83	-0.847	3.98	-0.773	3.96	-0.776	3.89	0.124	3.94	-0.707
4.25	-0.548	4.33	-0.549	4.48	-0.473	4.46	-0.476	4.39	0.478	4.44	-0.402
4.75	-0.251	4.83	-0.249	4.98	-0.172	4.96	-0.176	4.89	0.831	4.94	-0.093
5.25	0.046	5.33	0.047	5.48	0.129	5.46	0.121	5.39	1.184	5.44	0.194
5.75	0.345	5.83	0.347	5.98	0.428	5.96	0.422	5.89	1.537	5.94	0.494
6.25	0.638	6.33	0.645	6.48	0.73	6.46	0.722	6.39	1.89	6.44	0.794
6.75	0.935	6.83	0.94	6.98	1.031	6.96	1.022	6.89	2.243	6.94	1.094
7.25	1.226	7.33	1.24	7.48	1.328	7.46	1.321	7.39	2.596	7.44	1.394
7.75	1.517	7.83	1.535	7.98	1.627	7.96	1.622	7.89	2.949	7.94	1.694
8.25	1.805	8.33	1.828	8.48	1.93	8.46	1.921	8.39	3.302	8.44	1.994
8.75	2.092	8.83	2.122	8.98	2.232	8.96	2.223	8.89	3.655	8.94	2.294
9.25	2.384	9.33	2.422	9.48	2.531	9.46	2.527	9.39	4.008	9.44	2.594
9.75	2.674	9.83	2.723	9.98	2.834	9.96	2.831	9.89	4.361	9.94	2.894
10.25	2.966	10.33	3.027	10.48	3.139	10.46	3.131	10.39	4.714	10.44	3.194
10.75	3.241	10.83	3.323	10.98	3.435	10.96	3.424	10.89	5.067	10.94	3.574

Displacement = Displacement of LVDT from full extension (mm)
Vout = Voltage out (Volts)

Calibration Equipment

- LVDT s/n 6950, 6951, 6954, 6955, 6957, 6996
- LVDT type Schlumberger DG 5.0
- Power Supply Weir 4130
- Voltmeter Fluke 87 Digital Multimeter
- Micrometer GKN Shardlow Metrology Ltd

V_{max}
S/N 6950 0.585
6954 0.597
6955 0.599
6957 0.599
6956 0.596
6951 0.605

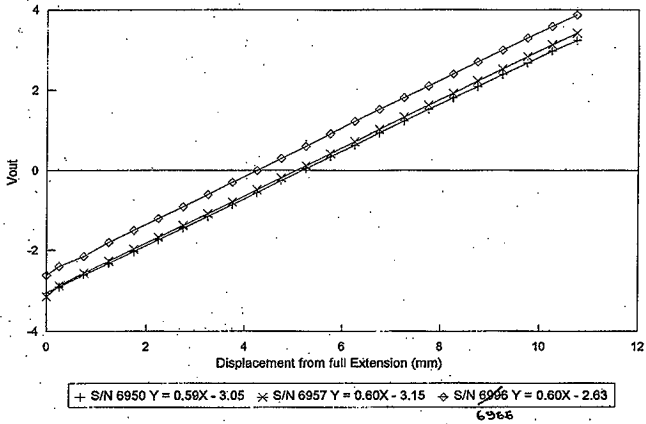
Fig A2.11a

Technology Division
Quality Assurance
Test File Index
Test: FT082 88797
Date: 17
File I



10/2/96

LVDT Calibration Results



LVDT Calibration Results

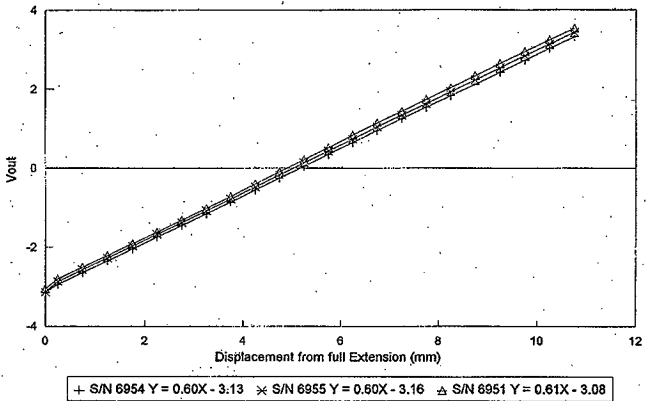


Fig A2.11b



DIAGNOSTIC INSTRUMENTS

Certificate number 9605034

CALIBRATION CERTIFICATE

Model type 01-2200

Serial Number 532

This is to certify that the above mentioned unit has been checked and re-calibrated in accordance with the manufacturer's procedure.

DC Calibration Results

RANGE	APPLIED SIGNAL	CHECK CH-1	CALIBRATED CH-1	CHECK CH-2	CALIBRATED CH-2
10V	9.004V	9.004V	9.004V	9.004V	9.003V
5V	4.502V	4.502V	4.501V	4.502V	4.501V
2V	1.801V	1.804V	1.800V	1.804V	1.800V
1V	900.4mV	900.418V	900.202V	900.418V	900.235V
500mV	450.2mV	450.453V	449.995V	450.453V	449.944V
200mV	180.1mV	180.084V	179.969V	180.084V	180.085V
100mV	90.04mV	90.237V	90.033V	90.237V	90.081V
50mV	45.02mV	45.192V	44.954V	45.192V	45.024V
20mV	18.01mV	18.215V	17.967V	18.215V	18.078V
10mV	9.00mV	9.111V	9.004V	9.111V	9.072V
5mV	4.50mV	—	—	—	—
1000Hz	1000Hz	1000Hz	1000Hz	1000Hz	1000Hz

delete where not applicable

uncertainties: (0.04% +/- 1 digit)
 (+/- 0.12Hz)

AC TEST	PASS/FAIL*	PASS/FAIL
* RELEVANT DOCUMENTATION ATTACHED.		

Calibrated By David Clarys

Date 96/05/29

Calibration Due 97/05/29

Calibration is traceable to recognised National Standards. Calibration was performed under a quality system that meets the requirements of BS5781. The uncertainties are for a confidence probability of not less than 95%.



RACAL - RECORDERS LIMITED
 Hardley Industrial Estate
 Hardley, Hythe
 Southampton SO45 3ZH
 England

Magnox
 Berkeley Centre
 Berkeley
 Glos
 GL13 9PB

CERTIFICATE OF CONFORMITY

Serial No: CSD00204

Date: 29 October, 1996

Telephone Hythe (01703) 843265

Fax: (01703) 848919

Contract No: BLO48695S00

Sub-Contract Order No:

Works Order Nos: DR79997

Item No:	Description	Qty	Serial Number
	V-Store	1	T562-005
Condition of material as despatched.			
Remarks		Inspector's Stamp	
Invoice Number S33547 refers			

Certified that the whole of the supplies detailed herein (or services described above) conform in all respects to the specifications, drawings and Contract/Order relative thereto; and that the supplies have been inspected and tested in accordance with the Conditions and requirements of the Contract.

Date: 29 October, 1996

Signed: *R. F. Wood*
 for RACAL RECORDERS LIMITED

Pink = Consignee with Goods Green = Consignee's Quality Manager

Fig A2.13



To: Task File
From: B J Brent
Conventional Equipment Group
Systems Engineering
Berkeley Centre

Ref: ETABZ 38797/16

Date: 2 October 1996

Hanford Tank Manipulator Tests

I hereby certify that Kiag Force Gauge type 9041, Serial No 85199 has been calibrated on 2 October 1996 and it has a calibration of 3.77 pC/N.

Calibration was performed with the force gauge installed in the actual 2 kg hammer to be used for the Hanford manipulator tests and testing was performed through impulses against a suspended reference mass and a reference accelerometer.

A handwritten signature in black ink, appearing to read "B J Brent".

B J Brent

SECTION 3
CORRECTION FACTOR FOR EXPONENTIAL WINDOW

Section 3 - Correction Factor for Exponential Windows

When an exponential window is used in the time domain on the Di-2200 Analyser, an exponential decay is added to the time domain record. The decay number (1 to 10) selected on the Di-2200 represents the negative exponential power to which the window decays at the end of the time record.

Damping decay is given by $e^{-\zeta\omega t}$ where ω is the natural frequency (radians), ζ is the viscous damping ratio, and t is the time. If c is the decay number set on the analyser then,

$$c = \zeta_1\omega T \text{ where } \zeta_1 \text{ is the window induced damping, and } T \text{ is the time record length.}$$

For a frequency bandwidth of b Hz, the sampling rate $s = 2.56 \times b$ samples/second, and if the time record contains n samples, then the time record length will be n/s seconds.

$$\text{Thus, } c = \zeta_1\omega n/2.56b$$

Since the loss factor $\eta = 2\zeta$ and $\omega = 2\pi f$, it follows that the window induced loss factor

$$\eta_w = 2.56cb/\pi fn \times 100 \%$$

and this value must be subtracted from the measured loss factor to produce the correct value.

For the current series of tests $c =$ See Table below
 $b = 100$ (acc) $= 50$ (lvdt)
 $n = 1024$

Tabulated values of c

	Test 1			Test 2			Test 2a			Test 3			Test 4			Test 5			Test 6			Test 7		
	X	Y	Z	X	Y	Z	X	Y	Z	X	Y	Z	X	Y	Z	X	Y	Z	X	Y	Z	X	Y	Z
acc	4	4	4	4	6	4	6	6	6	6	6	6	6	4	4	6	6	6	6	6	6	4	4	4
lvdt	2	2	2	2	2	2	2	2	2	2	2	2	2	2	2	2	2	2	2	2	2	2	2	2

EXAMPLE: Test 1Y Accelerometer Mode 2

- $f =$ frequency (Hz) = 7.70
- $\eta =$ measured loss factor (%) = 14.01
- $c = 4$ (from Table above)
- $b = 100$
- $n = 1024$
- $\therefore \eta_w = (2.56 \times 4 \times 100) / (\pi \times 7.70 \times 1024) \times 100\% = 4.13\%$

and the corrected Loss Factor would be $14.01 - 4.13 \approx 10\%$

SECTION 4
SUMMERY OF NATURAL FREQUENCIES
& DAMPING

TABLE No.	TITLE	Page No.
A4.1a	TESTS 1, 2, 2a and 3 Natural Frequencies and Damping, Un-corrected.	A35
A4.1b	TESTS 4, 5, 6 and 7 Natural Frequencies and Damping, Un-corrected.	A36
A4.2a	TESTS 1, 2, 2a and 3 Natural Frequencies and Damping, Corrected.	A37
A4.2b	TESTS 4, 5, 6 and 7 Natural Frequencies and Damping, Corrected.	A38

Natural Frequency f (Hz) and Loss Factor η (%)

LVDT f_0 (η_0)	LVDT f_1 (η_1)	Test No	accel f_1 (η_1)	accel f_2 (η_2)	accel f_3 (η_3)	accel f_4 (η_4)	accel f_5 (η_5)	accel f_6 (η_6)
		1	Fully extended horizontally rotational joints aligned for vertical operation (with a 10 kg (22 lb) payload)					
1.5	3.3 (14)	1X	3.2 (16)	12.3 (7)	19.1 (7)	29.9(6)	35.5 (8)	53.0 (11)
1.5 (28)	3.4	1Y	3.2 (16)	7.7 (14)	18.3 (14)	28.9 (8)	35.0 (9)	46.9 (12)
0.9	4.4 (13)	1Z	4.3(10)	8.3 (17)	19.7 (12)	30.0 (13)	39.3 (4)	53.0 (13)
		2	As Test 1 but with additional 50 kg (110 lb) added mass at tool-arm (Total payload including hanger = 62 kg (136 lb))					
1.2	3.2 (16)	2X	3.7		21.9	31.0	46.4	56.8
1.3 (35)	3.3	2Y	3.1 (19)	6.4 (16)	16.9 (13)	28.4 (10)	36.0 (10)	41.3 (19)
1.1	5.0 (5)	2Z	4.3 (10)	8.7 (17)	20.4 (8)	30.8 (10)	38.8 (7)	53.8 (14)
		2a	As Test 1 but with additional 20 kg (44 lb) added mass at tool-arm (Total payload including hanger = 32 kg (70 lb))					
1.4	3.2 (15)	2aX	3.8		21.4	30.2		
1.4 (62)	3.2	2aY	3.1 (29)	6.9 (17)	17.2 (13)	28.7 (8)	35.0 (8)	41.8 (12)
1.1	5.0 (4)	2aZ	4.3 (15)	8.1 (19)	19.8 (11)	30.2 (11)	39.7 (4)	53.0 (12)
		3	As Test 1 but with the wrist rotated +45° and the shoulder rotated -45°					
		3X	3.8	7.9		13.0	18.8	31.1
		3Y	3.4	8.1	9.1	13.1	18.6	30.6
		3Z	4.5	7.7	9.0	13.2	19.0	30.5

Results in **Bold** are based on multi-point testing, others on a single point test.
 Complex modes are shown shaded. Where no damping is shown, this is due to un-reliable data.

Fig A4.1a Tests 1, 2, 2a & 3 Natural Frequencies and Damping (Un-corrected)

Natural Frequency f (Hz) and Loss Factor η (%)

LVDT f_0 (η_0)	LVDT f_1 (η_1)	Test No	accel f_1 (η_1)	accel f_2 (η_2)	accel f_3 (η_3)	accel f_4 (η_4)	accel f_5 (η_5)	accel f_6 (η_6)
		4	As Test 1 but with the wrist rotated +90° and the shoulder rotated -90°					
1.6 (41)	3.8	4X	3.9	9.3		18.8	31.5	39.4
1.6	3.6	4Y	3.3 (32)	9.1 (14)	12.8 (20)	18.5 (19)	30.3 (5)	39.1 (8)
1.0 (30)	4.8	4Z	4.1 (20)	6.0 (35)	15.6 (27)	26.7 (21)	28.2 (17)	33.4 (21)
		5	As Test 1 but with pivot A rotated +45° and pivot B rotated -45°					
		5X	3.8	8.0		26.7	34.5	46.6
		5Y	3.5	7.8		18.4	26.1	34.5
		5Z	4.0	6.5	11.8	13.7	16.0	18.1
		6	As Test 1 but with pivot A rotated +90° and pivot B rotated -90°					
1.6 (21)	3.8	6X	3.9	8.5 (17)	13.2 (18)	18.1 (18)	22.1 (9)	32.3 (6)
1.5	3.9	6Y	3.8 (28)	8.3 (18)	15.3 (36)	18.3 (11)	20.3 (11)	31.5 (7)
		6Z	3.5	5.5 (19)	9.6 (22)	12.5 (22)	13.7 (19)	16.5 (11)
		7	As Test 1 but pivot J at 0°, pivot H at 45° and pivot G at 45°					
1.6 (42)	3.5	7X	3.6 (11)	9.2 (7)	21.1 (11)	27.5 (6)	46.5 (6)	
1.7	3.5 (13)	7Y	3.4 (13)	8.5 (14)	20.0 (12)	26.8 (8)	40.4 (16)	45.4 (8)
1.1	4.5 (11)	7Z	4.4 (16)	9.0 (24)	19.0 (14)	27.5 (10)	50.2 (7)	60.2 (4)

Results in **Bold** are based on multi-point testing, others on a single point test.
 Complex modes are shown shaded. Where no damping is shown, this is due to un-reliable data.

Fig A4.1b Tests 4, 5, 6 and 7 Natural Frequencies and Damping (Un-corrected)

Natural Frequency f (Hz) and Loss Factor η (%)

LVDT f_0 (η_0)	LVDT f_1 (η_1)	Test No	accel f_1 (η_1)	accel f_2 (η_2)	accel f_3 (η_3)	accel f_4 (η_4)	accel f_5 (η_5)	accel f_6 (η_6)
		1	Fully extended horizontally rotational joints aligned for vertical operation					
1.5	3.3 (12)	1X	3.2 (6)	12.3 (5)	19.1 (5)	29.9(5)	35.5 (7)	53.0 (10)
1.5 (23)	3.4	1Y	3.2 (6)	7.7 (10)	18.3 (12)	28.9 (7)	35.0 (8)	46.9 (11)
0.9	4.4 (11)	1Z	4.3(3)	8.3 (13)	19.7 (10)	30.0 (12)	39.3 (3)	53.0 (12)
		2	As Test 1 but with additional 50 kg (110lb) added mass at tool-arm (Total payload including hanger = 60 kg (136 lb))					
1.2	3.2 (13)	2X	3.7		21.9	31.0	46.4	56.8
1.3 (29)	3.3	2Y	3.1 (3)	6.4 (10)	16.9 (10)	28.4 (8)	36.0 (9)	41.3 (18)
1.1	5.0 (3)	2Z	4.3 (3)	8.7 (13)	20.4 (6)	30.8 (9)	38.8 (6)	53.8 (13)
		2a	As Test 1 but with additional 20 kg (44lb) added mass at tool-arm (Total payload including hanger = 32 kg (70 lb))					
1.4	3.2 (12)	2aX	3.8		21.4	30.2		
1.4 (56)	3.2	2aY	3.1 (13)	6.9 (10)	17.2 (10)	28.7 (6)	35.0 (7)	41.8 (11)
1.1	5.0 (2)	2aZ	4.3 (3)	8.1 (13)	19.8 (9)	30.2 (9)	39.7 (3)	53.0 (11)
		3	As Test 1 but with the wrist rotated +45° and the shoulder rotated -45°					
		3X	3.8	7.9		13.0	18.8	31.1
		3Y	3.4	8.1	9.1	13.1	18.6	30.6
		3Z	4.5	7.7	9.0	13.2	19.0	30.5

Results in **Bold** are based on multi-point testing, others on a single point test.
 Complex modes are shown shaded. Where no damping is shown, this is due to un-reliable data.

Fig A4.2a Tests 1, 2, 2a & 3 Natural Frequencies and Damping (Corrected)

Natural Frequency f (Hz) and Loss Factor η (%)

LVDT f_0 (η_0)	LVDT f_1 (η_1)	Test No	accel f_1 (η_1)	accel f_2 (η_2)	accel f_3 (η_3)	accel f_4 (η_4)	accel f_5 (η_5)	accel f_6 (η_6)
		4	As Test 1 but with the wrist rotated +90° and the shoulder rotated -90°					
1.6 (36)	3.8	4X	3.9	9.3		18.8	31.5	39.4
1.6	3.6	4Y	3.3 (21)	9.1 (11)	12.8 (18)	18.5 (17)	30.3 (4)	39.1 (7)
1.0 (22)	4.8	4Z	4.1 (12)	6.0 (30)	15.6 (25)	26.7 (20)	28.2 (16)	33.4 (20)
		5	As Test 1 but with pivot A rotated +45° and pivot B rotated -45°					
		5X	3.8	8.0		26.7	34.5	46.6
		5Y	3.5	7.8		18.4	26.1	34.5
		5Z	4.0	6.5	11.8	13.7	16.0	18.1
		6	As Test 1 but with pivot A rotated +90° and pivot B rotated -90°					
1.6 (16)	3.8	6X	3.9	8.5 (11)	13.2 (14)	18.1 (15)	22.1 (7)	32.3 (5)
1.5	3.9	6Y	3.8 (16)	8.3 (12)	15.3 (15)	18.3 (9)	20.3 (9)	31.5 (5)
		6Z	3.5 (39)	5.5 (11)	9.6 (17)	12.5 (18)	13.7 (16)	16.5 (8)
		7	As Test 1 but pivot J at 0°, pivot H at 45° and pivot G at 45°					
1.7 (37)	3.5	7X	3.6 (2)	9.2 (4)	21.1 (9)	27.5 (5)	46.5 (5)	
1.7	3.5 (11)	7Y	3.4 (1)	8.5 (10)	20.0 (9)	26.8 (7)	40.4 (6)	45.4 (6)
1.1	4.5 (9)	7Z	4.4 (9)	9.0 (20)	19.0 (12)	27.5 (9)	50.2 (6)	60.2 (3)

Results in **Bold** are based on multi-point testing, others on a single point test.
 Complex modes are shown shaded. Where no damping is shown, this is due to un-reliable data.

Fig A4.2b Tests 4, 5, 6 & 7 Natural Frequencies and Damping (Corrected)

SECTION 5
MODE SHAPES

FIGURE No	TITLE	Page No.
A5.1	Test 1X, Modes 1 & 2.	A41
A5.2	Test 1X, Modes 3 & 4.	A42
A5.3	Test 1X, Modes 5 & 6.	A43
A5.4	Test 1Y, Modes 1 & 2.	A44
A5.5	Test 1Y, Modes 3 & 4.	A45
A5.6	Test 1Y, Modes 5 & 6.	A46
A5.7	Test 1Z, Modes 1 & 2.	A47
A5.8	Test 1Z, Modes 3 & 4.	A48
A5.9	Test 1Z, Modes 5 & 6.	A49
A5.10	Test 2Y, Modes 1 & 2.	A50
A5.11	Test 2Y, Modes 3 & 4.	A51
A5.12	Test 2Y, Modes 5 & 6.	A52
A5.13	Test 2Z, Modes 1 & 2.	A53
A5.14	Test 2Z, Modes 3 & 4.	A54
A5.15	Test 2Z, Modes 5 & 6.	A55
A5.16	Test 2aY, Modes 1 & 2.	A56
A5.17	Test 2aY, Modes 3 & 4.	A57
A5.18	Test 2aY, Modes 5 & 6.	A58
A5.19	Test 2aZ, Modes 1 & 2.	A59
A5.20	Test 2aZ, Modes 3 & 4.	A60
A5.21	Test 2aZ, Modes 5 & 6.	A61
A5.22	Test 4Y, Modes 1 & 2.	A62

FIGURE No	TITLE	Page No.
A5.23	Test 4Y, Modes 3 & 4.	A63
A5.24	Test 4Y, Modes 5 & 6.	A64
A5.25	Test 4Z, Modes 1 & 2.	A65
A5.26	Test 4Z, Modes 3 & 4.	A66
A5.27	Test 4Z, Modes 5 & 6.	A67
A5.28	Test 6X, Modes 1 & 2.	A68
A5.29	Test 6X, Modes 3 & 4.	A69
A5.30	Test 6X, Modes 5 & 6.	A70
A5.31	Test 6Y, Modes 1 & 2.	A71
A5.32	Test 6Y, Modes 3 & 4.	A72
A5.33	Test 6Y, Modes 5 & 6.	A73
A5.34	Test 6Z, Modes 1 & 2.	A74
A5.35	Test 6Z, Modes 3 & 4.	A75
A5.36	Test 6Z, Modes 5 & 6.	A76
A5.37	Test 7X, Modes 1 & 2.	A77
A5.38	Test 7X, Modes 3 & 4.	A78
A5.39	Test 7X, Modes 5 & 6.	A79
A5.40	Test 7Y, Modes 1 & 2.	A80
A5.41	Test 7Y, Modes 3 & 4.	A81
A5.42	Test 7Y, Modes 5 & 6.	A82
A5.43	Test 7Z, Modes 1 & 2.	A83
A5.44	Test 7Z, Modes 3 & 4.	A84
A5.45	Test 7Z, Modes 5 & 6.	A85

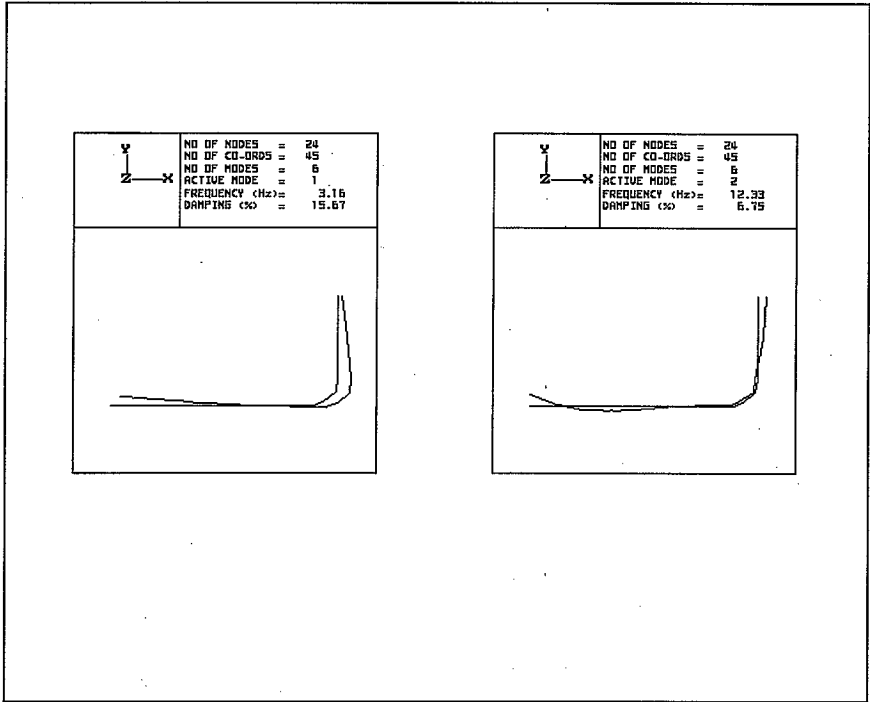


Fig A5.1 TEST 1X Modes 1& 2

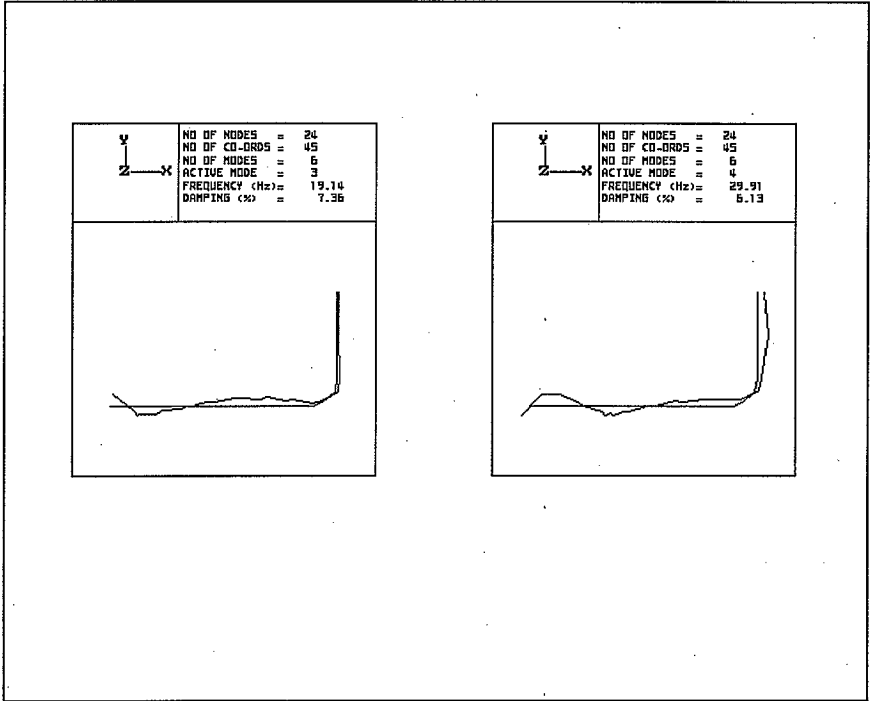


Fig A5.2 TEST 1X Modes 3 & 4

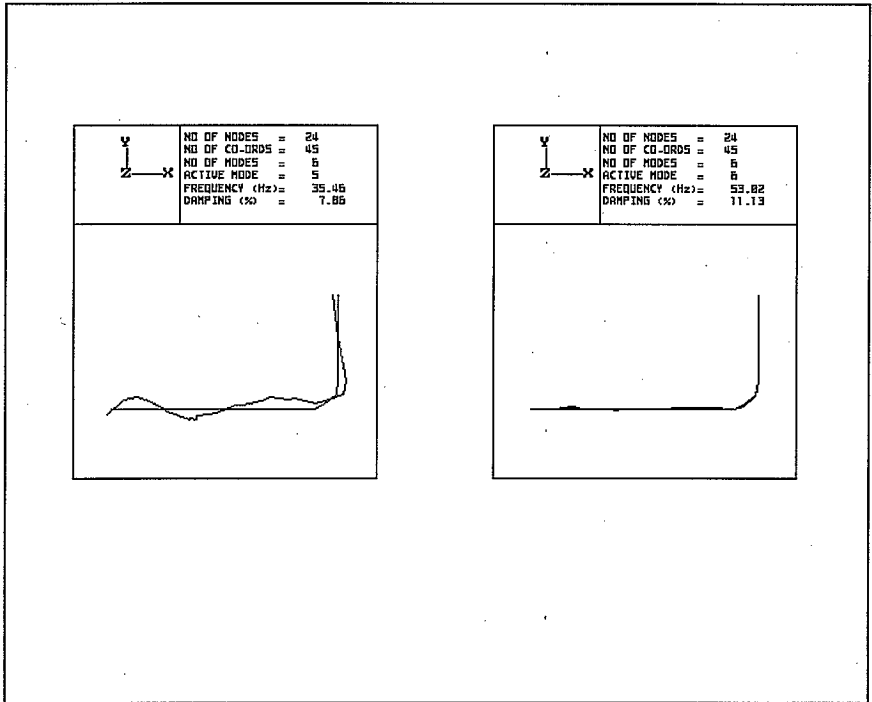


Fig A5.3 TEST 1X Modes 5 & 6

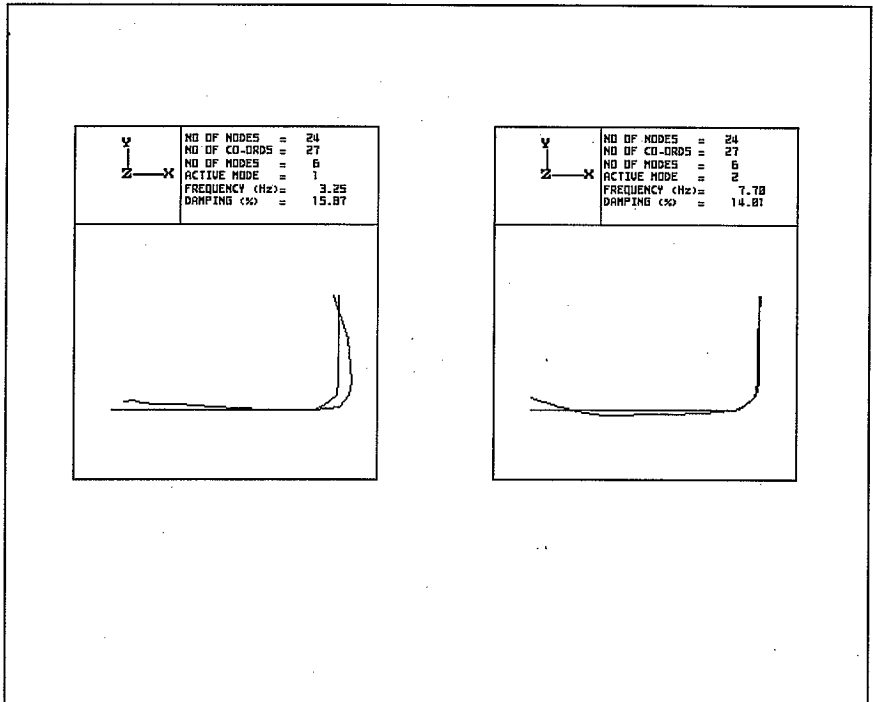


Fig A5.4 TEST 1Y Modes 1 & 2

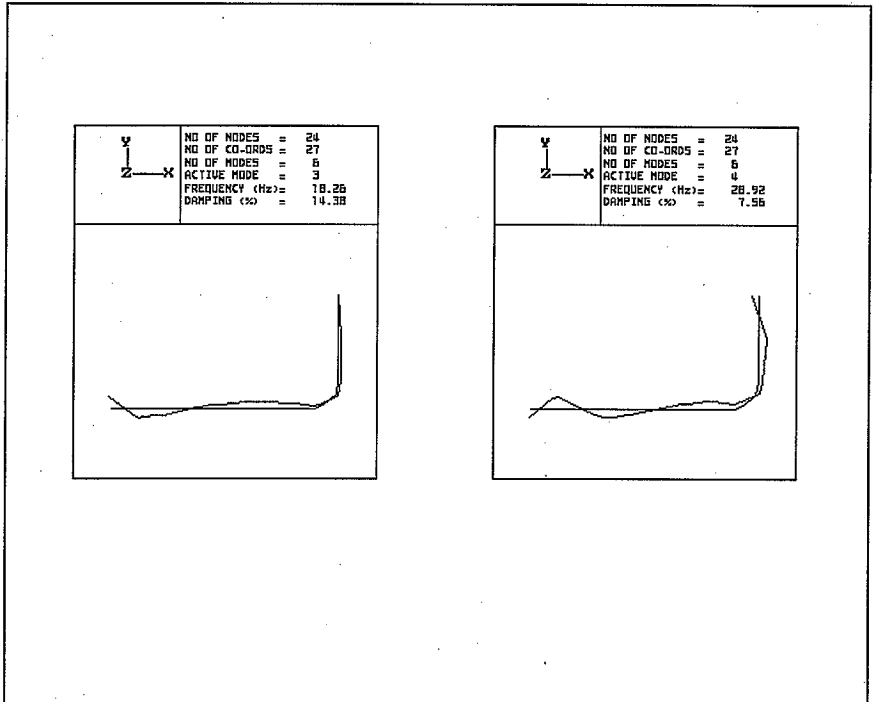


Fig A5.5 TEST 1Y Modes 3 & 4

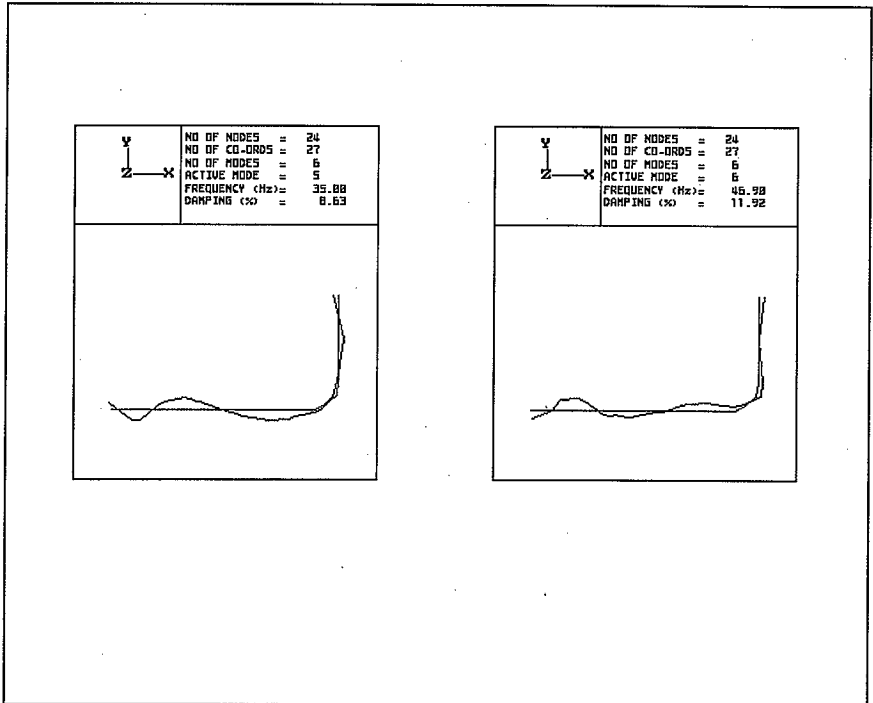


Fig A5.6 TEST 1Y Modes 5 & 6

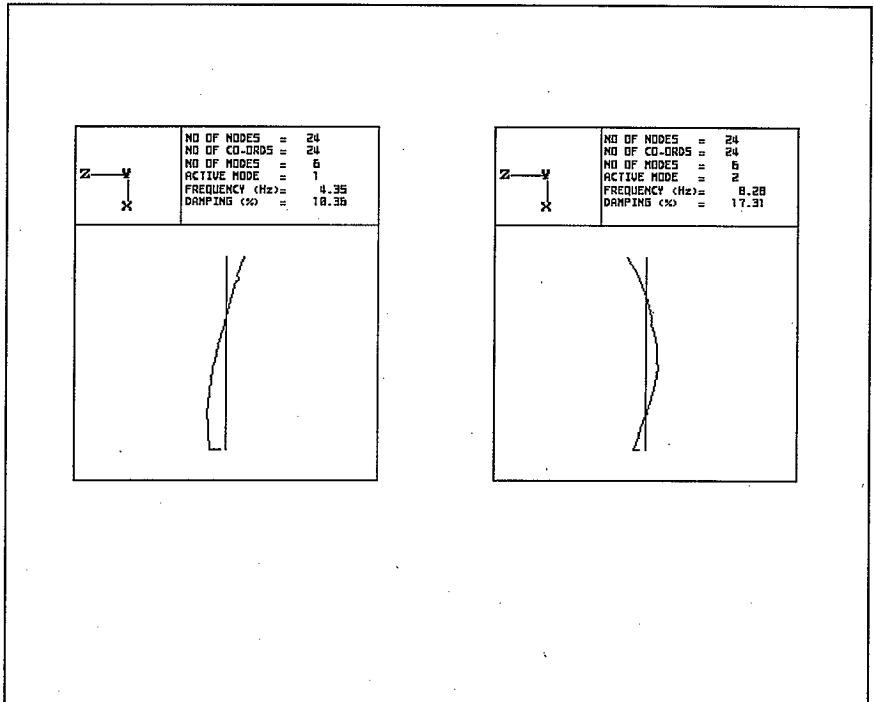


Fig A5.7 TEST 1Z Modes 1 & 2

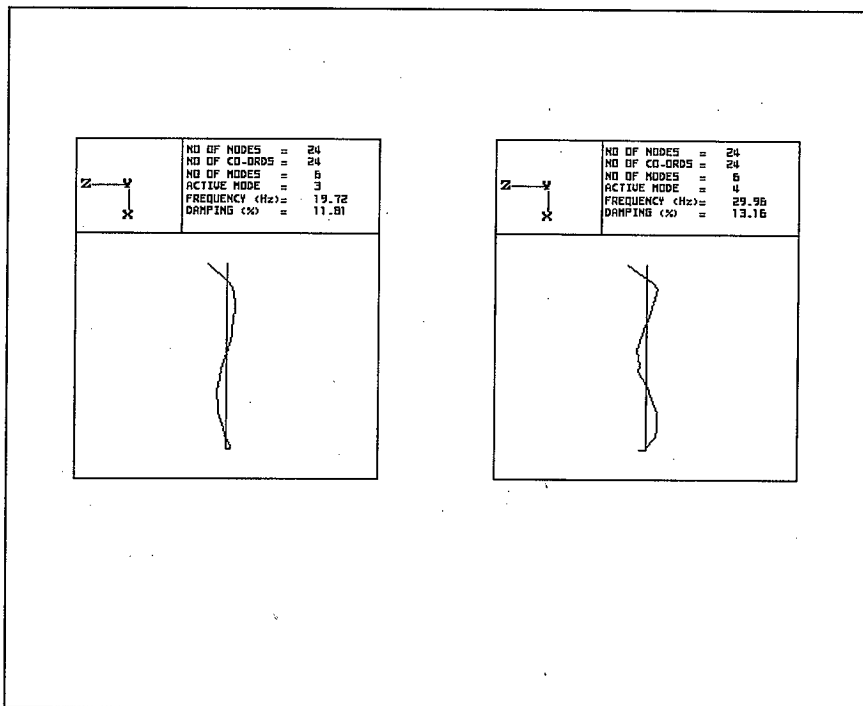


Fig A5.8 TEST 1Z Modes 3 & 4

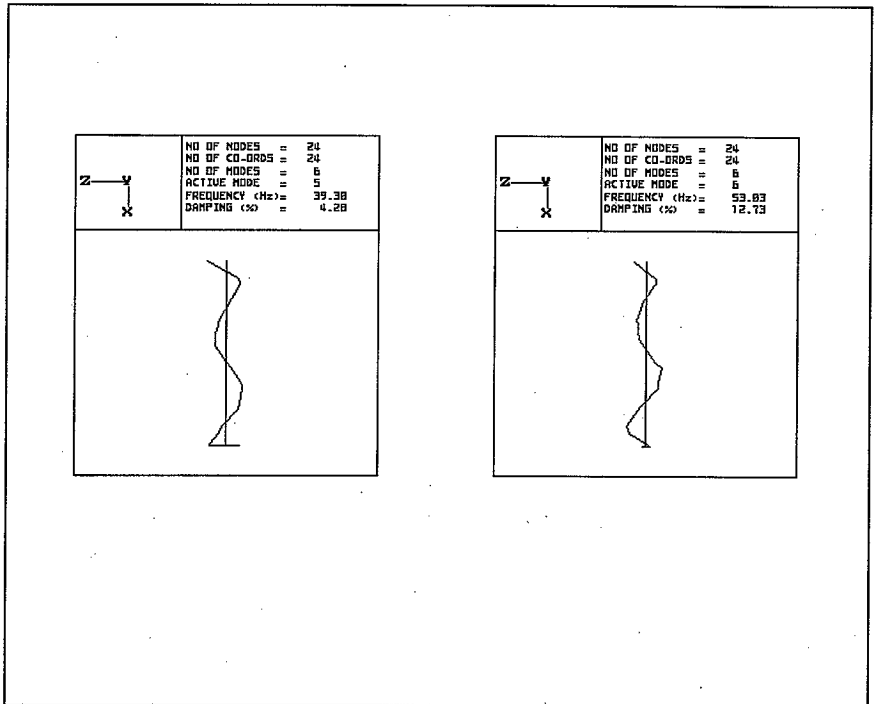


Fig A5.9 TEST 1Z Modes 5 & 6

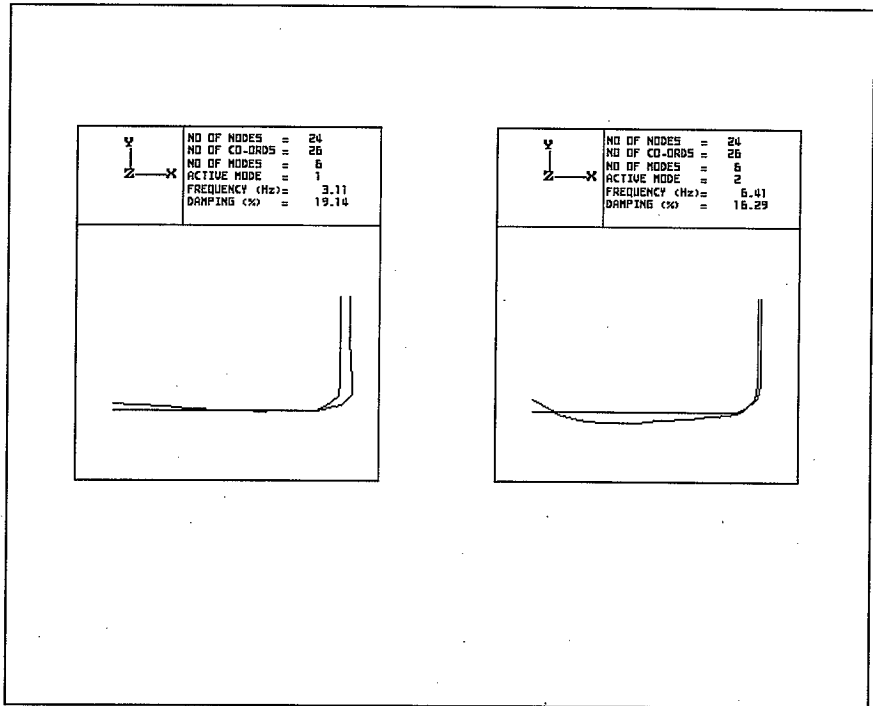


Fig A5.10 TEST 2Y Modes 1 & 2

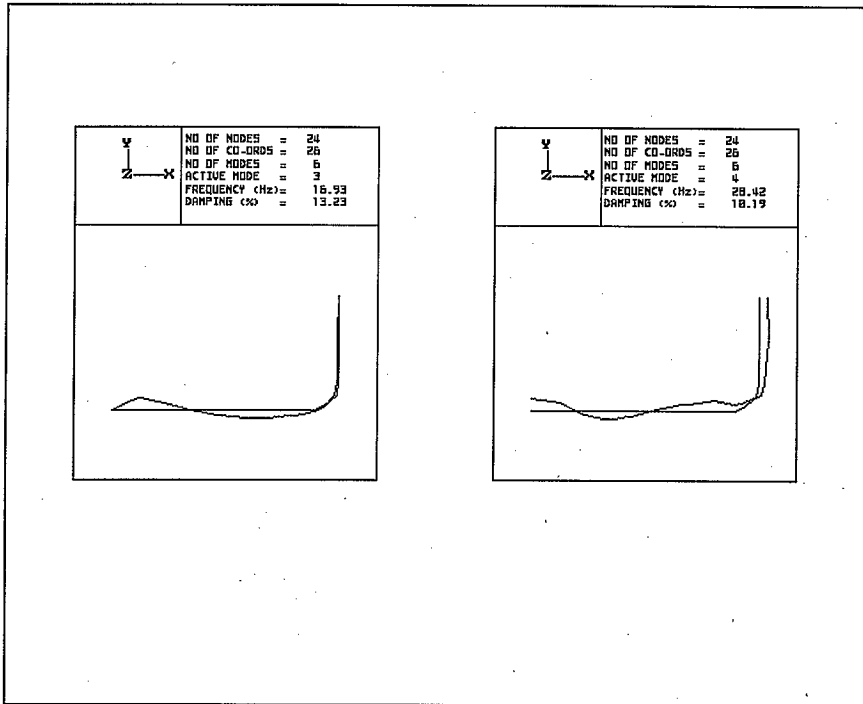


Fig A5.11 TEST 2Y Modes 3 & 4

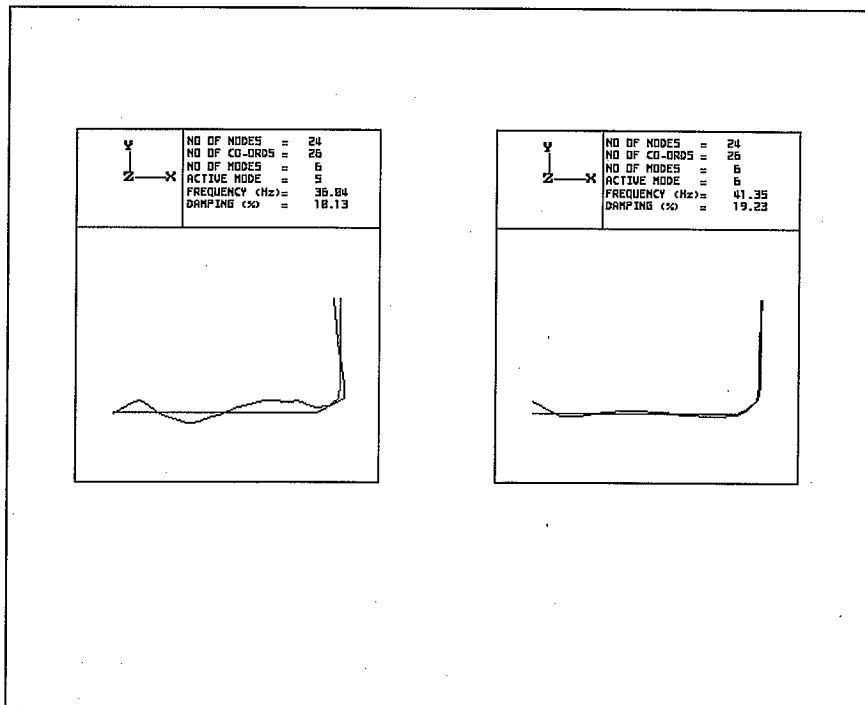


Fig A5.12 TEST 2Y Modes 5 & 6

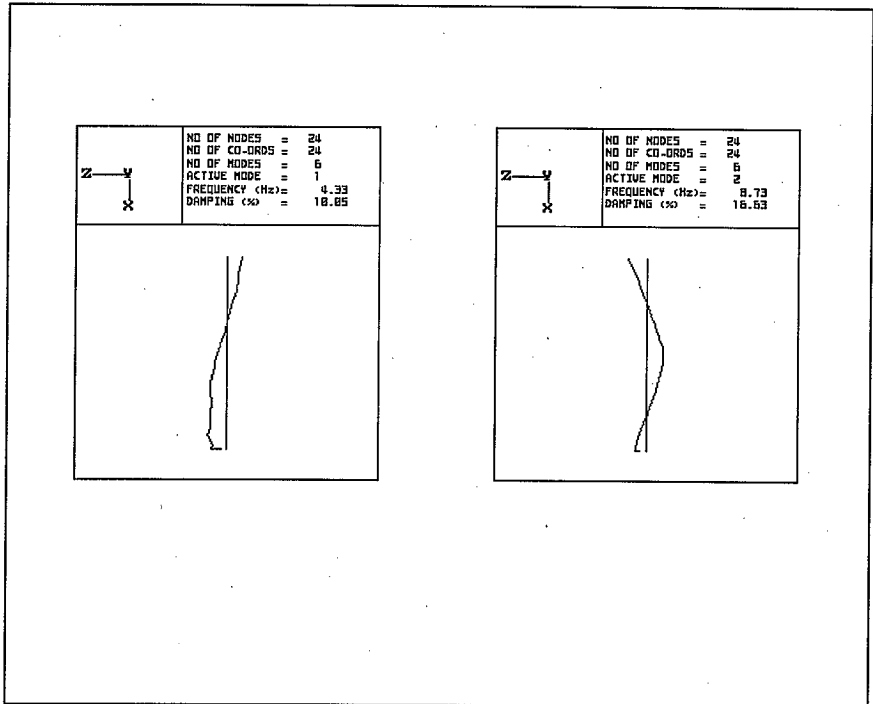


Fig A5.13 TEST 2Z Modes 1 & 2

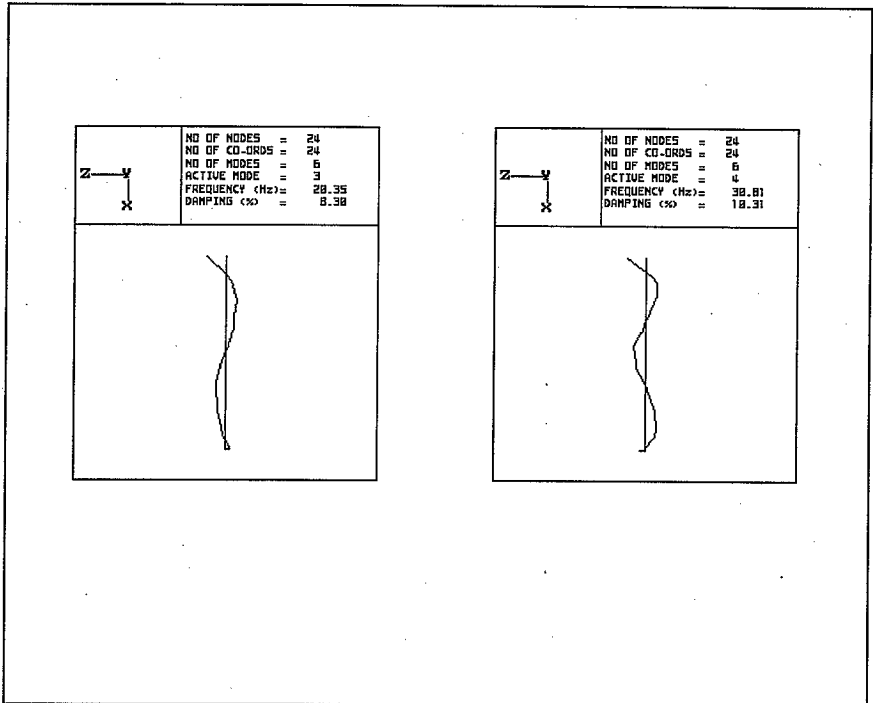


Fig A5.14 TEST 2Z Modes 3 & 4

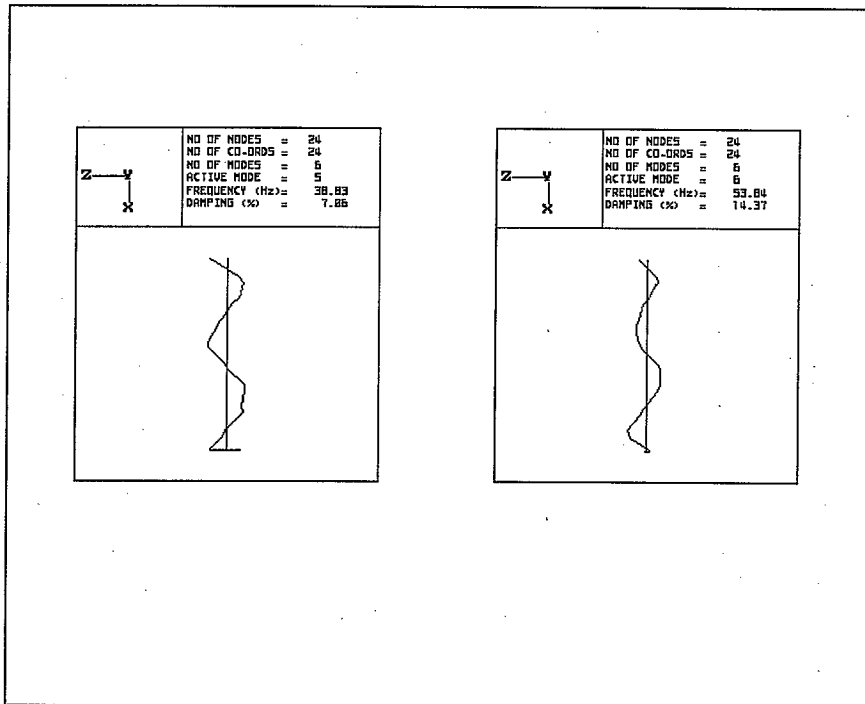


Fig A5.15 TEST 2Z Modes 5 & 6

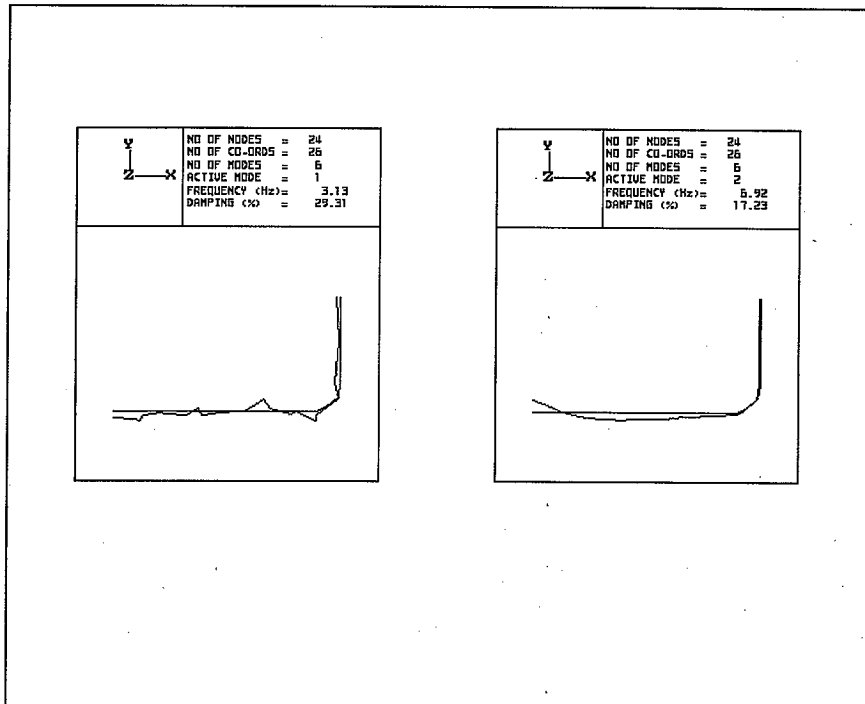


Fig A5.16 TEST 2aY Modes 1 & 2

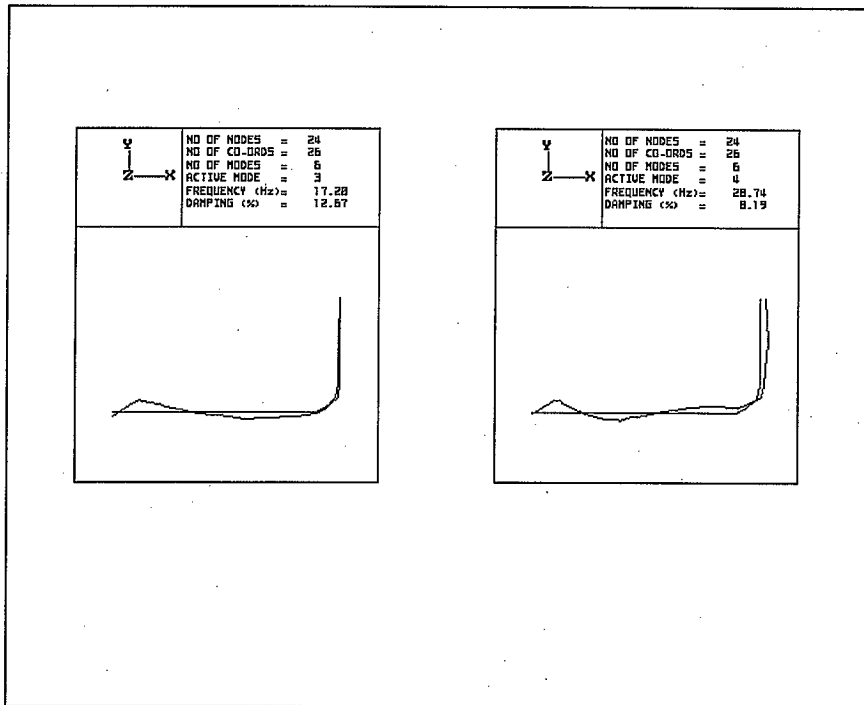


Fig A5.17 TEST 2aY Modes 3 & 4

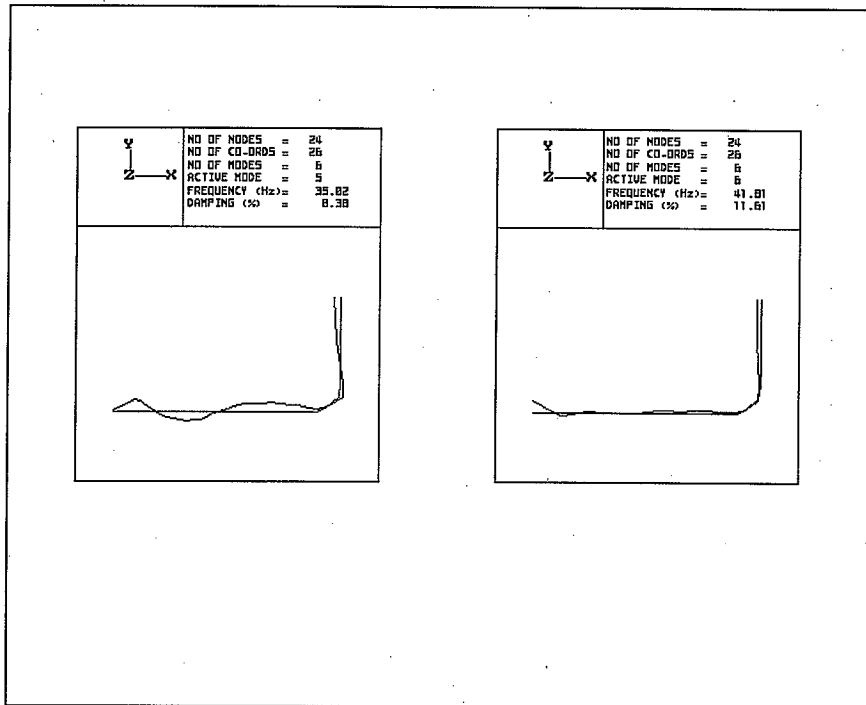


Fig A5.18 TEST 2aY Modes 5 & 6

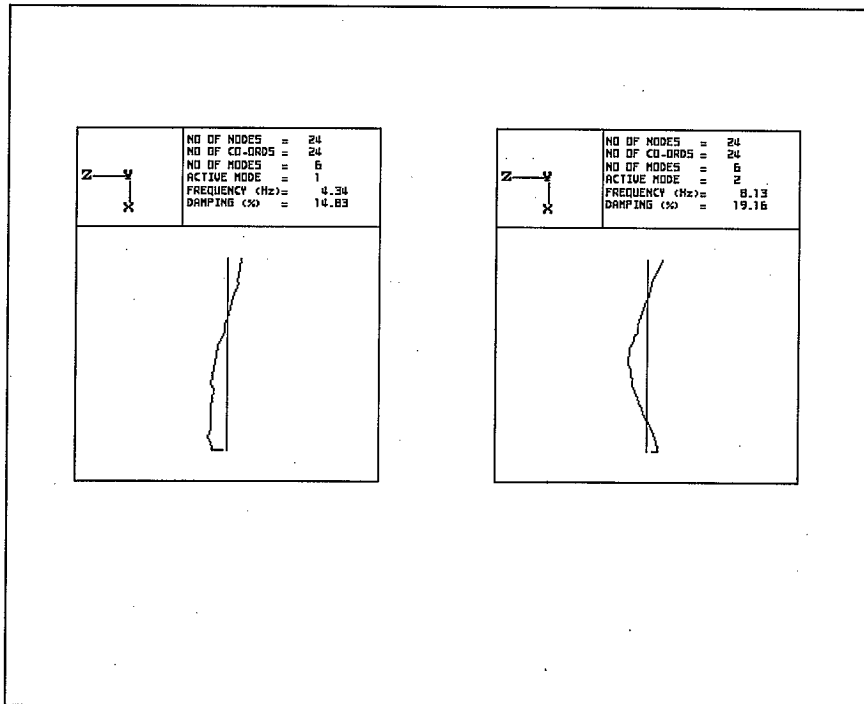


Fig A5.19 TEST 2aZ Modes 1 & 2

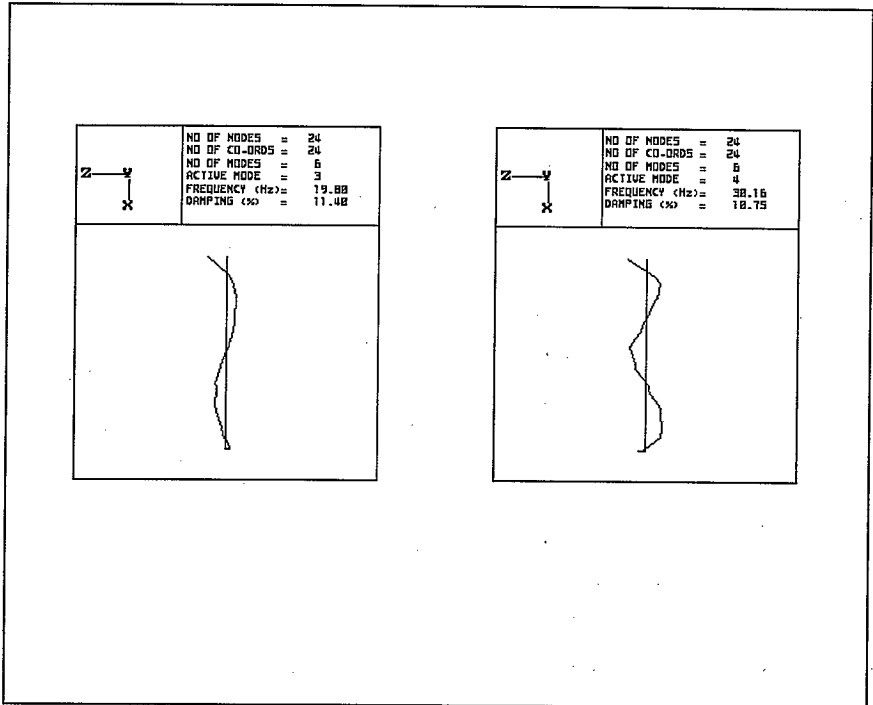


Fig A5.20 TEST 2aZ Modes 3 & 4

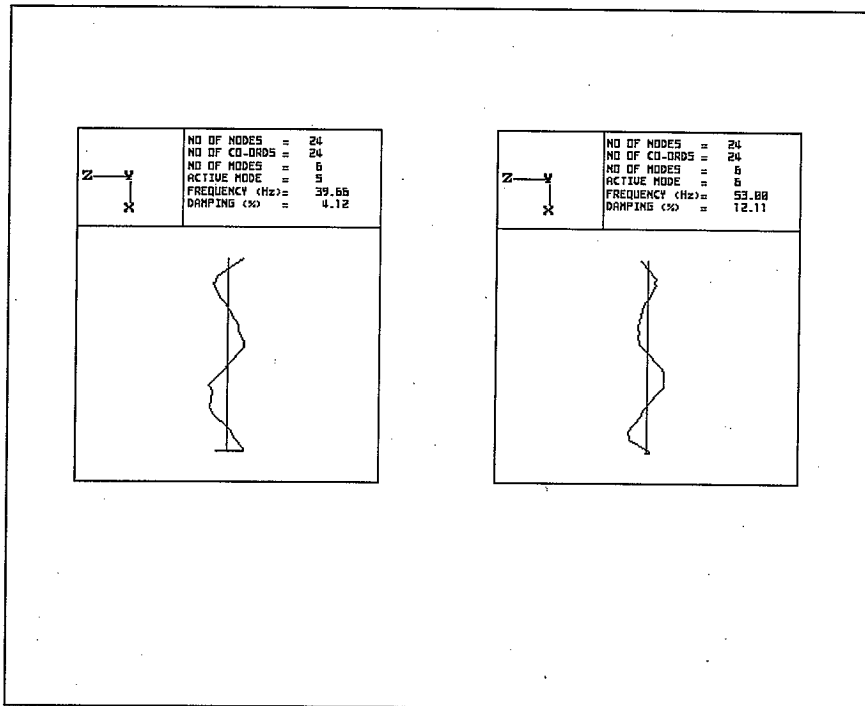


Fig A5.21 TEST 2aZ Modes 5 & 6

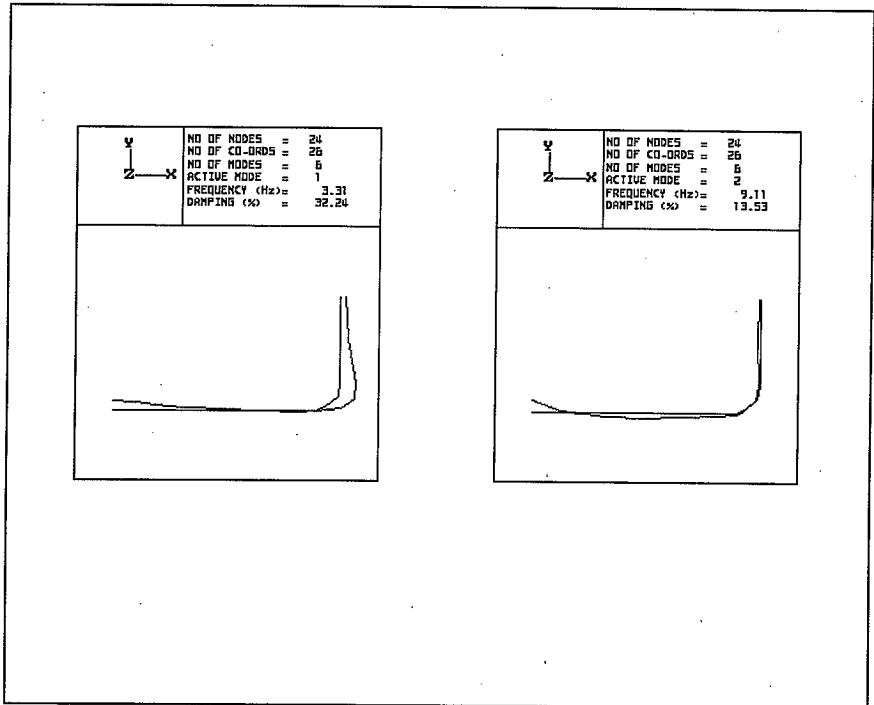


Fig A5.22 TEST 4Y Modes 1 & 2

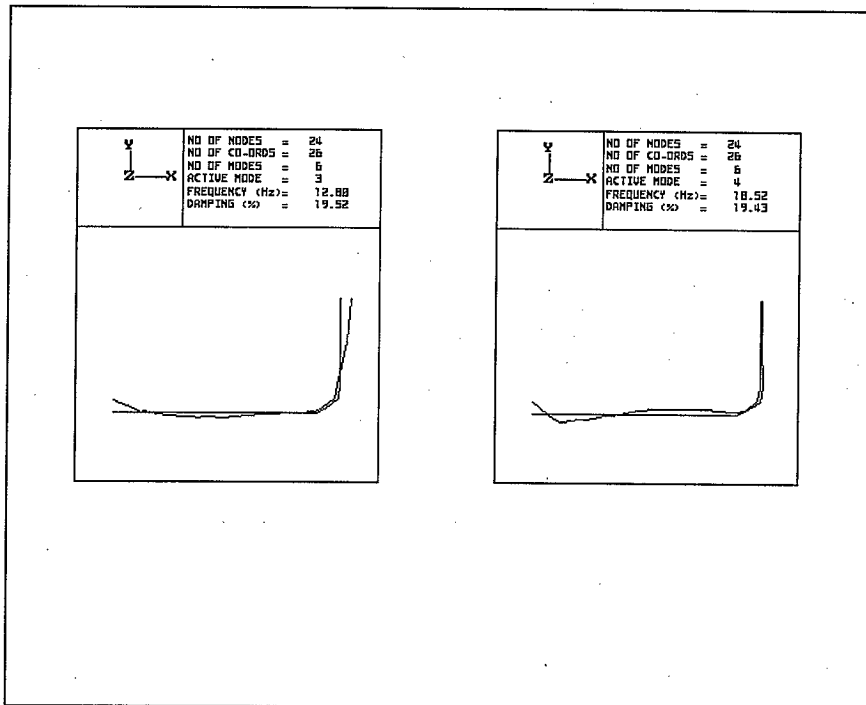


Fig A5.23 TEST 4Y Modes 3 & 4

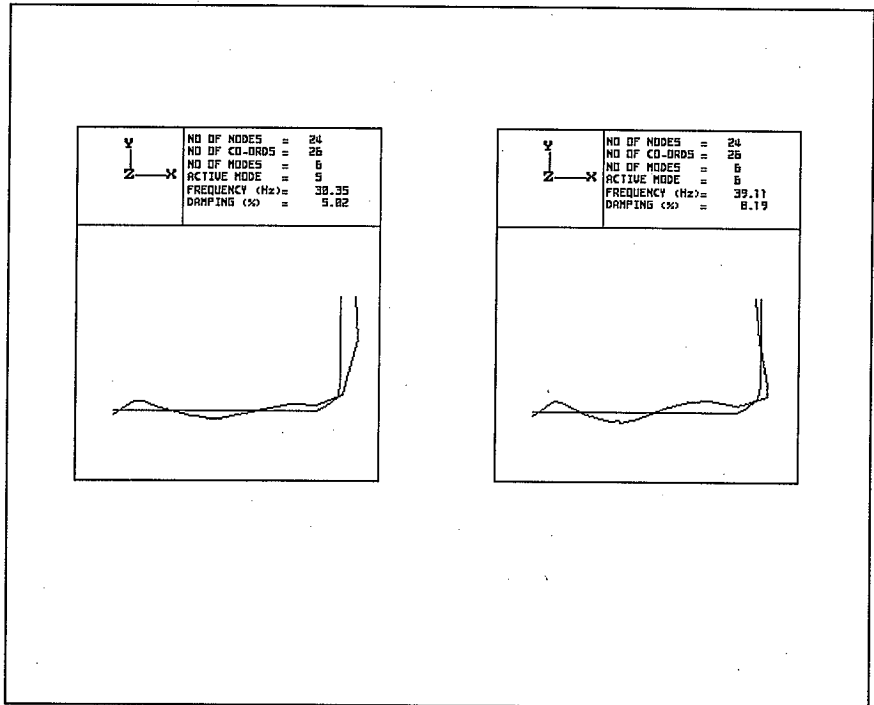
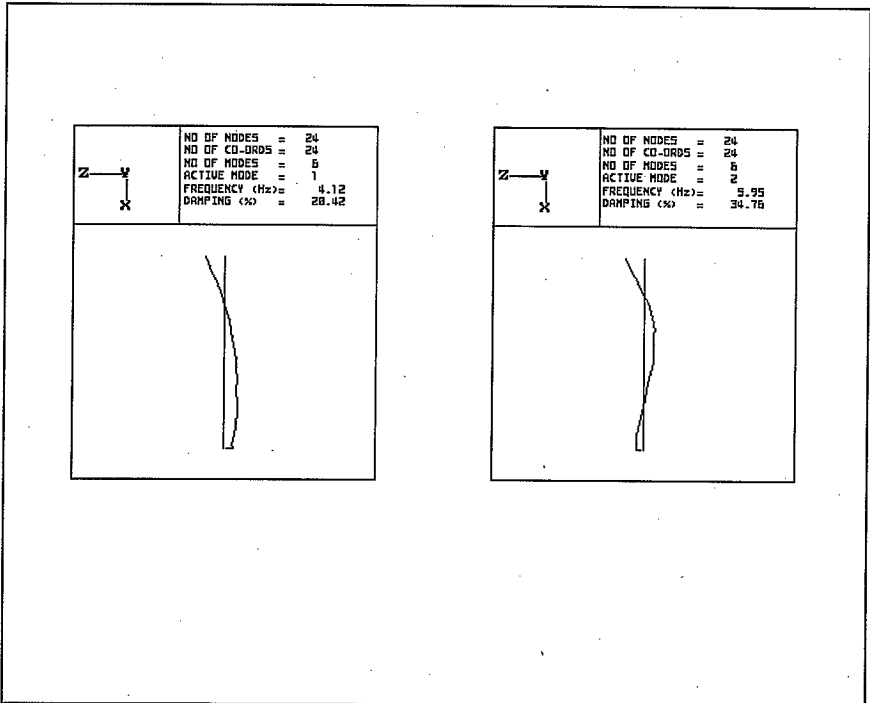


Fig A5.24 TEST 4Y Modes 5 & 6



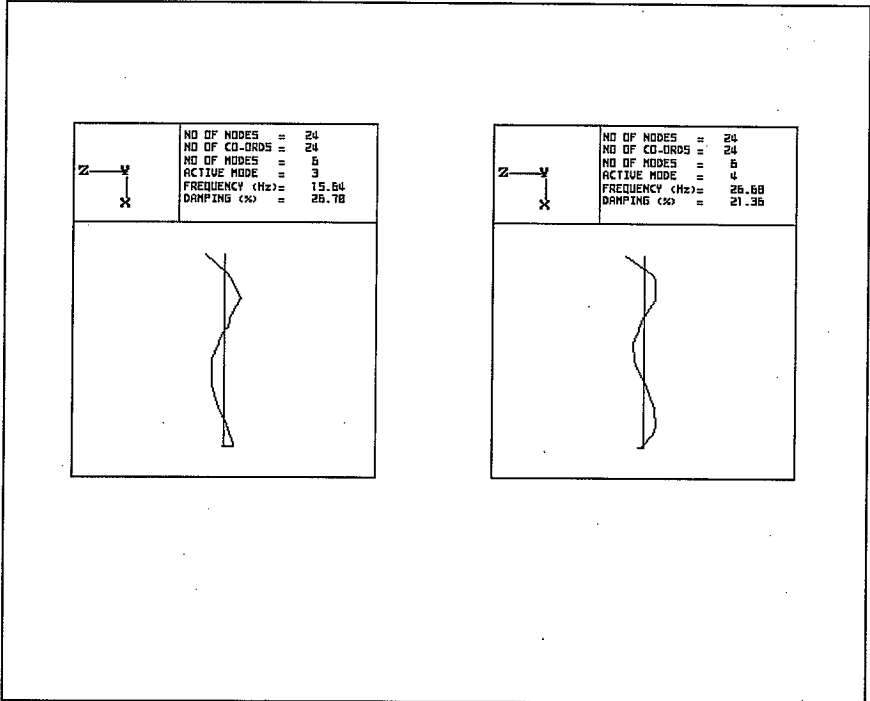


Fig A5.26 TEST 4Z Modes 3 & 4

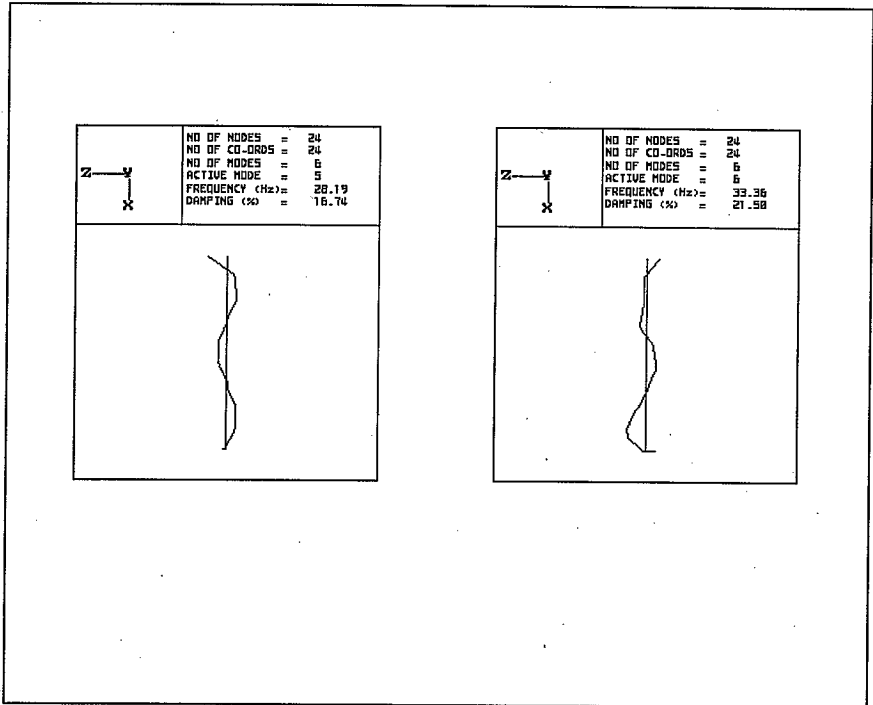


Fig A5.27 TEST 4Z Modes 5 & 6

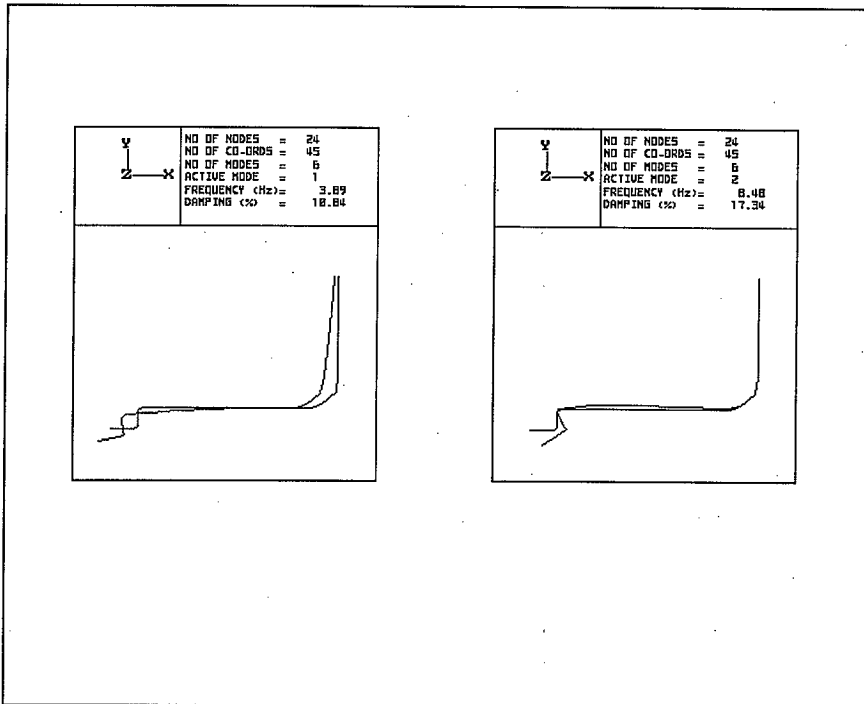


Fig A5.28 TEST 6X Modes 1 & 2

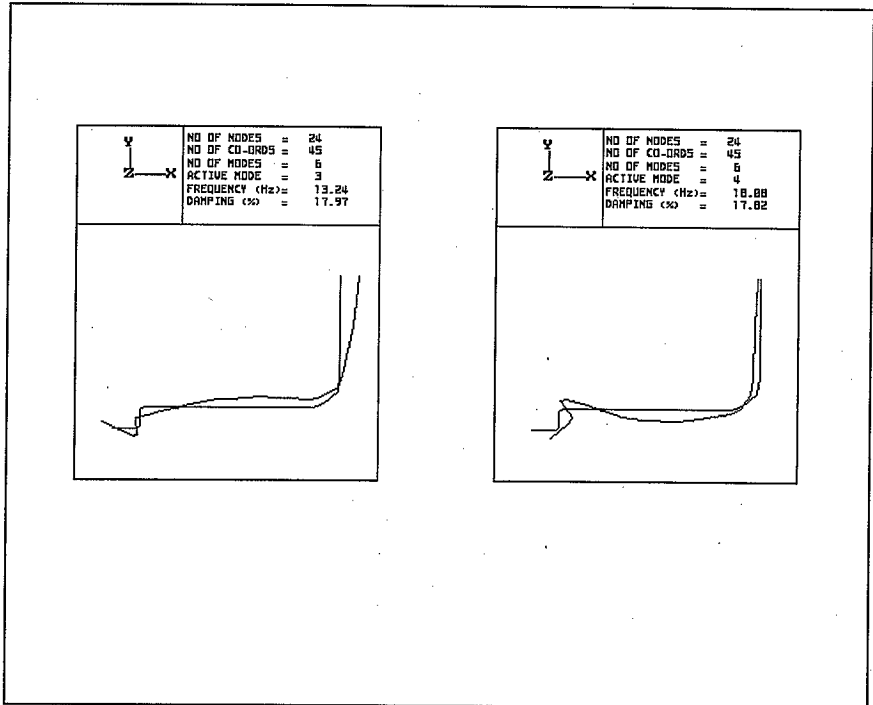


Fig A5.29 TEST 6X Modes 3 & 4

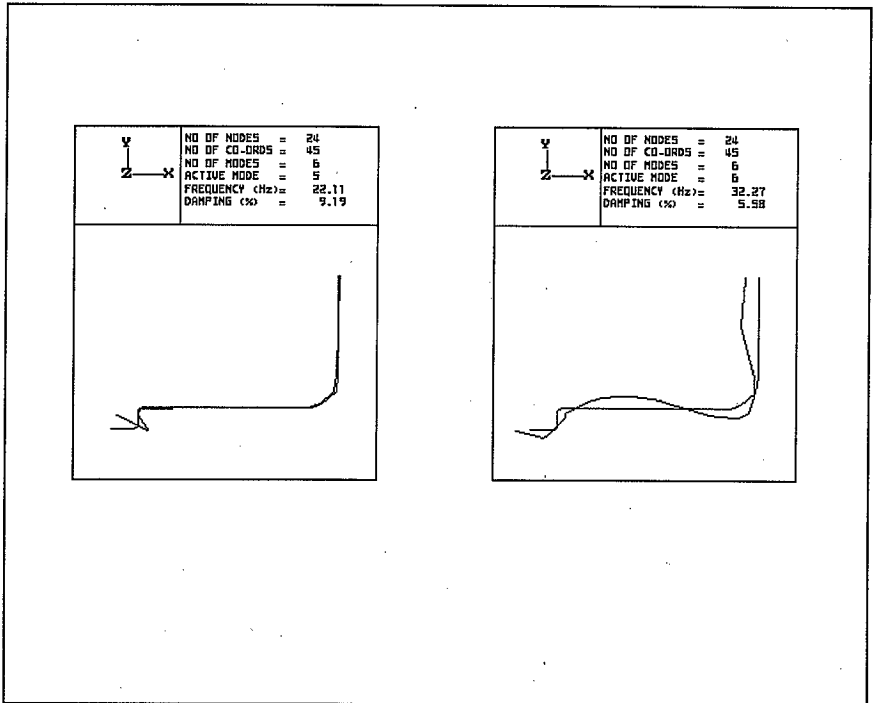


Fig A5.30 TEST 6X Modes 5 & 6

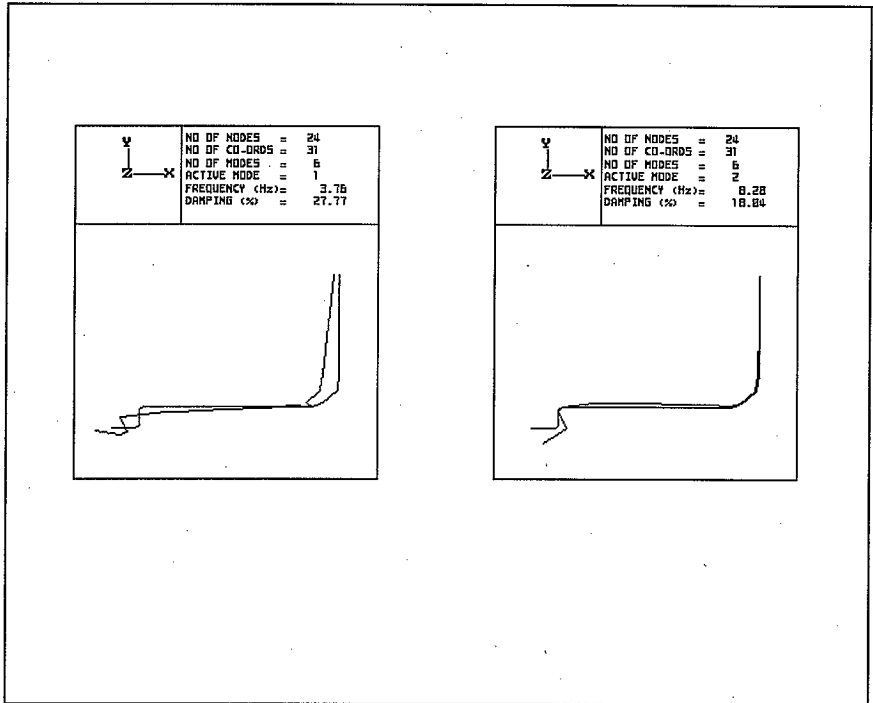


Fig A5.31 TEST 6Y Modes 1 & 2

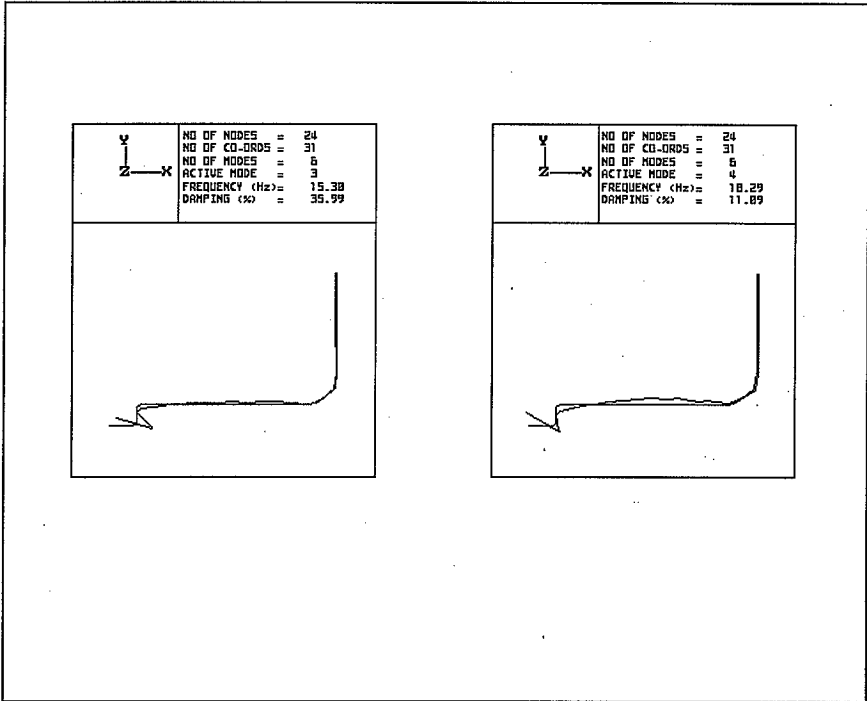


Fig A5.32 TEST 6Y Modes 3 & 4

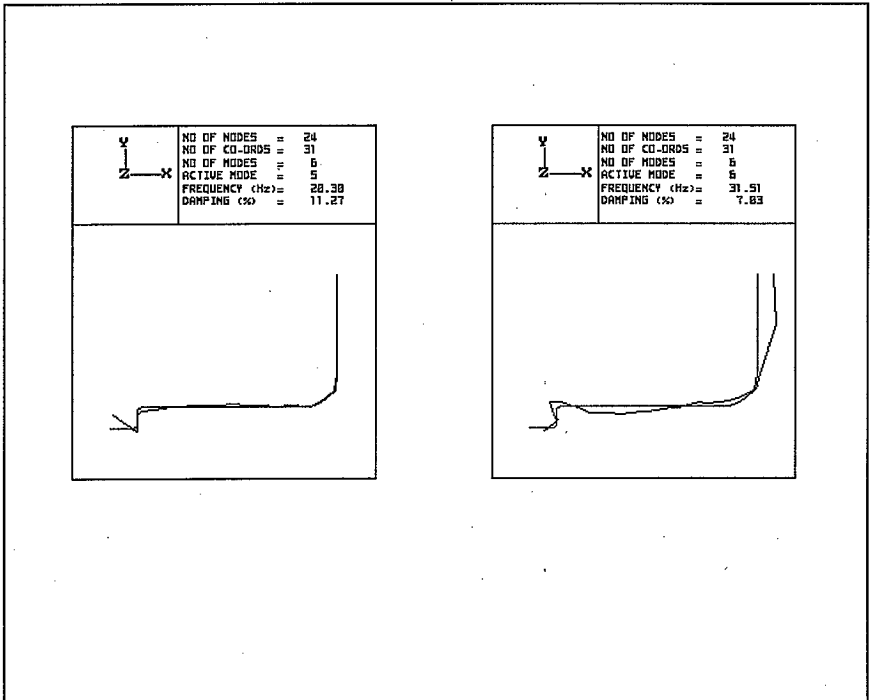


Fig A5.33 TEST 6Y Modes 5 & 6

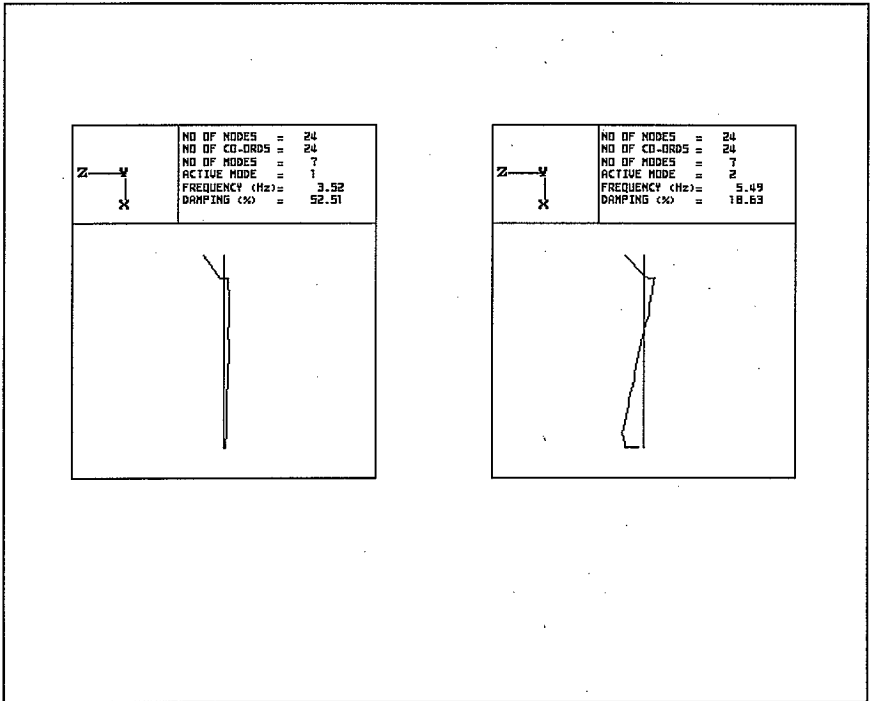


Fig A5.34 TEST 6Z Modes 1 & 2

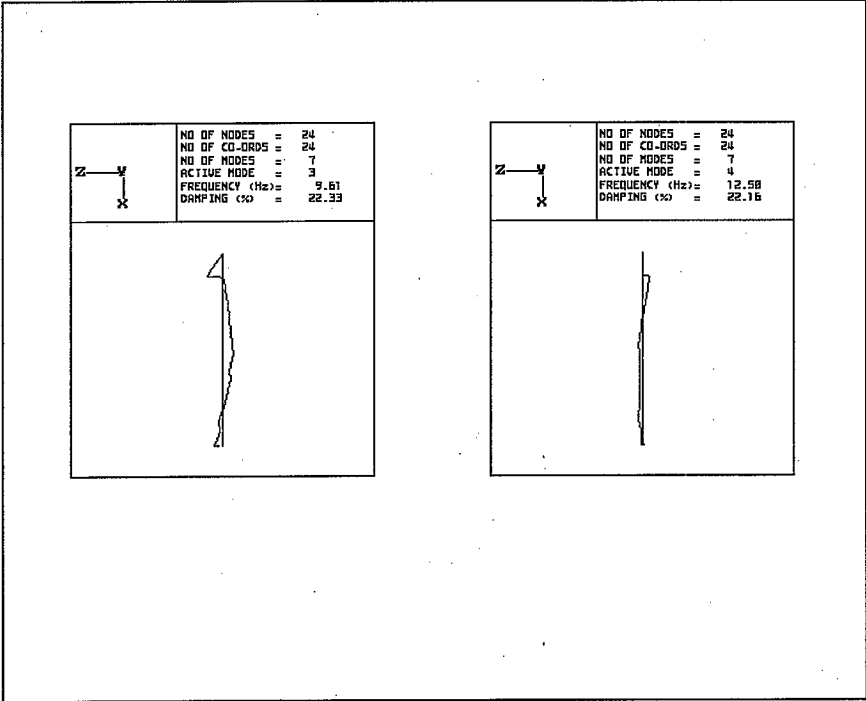


Fig A5.35 TEST 6Z Modes 3 & 4

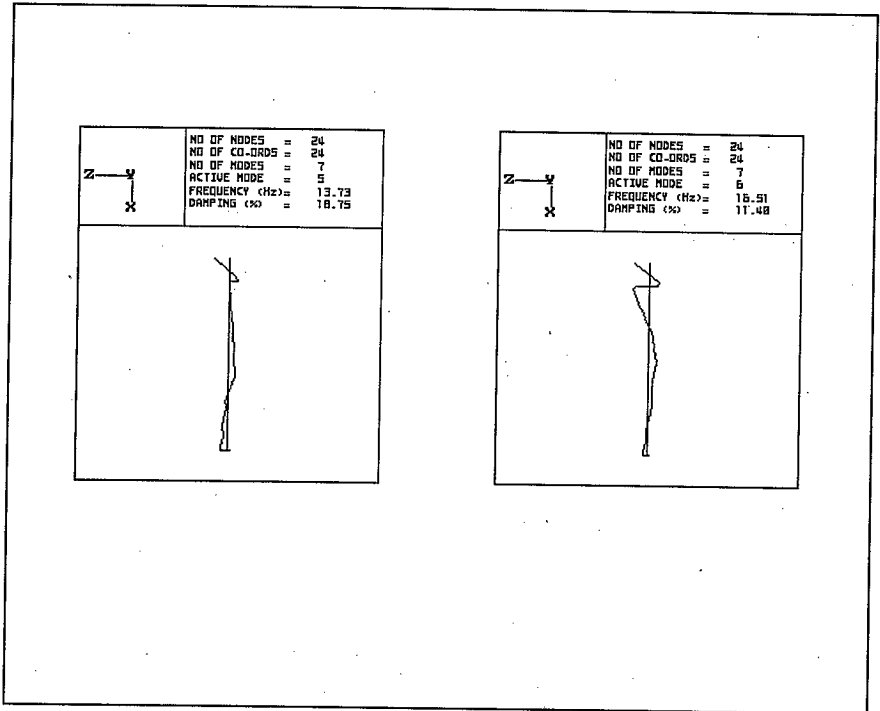


Fig A5.36 TEST 6Z Modes 5 & 6

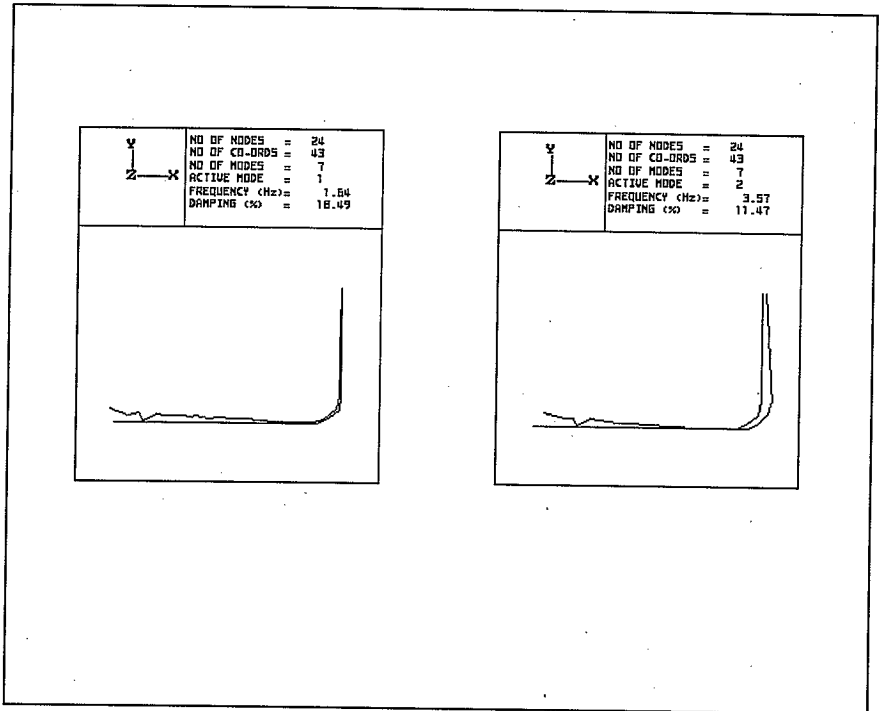


Fig A5.37 TEST 7X Modes 1 & 2

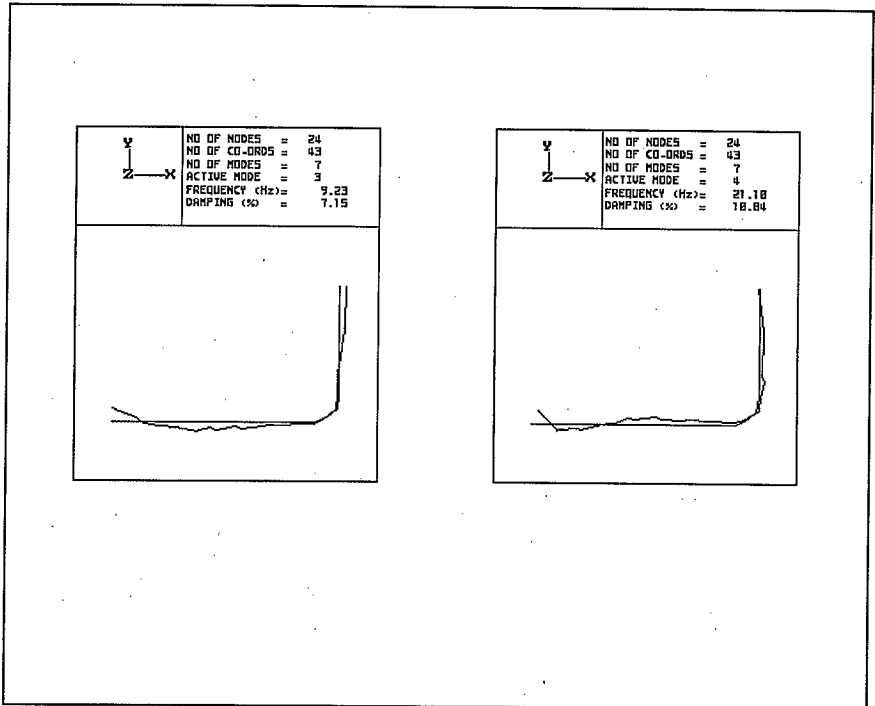


Fig A5.38 TEST 7X Modes 3 & 4

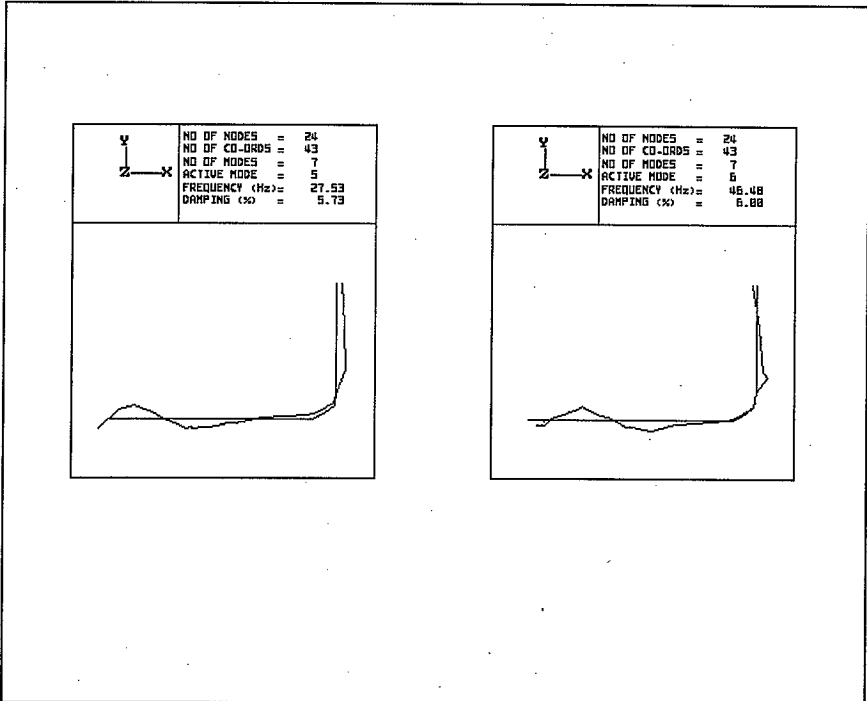


Fig A5.39 TEST 7X Modes 5 & 6

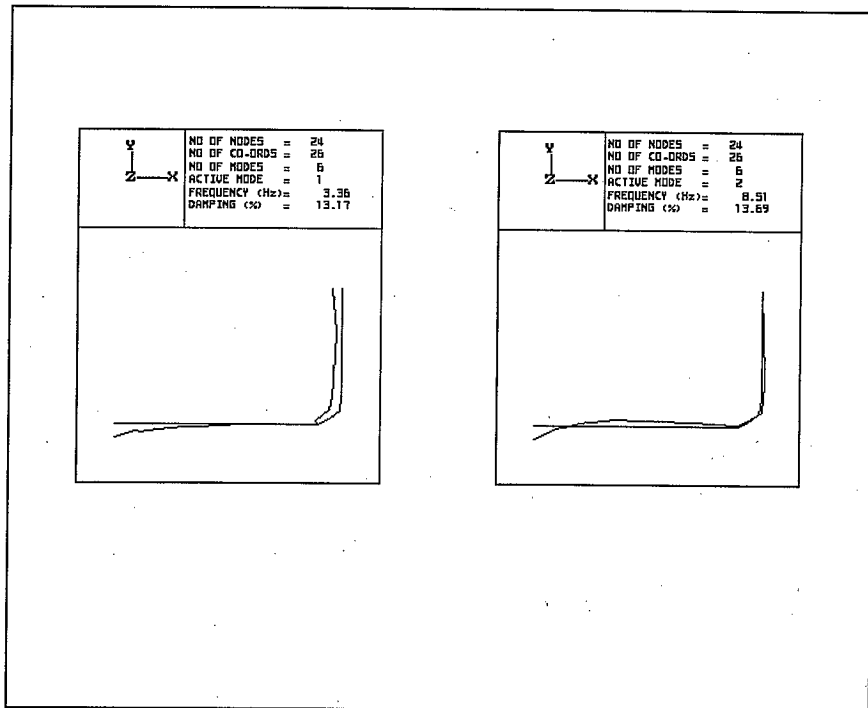


Fig A5.40 TEST 7Y Modes 1 & 2

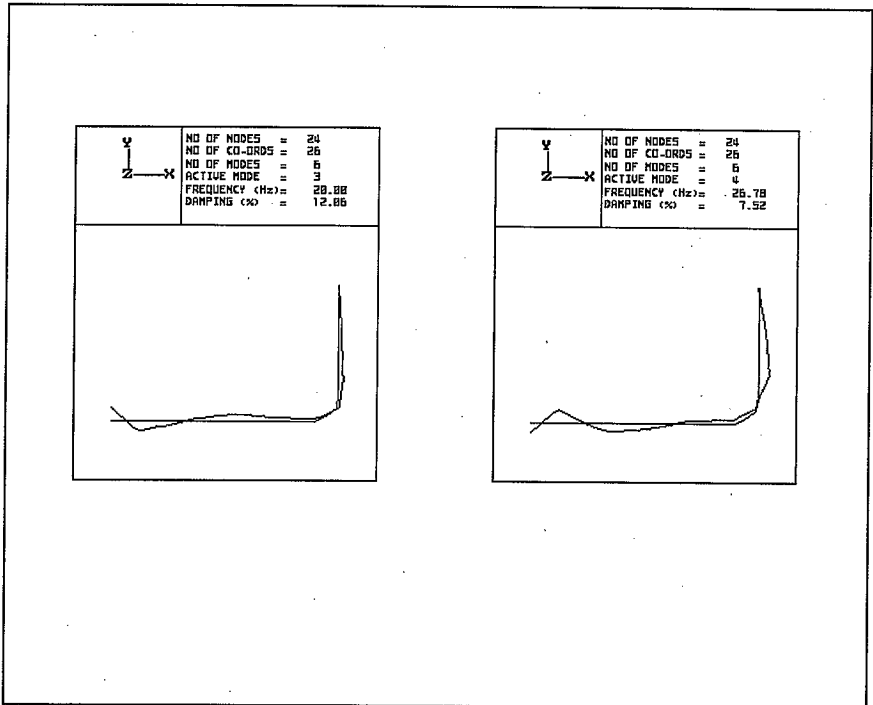


Fig A5.41 TEST 7Y Modes 3 & 4

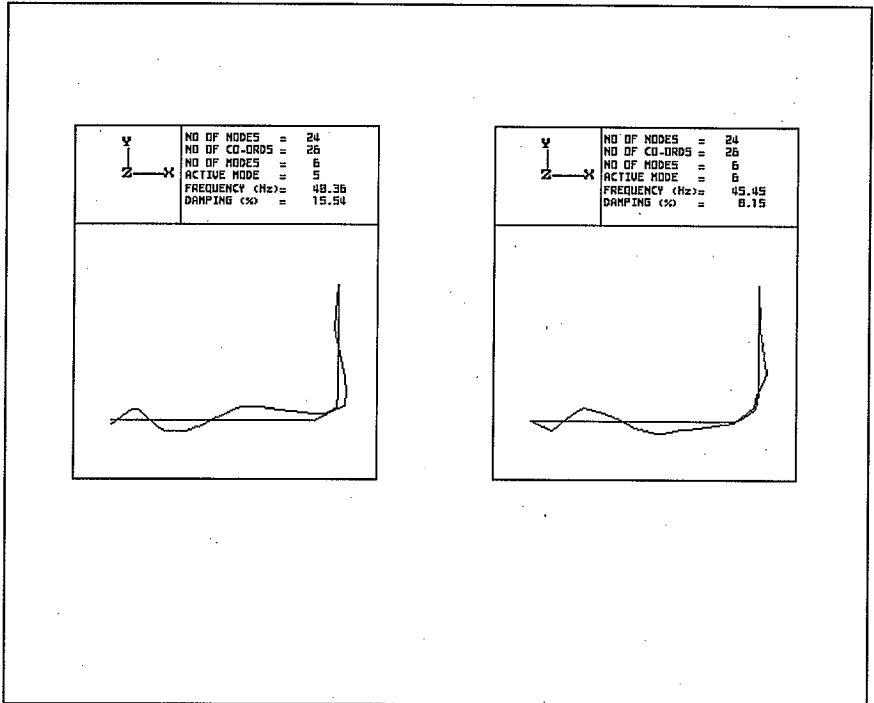


Fig A5.42 TEST 7Y Modes 5 & 6

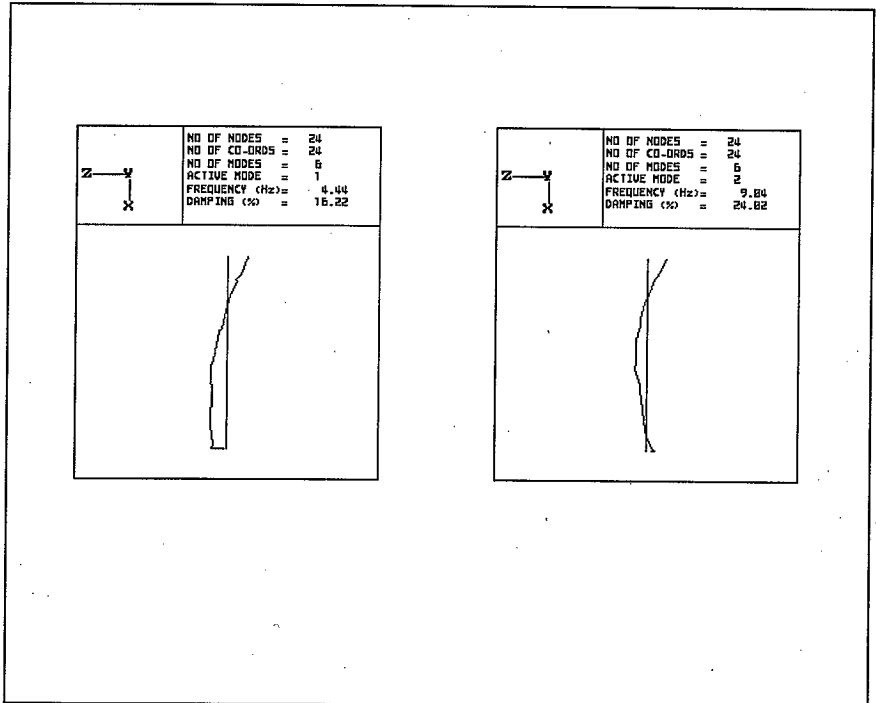


Fig A5.43 TEST 7Z Modes 1 & 2

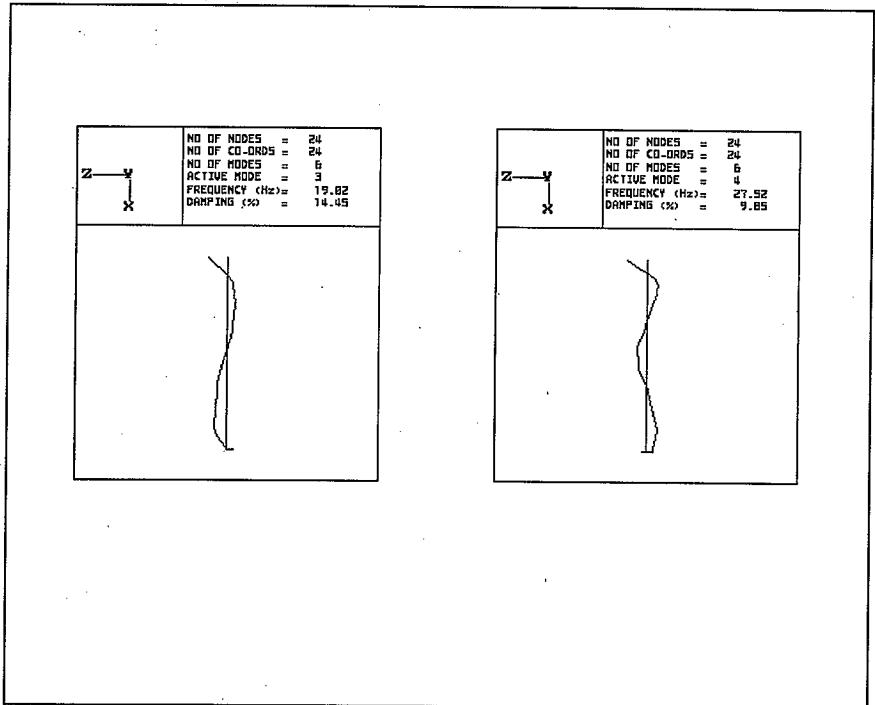


Fig A5.44 TEST 7Z Modes 3 & 4

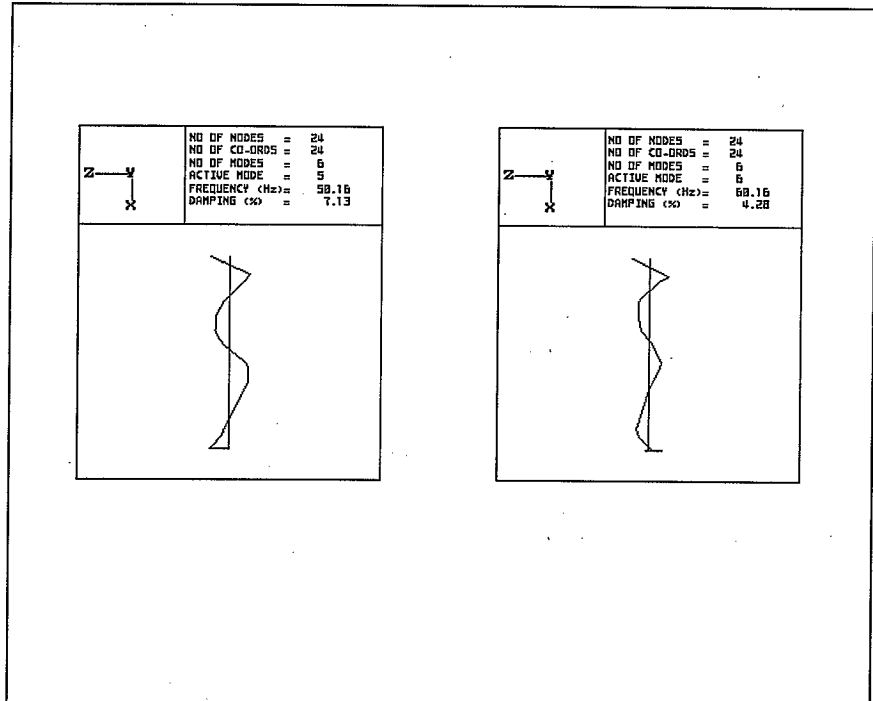
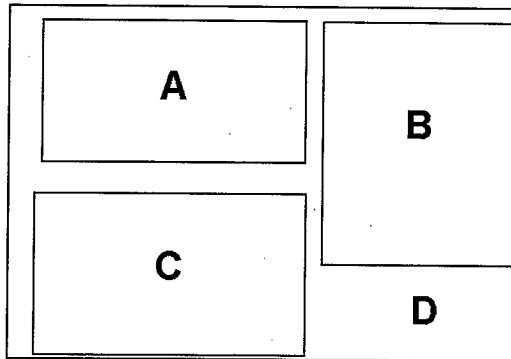


Fig A5.45 TEST 7Z Modes 5 & 6

SECTION 6
DRIVING POINT COMPLIANCE PLOTS

FIGURE No	TITLE	Page No.
A6.1	Key for Driving Point Compliance Plots.	A87
A6.2	Driving Point Compliances for Test 1X.	A88
A6.3	Driving Point Compliances for Test 1Y.	A89
A6.4	Driving Point Compliances for Test 1Z.	A90
A6.5	Driving Point Compliances for Test 2X.	A91
A6.6	Driving Point Compliances for Test 2Y.	A92
A6.7	Driving Point Compliances for Test 2Z.	A93
A6.8	Driving Point Compliances for Test 2aX.	A94
A6.9	Driving Point Compliances for Test 2aY.	A95
A6.10	Driving Point Compliances for Test 2aZ.	A96
A6.11	Driving Point Compliances for Test 4X.	A97
A6.12	Driving Point Compliances for Test 4Z.	A98
A6.13	Driving Point Compliances for Test 6X.	A99
A6.14	Driving Point Compliances for Test 7X.	A100
A6.15	Driving Point Compliances for Test 7Y.	A101
A6.16	Driving Point Compliances for Test 7Z.	A102



KEY

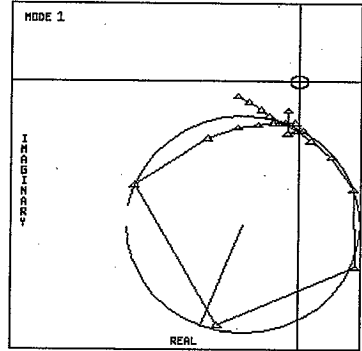
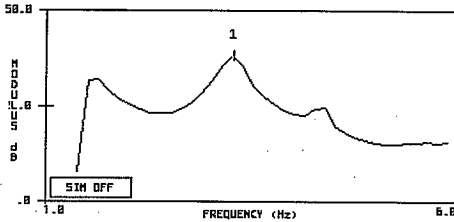
- A** Driving Point Compliance frequency response function showing the mode numbers that have been identified.
X-axis Frequency (Hz)
Y-axis Modulus of Compliance (dB)

- B** Nyquist Plot showing real and imaginary parts of frequency response function of the mode shown in the top left hand corner.
X-axis Real part
Y-axis Imaginary part

- C** Carpet plot qualitatively showing deviation from text book viscous damping. There is a redundancy of information available allowing many independent estimates to be made of the damping. This plot shows these various damping estimates as the Y-axis. Classical viscous damping would produce a horizontal co-planar plot, whereas any deviation from this is indicative of non-linearities, noise, bad measurements etc.

- D** Data giving Identified Mode Number
 Natural Frequency (Hz)
 % Damping (Loss Factor)

Fig A6.1 Key for Driving Point Compliance Plots



O-FIT FOR MODE 1
 NAT. FREQUENCY (Hz) = 3.26
 % STRUCTURAL DAMPING = 13.9404

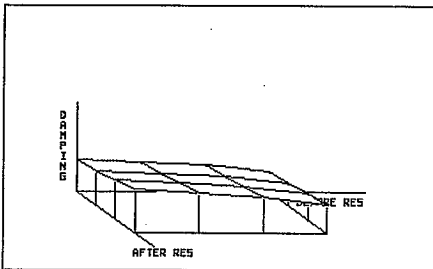
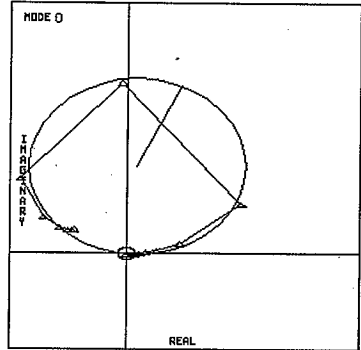
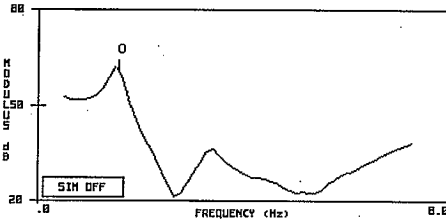


Fig A6.2 Driving Point Compliance for Test 1X



O-FIT FOR MODE 0
NAT. FREQUENCY (Hz) = 1.54
% STRUCTURAL DAMPING = 28.3975

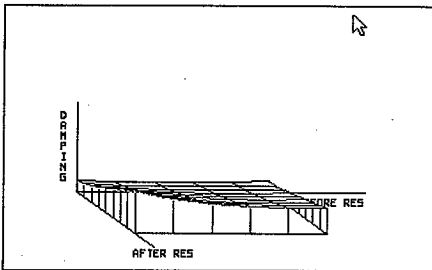
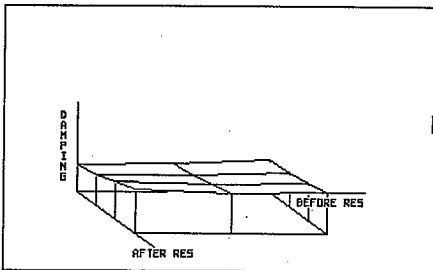
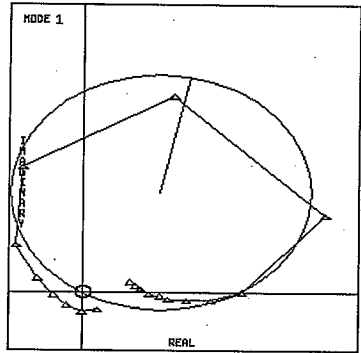
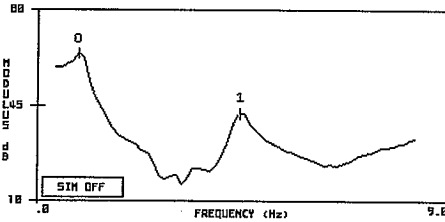
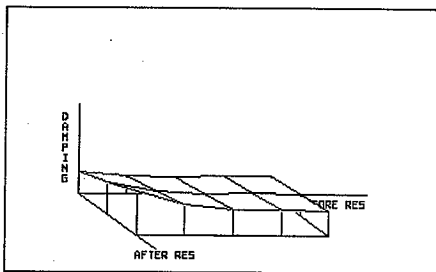
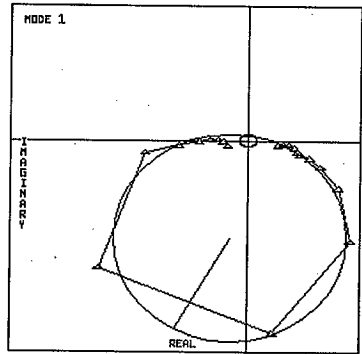
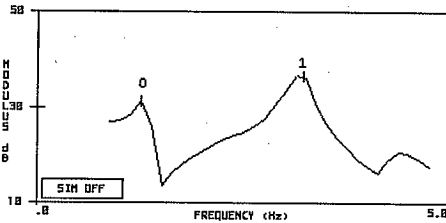


Fig A6.3 Driving Point Compliance for Test 1Y



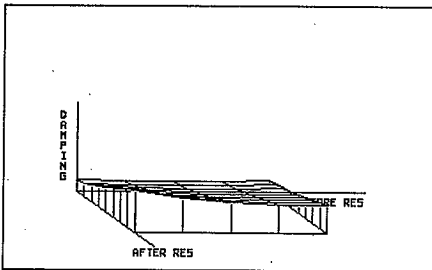
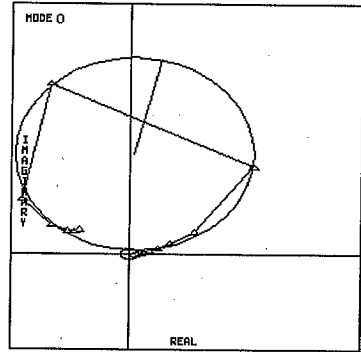
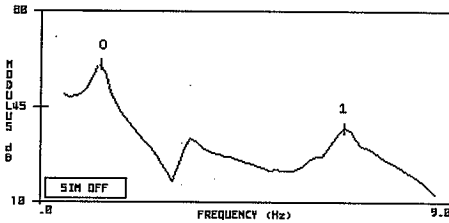
O-FIT FOR MODE 1
NAT. FREQUENCY (Hz) = 4.39
% STRUCTURAL DAMPING = 13.0749

Fig A6.4 Driving Point Compliance for Test 1Z



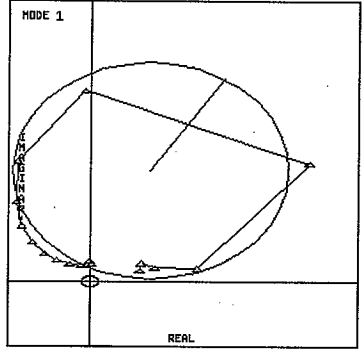
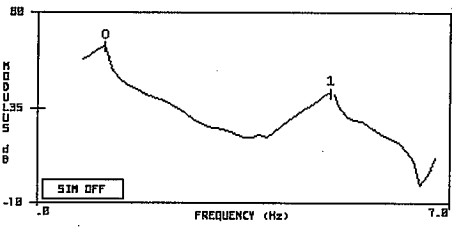
O-FIT FOR MODE 1
 NAT. FREQUENCY (Hz) = 3.21
 % STRUCTURAL DAMPING = 15.7078

Fig A6.5 Driving Point Compliance for Test 2X



O-FIT FOR MODE 0
NAT. FREQUENCY (Hz) = 1.31
% STRUCTURAL DAMPING = 34.5970

Fig A6.6 Driving Point Compliance for Test 2Y



O-FIT FOR MODE 1
NAT. FREQUENCY (Hz) = 4.95
% STRUCTURAL DAMPING = 4.5358

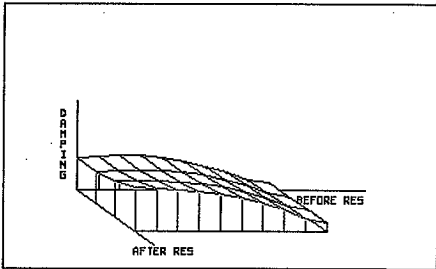
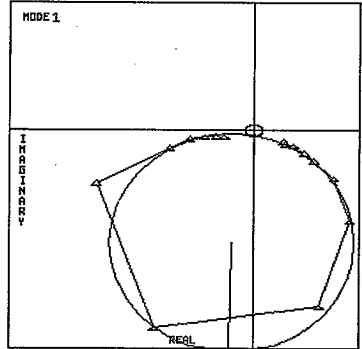
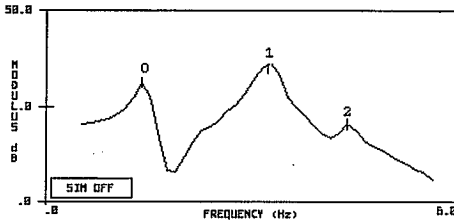


Fig A6.7 Driving Point Compliance for Test 2Z



O-FIT FOR MODE 1
 NAT. FREQUENCY (Hz) = 3.20
 % STRUCTURAL DAMPING = 14.6989

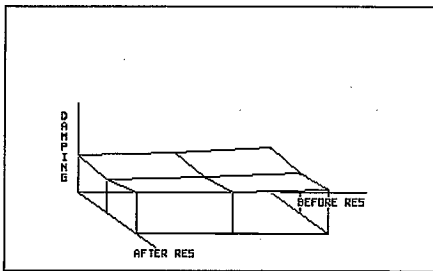
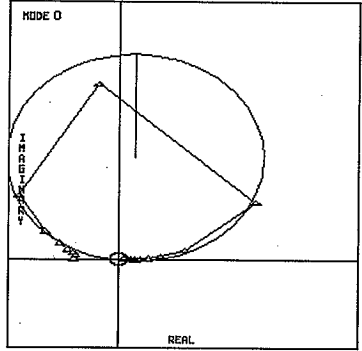
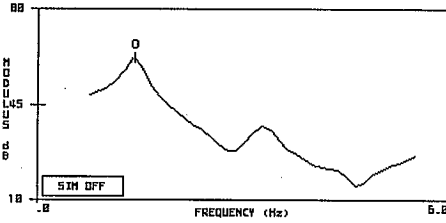


Fig A6.8 Driving Point Compliance for Test 2aX



O-FIT FOR MODE 0
NAT. FREQUENCY (Hz) = 1.39
% STRUCTURAL DAMPING = 62.4103

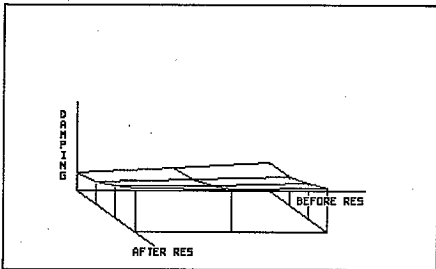
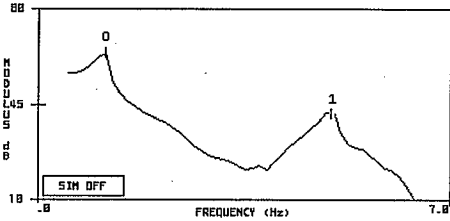
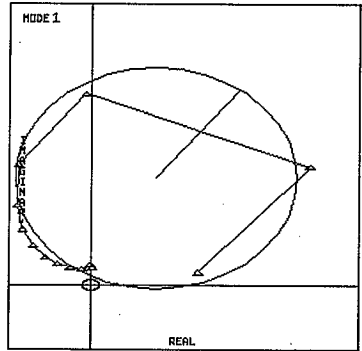


Fig A6.9 Driving Point Compliance for Test 2aY

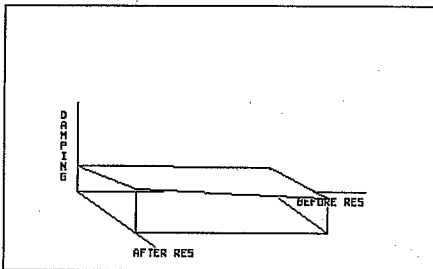
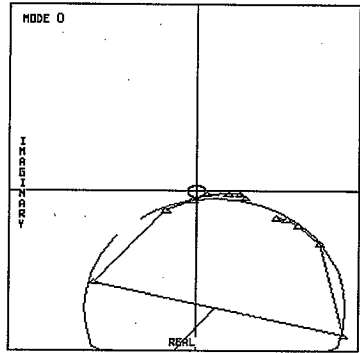
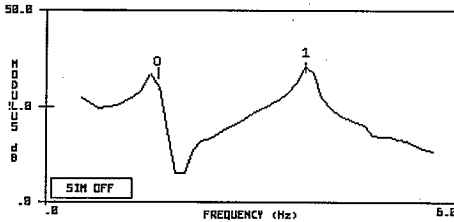


No Plot



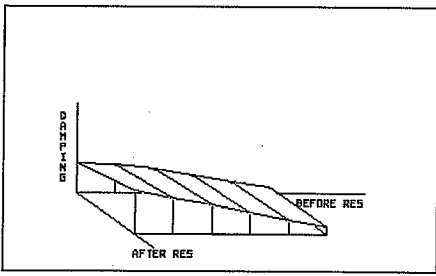
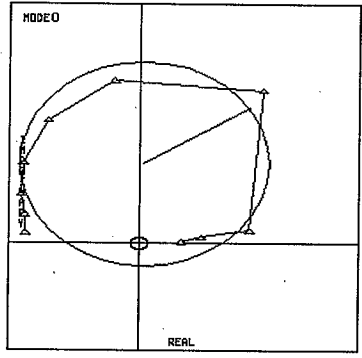
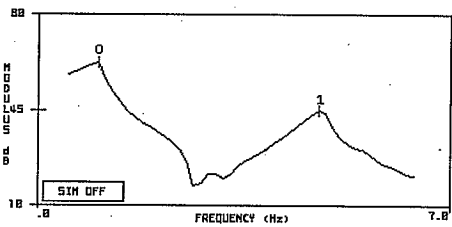
O-FIT FOR MODE 1
NAT. FREQUENCY (Hz) = 4.96
% STRUCTURAL DAMPING = 3.9397

Fig A6.10 Driving Point Compliance for Test 2aZ



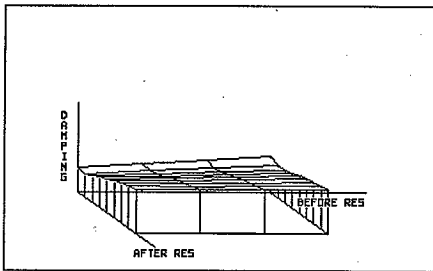
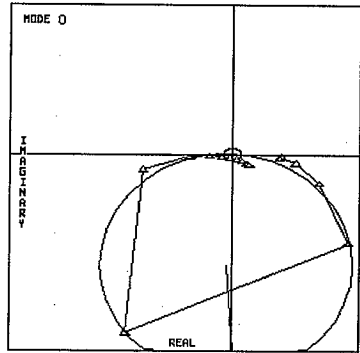
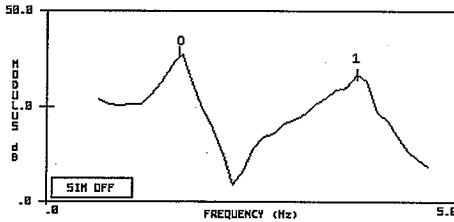
O-FIT FOR MODE 0
 NAT. FREQUENCY (Hz) = 1.61
 % STRUCTURAL DAMPING = 49.8685

Fig A6.11 Driving Point Compliance for Test 4X



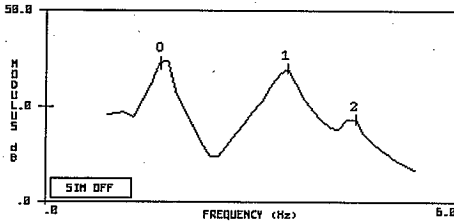
O-FIT FOR MODE 0
 NAT. FREQUENCY (Hz) = 1.01
 % STRUCTURAL DAMPING = 29.8192

Fig A6.12 Driving Point Compliance for Test 4Z

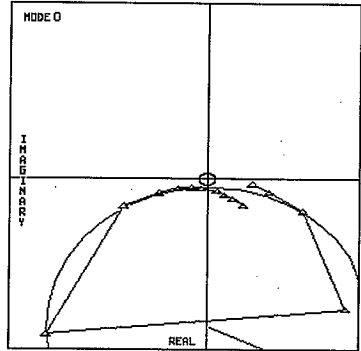


O-FIT FOR MODE 0
 NAT. FREQUENCY (Hz) = 1.59
 % STRUCTURAL DAMPING = 20.8691

Fig A6.13 Driving Point Compliance for Test 6X

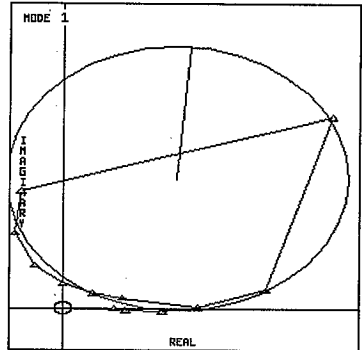
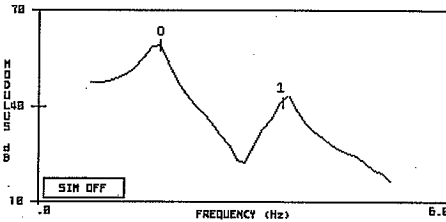


NO PLOT



O-FIT FOR MODE 0
NAT. FREQUENCY (Hz) = 1.65
% STRUCTURAL DAMPING = 41.7116

Fig A6.14 Driving Point Compliance for Test 7X



O-FIT FOR MODE 1
NAT. FREQUENCY (Hz) = 3.55
% STRUCTURAL DAMPING = 12.7655

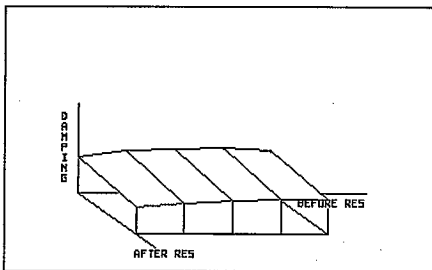
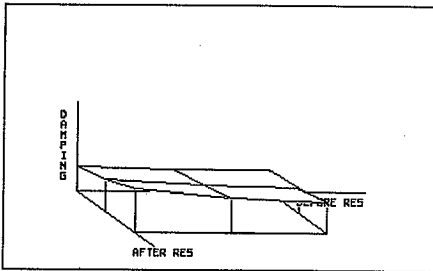
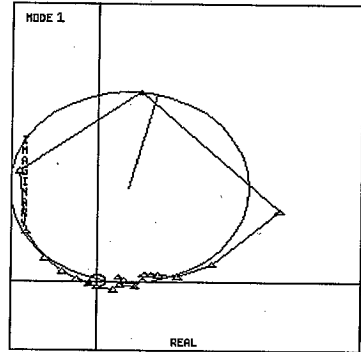
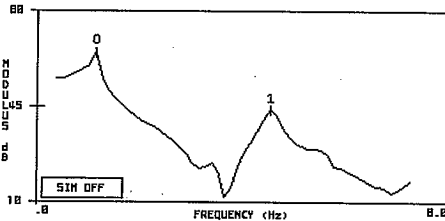


Fig A6.15 Driving Point Compliance for Test 7Y



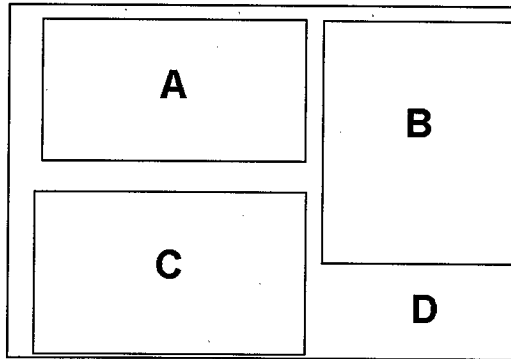
O-FIT FOR MODE 1
NAT. FREQUENCY (Hz) = 4.53
% STRUCTURAL DAMPING = 11.2967

Fig A6.16 Driving Point Compliance for Test 7Z

SECTION 7

DRIVING POINT INERTANCE

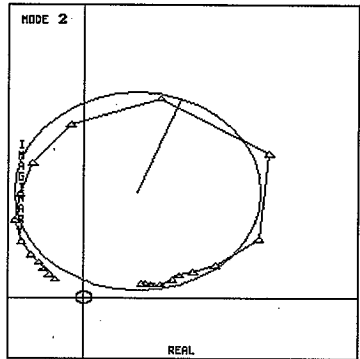
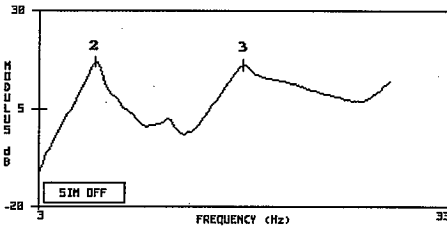
FIGURE No	TITLE	Page No.
A7.1	Key for Driving Point Inertance Plots.	A104
A7.2	Modal v Point Data Comparison. (Test 1Y Point Inertance 80018001)	A105
A7.3	Modal v Point Data Comparison. (Test 1Y Point Inertance 80018008)	A106
A7.4	Modal v Point Data Comparison. (Test 1Y Point Inertance 80018016)	A107
A7.5	1st Repeat of Test 1Y Point Inertance 80018001.	A108
A7.6	2nd Repeat of Test 1Y Point Inertance 80018001.	A109
A7.7	Driving Point Inertances for Test 2X.	A110
A7.8	Driving Point Inertances for Test 2aX.	A111
A7.9	Driving Point Inertances for Test 3X.	A112
A7.10	Driving Point Inertances for Test 3Y.	A113
A7.11	Driving Point Inertances for Test 3Z.	A114
A7.12	Driving Point Inertances for Test 4X.	A115
A7.13	Driving Point Inertances for Test 5X.	A116
A7.14	Driving Point Inertances for Test 5Y.	A117
A7.15	Driving Point Inertances for Test 5Z.	A118



KEY

- A** Driving Point Inertance frequency response function showing the mode numbers that have been identified.
X-axis Frequency (Hz)
Y-axis Modulus of Compliance (dB)
- B** Nyquist Plot showing real and imaginary parts of frequency response function of the mode shown in the top left hand corner.
X-axis Real part
Y-axis Imaginary part
- C** Carpet plot qualitatively showing deviation from text book viscous damping. There is a redundancy of information available allowing many independent estimates to be made of the damping. This plot shows these various damping estimates as the Y-axis. Classical viscous damping would produce a horizontal co-planar plot, whereas any deviation from this is indicative of non-linearities, noise, bad measurements etc.
- D** Data giving Identified Mode Number
Natural Frequency (Hz)
% Damping (Loss Factor)

Fig A7.1 Key for Driving Point Inertance Plots



O-FIT FOR MODE 2
NAT. FREQUENCY (Hz) = 7.80
% STRUCTURAL DAMPING = 15.5635

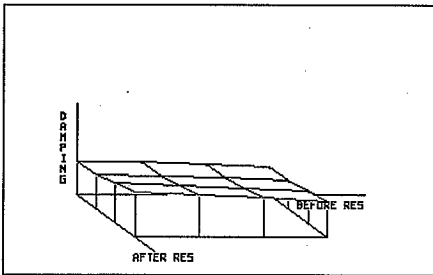
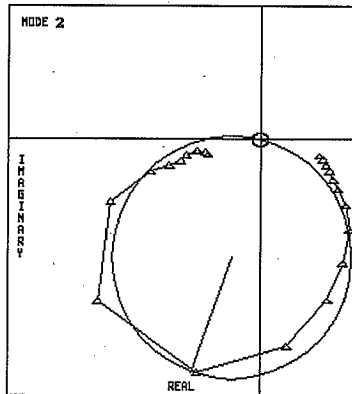
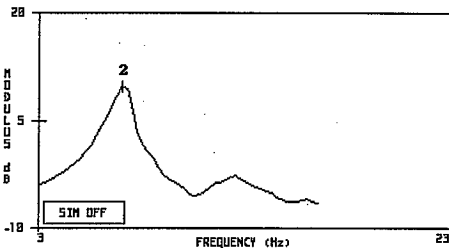


Fig A7.2 Modal v Point Data Comparison (Test 1Y Point Inertance 80018001)



O-FIT FOR MODE 2
 NAT. FREQUENCY (Hz) = 7.78
 % STRUCTURAL DAMPING = 16.6564

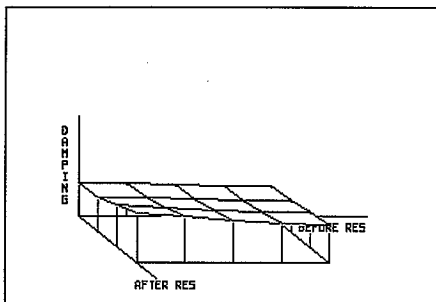
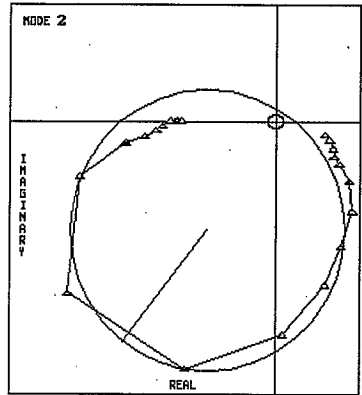
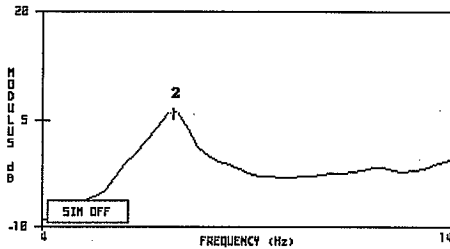


Fig A7.3 Modal v Point Data Comparison (Test 1Y Point Inertance 80018008)



O-FIT FOR MODE 2
 NAT. FREQUENCY (Hz) = 7.89
 % STRUCTURAL DAMPING = 12.4253

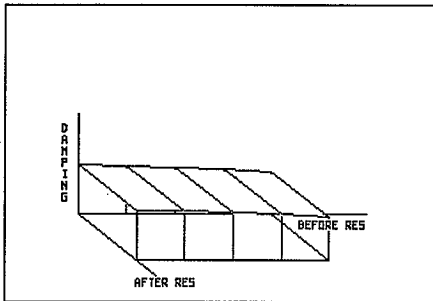
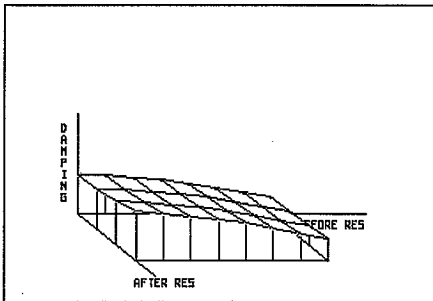
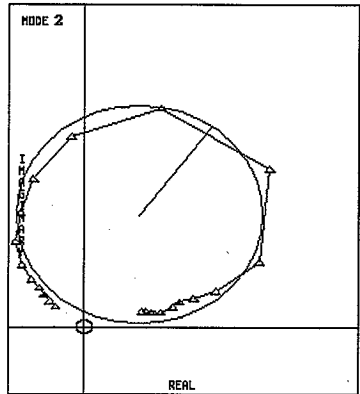
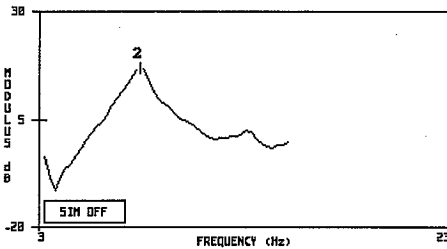
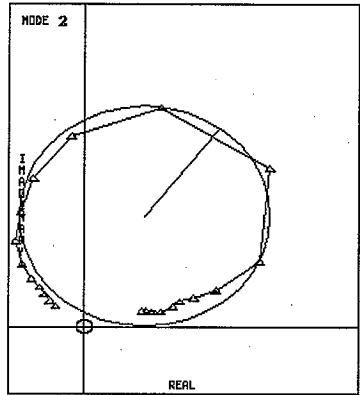
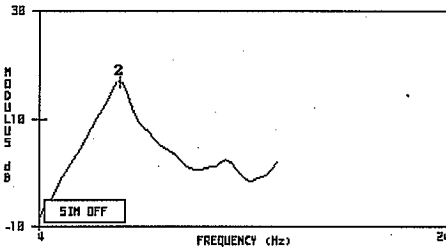


Fig A7.4 Modal v Point Data Comparison (Test 1Y Point Inertance 80018016)



O-FIT FOR MODE 2
NAT. FREQUENCY (Hz) = 7.88
% STRUCTURAL DAMPING = 10.8220

Fig A7.5 1st Repeat of Test 1Y Point Inertance 80018001



O-FIT FOR MODE 2
NAT. FREQUENCY (Hz) = 7.89
% STRUCTURAL DAMPING = 11.8266

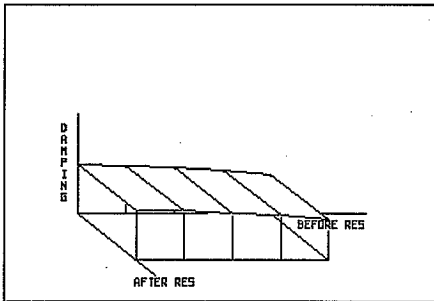


Fig A7.6 2nd Repeat of Test 1Y Point Inertance 80018001

Inertance m/s^2 per N

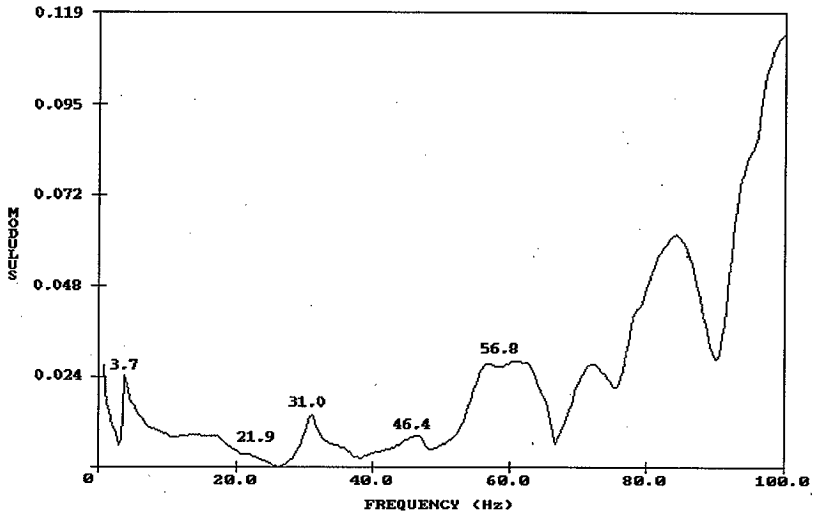


Fig A7.7 Driving Point Inertance for Test 2X

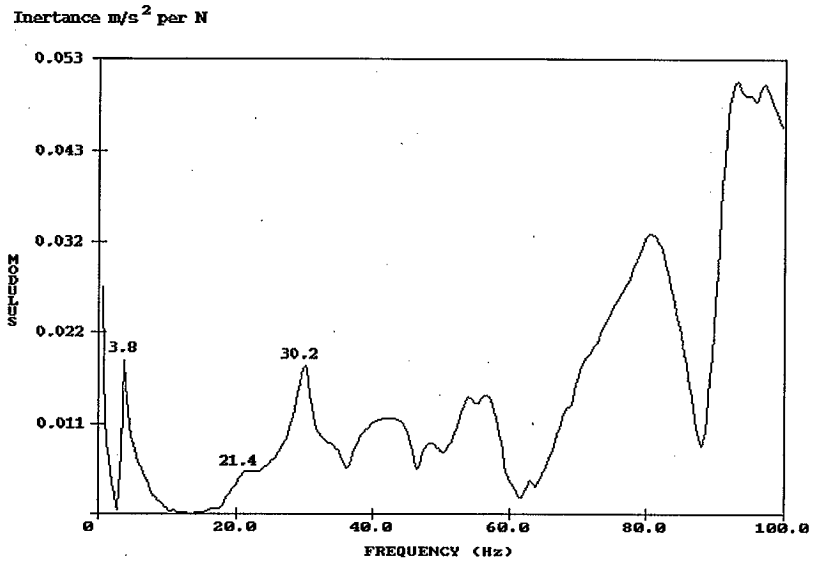


Fig A7.8 Driving Point Inertance for Test 2aX

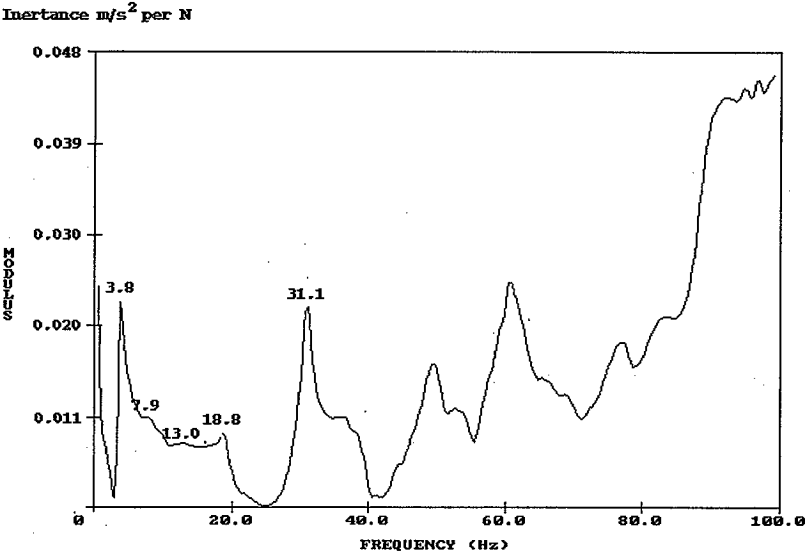


Fig A7.9 Driving Point Inertance for Test 3X

Inertance m/s^2 per N

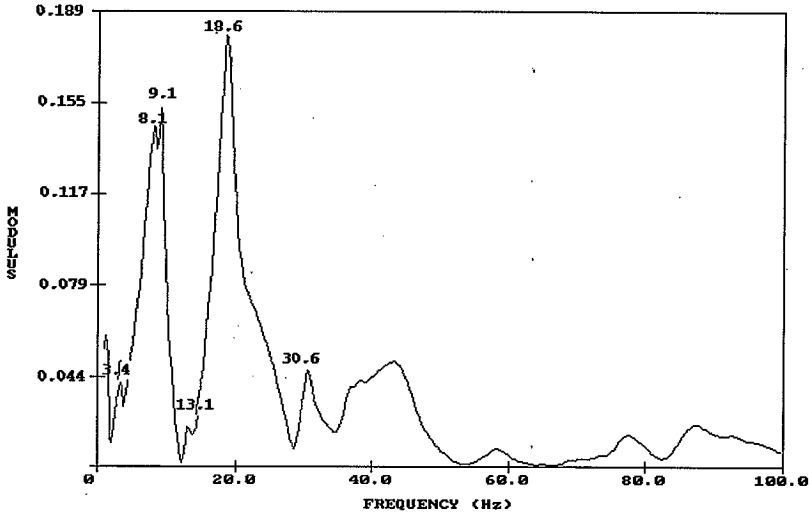


Fig A7.10 Driving Point Inertance for Test 3Y

Inertance m/s^2 per N

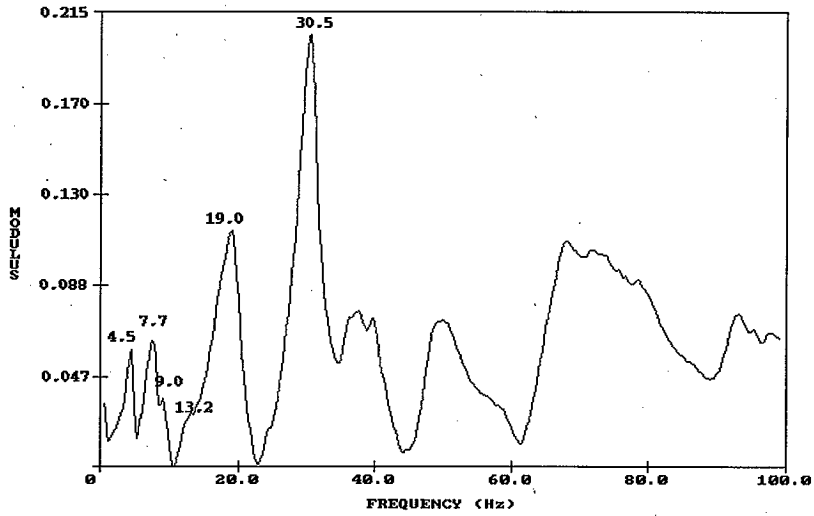


Fig A7.11 Driving Point Inertance for Test 3Z

Inertance m/s^2 per N

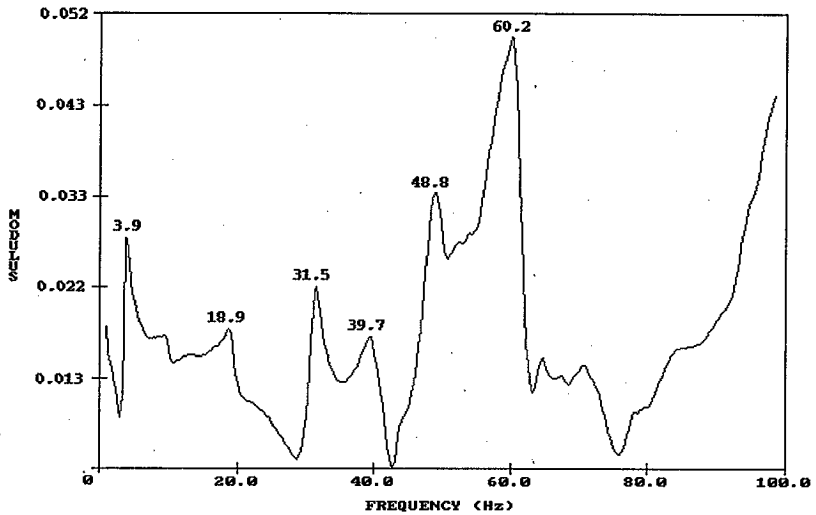


Fig A7.12 Driving Point Inertance for Test 4X

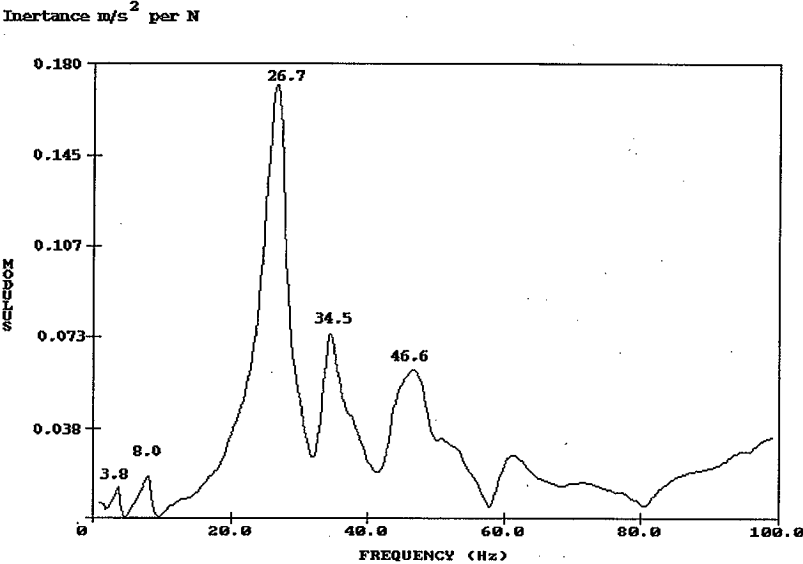


Fig A7.13 Driving Point Inertance for Test 5X

Inertance m/s^2 per N

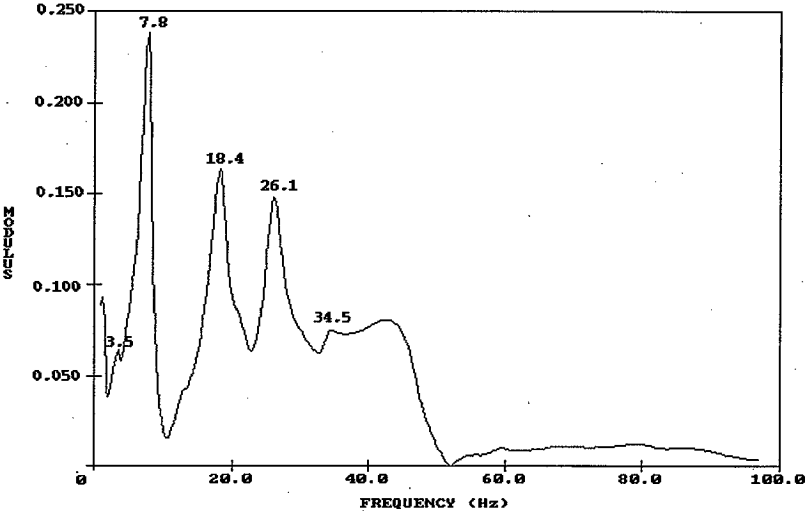


Fig A7.14 Driving Point Inertance for Test 5Y

Inertance m/s^2 per N

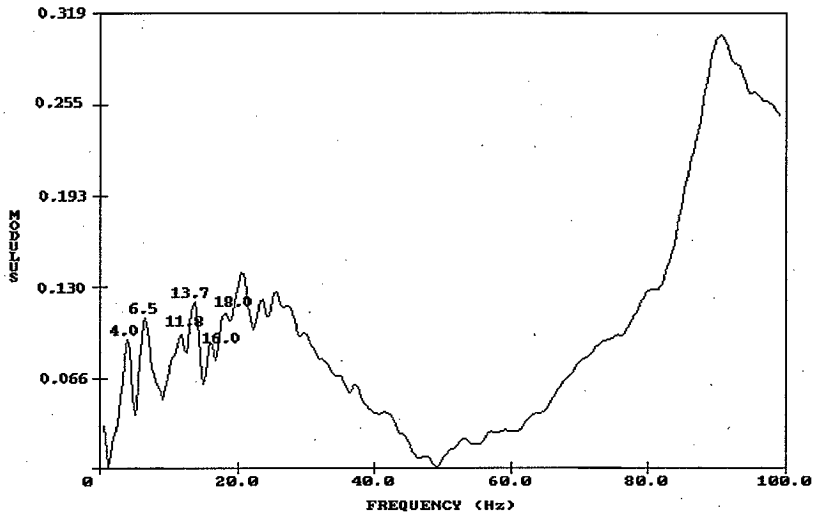


Fig. A7.15 Driving Point Inertances for Test 5Z

SECTION 8
SENSITIVITY TO LOADING

FIGURE No	TITLE	Page No.
A8.1	Static Loading in the \pm X Direction.	A120
A8.2	Static Loading in the \pm Y Direction.	A121
A8.3	Sensitivity to Dynamic loading in the X Direction.	A122
A8.4	Sensitivity to Dynamic loading in the Y Direction.	A123
A8.5	Sensitivity to Dynamic loading in the Z Direction.	A124

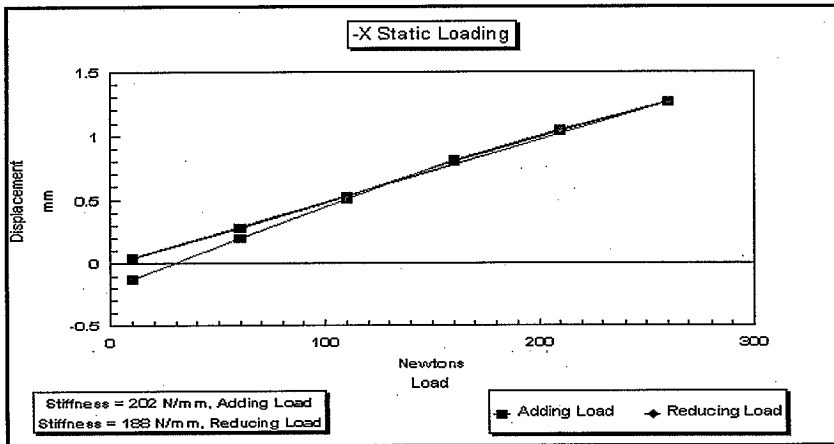
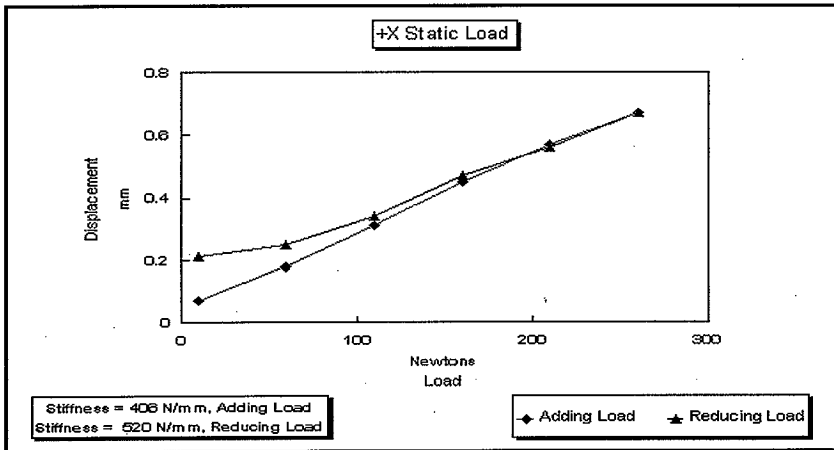


Fig A8.1 Static Loading in the ± X Direction

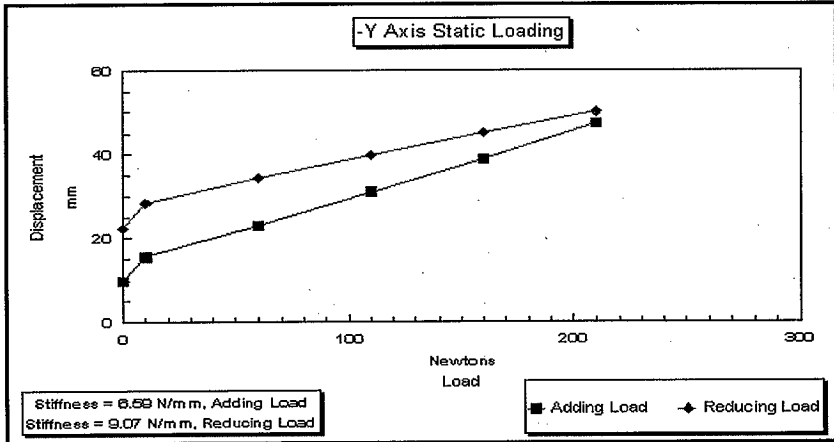
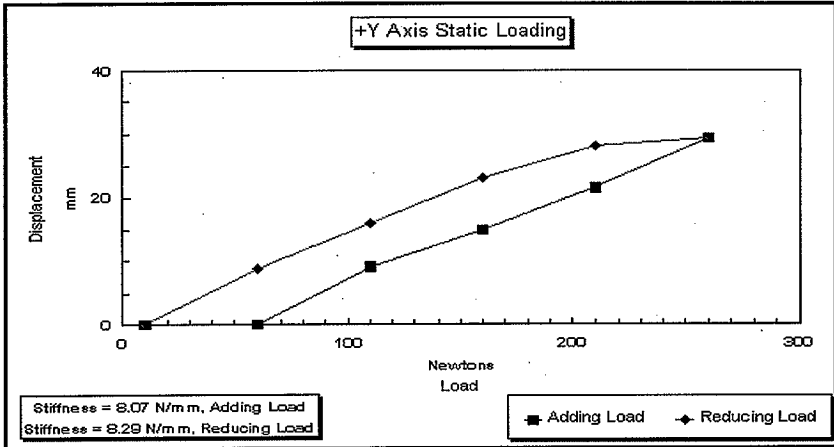


Fig A8.2 Static Loading in the \pm Y Direction

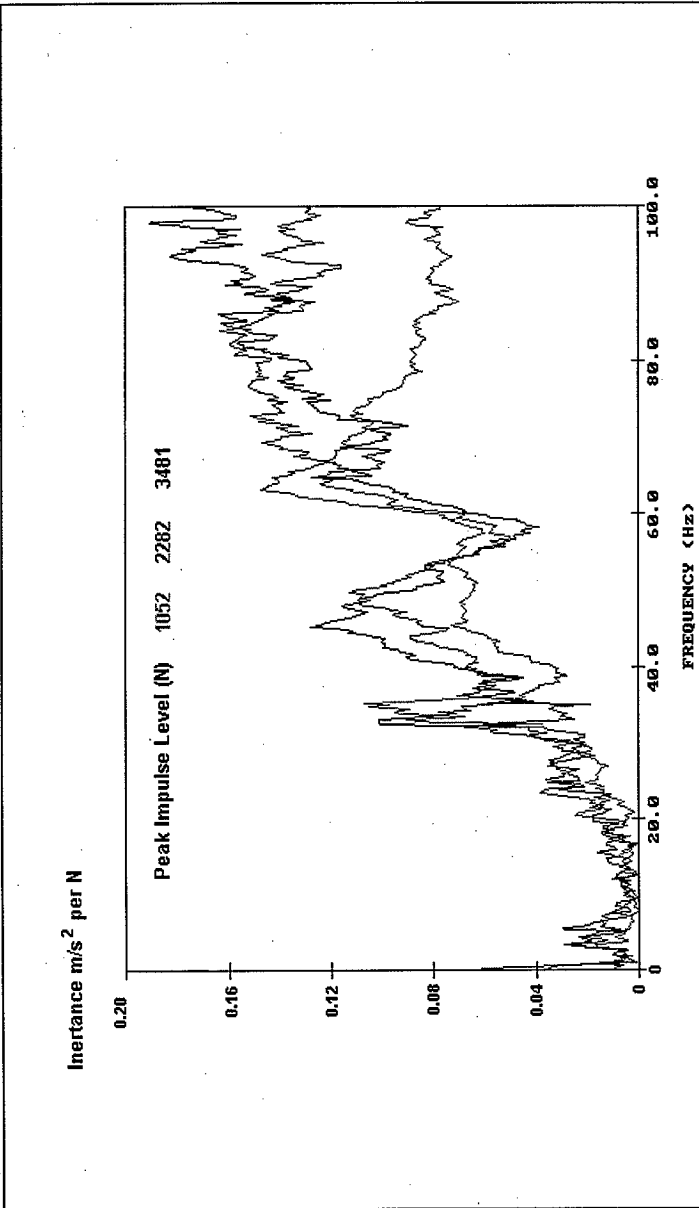


Fig 8.3 Sensitivity to Dynamic Loading in the X Direction

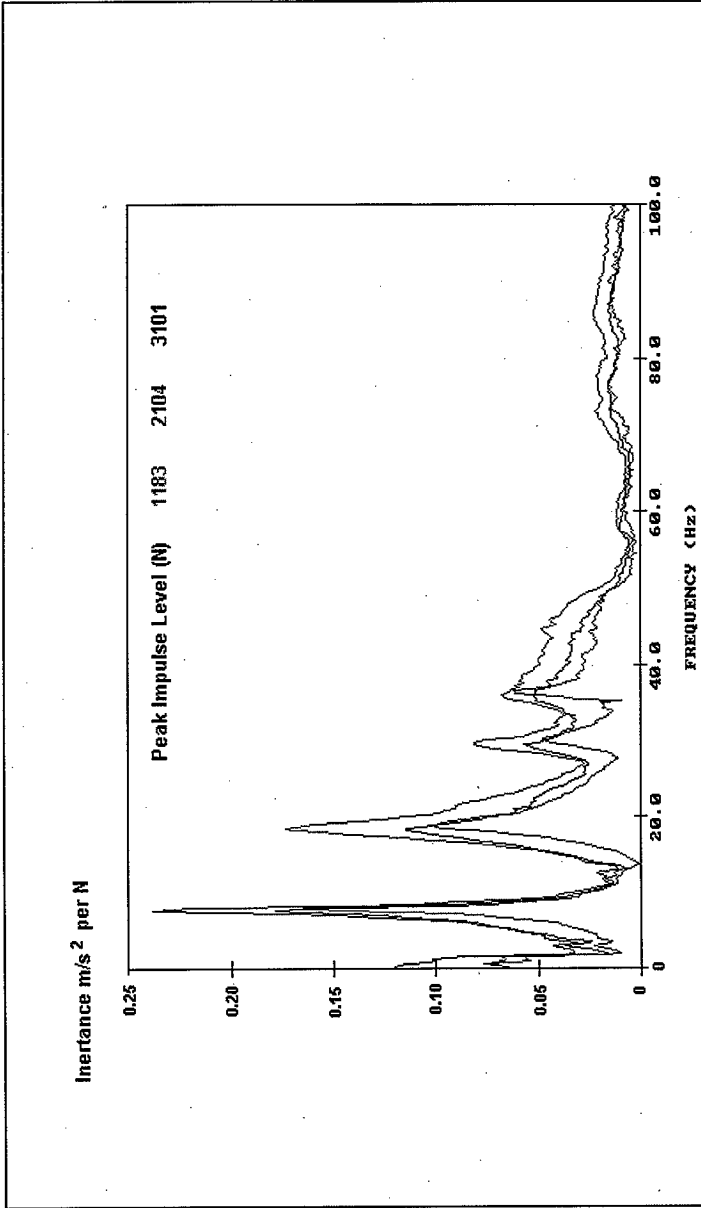


Fig 8.4 Sensitivity to Dynamic Loading in the Y Direction

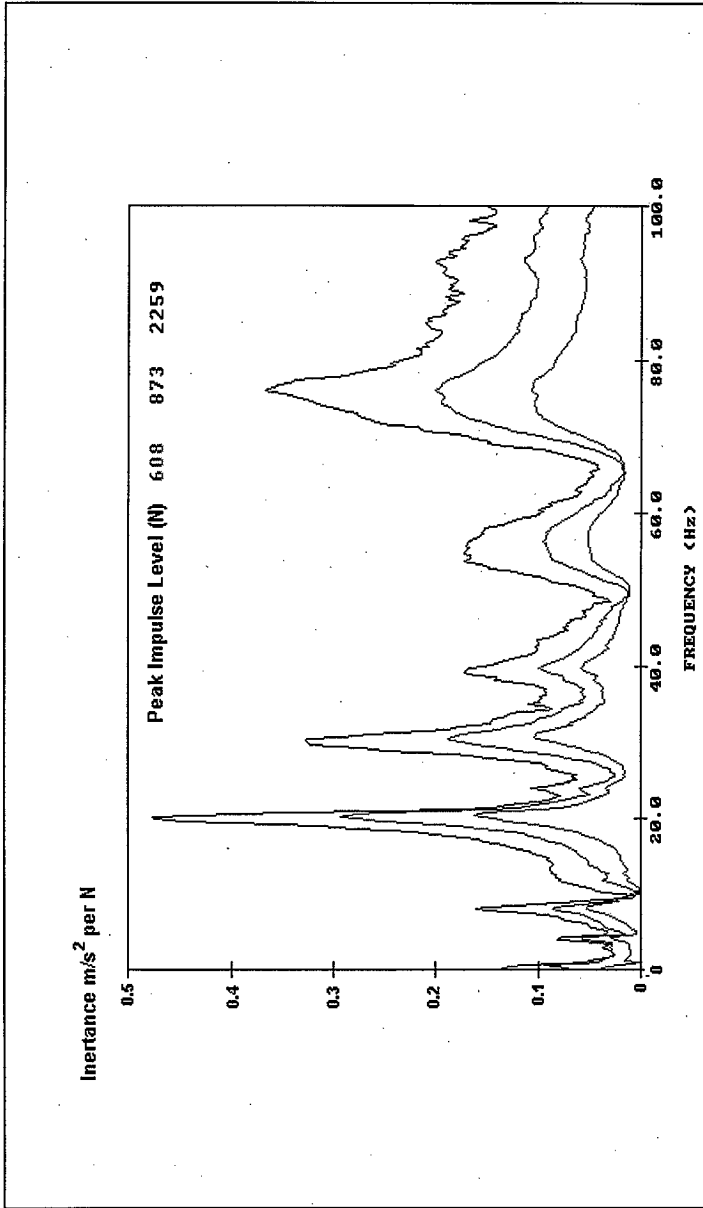


Fig A8.5 Sensitivity to Dynamic loading in the Z Direction

APPENDIX B
SLUICER DATA

Section No	CONTENTS	Page No.
1	Test Notation and Definitions.	B2
2	Instrumentation.	B8
3	Low frequency Data.	B14
4	High Frequency Data.	B34A
5	Photographs.	B52
6	Manufacturer's Information.	B67

TEST NOTATION AND DEFINITIONS

FIGURE No	TITLE	Page No.
B1.1	Confined Sluicer for Hanford Tests.	B3
B1.2	Sluicer and Backhoe Interface.	B4
B1.3	Test Site Layout.	B5
B1.4	Pump and Piping Layout.	B6
B1.5	Summary of Test Runs.	B7

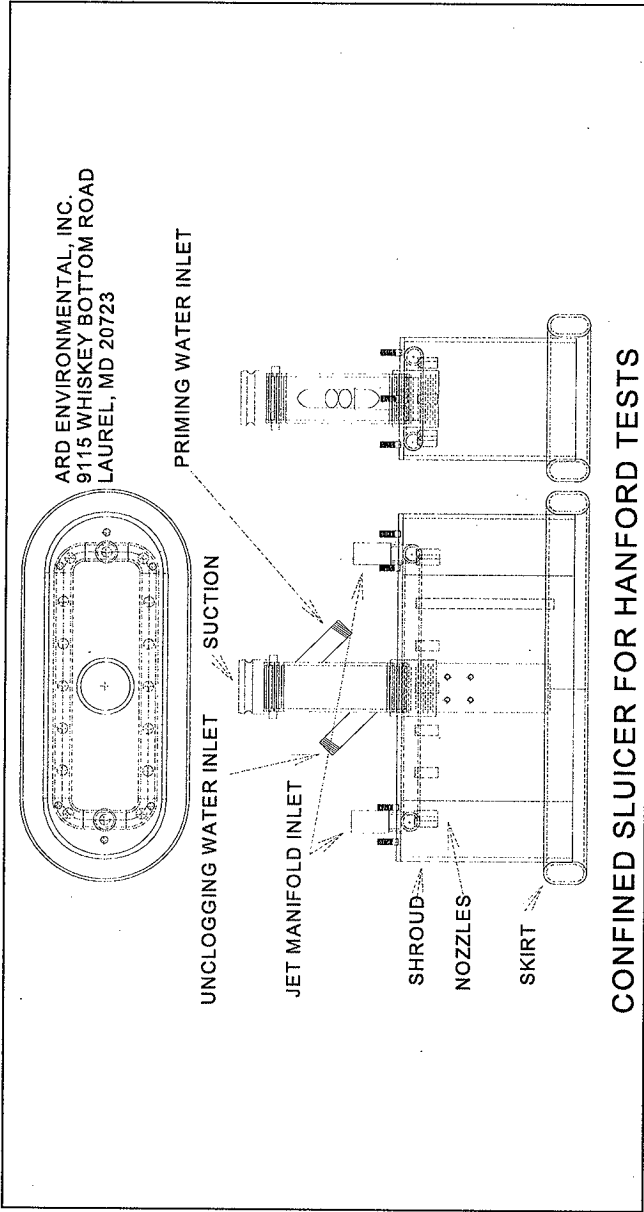


Fig B1.1

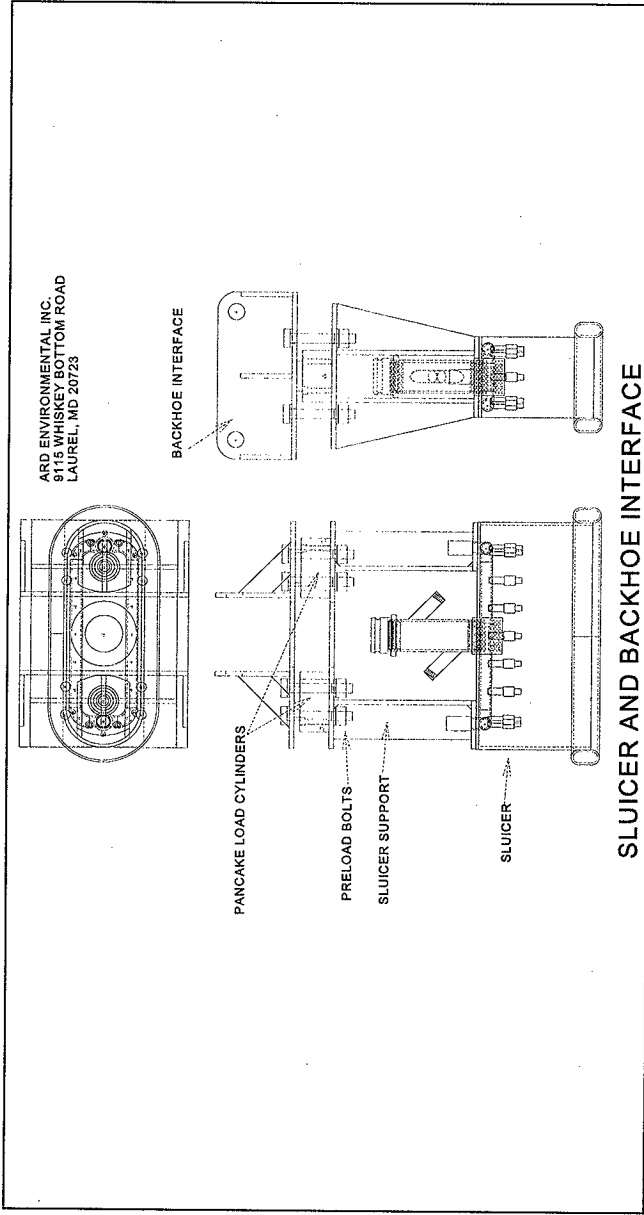


Fig B1.2

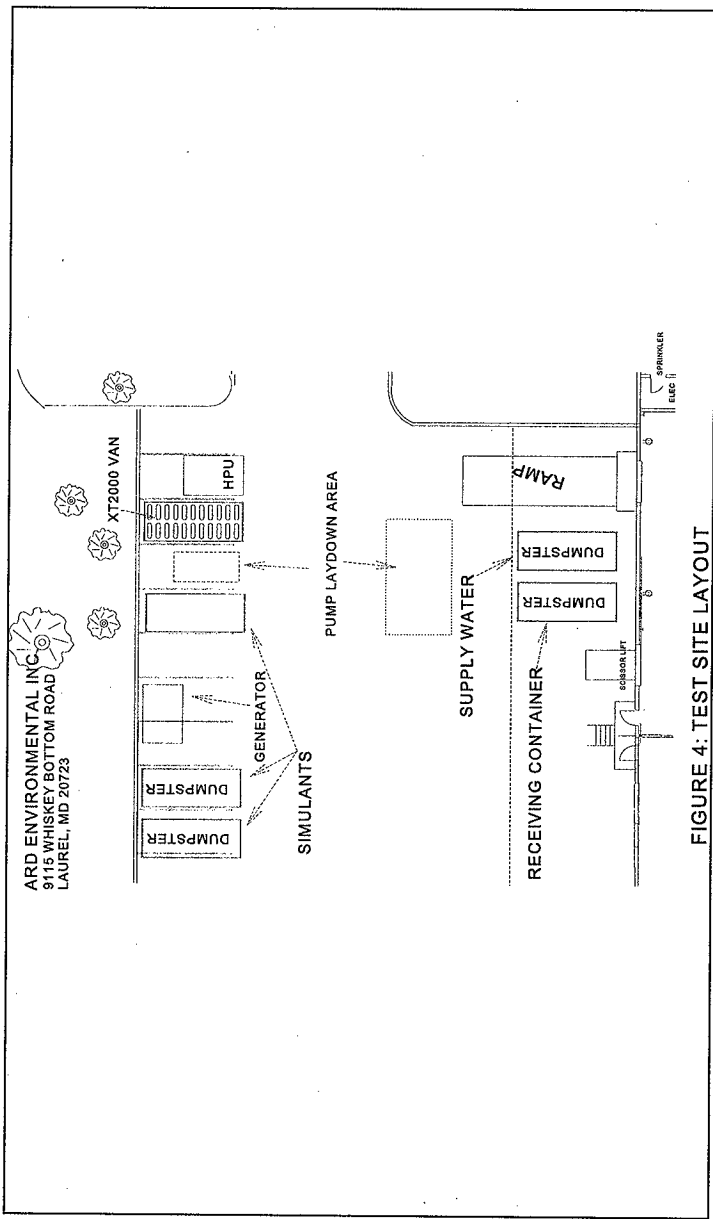


FIGURE 4: TEST SITE LAYOUT

Fig B1.3

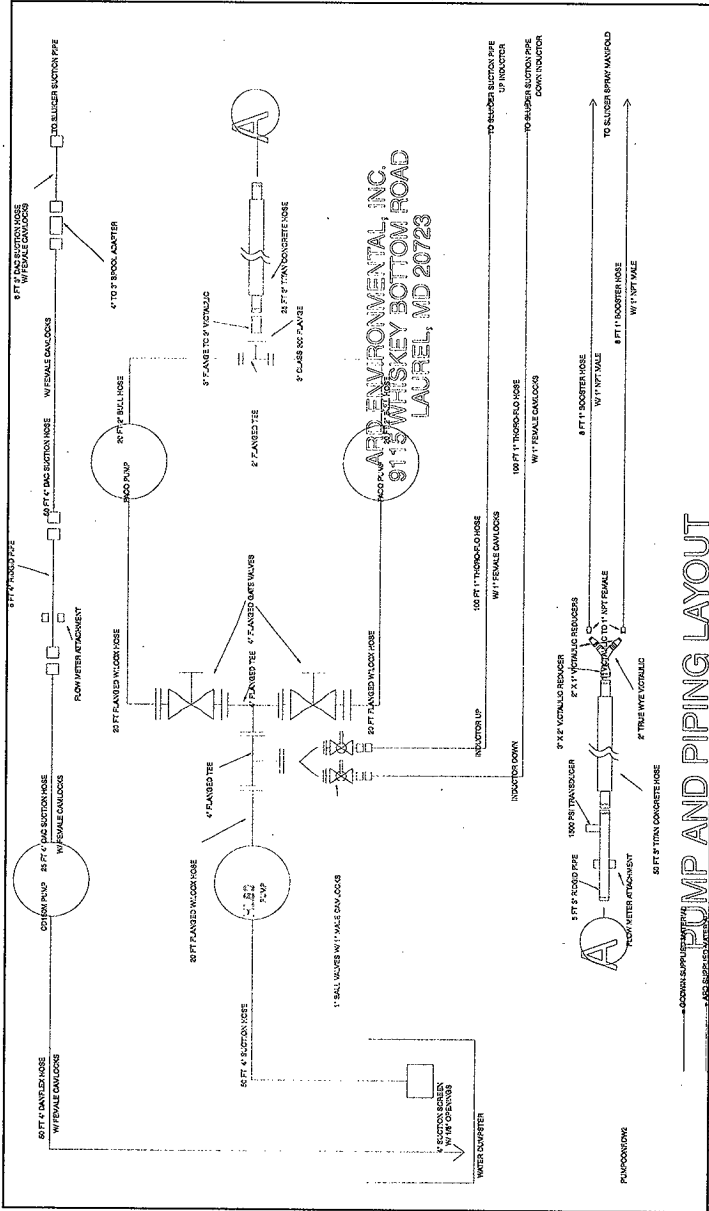


Fig B1.4

SUMMARY OF TEST RUNS - SLUICER ON BACKHOE				
TEST # AND DESCRIPTION	DATA RUNS	FIGURES	DESCRIPTION	LABVIEW FILES
1: STATIC THRUST	N/A	N/A	SLUICER SUSPENDED FROM LOAD CELL	N/A
2: SALTCAKE		LF1,2 LF3,4 LF5,6 LF7,8 LF9,10	LF1,2,3,4 HF5,6 HF7	SSLUICE1.BIN SSLUICE2.BIN SSLUICE3.BIN SSLUICE4.BIN SSLUICE5.BIN
3: BLOCKED SHROUD		LF11,12 LF13,14 LF15,16	HF9 HF10,11,12 HF13	SSLUICE7.BIN SSLUICE8.BIN SSLUICE9.BIN
4: HARDPAN	10	LF17,18 HF14,15,16	SLUICER ON BACKHOE OPERATING AGAINST SIMULANT SLAB	SSLUICE10.BIN

NOTE: INSTRUMENTATION WAS AS SHOWN IN FIGURE 7 FOR TESTS 2,3,4. LOAD CELL ONLY FOR TEST 1.

SUMMARY OF TEST RUNS

Fig B1.5

SECTION 2
INSTRUMENTATION

FIGURE No	TITLE	Page No.
B2.1	Sluicer Jet Characteristics.	B9
B2.2	Sensor Type, Range and Location.	B10
B2.3	Hanford Hardware Instrumentation Diagram.	B11
B2.4	Labview Data Acquisition.	B12
B2.5	Labview Data Analysis.	B13

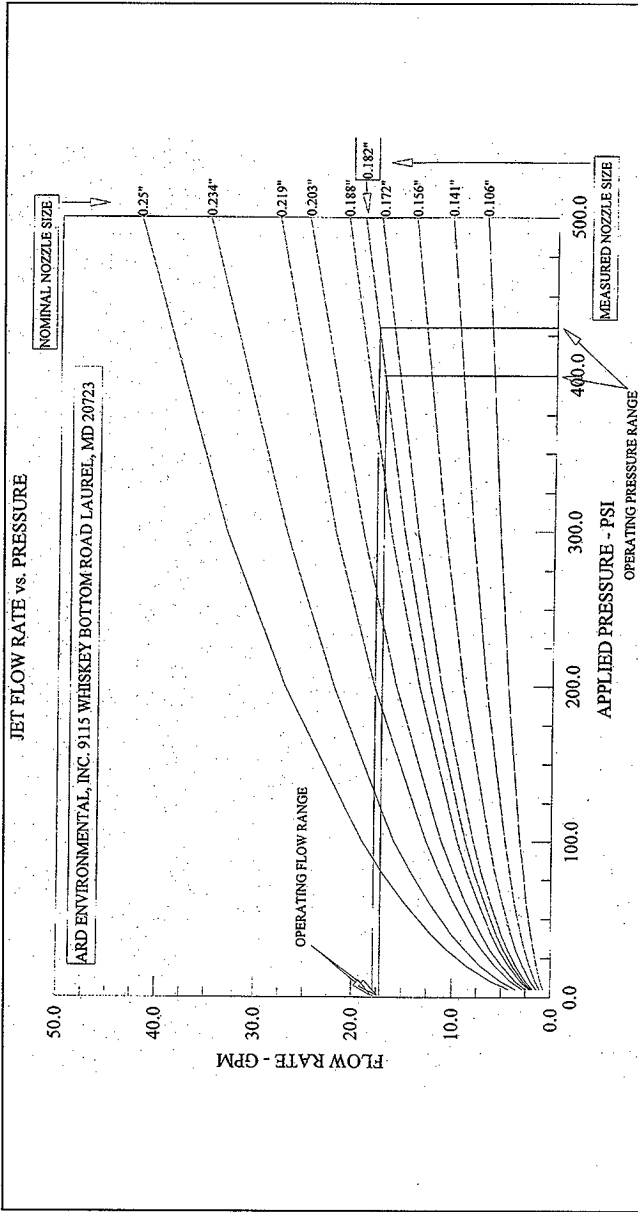


Fig B2.1 SLUICER JET CHARACTERISTICS (Based on manufacturers information)

ARD ENVIRONMENTAL, INC. 9115 WHISKEY BOTTOM ROAD LAUREL, MD 20723

CHANNEL	LOCATION	DESCRIPTION	SPECIFICATION	RANGE
00	SLUICER SHROUD (X)	TRIAXIAL ACCELEROMETER	10 mV/g	500 g
01	SLUICER SHROUD (Y)	TRIAXIAL ACCELEROMETER	10 mV/g	500 g
02	SLUICER SHROUD (Z)	TRIAXIAL ACCELEROMETER	10 mV/g	500 g
04	4" SUCTION TO DUMPSTER	FLOW METER W/TRANSMITTER	4-20 ma	600 GPM
05	3" CLEAN WATER FEED	FLOW METER W/TRANSMITTER	4-20 ma	600 GPM
06	SLUICER - LOADCELL	PRESSURE TRANSMITTER	4-20 ma	1500 PSI
07	SLUICER: WATER FEED	PRESSURE TRANSMITTER	4-20 ma	750 PSI
16	SLUICER: WATER SHROUD PRESSURE FEED	PRESSURE TRANSMITTER	4-20 ma	3000 PSI

SENSOR TYPE, RANGE AND LOCATION

Fig B2.2

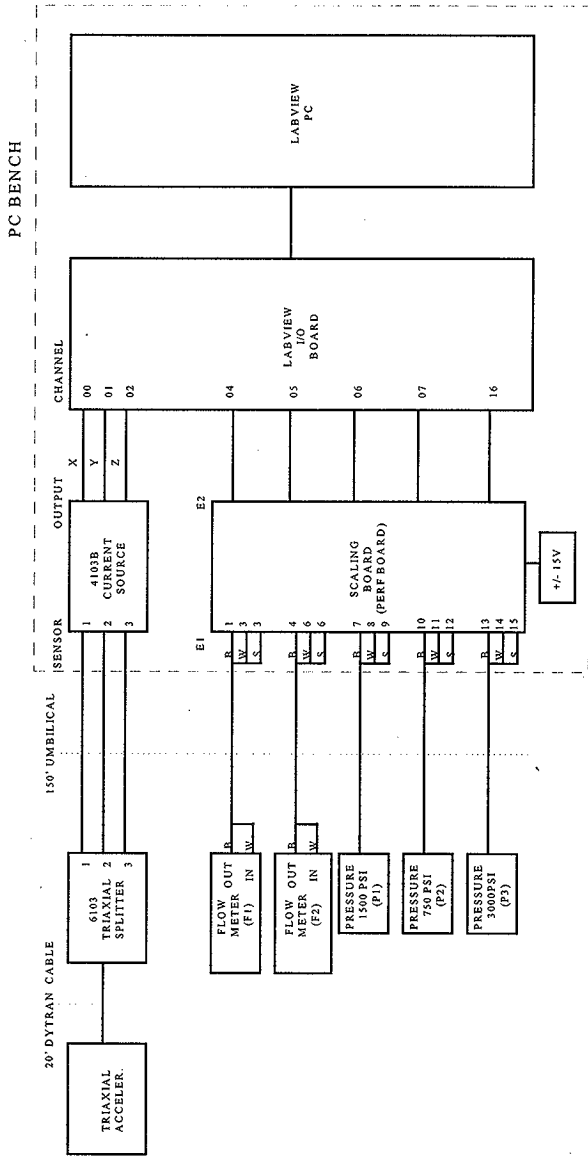


Figure 7. HANFORD HARDWARE INSTRUMENTATION DIAGRAM

Fig B2.3

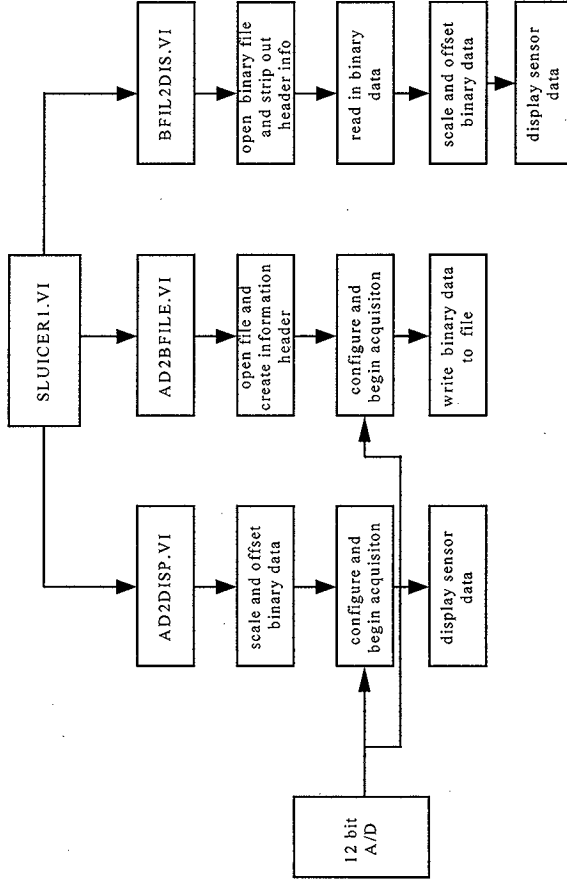


Figure 8. LABVIEW DATA ACQUISITION

Fig B2.4

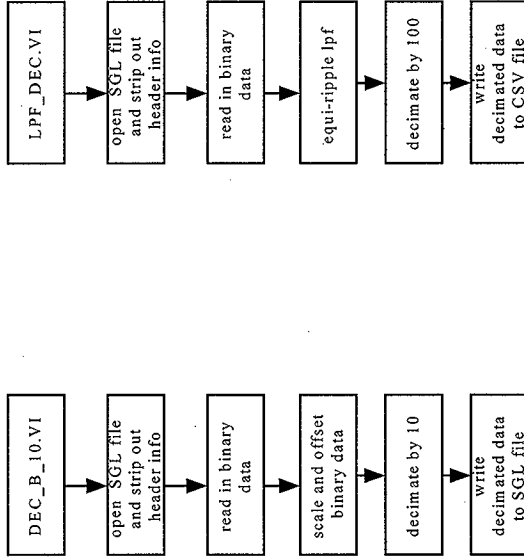


Figure 9. LABVIEW DATA ANALYSIS

SECTION 3

LOW FREQUENCY DATA

FIGURE No	CONTENTS	Page No.
LF1	Sluicer Test 2, Run 1: Saltcake.	B17
LF2	Sluicer Test 2, Run 1: Saltcake.	B18
LF3	Sluicer Test 2, Run 2: Saltcake.	B19
LF4	Sluicer Test 2, Run 2: Saltcake.	B20
LF5	Sluicer Test 2, Run 3: Saltcake.	B21
LF6	Sluicer Test 2, Run 3: Saltcake.	B22
LF7	Sluicer Test 2, Run 4: Saltcake.	B23
LF8	Sluicer Test 2, Run 4: Saltcake.	B24
LF9	Sluicer Test 2, Run 5: Saltcake.	B25
LF10	Sluicer Test 2, Run 5: Saltcake.	B26
LF11	Sluicer Test 3, Run 7: Blocked Shroud No Suction.	B27
LF12	Sluicer Test 3, Run 7: Blocked Shroud No Suction.	B28
LF13	Sluicer Test 3, Run 8: Blocked Shroud, Suction.	B29
LF14	Sluicer Test 3, Run 8: Blocked Shroud, Suction.	B30
LF15	Sluicer Test 4, Run 9: Blocked Shroud And Suction.	B31
LF16	Sluicer Test 3, Run 9: Blocked Shroud And Suction.	B32
LF17	Sluicer Test 4, Run 10: Hardpan.	B33
LF18	Sluicer Test 4, Run 10: Hardpan.	B34

Low Frequency Data

Each data run is shown in two graphs, see Figs LF1 to LF18. For runs 1 through 4, the first graph is the time series data for one of the horizontal accelerometers (Ay), the vertical accelerometer (Az), the load cylinder pressure (Pl) and the water pressure (Pw) to the sluicer. For runs 5 through 10, the times series data are Ay, Az, Pl and the pressure in the shroud, Ps.

The second graph for runs 1 through 4 are the FFT spectra for Ay, Az, and the cross-power spectrum of Ay*Az. For runs 5 through 10, the FFT spectrum of the shroud pressure is also shown.

The triaxial accelerometers have -3 db points at 0.32 Hz for Ax and Ay, and 0.4 Hz for Az. The table below shows the multiplier as a function of frequency to correct for the low frequency response of the accelerometers.

f (Hz)	0.1	0.2	0.3	0.4	0.5	0.6	0.7	0.8	0.9	1.0
Ax,Ay	3.35	1.89	1.46	1.28	1.19	1.13	1.10	1.08	1.06	1.05
Az	4.12	2.24	1.67	1.41	1.28	1.20	1.15	1.12	1.09	1.08

Runs 1

through 4: The acceleration levels in the low frequency data are very low, and generally random. Some energy appears to be coherent from about 0.18 to 0.28 Hz, but the levels are very low. The preload in the load cylinders was set at a nominal value of 200 psi, however this was not done correctly in run 1. The load cylinder data reflects the forces that were applied by the backhoe. The water pressure supplied to the shroud was essentially constant at 430 psi.

Run 5: Some low level coherent energy at around 0.38 Hz in the accelerometer data, the spectrum of the shroud pressure shows no coherent energy.

Run 6: This run was aborted and there are no test data.

Run 7: No coherent energy in any of the spectra. There is a correlation in the time series data between the rise in shroud pressure and the increase in load cylinder pressure. However, the shroud pressure rose because the sluicer was being pressed against the ground by the backhoe, and is the effect, not the cause.

Run 8: The acceleration levels increase towards the end of the run, corresponding to increased shroud pressure. This is due to the increased levels of turbulence as the shroud is pressed against the ground. The maximum shroud pressure achieved was about 25 psi. The spectra show no coherence in the data, supporting the supposition that the accelerations are due to turbulence.

Run 9: The acceleration levels increase towards the middle of the run, corresponding to increased shroud pressure. This is due to the increased levels of turbulence as the shroud is pressed against the ground. The maximum shroud pressure achieved was about 25 psi. The spectra show no coherence in the data, supporting the supposition that the accelerations are due to turbulence.

Run 10: The spectra show a spike of coherent energy at about 0.1 Hz. The time series acceleration data show a large transient about 40 seconds into the run, and about 10 seconds in duration. This is the only record that exhibits this type of feature, and is also the only record of sluicing in hardpan, however the cause of the transient is unknown.

SLUICER TEST 2, RUN 1: SALTCAKE

D1A.DW2

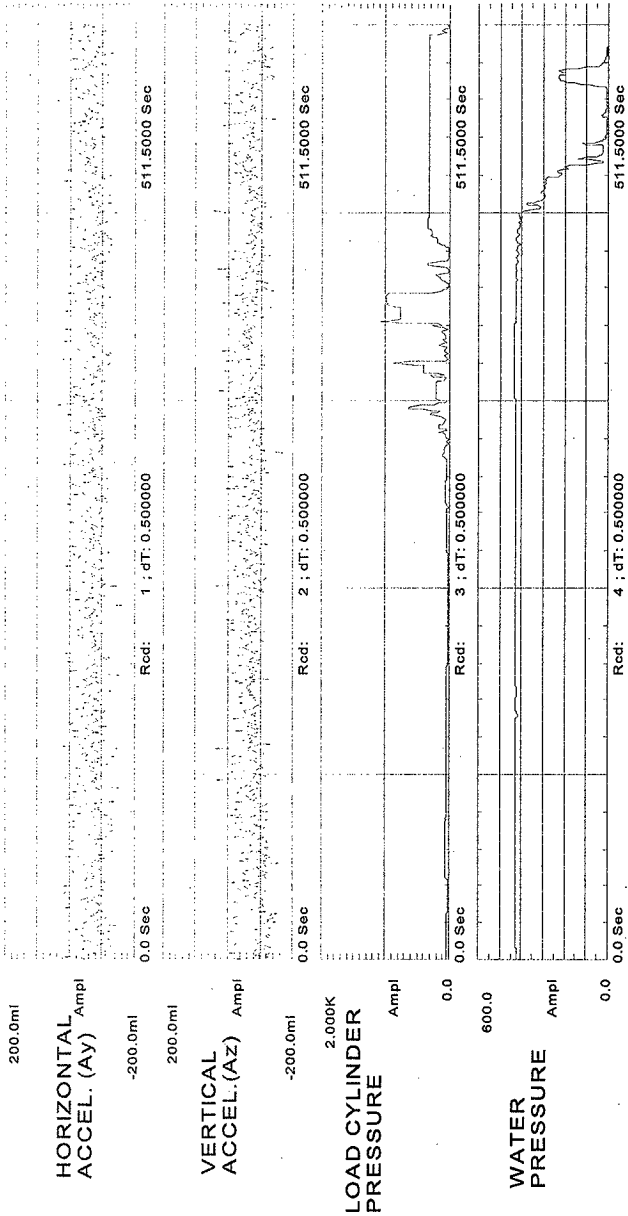


FIGURE LF1

ARD ENVIRONMENTAL, INC.

SPLICER TEST 2, RUN 1, SALTCAKE

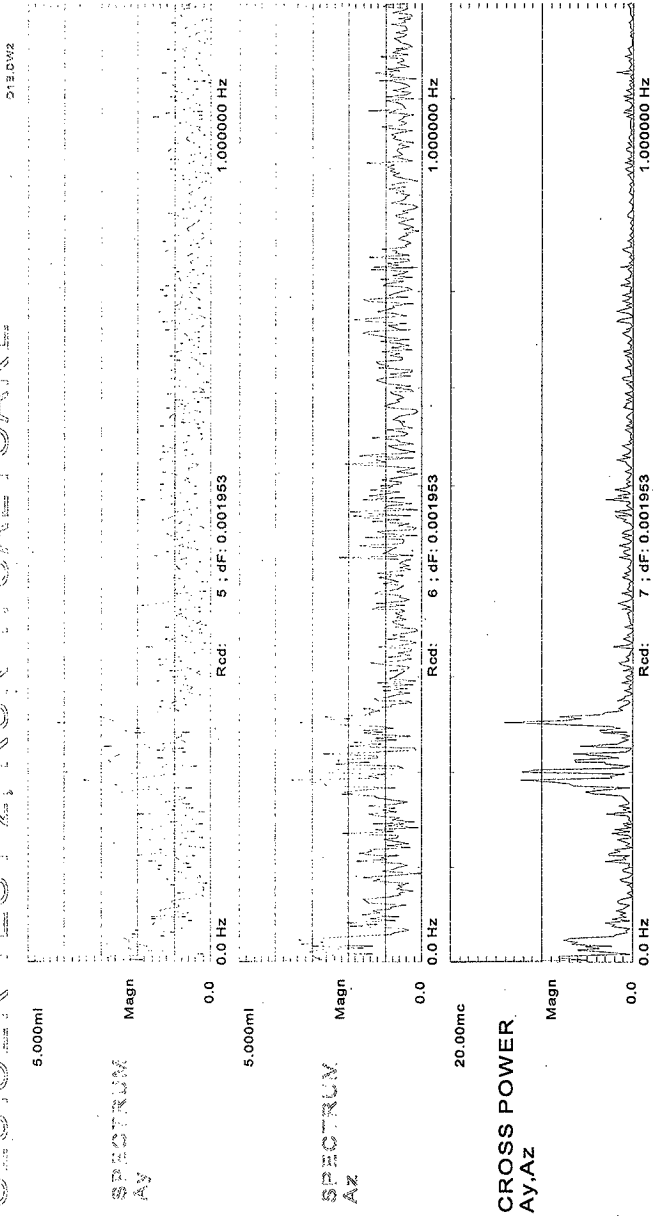


FIGURE LF2

ARD ENVIRONMENTAL, INC.

SLUICER TEST 2; RUN 2; SALTCAKE

SEP 01/92

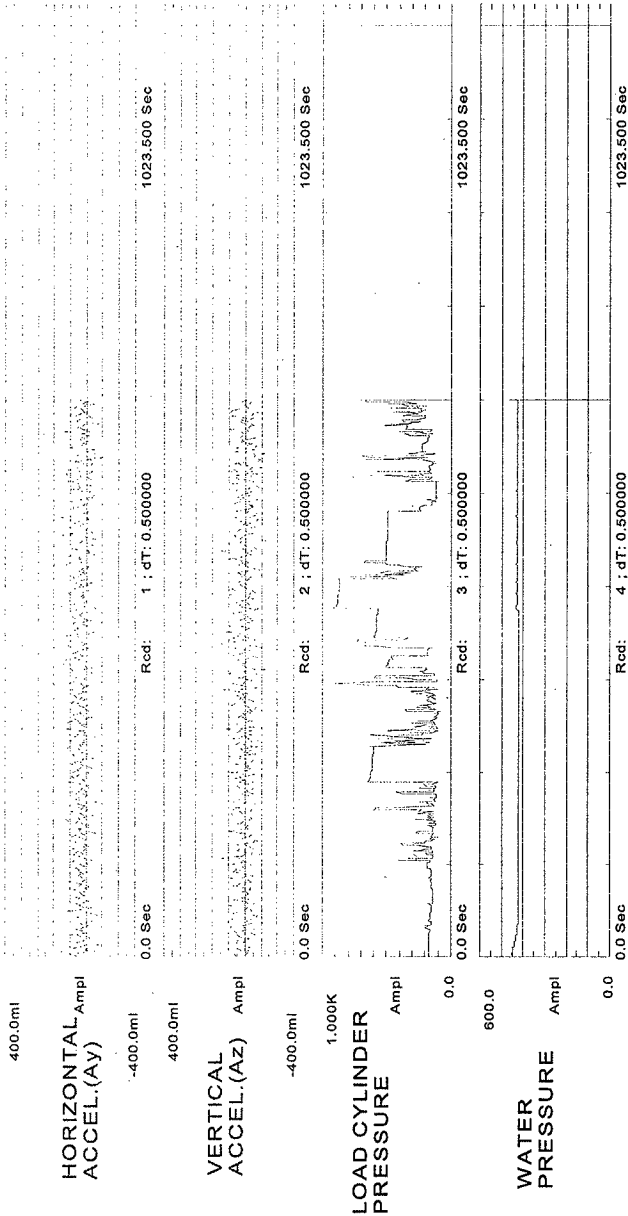


FIGURE LF3

ARD ENVIRONMENTAL, INC.

SPLICER TEST 2, RUN 2: SALTCAKE

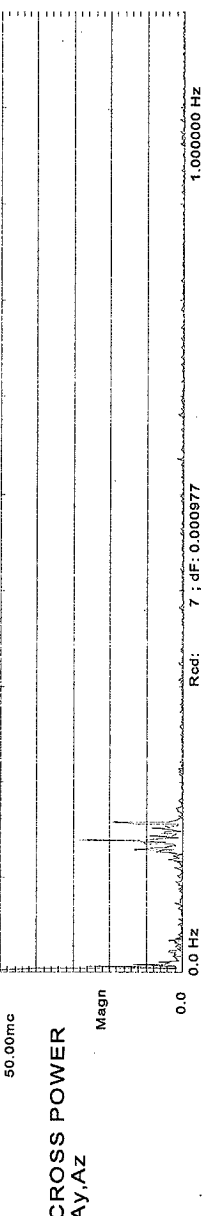
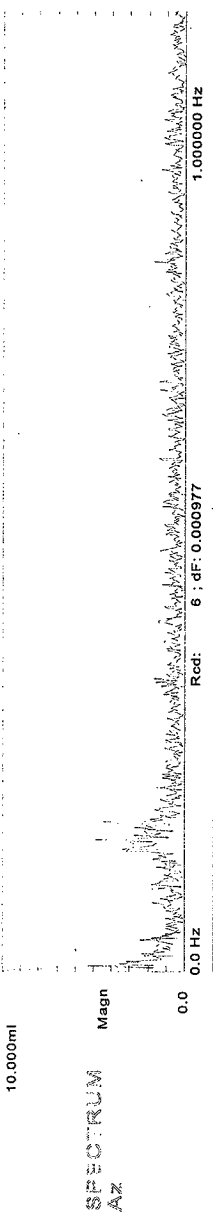
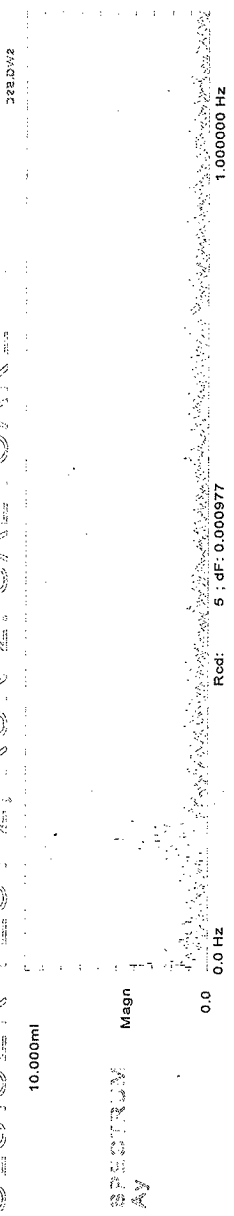


FIGURE LF4

ARD ENVIRONMENTAL, INC.

SLUICER TEST 2, RUN 3: SALTCAKE

38A.DV2

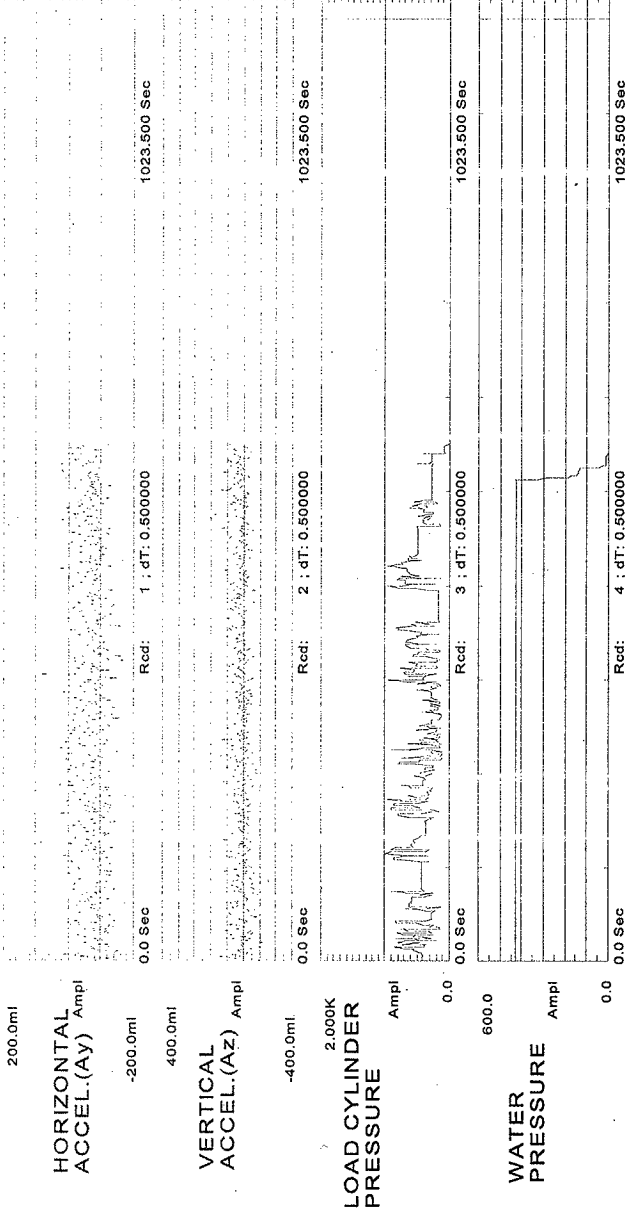


FIGURE LF5

ARD ENVIRONMENTAL, INC.

SPLICER TEST 2, RUN 3: SALTCAKE

538 DIV2

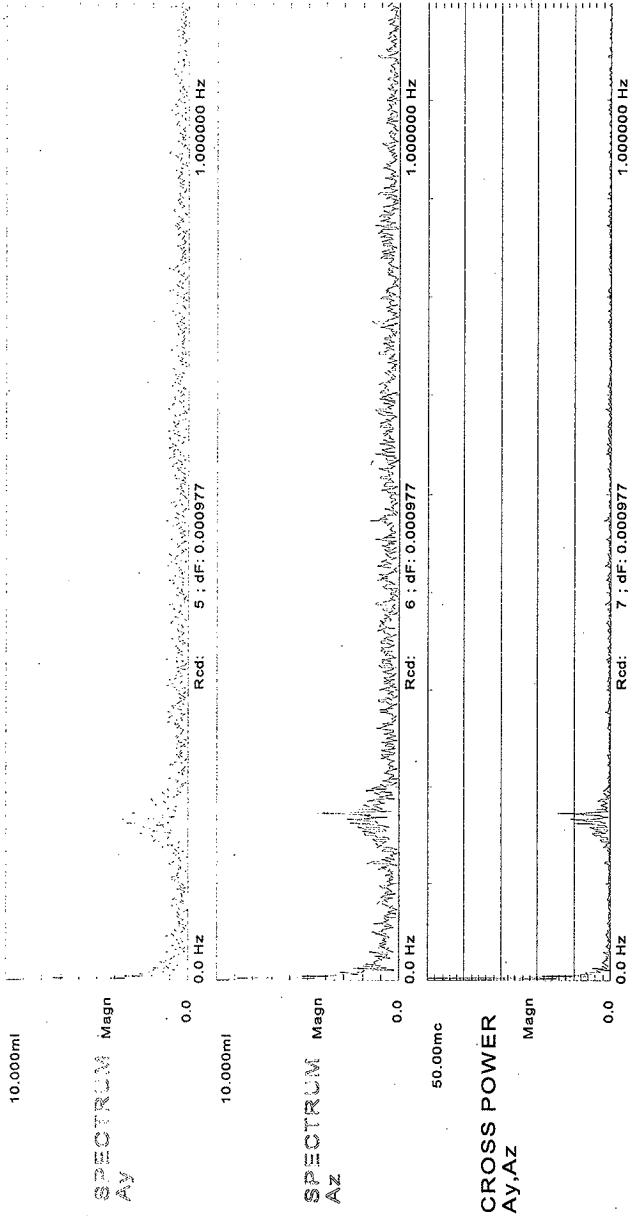


FIGURE LF6

ARD ENVIRONMENTAL, INC.

SLUICER TEST 2, RUN 4: SALTCAKE

34A.DW2

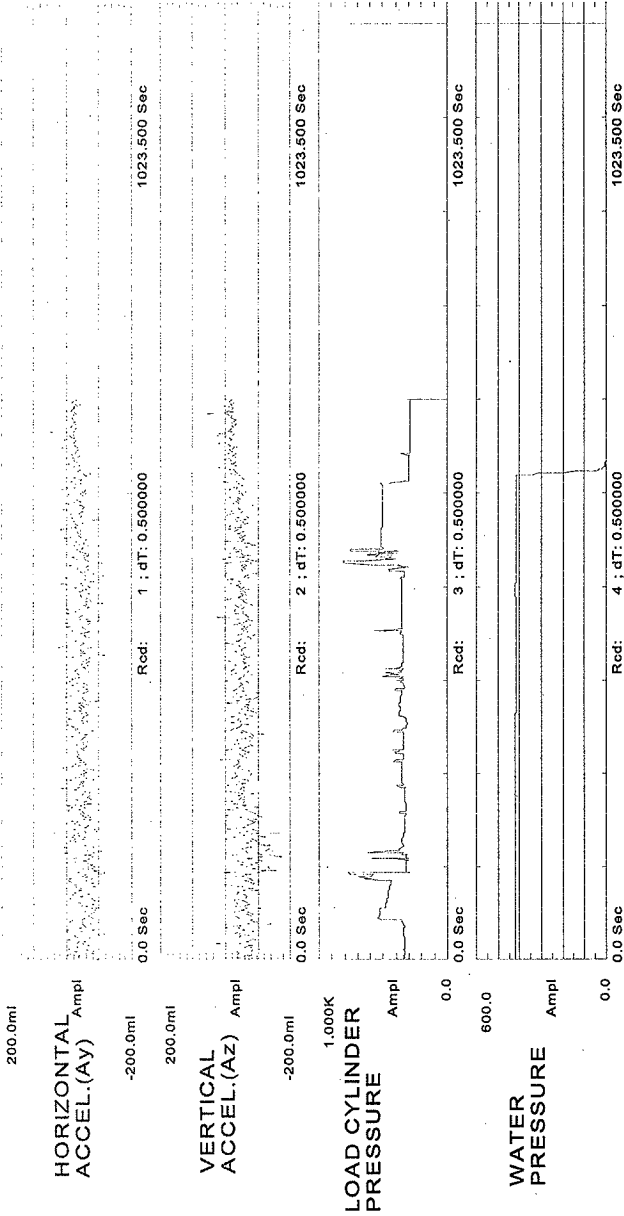


FIGURE LF7

ARD ENVIRONMENTAL, INC.

SLICER TEST 2, RUN 4: SALTCAKE

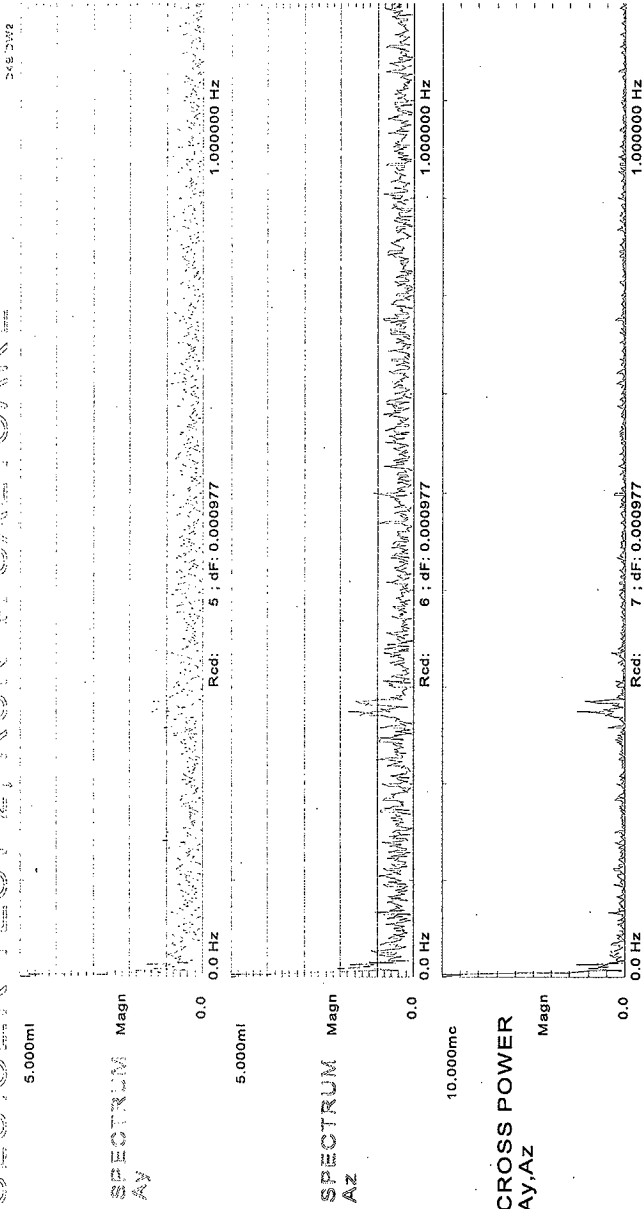


FIGURE LFB

ARD ENVIRONMENTAL, INC.

SLUICER TEST 2, RUN 3: SALTCAKE

36A.DV2

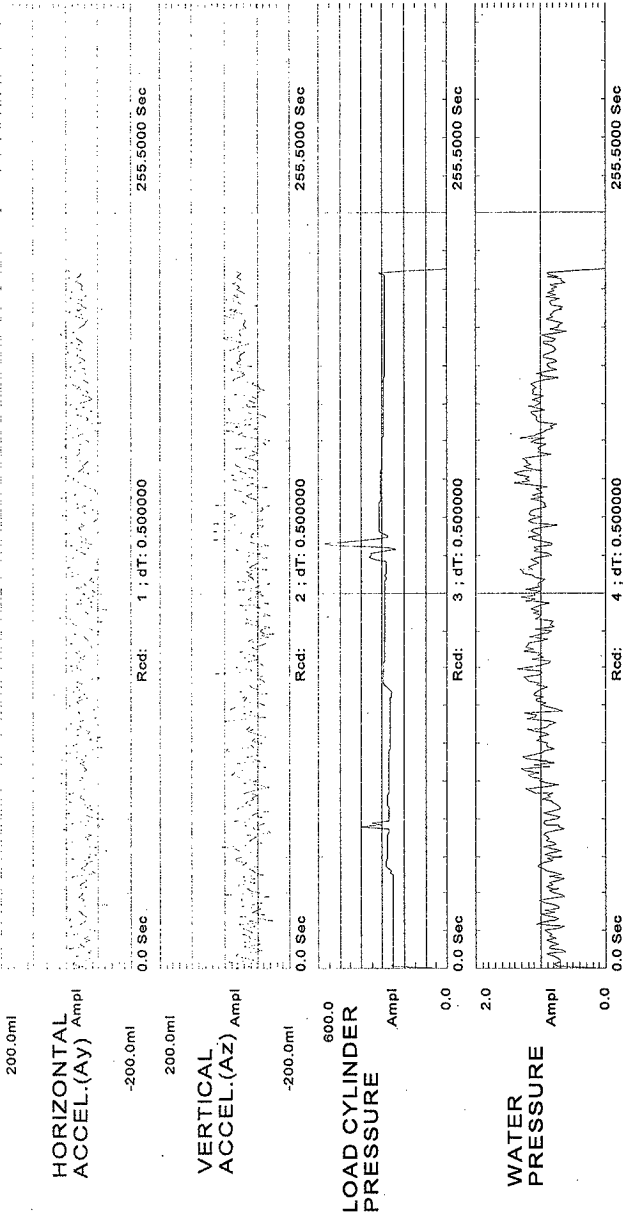


FIGURE LF9

ARD ENVIRONMENTAL, INC.

SLUICER TEST 2, RJN 5: SALT CAKE

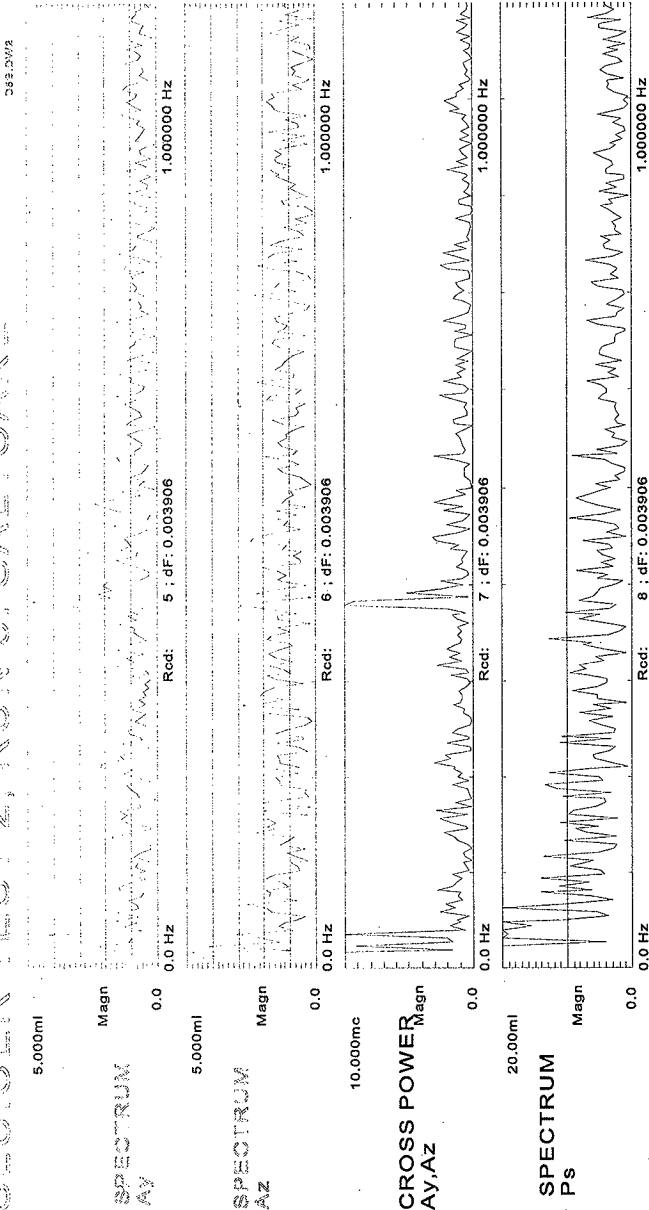


FIGURE LF10

ARD ENVIRONMENTAL, INC.

SLUGGER TEST 3, RUN 7; BLOCKED SHROUDING

07A.DP#E

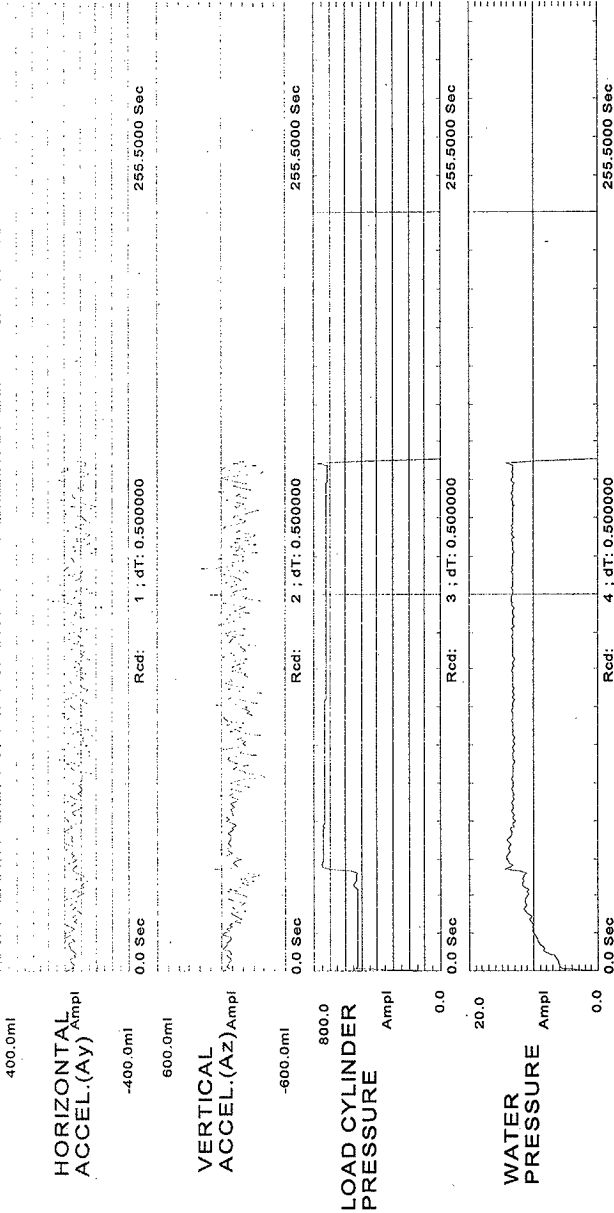


FIGURE LF11

ARD ENVIRONMENTAL, INC.

SILICER TEST 3, RUN 7, BLOCKED SHROUD NO. 37A 2042

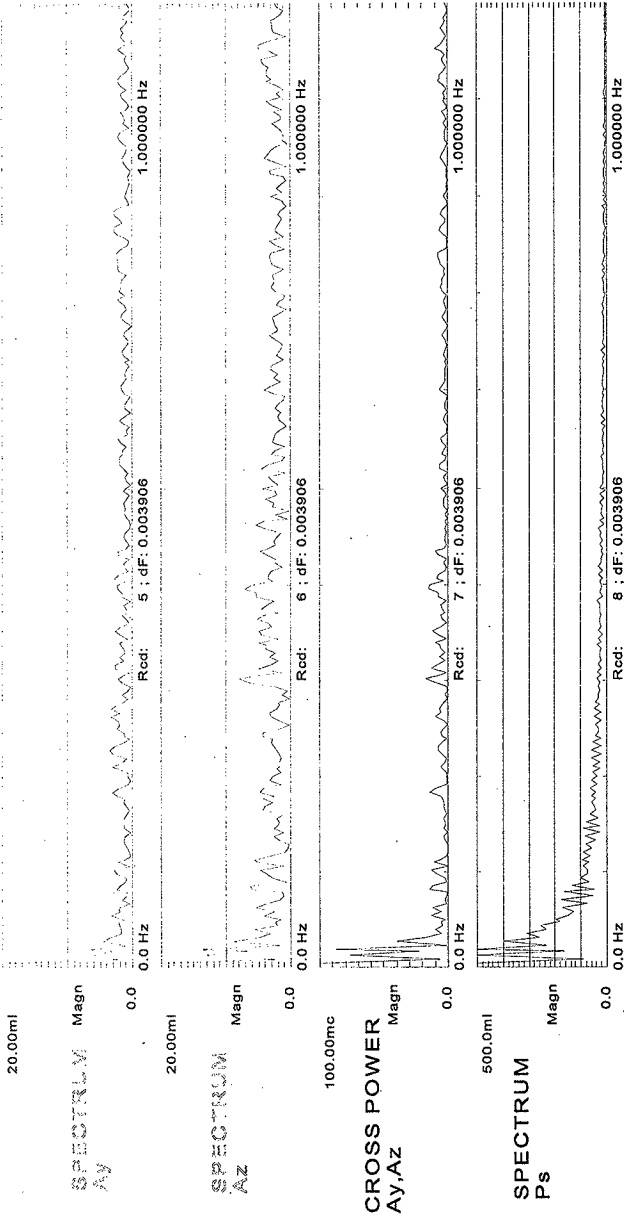


FIGURE LF12

SUBJECT TEST 3, RUN 8: BLOCKED SHROUDS

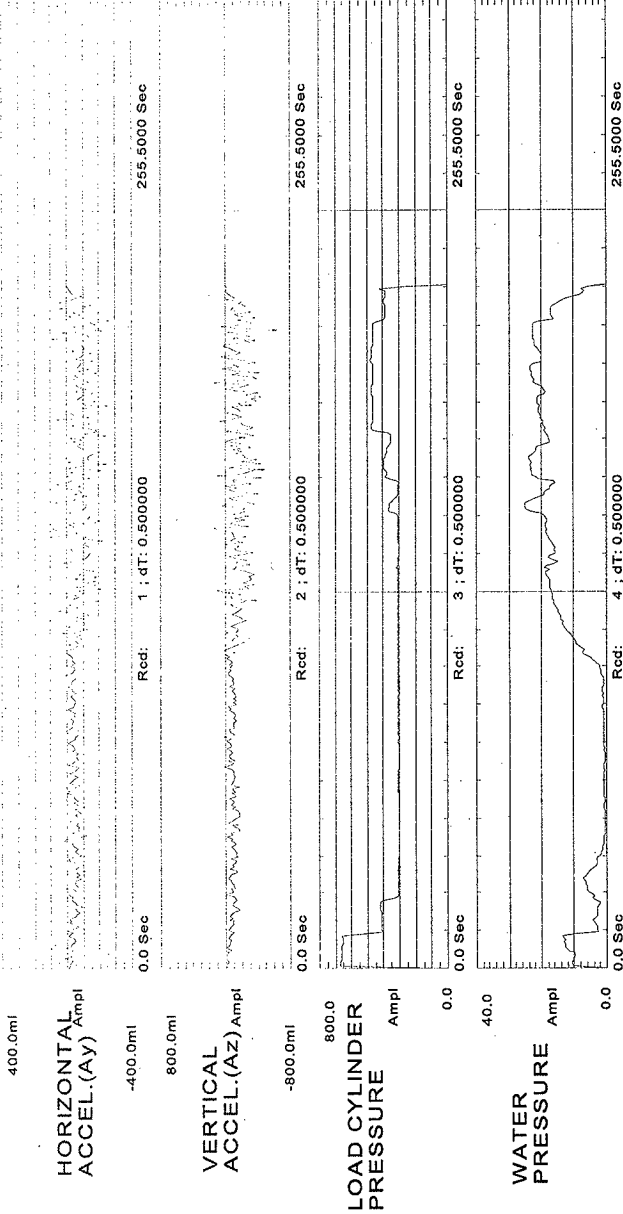


FIGURE LF13

ARD ENVIRONMENTAL, INC.

SLUICER TEST 3, RUN 8: BLOCKED SHROUD S

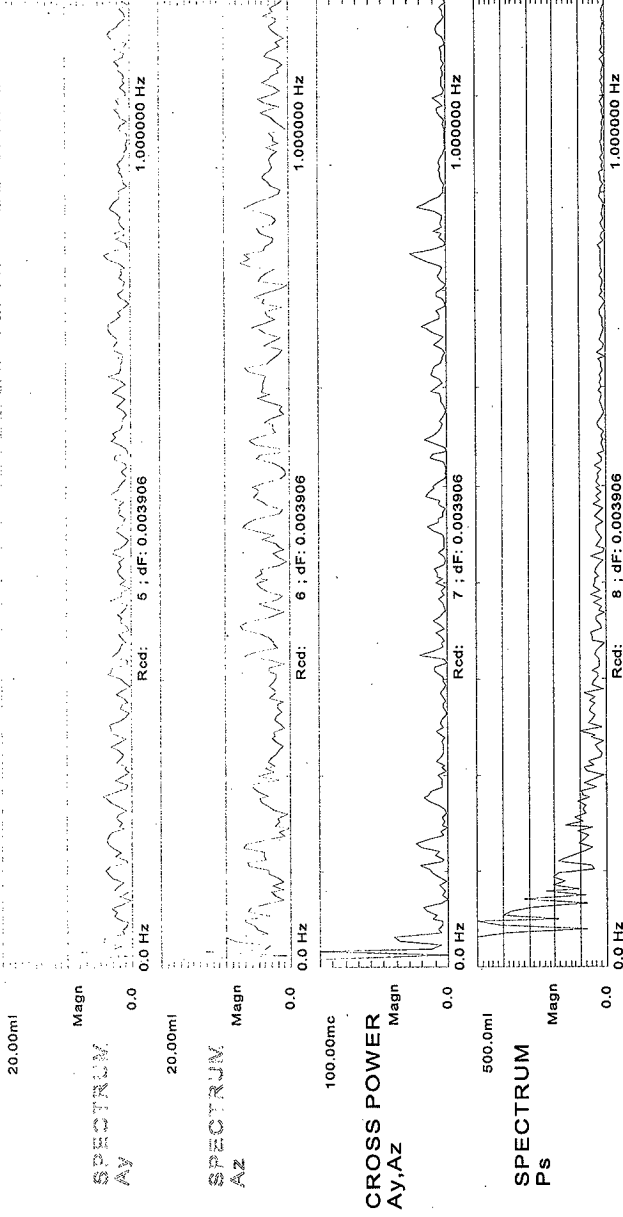


FIGURE LF14

SLUICER TEST 4, RUN 3: BLOCKED SHROUD

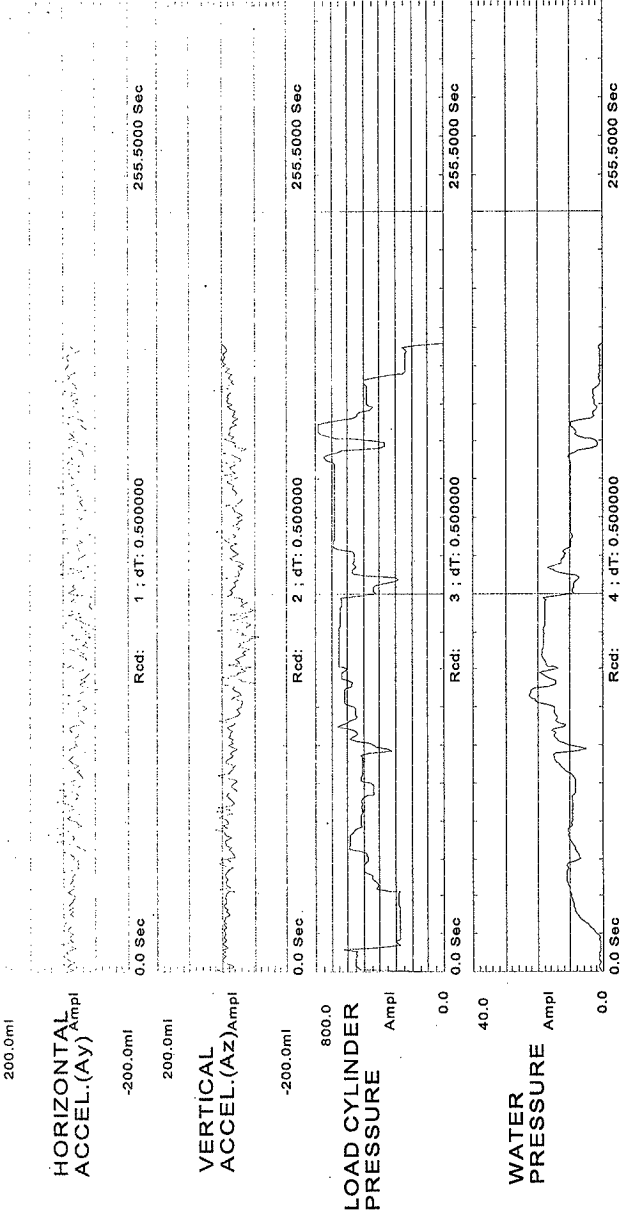


FIGURE LF15

SLICER TEST 3. RUN 9: BLOCKED SHROUD AN

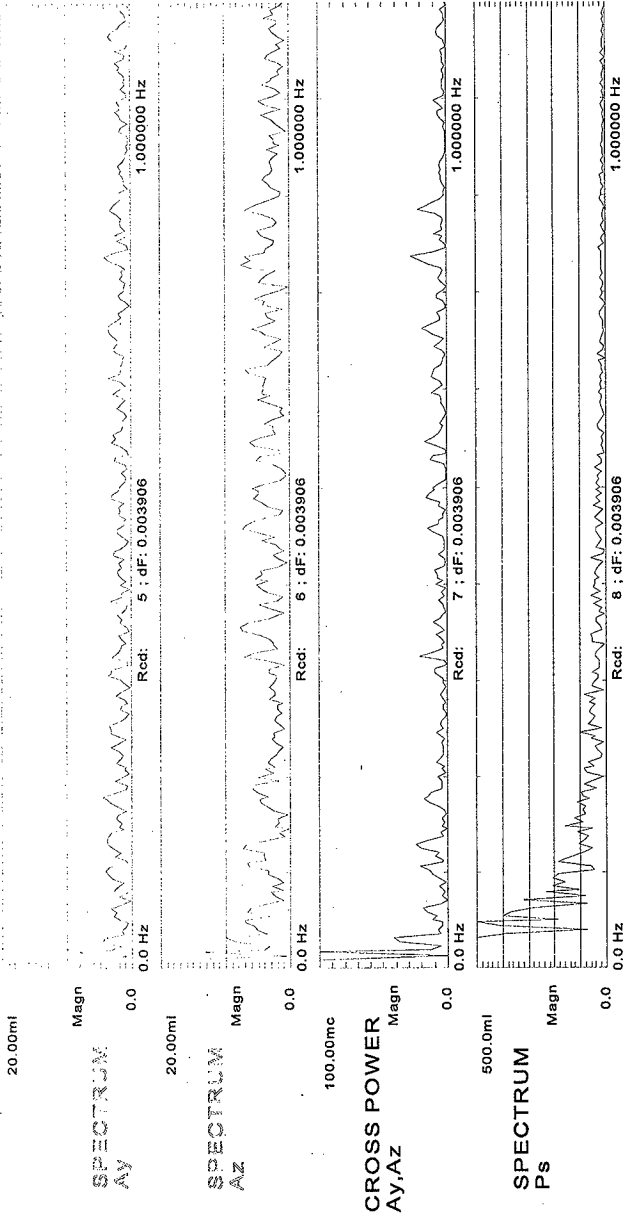


FIGURE LF16

SPLICER TEST 4 RUN 10: HARDPAN

3726.0099

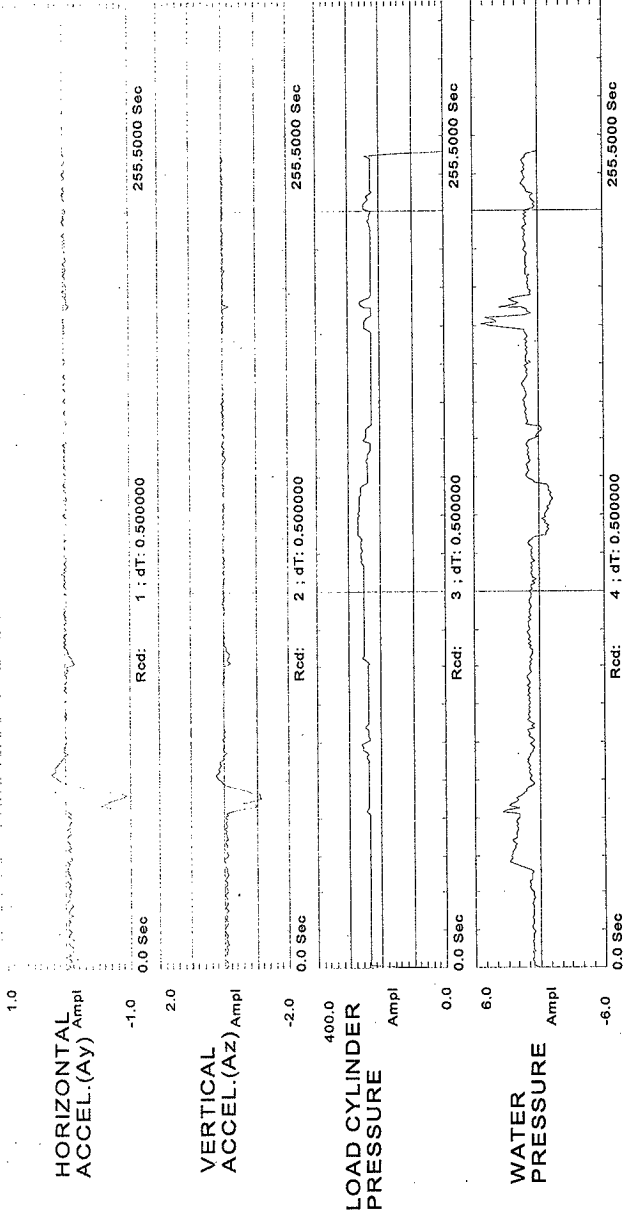


FIGURE LF17

ARD ENVIRONMENTAL, INC.

SLUGGER TEST 4, RUN 10 HARDPAN

D:\CB.DWE

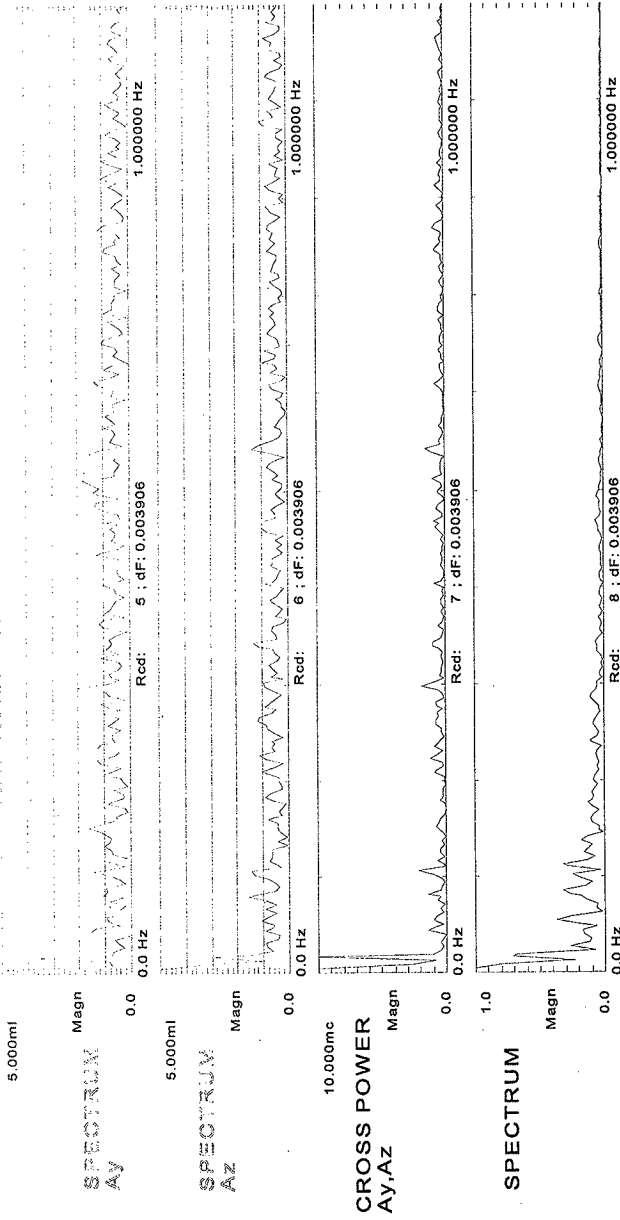


FIGURE LF18

ARD ENVIRONMENTAL, INC.

SECTION 4
HIGH FREQUENCY DATA

FIGURE No	CONTENTS	Page No.
HF1	Sluicer Test 2, Run 1: Saltcake.	B36
HF2	Sluicer Test 2, Run 1: Saltcake.	B37
HF3	Sluicer Test 2, Run 1: Saltcake.	B38
HF4	Sluicer Test 2, Run 1: Saltcake.	B39
HF5	Sluicer Test 2, Run 2: Saltcake.	B40
HF6	Sluicer Test 2, Run 2: Saltcake.	B41
HF7	Sluicer Test 2, Run 3: Saltcake.	B42
HF8	Sluicer Test 2, Run 5: Saltcake.	B43
HF9	Sluicer Test 3, Run 7: Blocked Shroud No Suction.	B44
HF10	Sluicer Test 3, Run 8: Blocked Shroud, Suction.	B45
HF11	Sluicer Test 3, Run 8: Blocked Shroud, Suction.	B46
HF12	Sluicer Test 3, Run 8: Blocked Shroud, Suction.	B47
HF13	Sluicer Test 3, Run 9: Blocked Shroud And Suction.	B48
HF14	Sluicer Test 4, Run 10: Hardpan.	B49
HF15	Sluicer Test 4, Run 10: Hardpan.	B50
HF16	Sluicer Test 4, Run 10: Hardpan.	B51

High frequency Data

Selected 1 second runs were extracted from the raw files and process to elicit any features that might be of importance to the operation of the arm.

Run 1, four data segments; run 2, two data segments, run 3, 1 data segment:

All four segments show coherent energy at about 30 Hz. The source of this energy is probably the backhoe. The only other possible source would be the Paco pumps, however they operate at 3500 rpm, which gives a fundamental frequency of 58.3 Hz. Since there are multiple blades in the impeller, blade frequency would be higher than the shaft frequency.

The feed pump to the Paco pumps was diesel-driven at 2400 rpm, which would give a fundamental of 40 Hz. Firing rate for the diesel and blade rate for the pump would be considerably higher, however the feed water pump was isolated from the Paco pumps by over 50' of hose, therefore it is difficult to see how any energy from the feed water pump could get to the accelerometers. In any event, the maximum acceleration was about 1g, corresponding to an excursion of about 0.28 mm if all the energy were at 30 Hz.

Run 5, 1 data segment:

Some coherent energy shows up at 30 and 40 Hz. In the cross-power spectrum, and a lesser peak shows up in the spectrum of Az at about 52 Hz. Again, the acceleration amplitude is about 1 g.

Run 7, 1 data segment:

A very small peak at 30 Hz., but the peak acceleration level is about 2 g.

Run 8, 3 data segments:

Some small amount of coherent energy at 30 and 40 Hz.

Run 9, 1 data segment:

Only the time series data are shown, and appear unremarkable.

Run 10, 3 data segments:

The shroud pressure spectrum shows some coherent energy at 20, 30 and 40 Hz., while the accelerometer spectra show energy primarily at 30 and 40 Hz. Again, levels are low, with the peak acceleration at about 1 g.

SLICER TEST 2, RUN 1: SALTCAKE

2_44.DW2

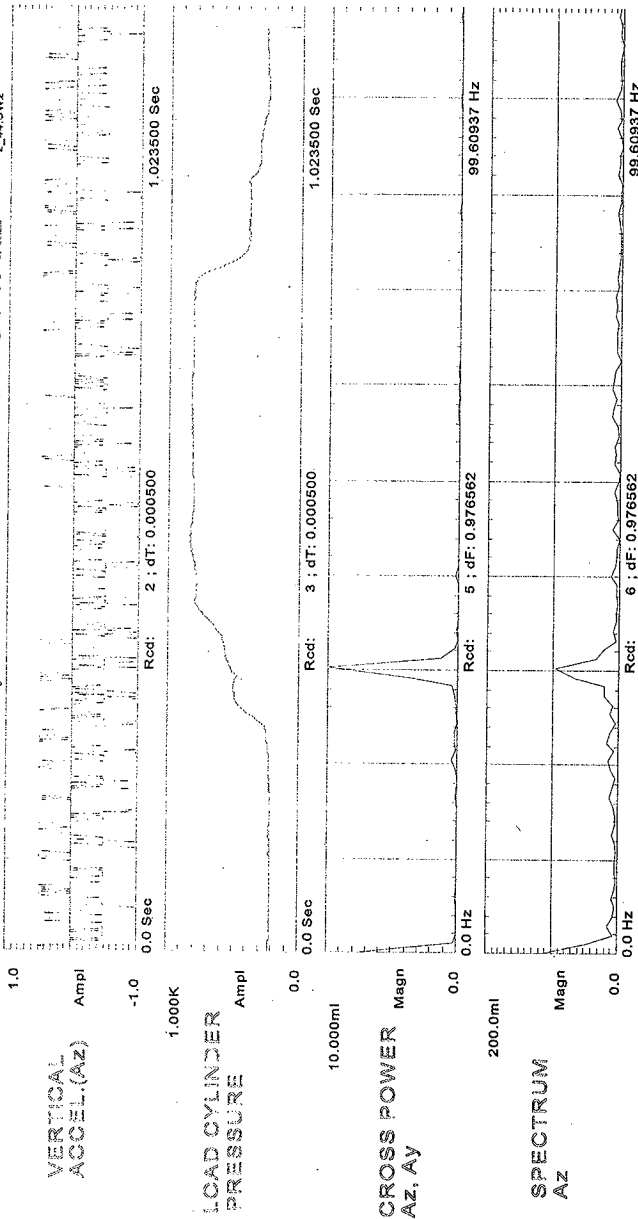


FIGURE HF1

SLUICER TEST 2, RUN 1: SALTCAKE

2.592.DW2

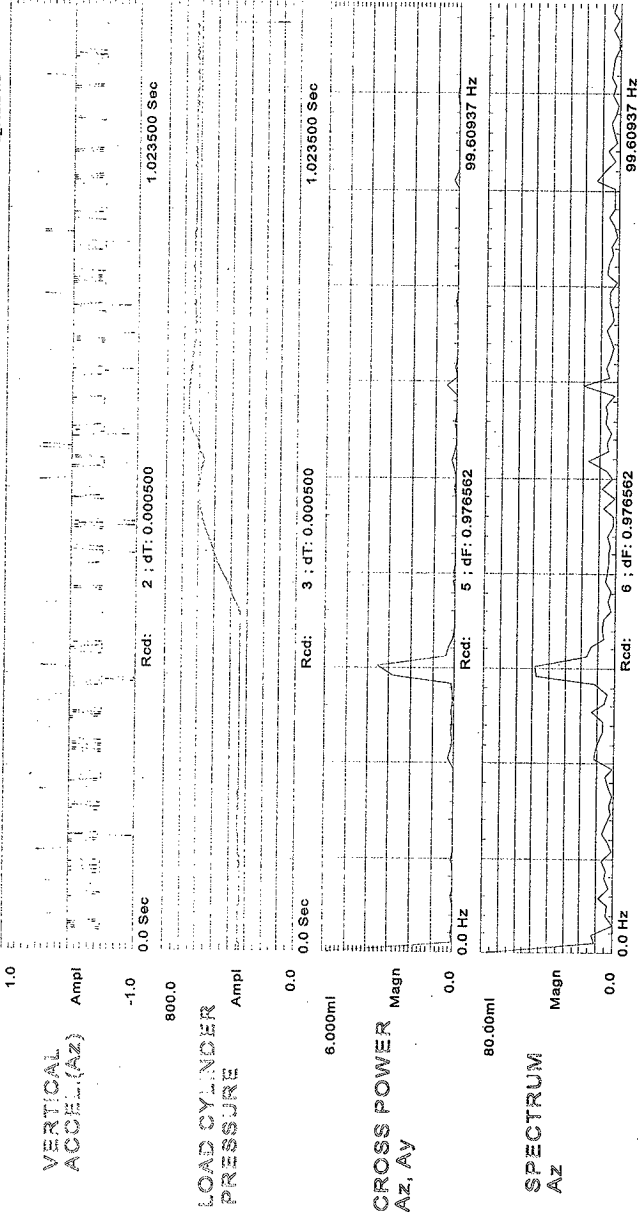


FIGURE HF2

ARD ENVIRONMENTAL, INC

SLICER TEST 2, RUN 1: SALTCAKE

2.84.DV2

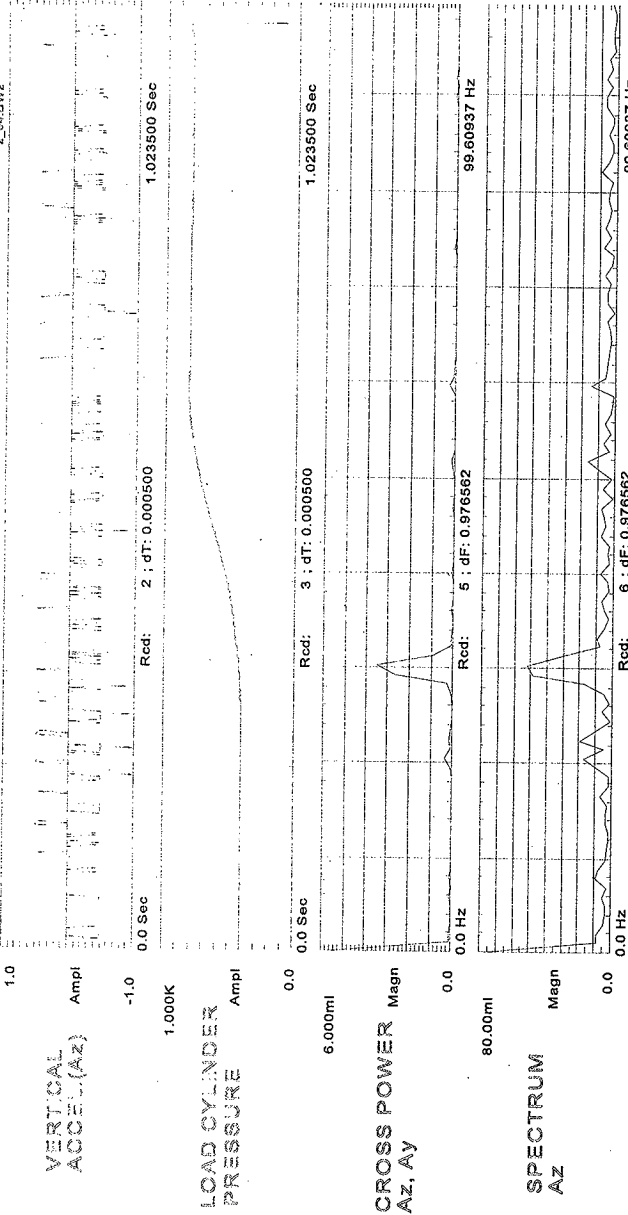


FIGURE HF3

SLUICER TEST 2, RUN 1: SALTCAKE

Z_584.CWZ

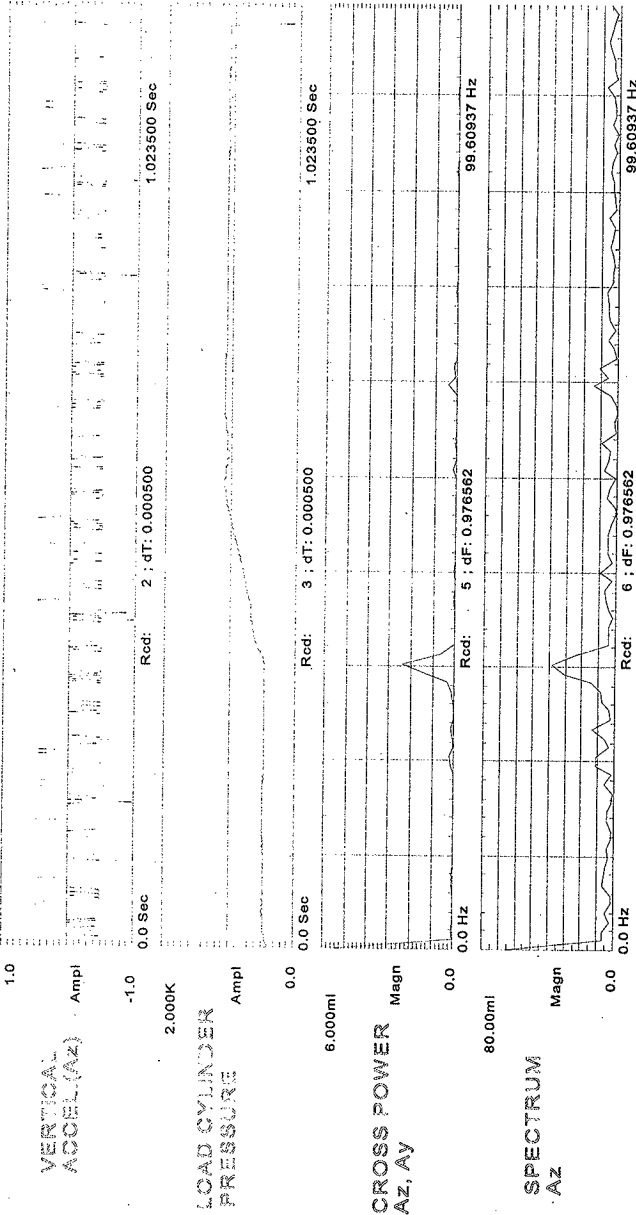


FIGURE HF4

SLICER TEST 2, RUN 2: SALTCAKE

2.48 DW2

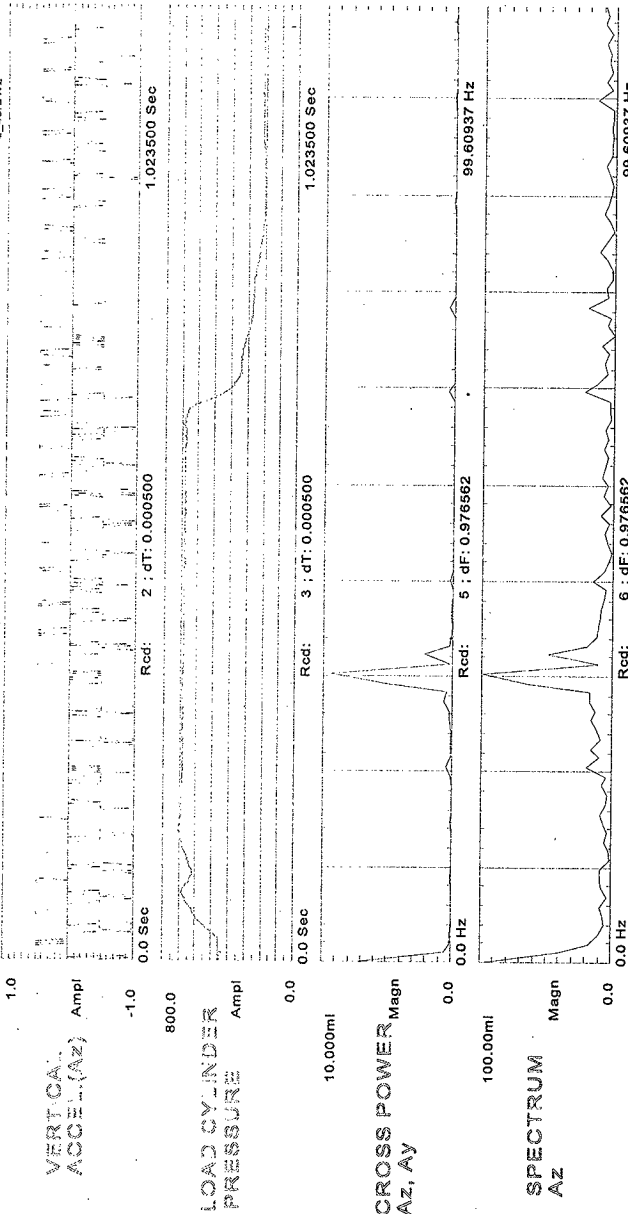
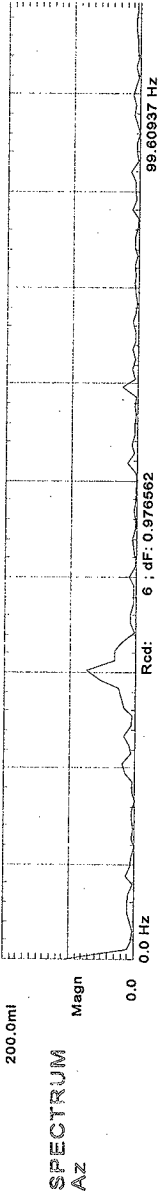
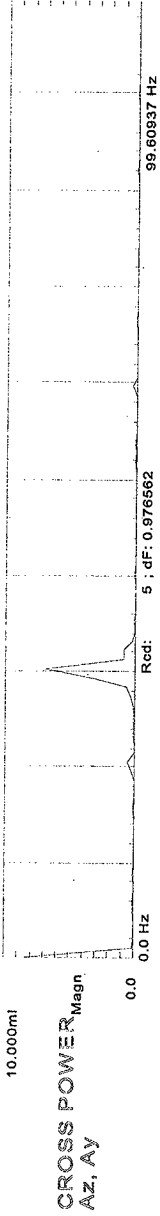
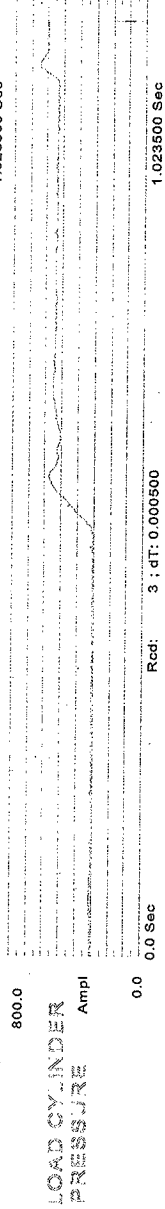


FIGURE HF5

ARD ENVIRONMENTAL, INC

SLUICER TEST 2, RUN 2: SALTCAKE

2_904.DW2



SLUICER TEST 2, RUN 3: SALTCAKE

2_324.DW2

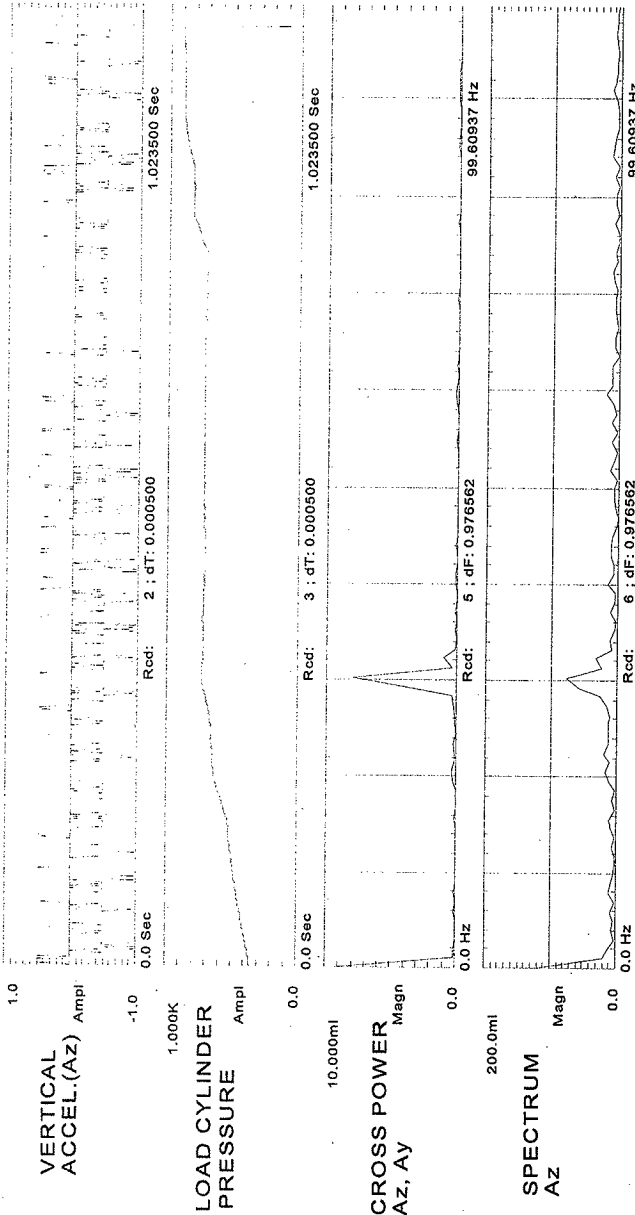


FIGURE HF7

ARD ENVIRONMENTAL, IN

SLUICER TEST 2, RUN 5: SALTCAKE

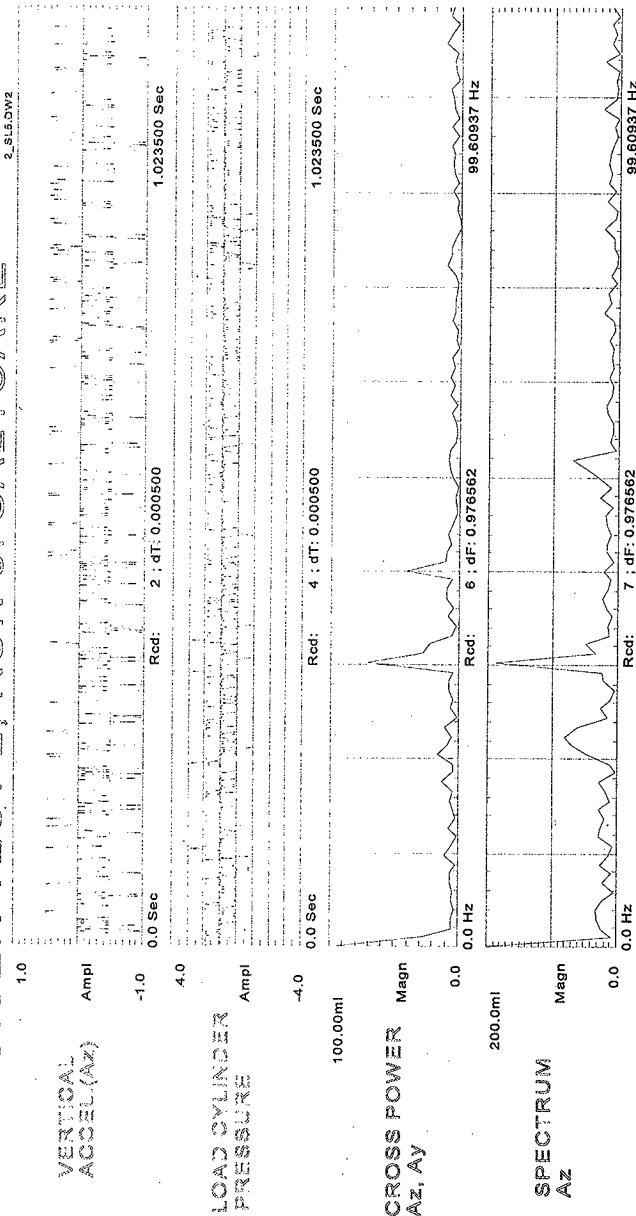
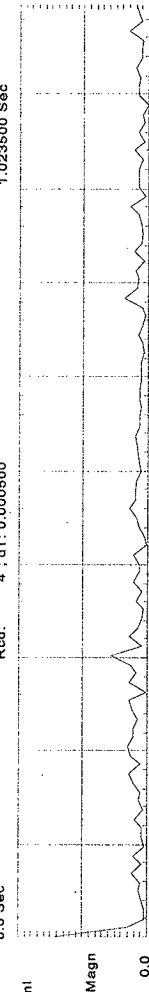
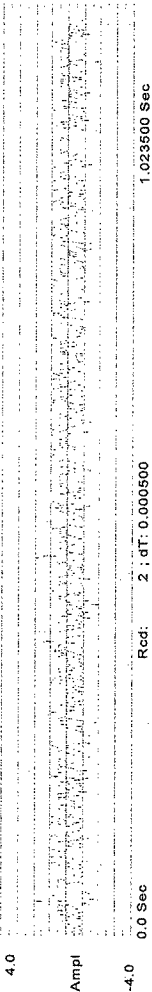


FIGURE HF8

ARD ENVIRONMENTAL, INC.

SLICER TEST 3, RUN 7: BLOCKED SHROUD NQ.S



SLUICER TEST 3, RUN 8: BLOCKED SHROUD, SUC1

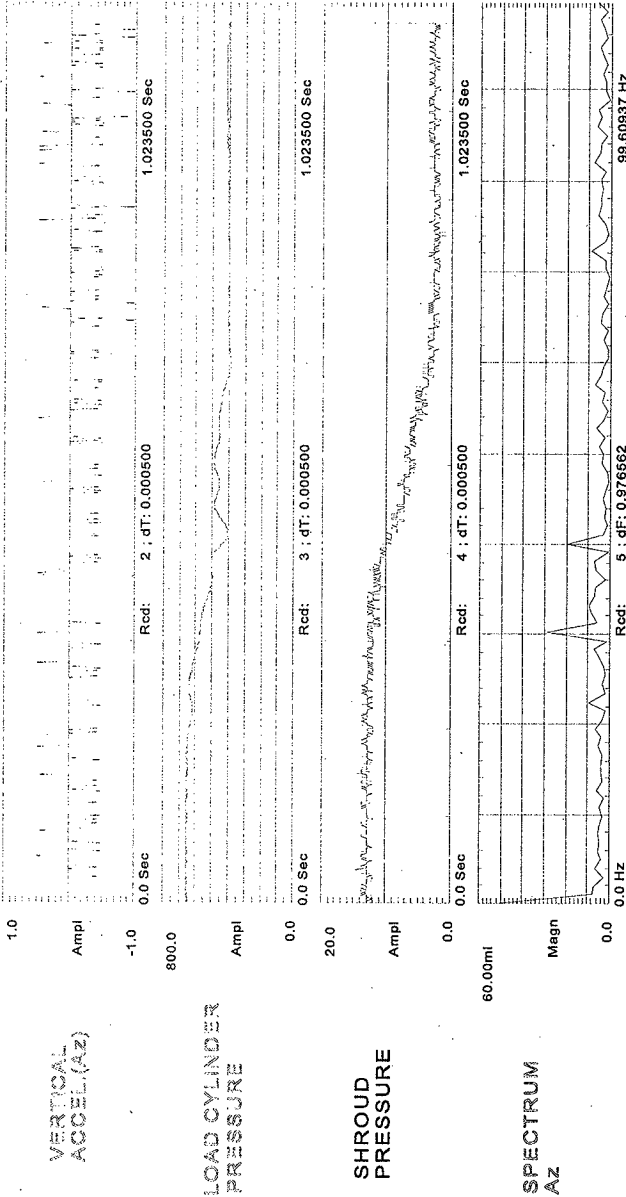


FIGURE HF10

SLICER TEST 3, RUN 8: BLOCKED SHROUD, SUB

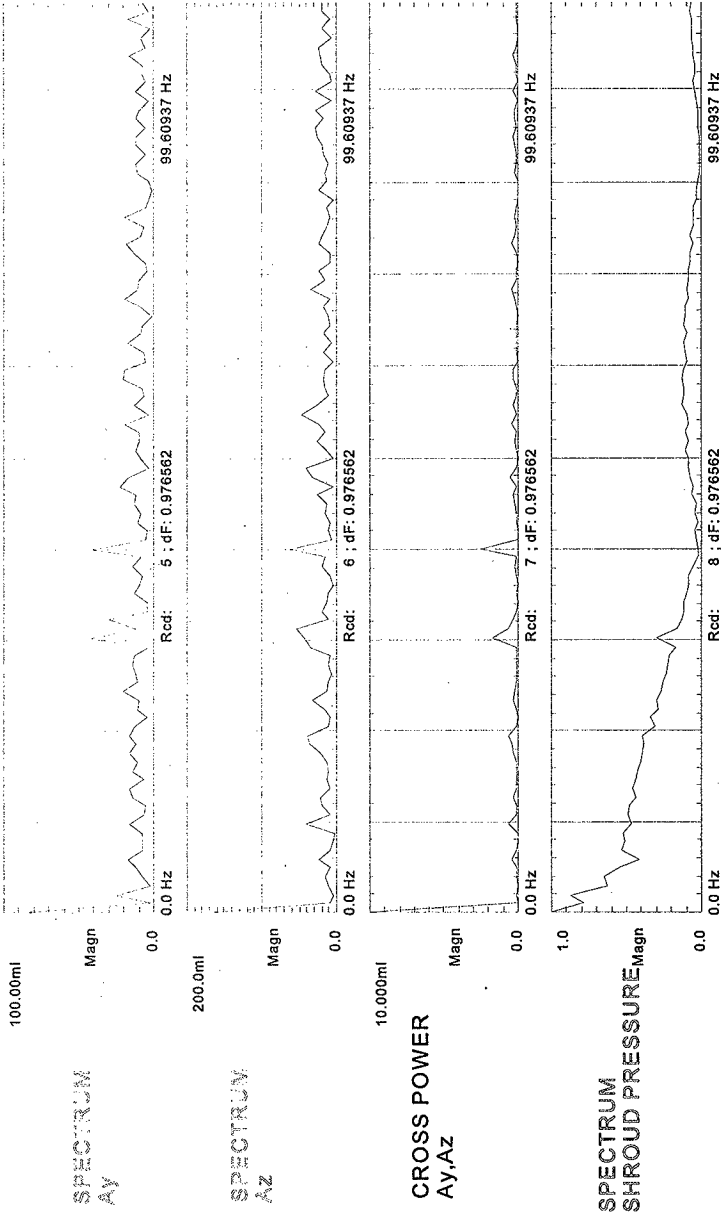


FIGURE HF11

SLUICER TEST 3, RUN 8: BLOCKED SHROUD, SUCTION

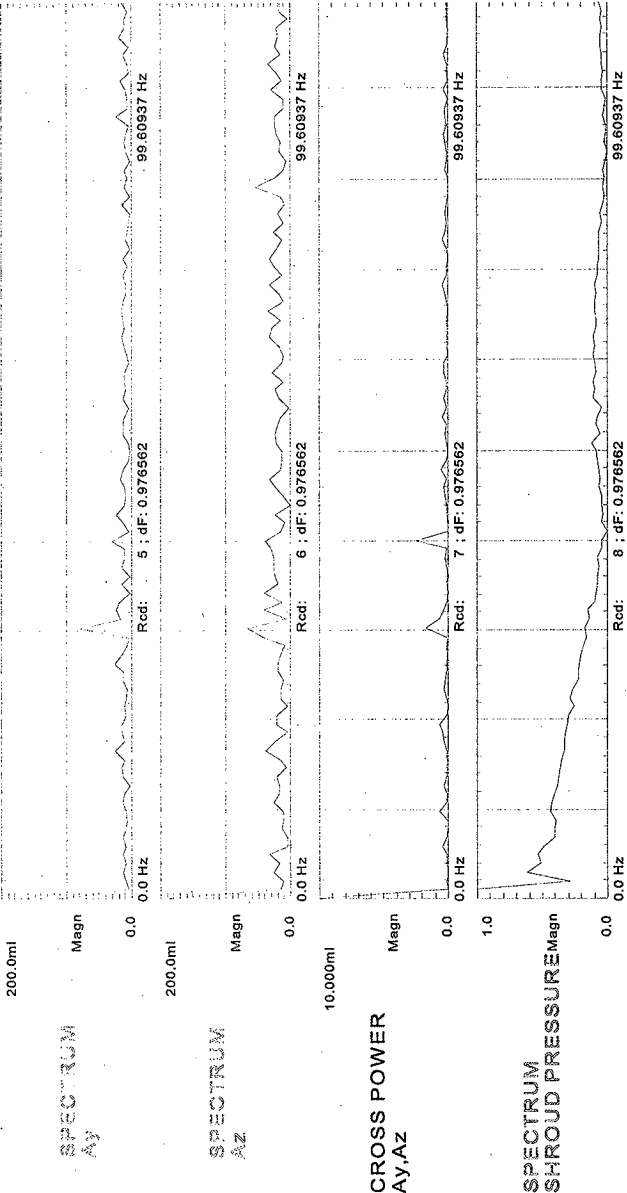


FIGURE HF12

SLICER TEST 3, RUN 9: BLOCKED SHROUD AND

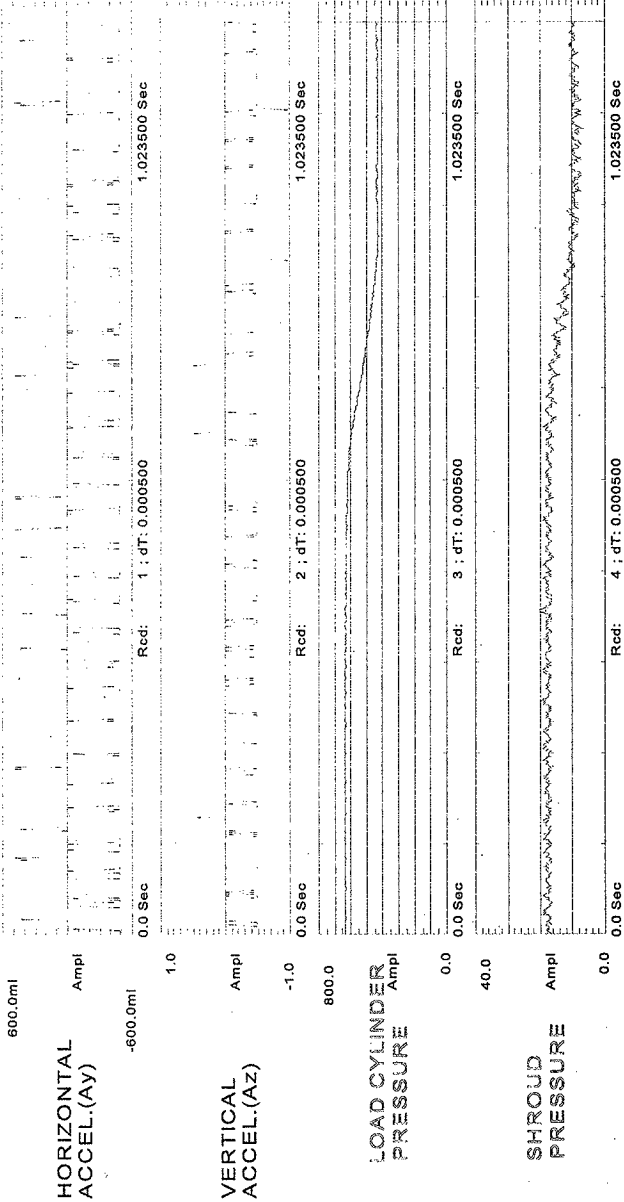


FIGURE HF13

SLICER TEST 4, RUN 10: HARDPAN

4_S110_4.DWZ

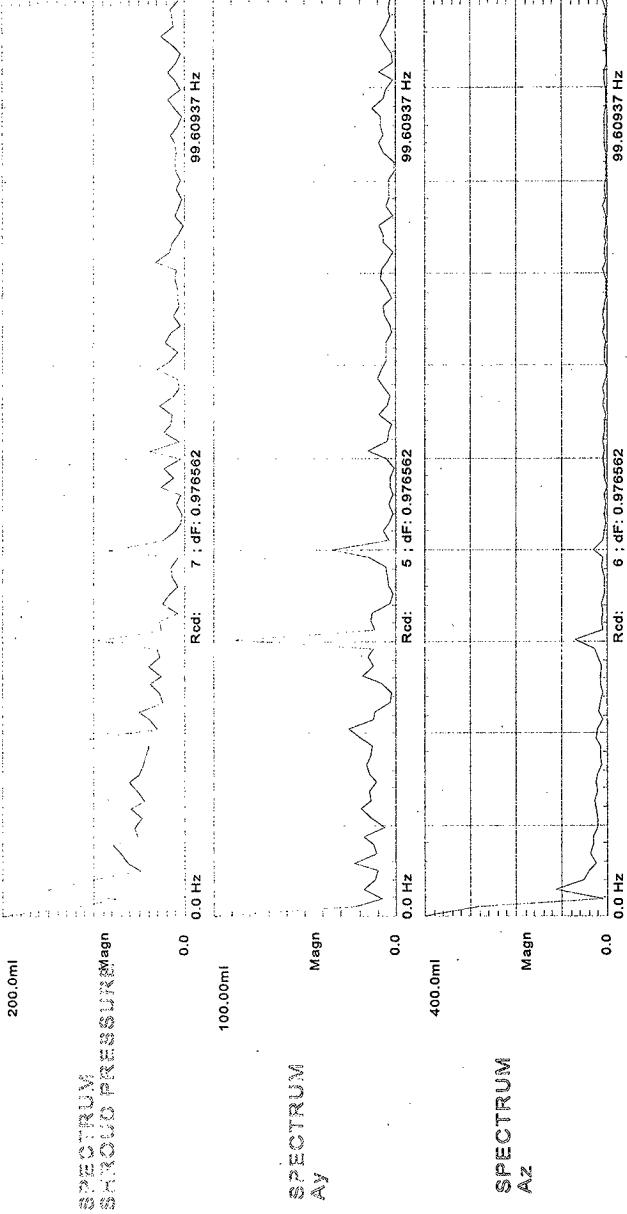


FIGURE HF14

ARD ENVIRONMENTAL, INC.

SLUICER TEST 4, RUN 10: HARDPAN

4_S10_7A.DWG

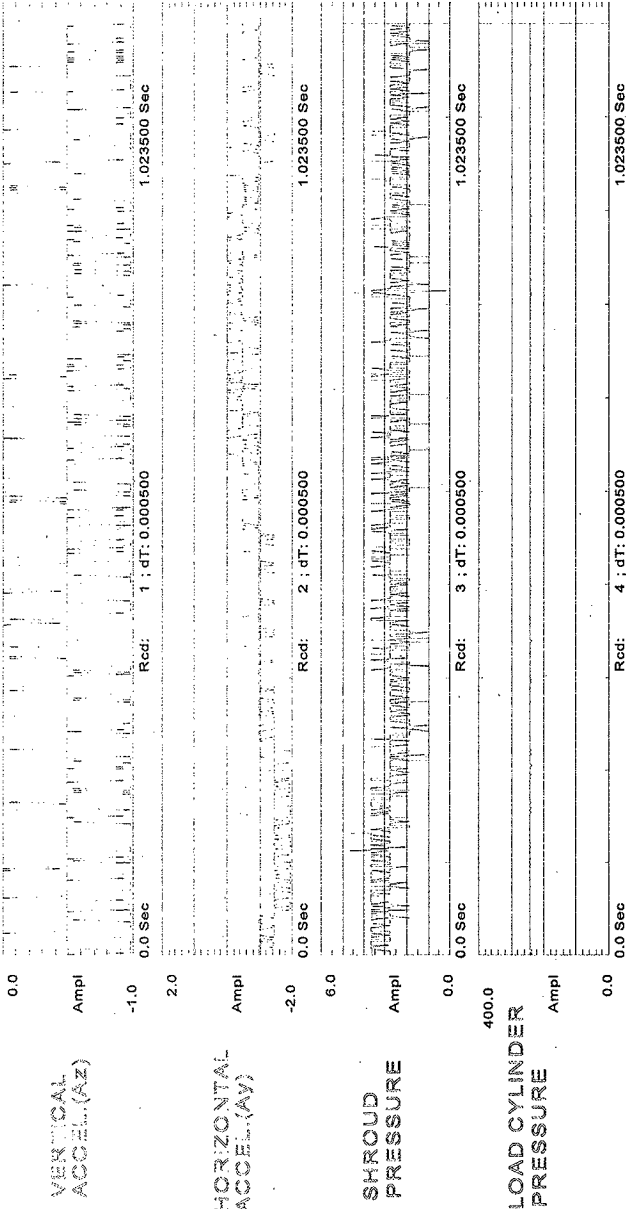


FIGURE HF15

ARD ENVIRONMENTAL, INC.

SLICER TEST 4 RUN 10: HARDPAN

4.SLIC.B.DW2

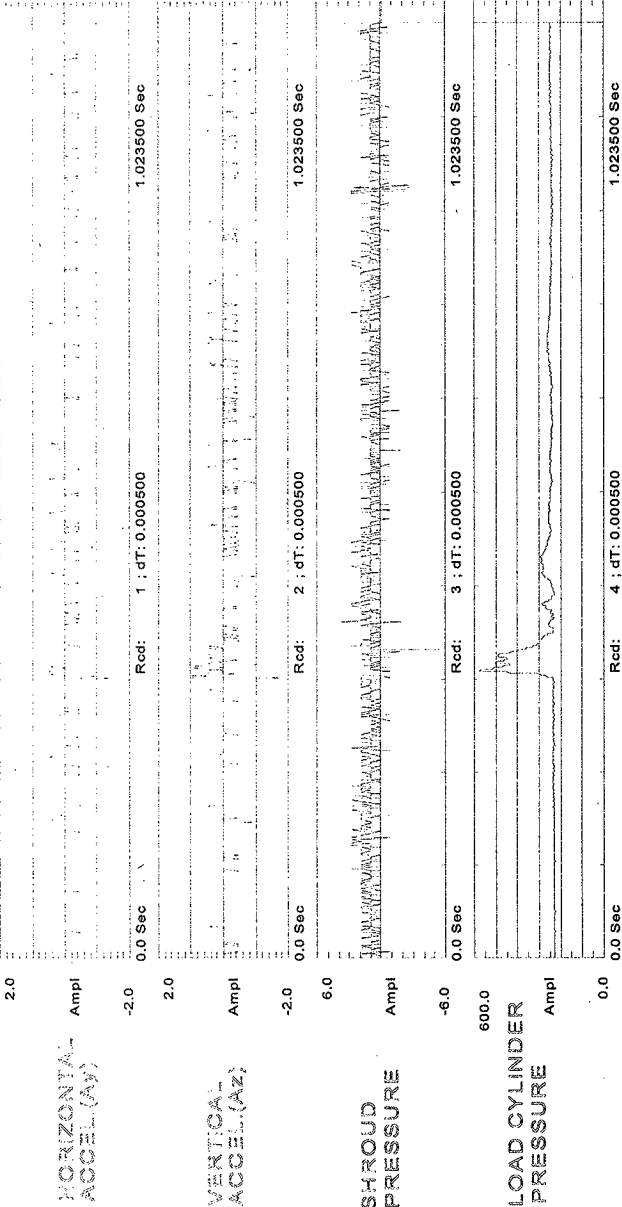


FIGURE HF16

ARD ENVIRONMENTAL, INC.

SECTION 5

PHOTOGRAPHS

FIGURE No	CONTENTS	Page No.
B5.1	Sluicer Assembly.	B53
B5.2	Sluicer and Backhoe Interface.	B54
B5.3	Backhoe and Sluicer.	B55
B5.4	Pump Layout.	B56
B5.5	Feedwater Flowmeter.	B57
B5.6	Sluicing Saltcake (1).	B58
B5.7	Sluicing Saltcake (2).	B59
B5.8	Sluicing Saltcake (3).	B60
B5.9	Sluicing Saltcake (4).	B61
B5.10	Sluicing Saltcake (5).	B62
B5.11	Sluicing Hardpan (1).	B63
B5.12	Sluicing Hardpan (2).	B64
B5.13	Sluicing Hardpan (3).	B65
B5.14	Mat after Blocked Sluicer.	B66



Fig B5.1

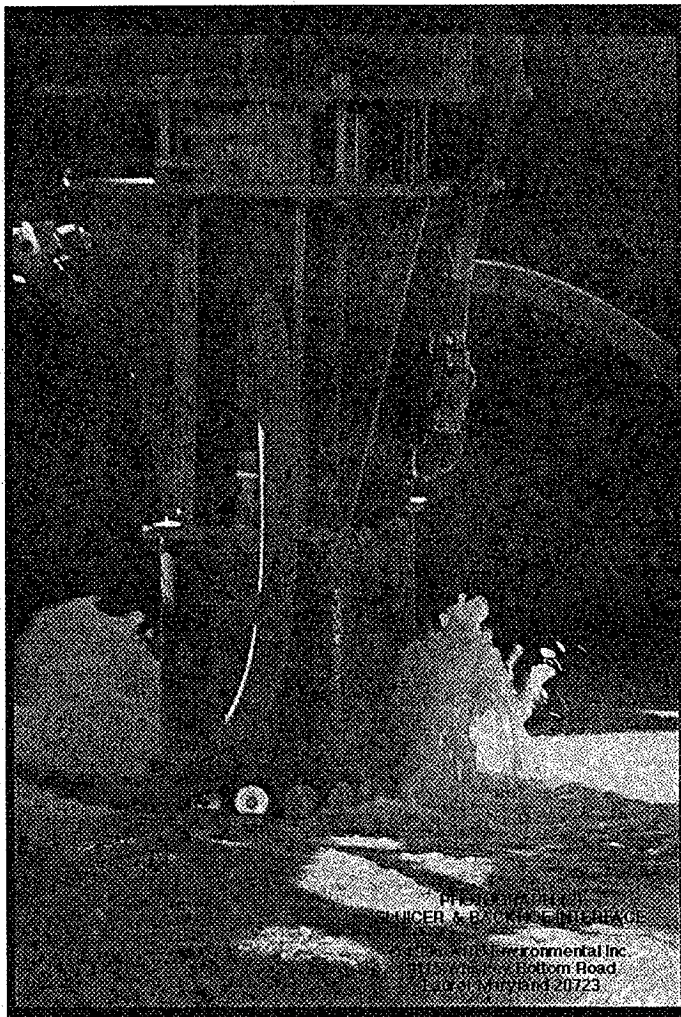
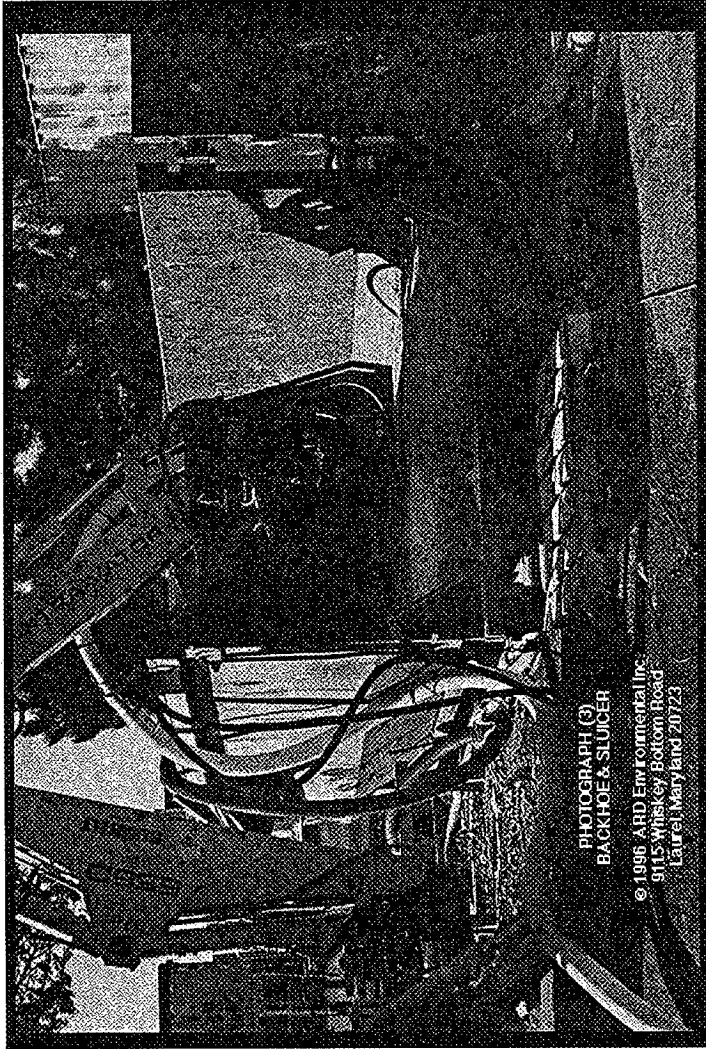


Fig B5.2



PHOTOGRAPH (3)
BACKHOE & SLUICER

© 1996 ARD Environmental Inc.
9115 Whiskey Bottom Road
Laurel, Maryland 20723

Fig B5.3

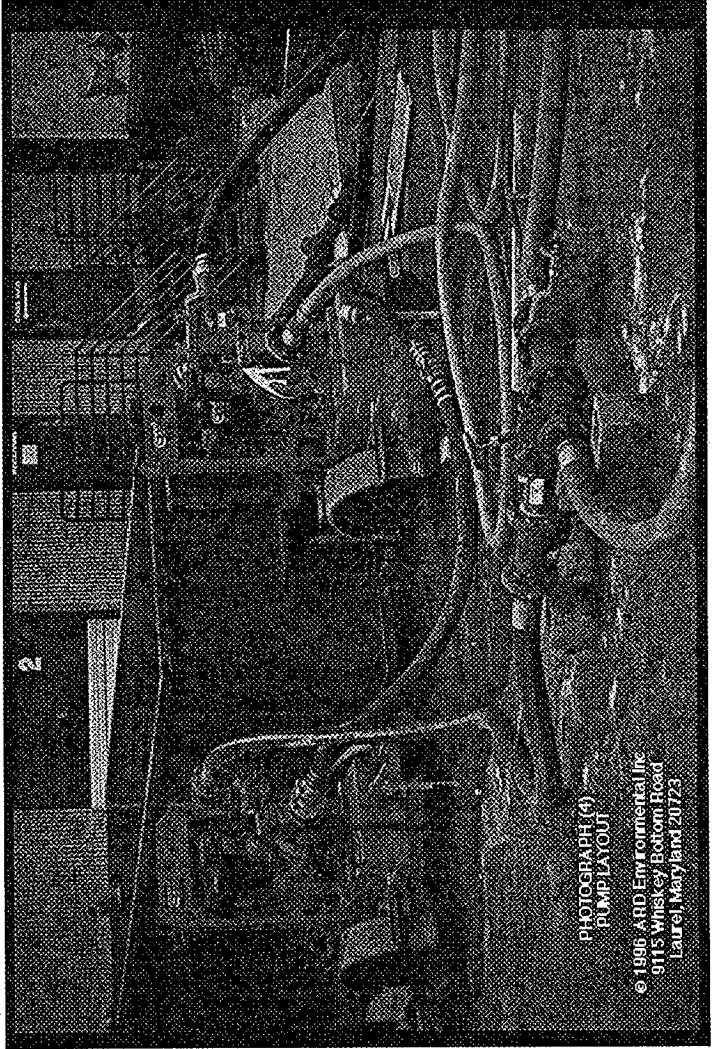


Fig B5.4

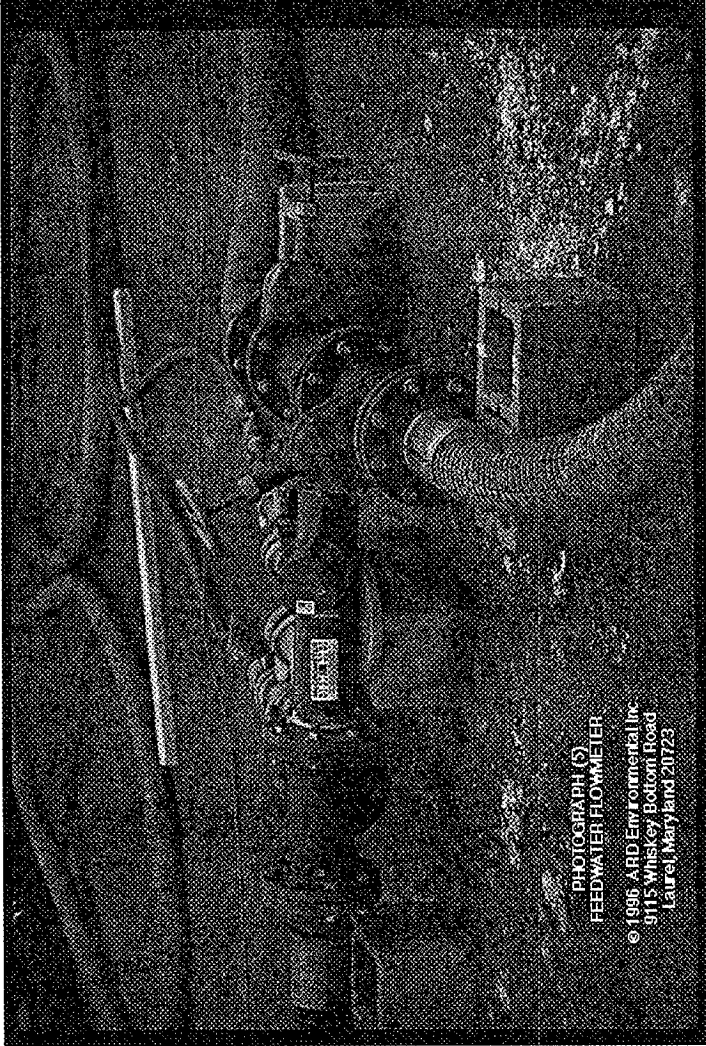


Fig B5.5

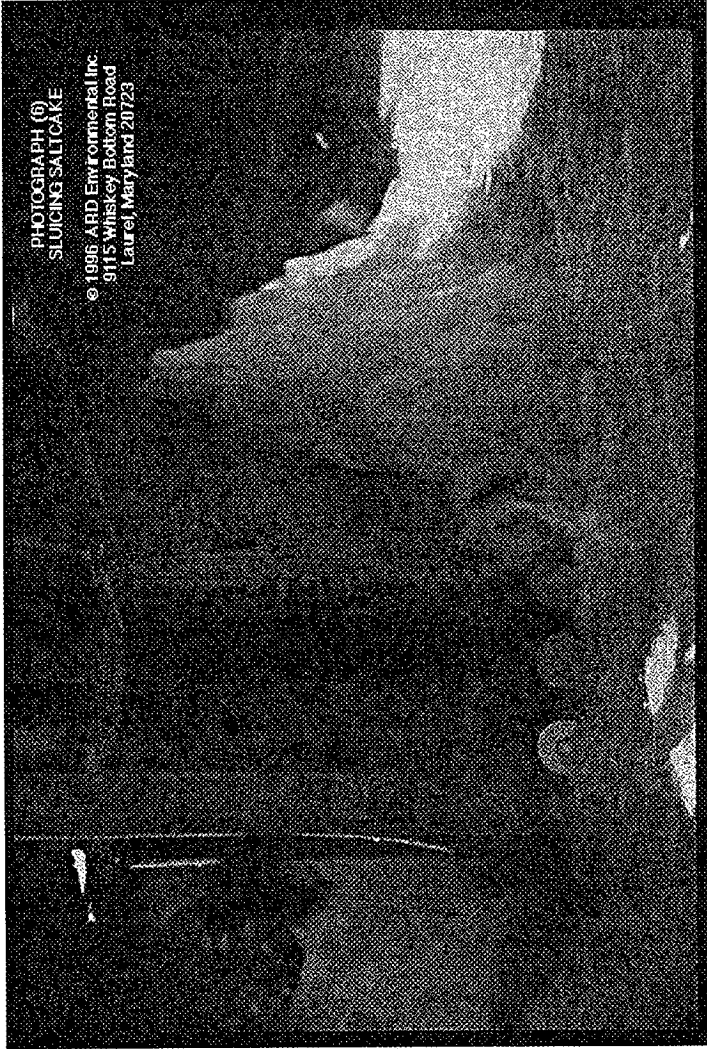


Fig B5.6



Fig B5.7



Fig B5.8

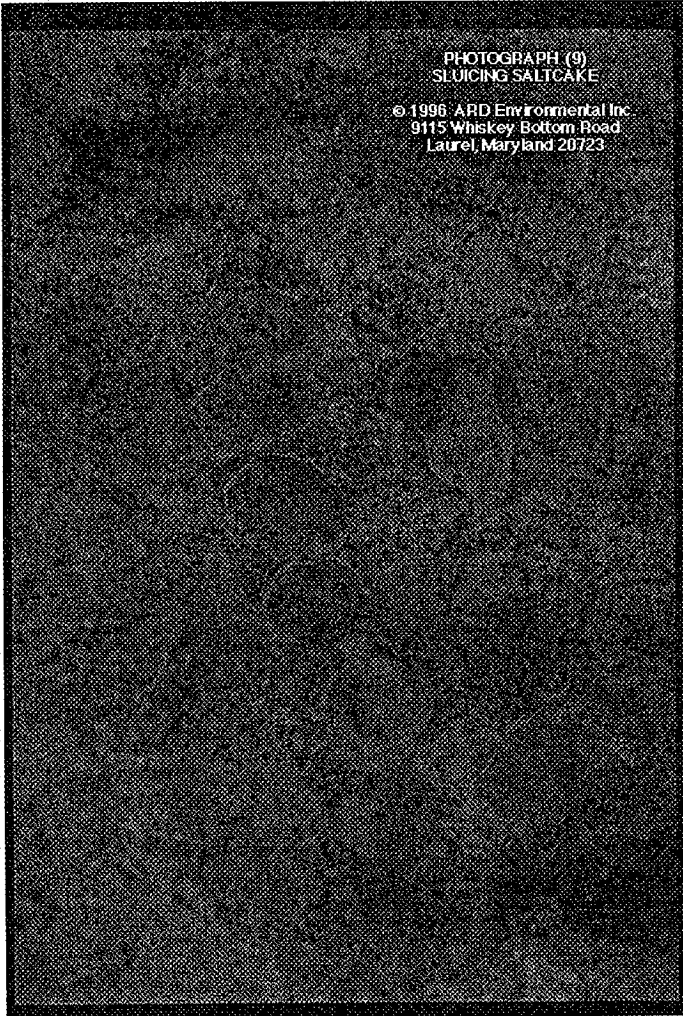


Fig B5.9

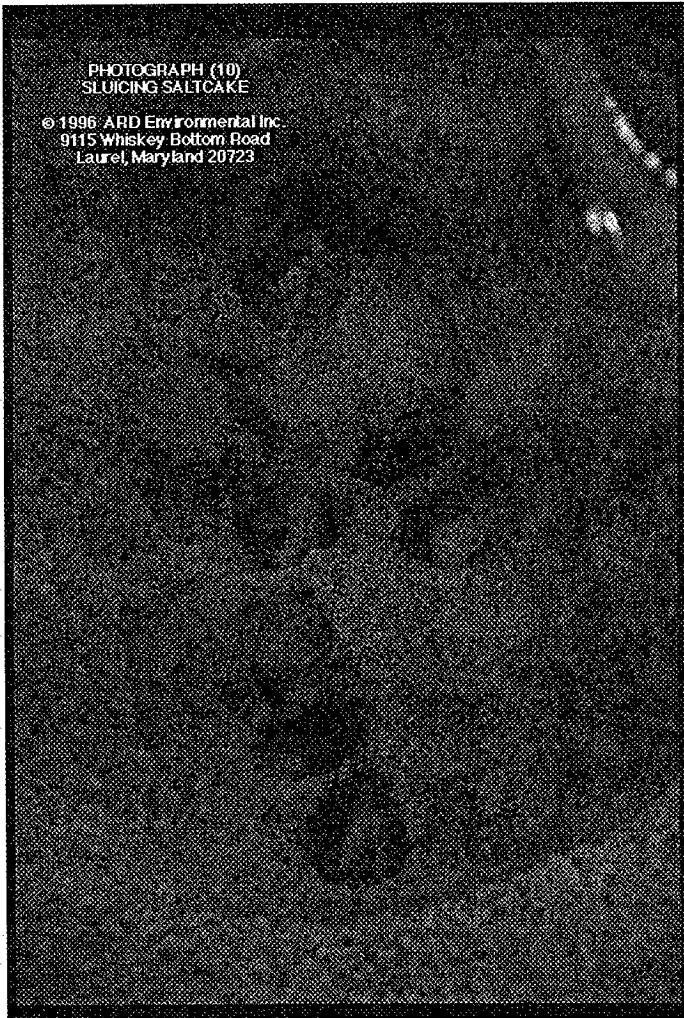


Fig B5.10

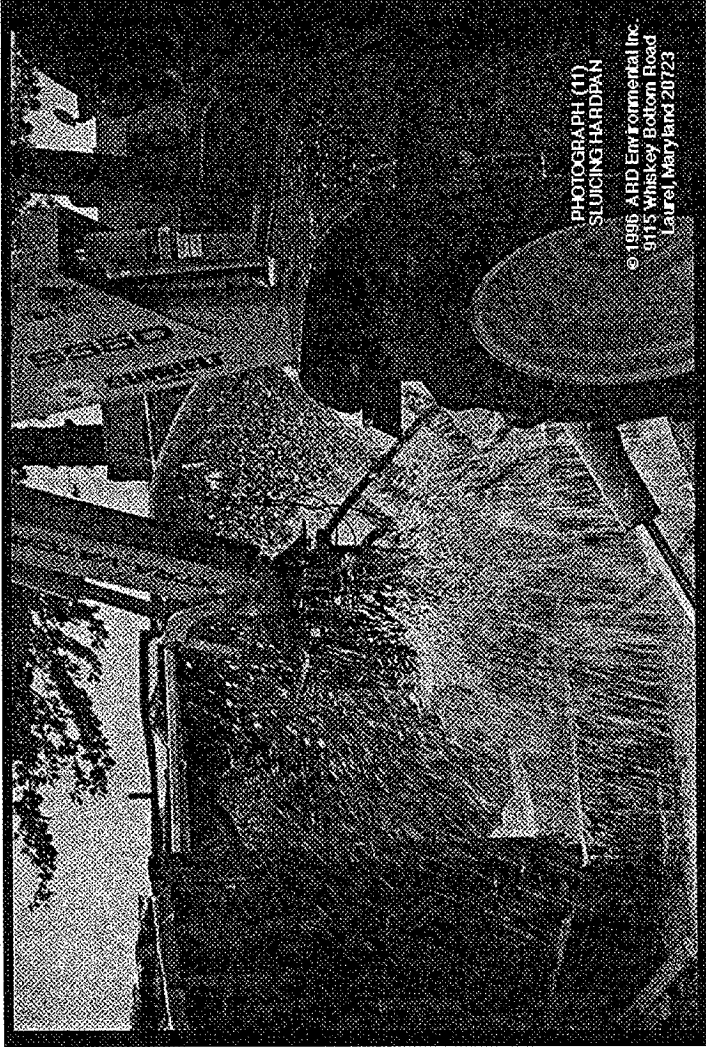


Fig 5B.11

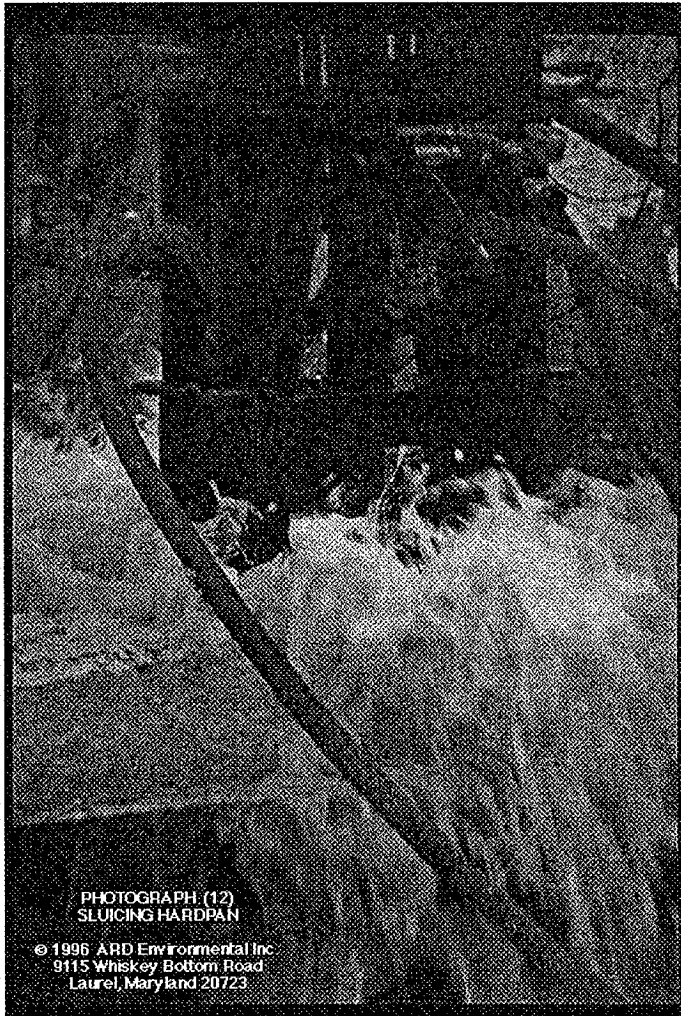


Fig B5.12

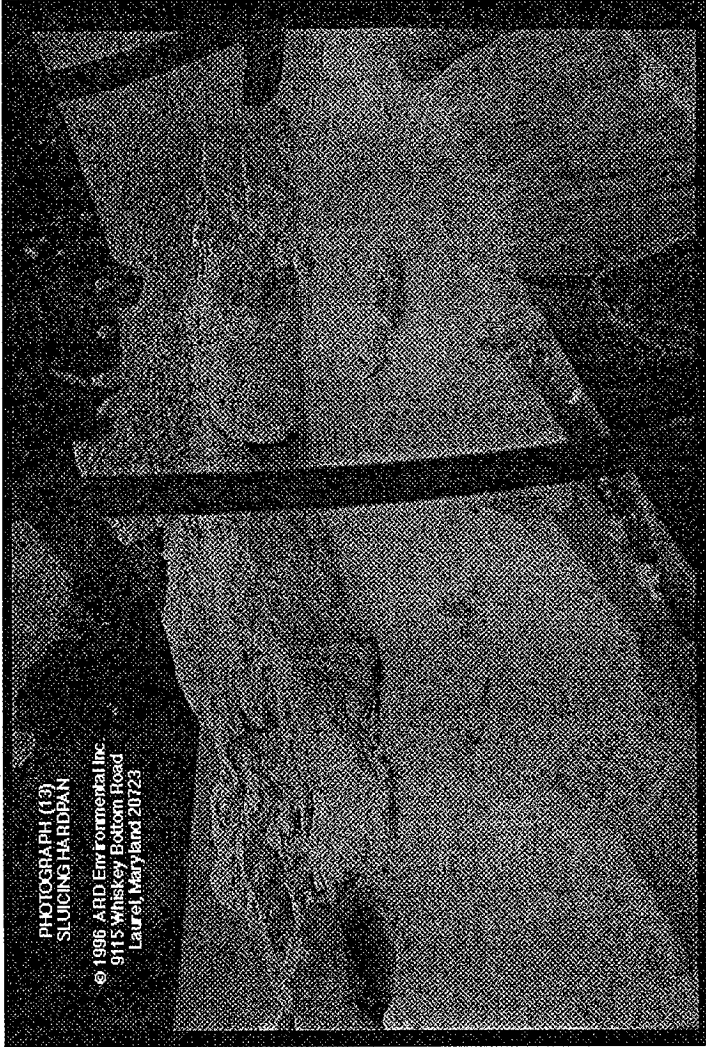


Fig B5.13

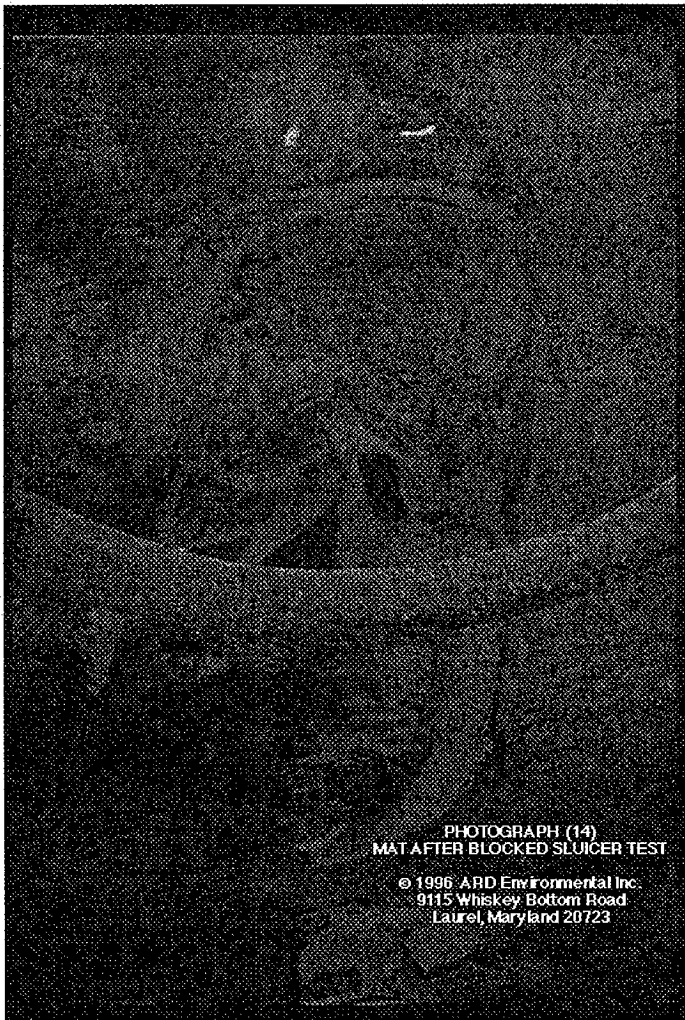
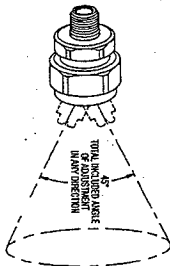


Fig B5.14

SECTION 6
EQUIPMENT INFORMATION

FIGURE No	CONTENTS	Page No.
1	Nozzle Specification	B68
2	Adjustable Ball Fittings	B69
3	CD 80 Pump	B70
4	CD 80 Pump Performance	B71
5	CD 150M Pump	B72
6	CD 150M Pump Performance	B73
7	Paco Pump Performance Curves	B74
8	McCROMETER MF100 Flowmeter	B75
9	McCROMETER MF100 Flowmeter Specification	B76
10	McCROMETER Propellor Flowmeter	B77
11	McCROMETER Propellor Flowmeter Specification	B78
12	McCROMETER Propellor Flowmeter Installation	B79
13	McCROMETER Schematic Diagram	B80
14	ISA I/O Boards Spec-1	B81
15	ISA I/O Boards Spec-2	B82
16	Dytran Schematic Diagram	B83
17	LIVM Sensors Specification-1	B84
18	LIVM Sensors Specification-2	B85
19	Triaxial Accelerometer Specification	B86
20	Dytran Calibration Certificate	B87
21	Dytran Current Source Diagram	B88
22	Dytran Current Source Calibration Certificate	B89
23	Model 4103B LIVM Power Unit	B90
24	Pressure Transducer Specification-1	B91

Adjustable BALL FITTINGS



male inlet, female outlet
 1/4" - 3/4" NPT or BSPT



male inlet, female outlet
 1" - 1 1/2" NPT or BSPT



male inlet, male outlet
 1 1/4" - 2 1/2" NPT or BSPT



DESIGN FEATURES

Adjustable ball fittings provide adjustable positioning of spray nozzles for more exact control of spray direction. They permit accurate pipe alignment and convenient nozzle positioning without disturbing pipe connections. Adjustable ball fittings are available in a wide range of pipe connections. They feature large internal passages

to minimize clogging and smooth finished sealing surfaces to assure leakproof connections.

The machined-type ball fitting features a lock ring that holds the nozzle in position when jarred or subjected to vibration. The fitting has a relatively small diameter for applications requiring a compact size. Its maximum

pressure rating is 300 psi (21 bar). Nozzle removal for cleaning and readjustment is quick and simple.

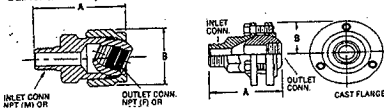
Cast-type fittings feature locking screws that hold the nozzle in position when jarred or subjected to vibration. They are rated for pressures up to 125 psi (9 bar).

DIMENSIONS & WEIGHTS

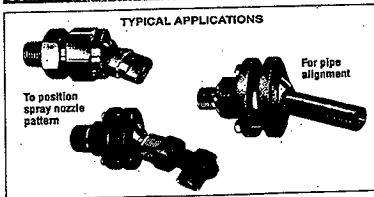
Inlet Pipe Conn. NPT or BSPT	Outlet Pipe Conn. NPT or BSPT	Adjustable Ball Fitting Ordering No.	Type Flanges	DIMENSIONS		Total Included Angle of Adjustment	Net Weight lbs.
				Overall Length inches	B inches		
1M	1F	1 x 1	CAST	3 3/8	1 3/8	40°	4
1 1/4M	1 1/4F	1 1/4 x 1 1/4	female outlet type	5 1/4	1 3/4	40°	4 1/2
1 1/2M	1 1/2F	1 1/2 x 1 1/2	female outlet type	5 1/2	1 3/8	40°	5
1 3/4M	1 3/4F	1 3/4 x 1 3/4	female outlet type	5 3/4	1 3/8	40°	5 1/2
1 3/4M	1 3/4M	1 3/4 x 1 3/4	CAST	5 3/4	1 3/8	40°	4 1/2
1 3/4M	1 3/4M	1 3/4 x 1 3/4	CAST	5 3/4	1 3/8	40°	4 1/2
2M	2M	2 x 2	CAST	9	3 1/2	40°	13 1/2
2 1/2M	2 1/2M	2 1/2 x 2 1/2	CAST	9	3 1/2	40°	13 1/2

Inlet Pipe Conn. NPT or BSPT	Outlet Pipe Conn. NPT or BSPT	Adjustable Ball Fitting Ordering No.	Material	DIMENSIONS		Total Included Angle of Adjustment	Net Weight oz.
				Overall Length inches	B inches		
3/4M	3/4F	38275-1/4 x 1/4	Brass	1 3/8	3/8		2
3/4M	3/4F	38275-1/4 x 1/4-SS	St. Steel	1 3/8	3/8		2
3/4M	3/4F	38275-1/4 x 1/4	Brass	1 3/4	1 1/4	45°	3
3/4M	3/4F	38275-1/4 x 1/4-SS	St. Steel	1 3/4	1 1/4	45°	3
3/4M	3/4F	38275-3/4 x 3/4	Brass	1 7/8	1 1/4		5.5
3/4M	3/4F	38275-3/4 x 3/4-SS	St. Steel	1 7/8	1 1/4		5.5
1/2M	1/2F	38275-1/2 x 1/2	Brass	2 1/4	1 1/2		10
1/2M	1/2F	38275-1/2 x 1/2-SS	St. Steel	2 1/4	1 1/2		10
3/4M	3/4F	38275-3/4 x 3/4	Brass	2 1/4	1 3/4		17
3/4M	3/4F	38275-3/4 x 3/4-SS	St. Steel	2 1/4	1 3/4		17

Call for availability of reducing sizes.



COMMON APPLICATIONS



ORDERING INFORMATION

38275 Type
 no material code = Brass
 SS = 303 Stainless Steel

Cast Type
 no material code = Brass
 I = Cast Iron
 SS = 303 Stainless Steel and
 Cast 316 Stainless Steel

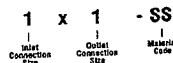
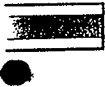
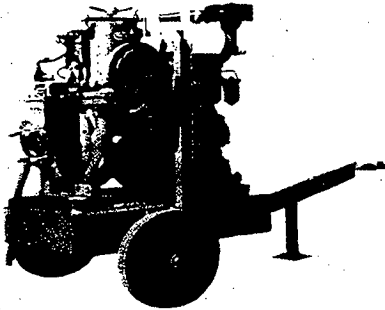


Fig 2



CD 80 Dri-Prime™ Pumps



Features:

Close mounted arrangement carrying pump and automatic priming compressor mounted to a diesel engine (Lister TS4 illustrated)

All metal construction solids handling pump end.

Extensive application flexibility - will handle raw sewage, slurries and liquids with solids up to 1 1/2 ins diameter.

Recessed impeller version available.

Continuously operated 'Godwin' patented air ejector priming device requiring no form of periodic adjustment or control.

Dry running, oil bath lubricated, mechanical seal with high abrasion resistant silicon carbide interfaces.

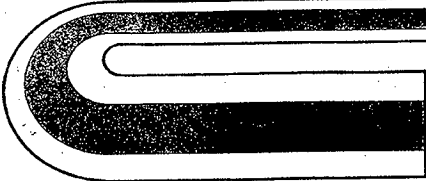
Solids handling, mushroom non-return valve with quick release access feature.

Compact unit mounted on two wheeled highway trailer incorporating integral overnight running fuel tank. Skid mounted versions are also available.

Very simple maintenance - normally confined to checking engine and seal cavity oil levels.

Available with a variety of engines including Lister, Hatz, Deutz and John Deere. Electric motor powered versions are also available.

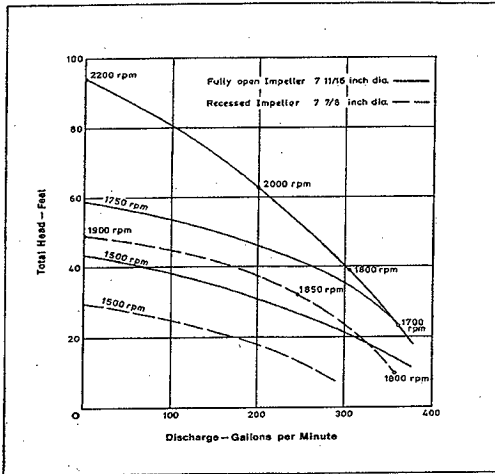
Stanced and unsilenced versions can be supplied.



godwin®
pumps

Fig 3

CD 80 Performance Curve



Performance Table

Diesel Set - Lister TS1 - 6.5 h.p. at 1750 r.p.m.
 Impeller Diameter 7 3/8 ins

Total Suction Head - Feet	Total Delivery Head - Feet				
	10	15	20	25	30
	Output		GPM		
10	370	355	330	300	265
15	355	330	300	265	210
20	330	300	265	210	150
25	320	265	210	150	90

MANOMETRIC or TOTAL Heads are given in the rating tables and curves based on water tests at sea level and 20°C.
 For maximum flows larger diameter pipes may be required.

	Dimensions in ins. - Dry Weight - lbs. (Approximate)			
	Highway Trailer			
	Length	Width	Height	Weight
CD80/TR1	90	54	58	1550

Technical Notes:

- Maximum operating speed: 2200 r.p.m.
- Maximum operating temperature: + 212°F
- Maximum working pressure: 41 p.s.i.
- Maximum suction pressure: 29.0 p.s.i.
- Maximum casing pressure: 61 p.s.i.
- Fuel tank capacity: 20 gallons
- Pipe connections: 3" A.S.A. 150

Material Specifications:

Pump casing, suction cover, separation tank, body and wearplates: close grained cast iron

Impeller: cast chromium steel hardened to minimum Brinell 341 HB

Shaft sleeve and shaft: 1 1/2 % nickel/chromium steel

Adaptor and ejector housing silicon aluminium

N.R.V. rubber: of high nitrile

Mechanical Seal Faces: solid silicon carbide



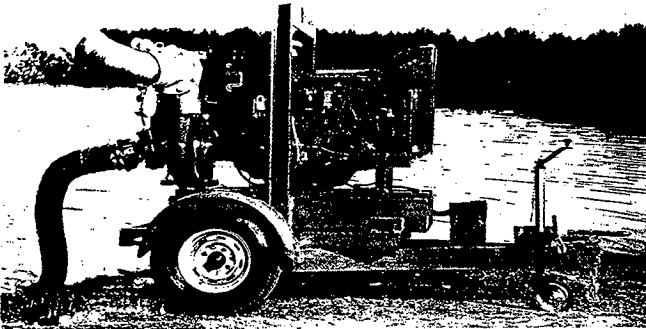
Godwin Pumps of America, Inc.
 Floodgate Road
 Bridgeport, NJ 08014
 Tel: (609) 467-3236
 Fax: (609) 467-4841

Specifications and illustrations are subject to revision without notice.

© Copyright 1991, Godwin Pumps of America, Inc.
 GPA/CD80/91

Fig 4

CD150M Dri-Prime™ Pumps



Features:

Close mounted arrangement carrying pump and vacuum priming compressor mounted to a diesel engine or electric motor.

All metal construction solids handling pump end.

Extensive application flexibility - will handle raw sewage, slimes and liquids with solids up to 3 in. in diameter.

Continuously operated 'Godwin' patented air ejector priming device requiring no form of periodic adjustment or control.

Dry running, oil bath, mechanical seal with high abrasion resistant silicon carbide interfaces.

Solids handling ball type non-return valve with renewable flexible rubber seat and quick release access feature.

Compact unit mounted on a skid base or two wheeled highway trailer both incorporating integral overnight running fuel tank.

Very simple maintenance - normally confined to checking engine and seal cavity oil levels.

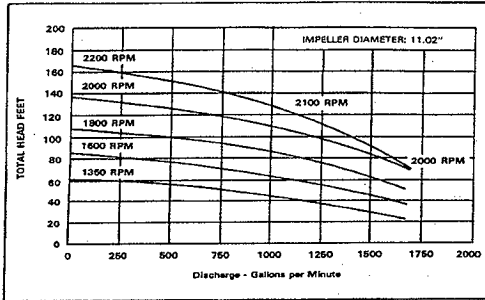
Available with a variety of engines including Lister, Hatz, Deutz, and John Deere.

Silenced and unsilenced versions can be supplied.

godwin®
pumps

Fig 5

CD150M Performance Curve



Performance Tables

Diesel Set - Hatz 3L40C - 24.1 h.p. at 1500 r.p.m.
 Impeller Diameter 10 3/4 in.

Total Suction Head - Feet	Total Delivery Head - Feet				
	10	20	30	40	50
10	1850	1700	1560	1355	1050
15	1740	1620	1485	1200	850
20	1700	1560	1355	1050	575
25	1535	1465	1225	850	120

Diesel Set - John Deere 4039D - 59 h.p. at 1800 r.p.m.
 Impeller Diameter 10.8 in.

Total Suction Head - Feet	Total Delivery Head - Feet				
	10	20	30	40	50
10	1980	1900	1850	1800	1680
15	1850	1810	1700	1520	1400
20	1670	1590	1500	1380	1240
25	1500	1400	1340	1240	1100

MANOMETRIC or TOTAL Heads are given in the rating tables and curves based on water tests at sea level and 20°C.

For maximum flows larger diameter pipes may be required.

Dimensions in in. - Dry Weight - lbs

	Highway Trailer			
	Length	Width	Height	Weight
Hatz 3L40C	90	56	51	2,540
John Deere 4039D	108	64	75	2,750

Technical Notes:

- Maximum operating speed: 2200 r.p.m.
- Maximum operating temperature: + 212°F
- Maximum working pressure: 58.5 p.s.i.
- Maximum suction pressure: 29.0 p.s.i.
- Maximum casing pressure: 88 p.s.i.
- Fuel tank capacity: 20 to 100 gal.
- Pipe connections: 6" A.S.A. 150

Material Specifications:

Pump casing, suction cover, separation tank and wearplates: close grained cast iron

Impeller: cast chromium steel hardness to minimum Brinell 341 HB

Shaft: 1 1/2% nickel chromium steel

NRV Body-Ejector Housing: silicon aluminium

N.R.V. Ball and Seat: high nitrile rubber

Mechanical Seal Faces: solid silicon carbide



Godwin Pumps of America, Inc.
 Floodgate Road
 Bridgeport, NJ 08014
 Tel: (609) 467-3636
 Fax: (609) 467-4841

Specifications and illustrations are subject to revision without notice.

*Copyright 1991, Godwin Pumps of America, Inc.
 GPA/CD150/91

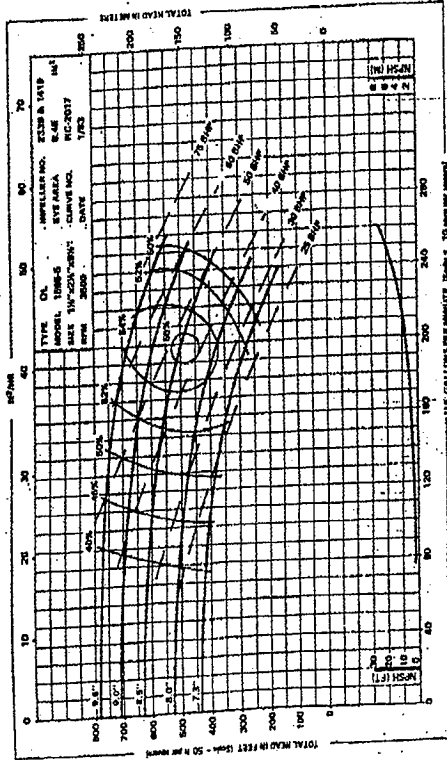
Fig 6



PACO Pumps, Inc.
P.O. Box 12824, 645 92nd Avenue
Oakland, California 94604-2924
(415) 635-3200 Telex: 33-5312

END SUCTION CENTRIFUGAL PUMPS
Type OL

PERFORMANCE CURVES — 3500 RPM



2.00
3.50
3.75
2.40

1783 NEW

Fig 7

JAN-30-97 10:44 FROM:GODVIN PUMPS - SALES

ID:16094674841

PAGE 2

McCrometer PRODUCT DATA

3255 WEST STETSON AVENUE, HEMET, CALIFORNIA 92545 PHONE: (909) 692-6011 TELE: 678-848 FAX: (909) 692-3078 BULLETIN MF100

FLANGED END FLOWMETER MODEL MF100

DESCRIPTION

The Model MF100 is designed to provide high pressure rating and excellent meter accuracy in an inexpensive package. Model MF100 meters are manufactured to comply with the applicable provisions of the American Water Works Association Standard No. C704-92 and latest revision for propeller type flowmeters. The impeller and drive assembly are easily accessed through the open end of the meter tube. As with all McCrometer propeller flowmeters, standard features include a magnetically coupled drive, instantaneous flowrate indicator and straight-reading, six-digit totalizer.

Impellers are manufactured of high-impact plastic, capable of retaining their shape and accuracy over the life of the meter. Each impeller is individually calibrated at the factory to accommodate the use of any standard McCrometer register, and since no change gears are necessary, the MF100 can be field-serviced without the need for factory recalibration. Factory lubricated, stainless steel bearings are

used to support the impeller shaft. The sealed bearing design limits the entry of materials and fluids into the bearing chamber providing maximum bearing protection.

An instantaneous flowrate indicator is standard and available in gallons per minute, cubic feet per second, liters per second and other units. The register is driven by a flexible steel cable encased within a protective vinyl liner. The register housing protects both the register and cable drive system from moisture while allowing clear reading of the flowrate indicator and totalizer.

INSTALLATION

Standard installation is horizontal mount. If the meter is to be mounted in the vertical position, please advise the factory. A straight run of full pipe the length of five diameters ahead and one diameter behind the meter is the minimum normally recommended.

APPLICATIONS

- Center pivot systems
- Sprinkler irrigation systems
- Drip irrigation systems
- Golf course and park water management
- Commercial nurseries
- Water and wastewater management

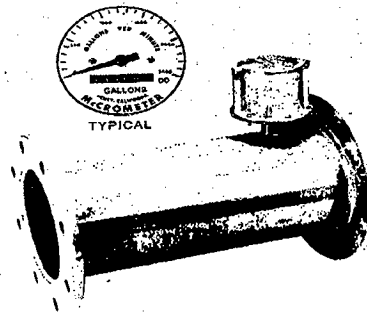


Fig 8

JAN-28-97 10:45 FROM:GODWIN PUMPS - SALES ID:16894674841 PAGE 3
 FLANGED END FLOWMETER MODEL MF100

SPECIFICATIONS

PERFORMANCE

ACCURACY / REPEATABILITY: ± 2% of reading guaranteed throughout full range. ± 1% over reduced range. Repeatability 0.25% or better.
MAXIMUM TEMPERATURE: (Standard Construction) 160°F constant.
PRESSURE RATING: 150 psf.

MATERIALS

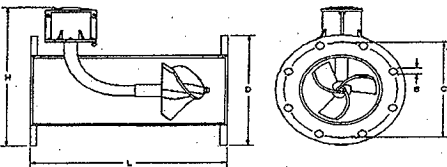
BEARING ASSEMBLY: Impeller shaft is 316 stainless steel. Ball bearings are 440C stainless steel.
MAGNETS: Permanent type, Cast or sintered alnico.
BEARING HOUSING: Brass; 316 stainless steel optional.
REGISTER: An instantaneous flowrate indicator and six-digit straight-reading totalizer are standard. The register is hermetically sealed within a die cast aluminum case. This protective housing includes a domed acrylic lens and hinged lens cover with locking hasp.

IMPELLER: Impellers are manufactured of high-impact plastic, retaining their shape and accuracy over the life of the meter. High temperature impeller is optional.

FLOW TUBE: Fusion-bonded epoxy-coated carbon steel.

OPTIONS

- Forward/reverse flow measurement
- Register extensions
- All stainless steel construction
- High temperature construction
- "Over Run" bearing assembly for higher than normal flowrates
- A complete line of flow recording/control instrumentation
- Flow straightening vanes
- Certified calibration test results



MF100	DIMENSIONS									
Meter and Nominal Pipe Size (Inches)	2	2 1/2	3	4	6	8	10	12		
Maximum Flow U.S. GPM	250	250	250	600	1200	1500	1800	2800		
Minimum Flow U.S. GPM	40	40	40	50	90	100	123	150		
Head Loss In Inches at Max. Flow	29.50	29.50	29.50	23.00	17.00	6.76	3.76	2.75		
Shipping Weight, lbs.	32	35	35	45	100	125	145	178		
B (Inches)	3/4	3/4	3/4	7/8	7/8	7/8	1	1		
C (Inches)	4 3/4	5 1/2	6	7 1/2	9 1/2	11 3/4	14 1/4	17		
D (Inches)	6	7	7 1/2	9	11	13 1/2	16	19		
H (Inches)	11 3/4	12 1/4	12 1/2	15	16	17 1/4	22 1/2	24		
L (Inches)	20	20	20	20	20	20	20	20		
No. of Bolts Per Flange	4	4	4	8	8	8	12	12		

Large flowmeters on special order. McCrometer reserves the right to change design or specifications without notice.

FOR MORE INFORMATION CONTACT:



3255 W. Station Ave.
 Houston, TX 77065
 (909) 652-0811 / Telex: 678 343
 Fax: (909) 652-3078

10WGD11-03/S00840

© 1993 by KETEMA, INC. / Printed in U.S.A.

Fig 9

McCrometer PRODUCT DATA

3255 WEST STETSON AVENUE, HEMET, CA 92345-7789 USA

PHONE 909 652-6811

FAX 909 652-9078

BULLETIN G1200

BASIC SPECIFICATIONS FOR McCROMETER PROPELLER FLOWMETERS

STANDARD INSTANTANEOUS FLOWRATE INDICATOR AND STRAIGHT READING TOTALIZER

Registers are six-digit, straight-reading type available in Gallons, Cubic Feet, Acre Feet, Cubic Meters and other standard measurements. Instantaneous flow indicator need to be of the magnetic cup design, and is available in Gallons per Minute, Cubic Feet per Second, Miner's Inches, Liters per Second and other standards.

Registers can be removed and replaced without interrupting service. The register case is hermetically sealed with a hinged lens cover and locking hasp. Material is die cast aluminum. Molded lens is domed, acrylic material.

Changes in calibration are accomplished on all McCrometer meters by exchanging the register assembly.

REGISTER OPTIONS

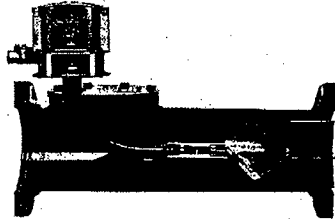
- Forward/reverse flow
- Test hand/index wheel
- Anti-reverse totalizer
- Custom scale
- Extended digit totalizer to increase maximum total reading

STANDARD FLEXIBLE DRIVE

The register is driven by a flexible steel cable encased in a protective vinyl liner which eliminates troublesome and costly worm or bevel gear drives. This unique cable drive allows the register to be extended toward.

STANDARD MAGNETIC DRIVE/BEARING ASSEMBLY

The stainless steel bearings support the propeller and allow it to freely rotate. The two permanent magnets on either side of the solid, one piece diaphragm transmit the rotation of the propeller to the flexible drive cable while preventing the process fluid from entering the hermetically sealed cable and register areas. Stainless steel bearings support the impeller and are lubricated at the factory. The shielded bearing design prevents entry of materials and fluids into the bearing chamber, providing maximum bearing protection. The standard bearing housing is made of brass with all stainless steel 440C ball bearings. The impeller shaft, bearing spacers and seal sleeve are 316 stainless steel.



BEARING OPTIONS

- All stainless steel construction, including housing, ball bearings and impeller shaft
- "Over Run" assembly for higher-than-normal flowrates
- Sealed bearings

STANDARD CALIBRATED IMPELLERS

Impellers are manufactured of high impact plastic which keeps its shape and accuracy over the life of the meter. The impellers are calibrated so that standard ratio registers may be used interchangeably. High impact resistance and broad chemical compatibility fit these impellers to a wide range of uses.

IMPELLER OPTIONS

- High temperature resistance impellers
- Acid and caustic resistance impellers

Fig 10

JAN-30-87 10:46 FROM:GDWIN PUMPS - SALES ID:16894874841 PAGE 6
 BASIC SPECIFICATIONS FOR McCROMETER PROPPELLER FLOWMETERS

BASIC SPECIFICATIONS

General: The meters furnished under these specifications shall comply with the applicable provisions of American Water Works Association Standard No. C704-91 for cold water meters applicable to the types of meters described in the bidding schedule as well as the specifications of the invitations for bids. In the event of conflict, the specifications herein shall prevail. Corrosion-resistant materials shall be used throughout the mechanical enclosure. Except for the register assembly, no aluminum materials shall be used. Surfaces of all other parts shall be treated with a fusion-bonded impervious coating. All rotating members, except members in the register assembly, shall be either jewel or ball bearing mounted.

Head Loss: Head loss shall not exceed _____ inches of water at _____ gallons per minute. (See flow range and head loss chart below.)

Impeller: The impeller shall be made of a plastic or other corrosion-resistant material of a rigid but resilient nature, that will not flex or otherwise change in dimension under a high flow of water, and be capable of withstanding temperatures of 160°F without slumping or warping. Impeller will be factory tested and adjusted to maintain an accuracy of plus or minus 2% over the normal flow range and remain accurate without use of change gears. The impeller shall be mounted on a non-corrosive shaft and bearing assembly and shall have a provision for sustaining thrusts at maximum flows. The impeller shall be magnetically coupled to connecting shafts

through a sealed housing to eliminate corrosion and friction. The drive mechanism from the impeller coupling to the register shall be a flexible drive line. The drive mechanism shall be lubricated and sealed at the factory.

Magnetic Drive: The meter instrument shall be driven by axial alnico magnets located on the impeller shaft and on the same axis and shall be completely sealed from water pressure.

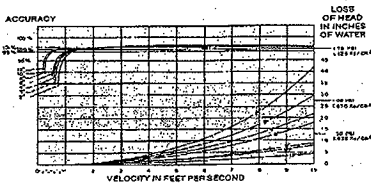
Register: The register shall be on a common axis with the impeller support and shall be rigidly supported by the housing support plate or drop pipe. The register shall consist of an instantaneous indicator and totalizer which shall be mounted perpendicular to the direction of flow and which can be viewed through a transparent cover. The totalizer shall be six-digit, straight-reading, driven by a positive direct drive mechanism from the impeller coupling, and shall register (acre feet, cubic feet, gallons, etc.). The flow indicator shall show flows instantaneously and be driven by a weighted drag mechanism from the impeller coupling. (See meter detail for available calibrations.) The meter shall be accurate within plus or minus 2% of true flow within the range specified. The register assembly shall be factory lubricated and sealed water-tight for infrequent submersion.

*Meter shall be McCrometer Model No. _____ or equal.

FLOW RANGE AND HEAD LOSS CHART

Water and Nominal Pipe Size	2"	2 1/2"	3"	4"	6"	8"	10"	12"	14"	16"	18"	20"	24"
Maximum Flow U.S. GPM	250	250	250	600	1200	1500	1800	2500	3000	4000	5000	8000	8500
Minimum Flow U.S. GPM	40	40	40	50	90	100	125	150	260	275	400	475	700
Maximum Head Loss (in. H ₂ O)	42.00	32.00	28.50	23.00	17.00	6.75	3.75	2.75	2.00	1.75	1.50	1.25	1.00

**ACCURACY AND HEAD LOSS CURVES
 3" TO 12" METERS**



NOTE TESTED IN STANDARD PIPE

STANDARD REGISTER FACE RANGES

Size	Gallons Per Minute	Liters Per Second	Cubic Feet Per Second	Million Gallon Days
2"	0-250	0-20	—	—
2 1/2"	0-250	0-20	—	—
3"	0-600	0-40	0-2	—
4"	0-1200	0-80	0-3	—
6"	0-2500	0-150	0-6	0-4
8"	0-3000	0-200	0-7	0-5
10"	0-3000	0-200	0-9	0-6
12"	0-3000	0-200	0-13	0-8
14"	0-3000	0-200	0-18	0-12
16"	0-3000	0-200	0-20	0-15
18" & 20"	0-10000	0-600	0-20	0-15
24" & 30"	0-15000	0-1000	0-35	0-25

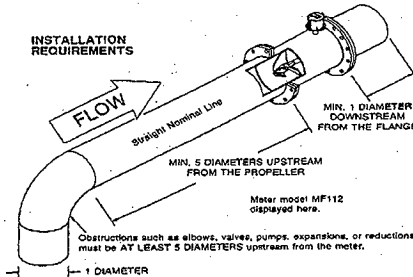
Fig 11

INSTALLATION INSTRUCTIONS

Proper meter installation is the first step to insure meter performance. Follow these instructions closely. Consult an authorized service representative or the factory for any circumstances encountered not covered in these instructions.

All McCrometer products are tested and inspected during manufacture and prior to shipping. An inspection should be performed at the time of unpacking to detect any damage that might have occurred during shipment.

INSTALLATION REQUIREMENTS

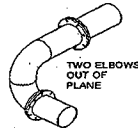


EXAMPLE:

A 3 inch nominal size meter:
 UPSTREAM: Requires 8" x 5 = 40"
 DOWNSTREAM: Requires 8" x 1 = 8"

STRAIGHTENING VANES:

Vanes can be added to insure steadier flow through the meter. Option # 6.



McCrometer propeller meters should be installed a minimum of five diameters downstream of any obstructions. Flowmeters are velocity sensing devices and are vulnerable to certain upstream disturbances. Because of this, meters need certain lengths of straight pipe runs before and after the meter. These distances usually relate to the diameter of the pipe used. Obstructions can include elbows, valves, pumps and changes in pipe diameter. The uneven flow created by these obstructions can vary with each system. If your applications provides for more than five diameters of upstream run, use the available distance.

Downstream run should be one diameter of straight pipe length after the meter.

NOTE: Special attention should be given to systems using two elbows "out of plane" or devices such as a centrifugal sand separator. These cause swirling flow in the line that affect propeller meters. Well developed swirls can travel up to 100 diameters downstream if unobstructed. Since most installations have less than 100 diameters to work with, straightening vanes become necessary to alleviate the problem. Straightening vanes will break-up most swirls and ensure more accurate measurement. McCrometer's mainline meters like the MV500 series have vanes included as a standard feature. If your model does not have straightening vanes (e.g., MO300 Bolt-On Saddle series), McCrometer actively encourages you to include them in the pipe just ahead of the meter.

OTHER INSTALLATION CONSIDERATIONS

- All propeller flowmeters are calibrated for a full pipe line. If the pipe isn't completely full, the flowmeter will overregister the flow. Although a minimum line pressure isn't necessary for an accurate measurement, a full pipe is!

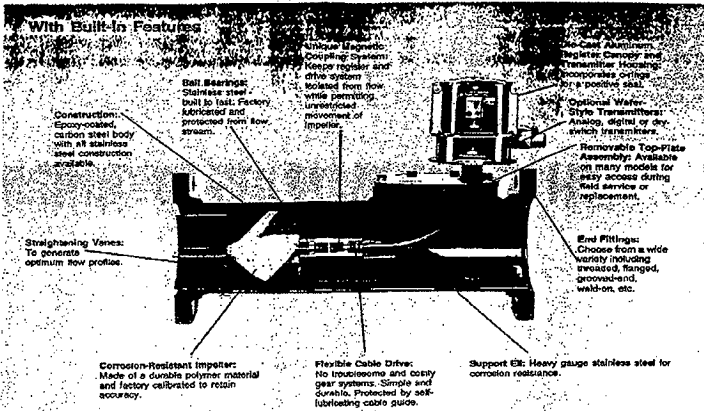
- McCrometer flowmeters can be mounted either horizontally or vertically. Although most applications are horizontally oriented, mounting the meter vertically actually offers some slight advantages. One reason is that gravity has a more pronounced flow-conditioning effect with lines in the vertical (as opposed to horizontal) orientation. The intended configuration of the meter must be specified when ordering.
- With the meter installed, check the rate-of-flow indicator. It should be stable to the point that it can be easily read. Some movement is normal, but if the indicator is moving erratically back and forth, disturbances exist and meter accuracy decreases.

SAFETY

- Any person installing, inspecting or maintaining a McCrometer flowmeter should have a working understanding of piping configurations and systems under pressure.
- Before adjusting or removing any meter, be certain the system has depressurized completely. **NEVER ATTEMPT TO REMOVE A METER UNDER PRESSURE!**
- Be careful when lifting meters. Meters can cause serious injury if dropped or lifted incorrectly.
- Only necessary and appropriate tools should be used when working on a meter.
- Before starting a system, make sure all connections are properly secured. Keep a safe and prudent distance away from the meter during system start-up.

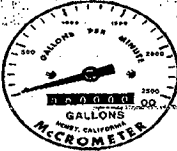
Fig 12

JAN-30-97 10:48 FROM:GODVIN PUMPS - SALES ID:16084674841 PAGE 7



Accuracy: $\pm 2\%$ of indicated reading; meets or exceeds all AWWA standards.

Variety of Sizes: Designs for 2" through 96" line size and larger.



Mechanical Register incorporates both a six-digit totalizer and instantaneous flow-rate indicator. Calibrations available in all common flow units.

McCrometer flowmeters are an economical choice for dependable flow measurement in a wide variety of water and wastewater applications including: main line metering, transfer lines, feeder lines, fire hydrant metering and water and wastewater treatment.

While most meters feature an epoxy-coated steel body, many are available in all stainless steel. The standard maximum constant temperature rating is 160°F, however, higher temperature ratings are available. The register case is hermetically sealed with a hinged lens cover and locking nasp.

McCrometer also offers the V-CONE™ differential pressure meter, which has no moving parts and provides compatibility with a wide range of fluids. This device offers all of the advantages of differential pressure flow metering with greatly improved performance.

- MCCROMETER Flowmeters are:**
- Economical to buy and maintain
 - Easily serviced by field personnel
 - Available with a variety of options
 - Ideal for all types of municipal water/wastewater applications

FOR MORE INFORMATION CONTACT:

MCCROMETER 3255 West Station Avenue
 Newark, CA 92245-7729 USA
 909 632-6811
 Fax 909 632-3078

Part Number 24228-0
 2505/01-05

© 1995 by McCrometer / Printed in USA

Fig 13

AT-MIO-64E-3

E Series Multifunction I/O Boards for ISA

AT-MIO-16E-1, AT-MIO-16E-2, AT-MIO-64E-3

Type of DAC.....	Double buffered, multiplying	Power-on state.....	Input (High-Z)
FIFO buffer size.....	2,048 samples	Data transfers.....	Programmed I/O
Data transfers.....	DMA, Interrupt, programmed I/O	Timing I/O.....	
DMA mode.....	Single transfer, demand transfer	Number of channels.....	2 up/down counter/fimers, 1 frequency scaler
Transfer Characteristics		Resolution.....	24 bits
Relative accuracy (INL).....		Counter/fimers.....	24 bits
After calibration.....	± 0.3 LSB typical, ± 0.5 LSB maximum	Frequency scalars.....	4 bits
Before calibration.....	± 4 LSB maximum	Compatibility.....	TTL/CMOS
DNL.....		Base clocks available.....	
After calibration.....	± 0.3 LSB typical, ± 1.0 LSB maximum	Counter/fimers.....	20 MHz, 100 kHz
Before calibration.....	± 3 LSB maximum	Frequency scalars.....	10 MHz, 100 kHz
Monotonicity.....	12 bits, guaranteed after calibration	Base clock accuracy.....	$\pm 0.01\%$
Other error.....		Maximum source frequency.....	20 MHz
After calibration.....	± 1.0 mV maximum	Minimum source pulse duration.....	10 ns in edge-detect mode
Before calibration.....	± 200 mV maximum	Minimum gate pulse duration.....	10 ns in edge-detect mode
Gain error (relative to internal reference).....		Data transfer.....	DMA, Interrupt, programmed I/O
After calibration.....	$\pm 0.01\%$ of output maximum	DMA mode.....	Single transfer
Before calibration.....	$\pm 0.5\%$ of output maximum	Triggers	
Gain error.....		Analog Trigger	
(relative to external reference).....	$\pm 0\%$ to $\pm 0.5\%$ of output maximum, not adjustable	Source	
Voltage Output		AT-MIO-16E-1, AT-MIO-16E-2... ACH-0.15%, PFI0/TRIG1	
Ranges.....	± 10 V to ± 10 V, \pm EXTREF, 0 to EXTREF	AT-MIO-64E-3... ACH-0.05%, PFI0/TRIG1	
Output coupling.....	DC	Level.....	\pm full-scale, internal; ± 10 V, external
Output impedance.....	0.1 Ω maximum	Slope.....	Positive or negative (software selectable)
Current drive.....	± 5 mA maximum	Resolution.....	3 bits, 1 to 256
Protection.....	Short-circuit to ground	Hysteresis.....	Programmable
Power-on state.....	0 V	Bandwidth (3 dB).....	1.5 MHz internal, 7 MHz external
External reference input.....		External input (PFI0/TRIG1).....	
Range.....	± 11 V	Impedance.....	10 k Ω
Overvoltage protection.....	± 25 V powered on, ± 15 V powered off	Coupling.....	DC
Input impedance.....	10 k Ω	Protection.....	-0.5 to $V_{cc} + 0.5$ V when configured as a digital signal; ± 35 V when configured as an analog trigger signal or disabled; ± 35 V powered off
Bandwidth (3 dB).....	1 MHz	Digital Trigger	
Dynamic Characteristics		Compatibility.....	TTL
Settling time for full-scale step.....	3 μ s to ± 0.5 LSB accuracy	Response.....	Rising or falling edge
Slew rate.....	20 V/ μ s	Tube width.....	10 ns minimum
Noise.....	200 μ Vrms, DC to 1 MHz	Trigger lines.....	7
Glitch energy (at midscale transition).....		Compatibility.....	Slave
Magnitude.....		Power Requirement	1.0 A
Reglitching disabled.....	± 200 mV	Purver available at I/O connector.....	-4.65 VDC to $+5.25$ VDC at 1 A
Reglitching enabled.....	± 30 mV	Physical	
Duration.....	1.5 μ s	Dimensions	
Stability.....		(not including connectors)..... 33.8 by 9.9 cm (13.3 by 3.9 in.)	
Offset temperature coefficient.....	± 50 mV/ $^{\circ}$ C	I/O connectors.....	
Gain temperature coefficient.....	± 25 ppm/ $^{\circ}$ C	AT-MIO-16E-1.....	
Internal reference.....	± 25 ppm/ $^{\circ}$ C	AT-MIO-16E-2..... 68-pin male SCSI-II type	
External reference.....	± 25 ppm/ $^{\circ}$ C	AT-MIO-64E-3..... 100-pin female 0.050 D-type	
On-board calibration reference.....		Environment	
Level.....	5,000 V (± 2.5 mV) (actual value stored in EEPROM)	Operating temperature..... 0 $^{\circ}$ to 55 $^{\circ}$ C	
Temperature coefficient.....	± 5 ppm/ $^{\circ}$ C maximum	Storage temperature..... -55 $^{\circ}$ to 150 $^{\circ}$ C	
Long-term stability.....	± 15 ppm/1,000 h	Relative humidity..... 5% to 90% noncondensing	
Digital I/O			
Number of channels.....	8 input/output		
Compatibility.....	TTL/CMOS		
Digital logic levels.....			

Level	Minimum	Maximum
Input low voltage (I_{OL})	0 V	0.6 V
Input high voltage (I_{OH})	2 V	5 V
Input low current (I_{OL})	-	-320 μ A
Input high current (I_{OH})	-	30 μ A
Output low voltage (V_{OL})	-	0.4 V
Output high voltage (V_{OH})	4.25 V	-

Fig 14

AT-MIO-64E-3

E Series Multifunction I/O Boards for ISA

Specifications

Typical specifications are typical at 25°C unless otherwise noted.

Analog Input

- Input Characteristics
Number of channels
AT-MIO-16E-1 16 single-ended or 8 differential (software selectable)
AT-MIO-16E-2 64 single-ended or 32 differential (software selectable)
AT-MIO-64E-3 500 kS/s
Type of ADC Successive approximation
Resolution 12 bits, 1 in 4,096
Maximum sampling rate
AT-MIO-16E-1 1.25 MS/s
AT-MIO-16E-2 500 kS/s
AT-MIO-64E-3 500 kS/s single channel sampling
333 kS/s multichannel scanning
Throughput to system memory
EISA machines 1.0 - 1.25 MS/s
ISA machines 600 - 900 kS/s
Input signal ranges

Gain (Software Selectable)	Range (Software Selectable)
	Micro V
0.5	±50V
1	±25V
2	±12.5V
5	±500 mV
10	±250 mV
50	±100 mV
100	±50 mV

- Input coupling DC
Maximum working voltage ±11 V @ ground
Signal = common mode Each input should remain within
Overvoltage protection ±25 V powered on, ±15 V powered off
Inputs protected
AT-MIO-16E-1 ACH<0.15>, AISENSE
AT-MIO-16E-2 ACH<0.63>, AISENSE, AISENSE2
AT-MIO-64E-3 8,192 samples
RIFO buffer size
AT-MIO-16E-1 2,048 samples
AT-MIO-16E-2 2,048 samples
AT-MIO-64E-3 2,048 samples
Data transfer DMA, Interrupts, programmed I/O
DMA modes Single transfer, demand transfer
Configuration memory size 512 words
Transfer Characteristics
Relative accuracy ±0.5 LSB typical dithered,
±1.5 LSB maximum undithered
DNL ±0.5 LSB typical, ±1.0 LSB maximum
No. of flag codes 12 bits, guaranteed
Offset Error
Pregain error after calibration ±12 µV maximum
Pregain error before calibration ±2.5 mV maximum
Pregain error after calibration ±0.5 mV maximum
Pregain error before calibration ±100 mV maximum
Gain error (relative to calibration reference)
After calibration (gain = 1) ±0.02% of reading maximum
Before calibration ±2.5% of reading maximum
Gain = 1 with gain error ±0.02% of reading maximum
Assumed to 0 at gain = 1 ±0.02% of reading maximum

Amplifier Characteristics

- Input impedance
Normal powered on 100 Ω in parallel with 100 pF
Powered off 820 Ω minimum
Overload 820 Ω minimum
Input bias current ±200 pA
Input offset current ±100 pA
CMRR, DC to 60 Hz

Gain	CMRR
15	700 dB
2.5	100 dB
	106 dB

Dynamic Characteristics

Bandwidth

Board	Small Signal (3 dB)	Large Signal (EN THD)
AT-MIO-16E-1	1.6 MHz	1 MHz
AT-MIO-16E-2	1 MHz	300 kHz
AT-MIO-64E-3	1 MHz	300 kHz

Settling time to full-scale step

Board	Gain	Accuracy		
		±0.012% (±0.5 LSB)	±0.024% (±1 LSB)	±0.098% (±4 LSB)
AT-MIO-16E-1	0.5	2 µs typical	1.5 µs typical	1.5 µs typical
		2 µs maximum	2 µs maximum	2 µs maximum
		1.5 µs typical	1.5 µs typical	1.5 µs typical
	1	2 µs typical	1.5 µs typical	1.5 µs typical
		2 µs maximum	1.5 µs maximum	1.3 µs maximum
		2 µs typical	1.5 µs typical	1.5 µs typical
2 to 50	2 µs typical	1.5 µs typical	1.5 µs typical	
	2 µs maximum	1.5 µs maximum	1.5 µs maximum	
	2 µs typical	1.5 µs typical	1.5 µs typical	
100	2 µs typical	1.5 µs typical	1.5 µs typical	
	2 µs maximum	1.5 µs maximum	1.5 µs maximum	
	2 µs typical	1.5 µs typical	1.5 µs typical	
AT-MIO-16E-2	All	2 µs typical	1.5 µs typical	1.5 µs typical
AT-MIO-64E-3	All	2 µs typical	2 µs typical	2 µs typical
		2 µs maximum	2 µs maximum	2 µs maximum
		2 µs typical	2 µs typical	2 µs typical

System noise (LSBs rms, not including quantization)

Board	Gain	Offset Error	Dither On
AT-MIO-16E-1	0.5 to 10	0.25	0.8
		20	0.4
		100	0.5
AT-MIO-16E-2	0.5 to 10	0.15	0.8
		20	0.3
		100	0.5

Crosstalk -80 dB, DC to 100 kHz

Stability
Recommended warm-up time 15 minutes

Offset temperature coefficient
Pregain ±5 µV/°C

Pregain ±240 µV/°C

Gain temperature coefficient ±20 ppm/°C

Onboard calibration reference
Level 5,000 V (±2.5 mV)

Temperature coefficient ±5 ppm/°C maximum

Long-term stability ±15 ppm/V_{1000h}

Continued on page 3-76

Fig 15

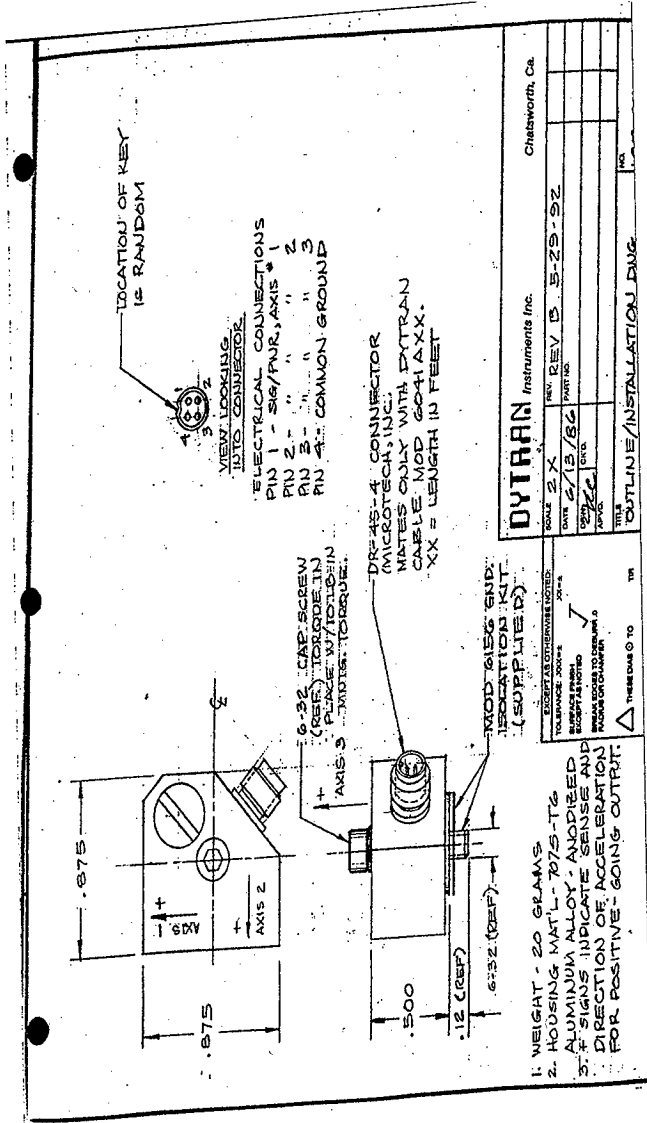


Fig 16

Low Frequency Response and Quasi-Static Behavior of LIVM Sensors

First, let's define the terms "Low Frequency Response," "Quasi-static Behavior" and "Discharge Time Constant" as they apply to the context of this article.

Low Frequency Response – The ability of a sensor to measure very low frequency sinusoidal or periodic inputs (pressure, force and acceleration) with accuracy. This ability is best characterized by a graph of sensitivity vs. frequency with input amplitude held constant.

Quasi-Static Behavior – The response of a piezoelectric sensor to static (steady state) events, characterized by a graph of sensor output vs. time. This is a measure of the length of time meaningful information is retained after the initial application of a steady state measured. ("Quasi" means "nearly or almost." Its use here is appropriate since piezoelectric sensors do not have true static response, but can only approximate static behavior.)

Discharge Time Constant – The time (in seconds) required for a sensor output voltage signal to discharge 63% of its initial value immediately following the application of a long term, steady state input change.

– Sensor Discharge Time Constant –

The discharge time constant (TC) of the Low Impedance Voltage Mode (LIVM) sensor and the coupling time constant of AC coupled power units are very important factors when considering the low frequency and the quasi-static static response capabilities of an LIVM system. For the time being we will consider only the sensor discharge TC and not the power unit coupling TC. As you will see, direct-coupled power units are available which remove the limiting effect of AC coupled power units on system behavior.

The term "Discharge Time Constant" or simply "TC," is referred to often on data sheets and specifications for piezoelectric sensors. It is important to understand the meaning of this term to understand how this influential design parameter controls both quasi-static behavior and low frequency response.

As we describe sensor discharge TC, its effect on quasi-static behavior will be quite apparent so we will relate these two topics first, then examine how TC relates to low frequency response.

– Discharge TC and Quasi-Static Response –

In the following explanation, we will refer to the term "step function" input. This type of input is obtained, for example, by using static means such as a dead weight tester to calibrate a pressure sensor and a proving ring to calibrate a force sensor.

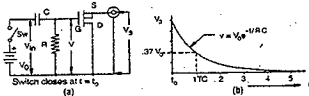


Figure 1: Discharge Time Constant (TC) Output vs. Time

For purposes of TC analysis, the sensor piezo element and internal amplifier may be represented schematically by the RC circuit, battery & switch shown in Figure 1a. Gate voltage (v) responds as shown in Figure 1b when voltage step (V₀) is impressed across the input terminals at t₀. Such a step function voltage input would be generated by a sensor element in response to a sudden change in pressure or force input. At voltage (v) instantly assumes value V₀, then immediately begins to discharge (or decay) exponentially with time. The decay function is described by the following equation:

$$v = V_0 e^{-t/TC} \quad (\text{Eq. 1})$$

Where:

- v = instantaneous gate voltage (Volts)
- V₀ = initial voltage at time t₀ (Volts)
- e = base of natural logarithm (Ohms)
- R = gate resistance (Ohms)
- C = total shunt capacitance (Farads)

It is important to note here that the resistance (R) is the value of the resistor placed across the piezoelectric element to bias the MOSFET sensor.

The capacitance (C) is comprised of the self-capacitance of the piezo crystal, the input capacitance of the amplifier, stray capacitance and any ranging capacitance placed across the crystal to reduce sensitivity (if need be). The product RC is the sensor discharge TC, in seconds.

$$RC = TC, (\text{Ohms}) \times (\text{Farads}) = (\text{Seconds}) \quad (\text{Eq. 2})$$

Referring again to Figure 1b, we should point out a few important features of the exponential decay curve. First, if we let time (t) equal t then Equation 1 reduces to:

$$v = V_0 e^{-1} = V_0/e = .37 V_0 \quad (\text{Eq. 3})$$

This result states that at time t=TC (one time constant) the signal is discharged to 37% of V₀, or put in another way, has lost 63 (63%) of its initial value V₀ in 5 x TC seconds (five time constants), the output will have decayed essentially to zero.

Another important point is that the curve shown in Figure 1b is relatively linear to about 10% TC, i.e., in 1% of the TC, the sensor will discharge 1% and so on up to 10% TC. In fact, we may draw the conclusion that to have at least 1% accuracy in quasi-static force or pressure measurement, we must take the reading of the output within a time window of 1% of the sensor TC.

Static response is most closely approximated when the event time is a very small percentage of the sensor (or system) discharge TC. This situation is best illustrated by example:

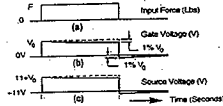


Figure 2: Approaching Static Response

Figure 2 illustrates a hypothetical situation where the static event lasts 1% of the sensor TC. (Assume a force sensor with a 1000 sec. TC and a 1 sec. event time.) Figure 2a is the force-time history showing input force F

applied to the sensor, starting at time t_0 and holding steady for ten seconds. At time $t_0 + 10$ seconds, the force is removed.

Figure 2b shows the corresponding gate voltage V. At time t_0 , this voltage instantly assumes value V_0 (sensor sensitivity X force F). After time $t_0 + 10$ sec., voltage has decayed in accordance with Equation 1, losing 1% of its initial value. At time $t_0 + 10$, the input force F is abruptly removed. Voltage V instantly drops to a point 1% below the original baseline (again responding with voltage change V_0), then begins to charge toward the baseline in accordance with Equation 1.

Figure 2c shows the corresponding output voltage measured at the output of the sensor (at the source terminal of the TC). Notice that the voltage waveform is similar in form, but elevated upward by the sensor bias voltage (approximately +11 Volts DC).

If we were attempting to calibrate this sensor by static means we would have .01 x 1000 or 10 seconds to take the reading of the output voltage after the application of the input step for a reading with 1% accuracy. A means of transient signal capture such as a digital storage oscilloscope facilitates such calibrations.

— Low Frequency Response —

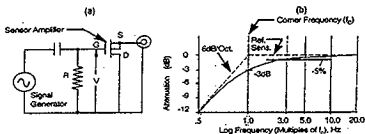


Figure 3: Low Frequency Response Characteristics

The RC circuit shown in Figure 1a is also a first order high-pass filter illustrated in Figure 3a above. We now switch to the frequency domain to describe the effect of TC on low frequency response.

Figure 3b is a Bode plot or graph of the low frequency response of an LVM sensor. A very significant point on the graph is the corner frequency f_c . At this frequency the output from the sensor has decreased by 3dB or approximately 30% from its reference sensitivity (the sensitivity that would be obtained at about 1 decade (10X) above the corner frequency). The slope or rolloff rate of the sensor is always -6dB/octave, standard for a first order high pass filter. In the Bode plot, this slope line crosses the reference axis at f_c . The phase shift at f_c is 45°.

Corner frequency f_c is set by the TC. To find f_c for your sensor, first consult the calibration certificate or data sheet supplied to obtain the TC, then solve for the corner frequency as follows.

$$\text{Corner Freq.} = f_c = .16 / \text{TC (Sec)} / (\text{Hz}) \quad (\text{Eq. 4})$$

Another important frequency is where the output is down by 5% from the reference sensitivity. This point is approximately 3 x the corner frequency on

$$-5\% \text{ Freq.} = 1.5\% = 3 \times f_c (\text{Hz}) \quad (\text{Eq. 5})$$

Figure 4 is a chart of attenuation and phase shift vs. frequency for a high pass filter. The values for these two parameters can be determined at multiples of the corner frequency with this chart.

Multiples of Corner Frequency f_c	Attenuation Factor	Attenuation (dB)	Phase Shift (degrees)
1/2	.10	-20	-64.3
1/3	.05	-30	-69.0
1/4	.03	-39	-71.5
1/5	.02	-48	-76.0
1/6	.017	-56	-78.7
1/8	.013	-68	-84.3
1/10	.010	-80	-89.4

Figure 4: Attenuation & Phase Shift vs. Multiples of Corner Frequency

— High Frequency Response —

The relationship between TC and high frequency response and/or rise time is often misunderstood so some clarification may be in order. Sensor is often power unit coupling TC have absolutely no effect on these two characteristics.

High frequency response and rise time for any sensor are controlled by mechanical design characteristics and may also be affected by system factors such as drive current, cable length, mounting techniques, passage resonances, mass loading, etc. These topics are covered in other sections of this catalog.

— The LVM Power Unit as It Effects —

Low Frequency Response and Quasi-Static Capability

At the beginning of this section you were told to ignore the power unit for the time being. You cannot ignore it completely however, because the AC coupled power unit is often the limiting factor in low frequency and quasi-static system capability rather than the sensor itself. All AC (capacitively coupled) power units are high pass filters, which can impair the low frequency response and quasi-static behavior of your system. (Refer to the section "System Low Frequency Response" in the article "Introduction to LVM Accelerometers" for a more complete treatment of the effect of power unit on LF & Q-S response.)

— The DC Coupled Power Unit —

One way to take full advantage of the long TC built into your sensor is to use the Model 4115B DC coupled power unit. This unit uses a summing op-amp circuit rather than a capacitor to direct couple the sensor to the readout.

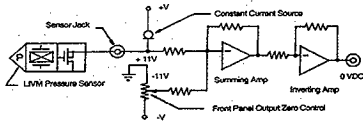


Figure 5: Functional Schematic, Model 4115B

A user-variable negative DC voltage is applied to the summing junction of the amplifier to exactly null the DC bias voltage from the sensor allowing precise zeroing of the output signal. This versatile power unit is especially useful for calibration of pressure and force sensors by static means. The 4115B also has an "AC" coupling mode for use with sensors in thermally unstable environments or for strictly dynamic use. Consult the summary product data sheet on Model 4115B elsewhere in this catalog for specifications and features.

— Transient Thermal Effects —

When using LVM sensors with very long time constants (greater than several minutes) with DC coupled power units such as the 4115B, varying temperatures can affect crystal preload structure, generating slowly changing output voltages, which may appear as annoying baseline shift in the output signal. In situations like this, it is important to insulate the sensor against transient (sudden) thermal inputs. Dytran can provide insulating jackets (or boots) for many sensors to minimize this problem. Consult the factory for details.

SPECIFICATIONS, MODEL 3014A TRIAXIAL ACCELEROMETER

SPECIFICATIONS	VALUE	UNITS
RANGE, F.S. (each axis)	± 500	g
SENSITIVITY, ± 10% [1]	10.0	mV/g
FREQUENCY RESPONSE, ± 5%	2 to 2000	Hz
DISCHARGE TIME CONSTANT, NOM.	0.5	SEC
EQUIVALENT ELECTRICAL NOISE	.007	g, RMS
LINEARITY [2]	1	%F.S.
TRANSVERSE SENSITIVITY, MAX.	5	%
OUTPUT BIAS VOLTAGE, NOM.	+11	VDC
OUTPUT IMPEDANCE, TYP.	100	OHMS
TEMPERATURE RANGE	-60 to +250	°F
COEFFICIENT OF THERMAL SENSITIVITY	.03	%/°F
MAXIMUM VIBRATION	± 600	g
MAXIMUM SHOCK	1000	g
SIZE (HEIGHT x WIDTH x DEPTH)	0.5 x .875 x .875	INCHES
WEIGHT	21	GRAMS
CONNECTOR	4-PIN [3]	
SUPPLY CURRENT RANGE, (each axis) [4]	2-to 20	mA
COMPLIANCE (SUPPLY) VOLTAGE RANGE (each axis)	+18 to +30	VDC
MATERIAL, HOUSING/CONNECTOR	ALUMINUM ALLOY/BRASS	
ENVIRONMENTAL SEAL	EPOXY	
MOUNTING [5]	CENTRAL 6-32 SCREW	SUPPLIED

ACCESSORIES SUPPLIED: (1) Model 6156 Ground Isolation Installation Kit.

[1] Reference sensitivity measured at 100 Hz, 1 G RMS per ISA RP 37.2

[2] Linearity is % of specified full scale (or any lesser full scale range), zero-based best fit straight line method.

[3] Connector mates only with Dytran cable Assy, Model 6041Axx, (xx = length in feet)

[4] Power only with Dytran LIVM power unit or other Dytran-compatible constant current type power unit. If power is applied without current limiting protection, the internal amplifier will be immediately destroyed.

[5] Case ground isolation is achieved by mounting with the Model 6156 Ground Isolation Mounting Kit supplied with each 3014A. See the Outline/Installation Drawing.

Fig 19



Dynamic Transducers and Systems
 21592 Marilla St. • Chatsworth, CA 91311 • Phone 818-700-7818 • FAX 818-700-7880

**CALIBRATION CERTIFICATE
 TRIAXIAL LIVM ACCELEROMETER**

CUSTOMER ARD ENVIRONMENTAL P.O.# 8714
 ORDER NUMBER 94002 TEMP. 23 °C HUMIDITY 47 %
 MODEL 3014A SERIAL NO. 1172 RANGE, F.S. 500 G's

FREQUENCY RESPONSE (1) FREQUENCY (Hz)	Δx AXIS 1	Δy SENSITIVITY (mV/G) AXIS 2	Δz AXIS 3
20	<u>9.9</u>	<u>9.6</u>	<u>10.0</u>
30	<u>9.9</u>	<u>9.7</u>	<u>10.0</u>
50	<u>10.0</u>	<u>9.7</u>	<u>10.1</u>
100	<u>10.0</u>	<u>9.7</u>	<u>10.1</u>
300	<u>10.0</u>	<u>9.8</u>	<u>10.1</u>
500	<u>10.0</u>	<u>9.7</u>	<u>10.0</u>
1000	<u>10.1</u>	<u>9.8</u>	<u>10.1</u>
2000	<u>10.2</u>	<u>9.9</u>	<u>10.1</u>
3000	<u>N/A</u>	<u>N/A</u>	<u>N/A</u>
4000	<u>-</u>	<u>-</u>	<u>-</u>
5000	<u>-</u>	<u>-</u>	<u>-</u>
BIAS VOLTAGE (VDC)	<u>9.6</u>	<u>9.9</u>	<u>9.7</u>
DISCHARGE T.C. (sec)	<u>0.5</u>	<u>0.5</u>	<u>0.4</u>

[1] This calibration was performed in accordance with MIL-STD-45662A using the Back-to-Back Comparison Method per ISA RP37.2 and is traceable to the NIST through test report # 4632-130LH, 822/255150-95. Void date: 07-18-96.

CALIBRATION PERFORMED BY: [Signature] DATE: 3-21-96

CERTIFICATION OF CONFORMANCE

We certify that the products or services listed above are in conformance with the requirements of your purchase order. Objective evidence of manufacturing, inspection, and testing is on file and is available for review at our facility. Where materials or services incorporated in any of the items listed above have been procured by us from vendors, we certify that test reports or suitable evidence of compliance with the requirements of this purchase order have been obtained by us and are available from our files.

[Signature] 3/21/96
 Quality assurance Date
 CAL2019A.DOC

Fig 20

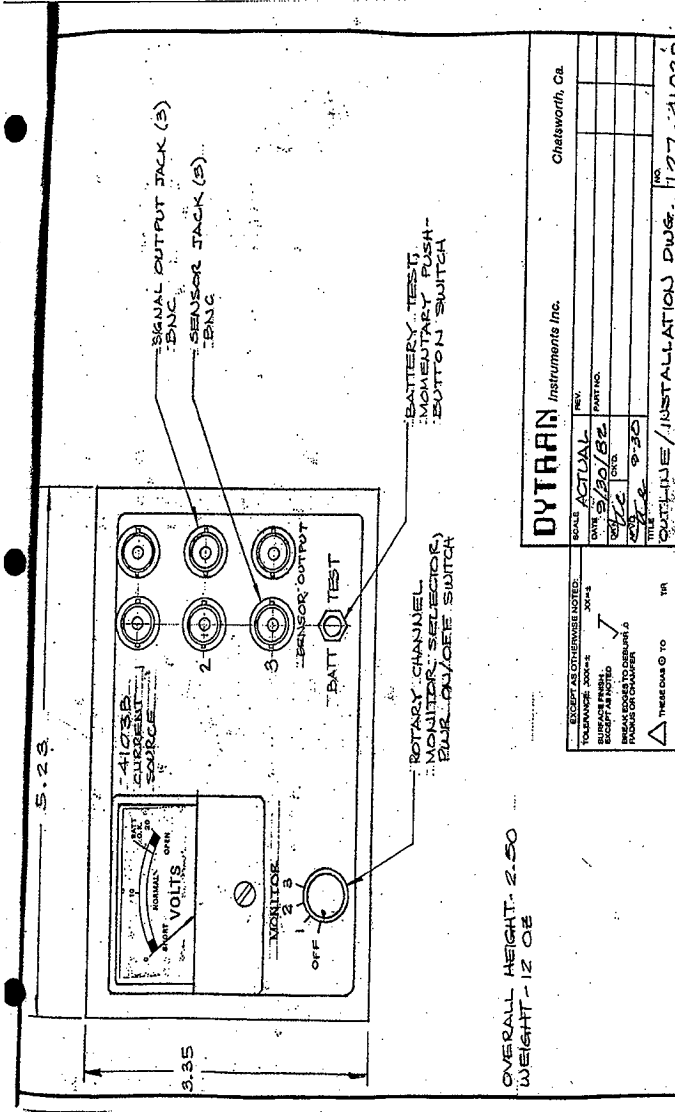


Fig 21



Dynamic Transducers and Systems
 21592 Marilla St. • Chatsworth, CA 91311 • Phone 818-700-7818 • FAX 818-700-7880

**CALIBRATION CERTIFICATE
 UNITY GAIN CURRENT SOURCE POWER UNITS**

MODEL 4002B SERIAL NO. 303

BATTERY POWERED LINE POWERED 115VAC 230VAC

TEMP. 22 °C

HUMIDITY 17 %

CALIBRATION DATA:

POWER SUPPLY VOLTAGE _____ VDC BATTERY VOLTAGE 18.8 VDC

METER ZERO METER CALIBRATION

SENSOR DRIVE CURRENT (mA)

CH1	CH2	CH3	CH4	CH5	CH6	CH7	CH8	CH9	CH10	CH11	CH12	CH13	CH14	CH15	CH16
1.7	1.5	1.5													

AS RECEIVED DATA:

GENERAL CONDITION _____

POWER SUPPLY VOLTAGE _____ VDC BATTERY VOLTAGE _____ VDC

CALIBRATE METER _____ REPLACED BATTERY YES NO

SENSOR DRIVE CURRENT (mA)

CH1	CH2	CH3	CH4	CH5	CH6	CH7	CH8	CH9	CH10	CH11	CH12	CH13	CH14	CH15	CH16

NOTES _____

This calibration was performed in accordance with MIL-STD-45662A.

CUSTOMER ARD ENVIRONMENTAL P.O.# 874

ORDER NO. 94002 DATE 3-18-96

CALIBRATION PERFORMED BY [Signature]

Fig 22

SPECIFICATIONS

MODEL 4103B 3-CHANNEL LIVM POWER UNIT

SPECIFICATIONS	VALUE	UNITS
SENSOR SUPPLY CURRENT, NOM.	1.4	mA
SENSOR EXCITATION VOLTAGE, FRESH BATTS.	+18	VDC
VOLTAGE GAIN	UNITY	
FRONT PANEL VOLTMETER, FS	+20	VDC
COUPLING CAPACITOR, EACH CHANN.	10	uF
PULLDOWN RESISTOR, EACH CHANN.	1.0	MEGOHMS
COUPLING TIME CONSTANT:		
INTO 1 MEGOHM READOUT LOAD	5	SEC
INTO 10 MEGOHM READOUT LOAD	9	SEC
LOWER -3db FREQUENCY:		
WITH 1 MEGOHM READOUT LOAD	.032	Hz
WITH 10 MEGOHM READOUT LOAD	.017	Hz
HIGH FREQUENCY RESPONSE:	DETERMINED BY SENSOR, CABLE LENGTH AND TYPE (TOTAL CAPACITANCE) AND OTHER FACTORS.	
NOISE, WIDEBAND	60	uV, RMS
BATTERY LIFE, NOMINALLY [1]	40	HOURS
BATTERIES, SUPPLIED (2)	9 VOLT TRANSISTOR RADIO TYPE	
SENSOR & OUTPUT CONNECTORS	BNC	JACK
SIZE (HEIGHT X WIDTH X DEPTH)	2.5 X 5.2 X 3.4	IN.
WEIGHT	1.2 (340)	OZ (GRAMS)

[1] BATTERY LIFE HOURS ASSUMES ALL THREE CHANNELS OPERATING CONTINUOUSLY WITH ALKALINE BATTERIES. OTHER TYPES OF BATTERIES MAY PROVIDE MORE OR LESS OPERATING HOURS DEPENDING UPON CHARACTERISTICS.

Fig 23

Pressure TRANSDUCERS



SERIES 100

4-20mA CURRENT OUTPUT PRESSURE TRANSDUCERS

DESCRIPTION

Noshok 100 Series Current Output Pressure Transducers were designed to provide a previously unequalled level of performance, utilizing Piezo Resistive or Thin film sensor technology dependent on pressure range. 100 Series Transducers are highly accurate, shock resistant and extremely stable over a long period of time. EMC, electromagnetic compatibility, to IEC 801 has been engineered in as a standard feature along with reverse polarity, overvoltage, and short circuit protection.

Advanced manufacturing techniques combined with technologically advanced standard features allow Noshok to offer a level of performance previously found only on transducers costing hundreds of dollars more.

A final electrical output and calibration inspection is performed on all Noshok Transmitters and Transmitters after final assembly and prior to shipment to insure 100% "out of the box" reliability.

FEATURES

- Thin film sensor, technology
- Current output signal
- High accuracy and long term stability
- Electromagnetic interference protection
- Available in gauge or absolute measuring ranges
- 0-5 and 0-10 PSI ranges available
- High alternating load resistance
- High overpressure protection
- Dynamic or static measurement capability
- Corrosion resistant stainless steel construction
- Compact size
- Mini-Hirschmann with mating connector electrical connection standard

(1) Compatible with Noshok 1900 series smart system indicators

APPLICATIONS

- Hydraulic and pneumatic systems
- Industrial machinery and machine tools
- Injection molding machines
- Stamping and forming presses
- Pumps and compressors
- Laboratory and test equipment
- Railroad equipment
- HVAC systems
- Medical
- Refrigeration equipment

SPECIFICATIONS

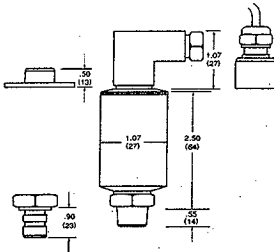
Output Signal	4-20mA, 2 wire
Pressure Ranges	Vacuum and compound through 0-15000 PSI; gauge and absolute
Proof Pressure	0-5, 0-10, 0-7500 through 0-15000 PSI; 1.5 times range 0-15 PSI through 0-6000 PSI; 2 times range
Burst pressure	0-5, 0-10, 0-7500 through 0-15000 PSI; 2 times range 0-15 PSI through 0-6000 PSI; 5 times range
Accuracy (RFSL or RSS) (includes repeatability, hysteresis and linearity)	± 0.5% full scale standard ± 0.25% full scale optional
Repeatability	± 0.05% full scale
Hysteresis	± 0.1% full scale
Stability	± 0.2% full scale per year
Input Excitation	12-30 VDC, unregulated
Temperature ranges	Compensated 32° to 175°F/0 to 80°C Effect = 0.03%/50°F Storage = -40° to 212°F/-40° to 100°C Medium = 22° to 212°F/-30° to 100°C Ambient = -40° to 185°F/-40 to 85° C
Response time	less than 1 ms (between 10-90% full scale)
Pressure cycle limit	150M
Operating life	100 million cycles
Adjustment	± 5% full scale of zero and span
Environmental protection	NEMA 4x, DIN IP65 (IEC 529)
Electromagnetic capability per IEC 801	Part 2 - ESD Level 2 Part 3 - Fields (RF) Level 2 Part 4 - Burst Level 3 Part 5 - Surge Level 2
Electrical protection	Reverse polarity, overvoltage and short circuit protection
Shock	Less than ± 0.05% full scale effect or 1000's @ 20ms on any axis
Vibration	Less than ± 0.05% full scale effect for 35g's @ 5-2000 Hz on any axis.

Fig 24

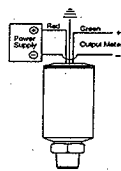


PRESSURE TRANSDUCERS SERIES 100

DIMENSIONS



WIRING DIAGRAMS AND ELECTRICAL CONNECTIONS



100 Series	4-20mA 2 WIRE
+ Supply	Red/1/A
+ Output	Green/2/B
Case ground	Blue (or non-shielded) 4/D

Example: Red/1/A = Applicable color wire/bendix pin or din plug number.

Load Limitations 4-20mA Output Only
 $V_{min} = 10V + (.022 \times R_L)$ 100 Series
 $V_{min} = 12V + (.022 \times R_L)$ 300 Series
 $R_L = R_s + R_w$
 R_L = Loop Resistance (ohms)
 R_s = Sense Resistance (ohms)
 R_w = Wire Resistance (ohms)

2 WIRE WIRING DIAGRAM EXAMPLE

ORDERING INFORMATION

SERIES 100

PRESSURE RANGES	30V	30*/200 PSIG	30/200	0-60 PSIG	60	0-600 PSIG	600	0-5000 PSIG	5000	0-15PSIA	15A
30*/15 PSIG	30/15	30*/300 PSIG	30/300	0-100 PSIG	100	0-750 PSIG	750	0-6000 PSIG	6000	0-30PSIA	30A
30*/30 PSIG	30/30	0-5 PSIG	5	0-150 PSIG	150	0-1000 PSIG	1000	0-7500 PSIG	7500	0-60PSIA	60A
30*/60 PSIG	30/60	0-10 PSIG	10	0-200 PSIG	200	0-1500 PSIG	1500	0-10000 PSIG	10000	0-100PSIA	100A
30*/100 PSIG	30/100	0-15 PSIG	15	0-300 PSIG	300	0-2000 PSIG	2000	0-15000 PSIG	15000	0-150PSIA	150A
30*/150 PSIG	30/150	0-30 PSIG	30	0-500 PSIG	500	0-3000 PSIG	3000			0-200PSIA	200A
										0-300PSIA	300A

PSIG = Gauge Pressure PSIA = Absolute Pressure Other ranges available on special request

ACCURACY (BFSL)	1 ± 0.5% FULL SCALE	2 ± 0.25% FULL SCALE
OUTPUT SIGNAL	1 4-20mA	
PROCESS CONNECTIONS	2 1/4" NPT MALE	3 7/16"-20 UNF (adjustable per SAE J-514) other connections available upon request
ELECTRICAL CONNECTIONS	1 36" CABLE (connected to option 7) 2 4 PIN BENDIX 3 6 PIN BENDIX	6 1/2" NPT CONDUIT (w/36" cable) 7 MINI-HIRSCHMANN (w/mating connector)
OPTION	SS THREADED ORIFICE ORF	

EXAMPLE

Series 100
 Pressure Range 3000 PSIG
 Accuracy ±0.25%
 Output Signal 4-20mA, 2 wire
 Process Connection 1/4" NPT MALE
 Electrical Connection MINI HIRSCHMANN

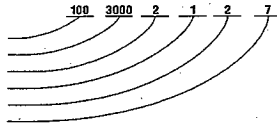


Fig 25